Production and Transport Processes of Carbon Dioxide in Soil Profiles of a Coniferous Forest and an Alpine Grassland

YVES LANIEL

January 1982

Production and Transport Processes of Carbon Dioxide in Soil Profiles at a Coniferous Forest and an Adjacent Grassland

Yohhei HAMADA

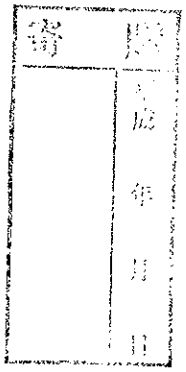

A dissertation submitted to the Doctoral Program
in Geoscience, the University of Tsukuba
in partial fulfillment of the requirements for the
degree of Doctor of Philosophy (Science)

January, 1999

Contents

Abstract

To quantitatively assess the processes of the production and transport of carbon dioxide in soil profiles, and to examine the effect of vegetation on the processes, the temporal and spatial distributions of the concentration and the content of carbon dioxide in soils were observed at a coniferous forest and an adjacent grassland in eastern Japan.

The concentration and the content of carbon dioxide varied largely by season and by depth at the observation sites. The concentration of carbon dioxide in soil air was always higher than that in the atmosphere and reached 1.26% at the forest site and 9.89% at the grassland site at the maximum. The concentrations increased from spring to summer and decreased from autumn to winter, and generally increased with depth. The carbon dioxide dissolved in soil water exhibited higher concentrations and the smaller temporal and spatial variations than that in soil air showed. Due to the volumetric water content higher than air-filled porosity, the total content of carbon dioxide in bulk soil was occupied mainly by the content dissolved in liquid phase of the soil.

The diffusive flux of carbon dioxide in soil air was dominant in the vertical transport of carbon dioxide in the soil profiles. The advective fluxes of carbon dioxide accompanied by the movement of soil air and soil water were generally small. However, the proportion of the advective flux of dissolved carbon dioxide increased with depth in the deep soils.

The production rate of carbon dioxide in the soil evaluated by the mass balance of carbon dioxide was largest near the ground surface and decreased with depth. The soil layer in which significant production rates were obtained ranged from the ground surface to a depth of 45 cm at the forest site and from the surface to 25 cm at the grassland site, reflecting the distribution of plant roots at both sites. The evaluated production rate exponentially increased in response to the linearly rising soil temperature. The mean residence time of CO_2 in the shallow soils was within a day at the forest site, while the time reached nearly two hundred hours at the grassland site.

From the discussion on the formation of concentration profiles of carbon dioxide, it was concluded that the shallow soil layer is important for the place of the production of carbon dioxide, while the deep soil layer is important as the place keeping high concentrations of carbon

dioxide and then determining the rate of the supply of carbonate species into groundwater. From the comparison of the results obtained at the forest and the grassland site, it was suggested that the difference in vegetation directly affects the production rate of carbon dioxide by the difference in the distribution of plant roots, and indirectly influences the transport processes of carbon dioxide, and then its concentration, by affecting the soil physical properties. By comparing the fluxes and the contents of carbon dioxide in soil air and soil water, it was indicated that the soil air is the important media in which much of carbon dioxide is transported while the soil water is important as the reservoir in which carbon dioxide is stored.

Key words: Carbon dioxide, microbial decomposition, molecular diffusion, pH, plant roots, and soil respiration.

List of Tables

List of Figures

List of Symbols

Symbol	Definition
A_C	Bottom area of the closed chamber (cm^2)
C_C	Concentration of CO_2 in the closed chamber ($gCO_2 \cdot cm^{-3}$)
C_g	Concentration of CO_2 in soil air ($gCO_2 \cdot cm^{-3}$)
$C_g(i)$	Concentration of CO_2 in soil air at the soil compartment i ($gCO_2 \cdot cm^{-3}$)
C_w	Concentration of CO_2 dissolved in soil water ($gCO_2 \cdot cm^{-3}$)
$C_w(i)$	Concentration of CO_2 dissolved in soil water at the soil compartment i ($gCO_2 \cdot cm^{-3}$)
C'_w	Molar concentration of CO_2 dissolved in soil water ($mol \cdot dm^{-3}$)
c_C	Concentration of CO_2 in the closed chamber (% in vol.)
c_{CO_2}	Corrected value of the concentration of CO_2 measured with the gas detection tubes (% in vol.)
c_{TUBE}	Uncorrected value of the concentration of CO_2 measured with the gas detection tubes (% in vol.)
D_0	Diffusion coefficient in free air at the standard state ($cm \cdot s^{-1}$)
D_a	Diffusion coefficient in free air
$D_a(i,j)$	Diffusion coefficient of CO_2 in free air between the soil compartments i and j ($cm \cdot s^{-1}$)
D_s	Diffusion coefficient in soil air
$D_s(i,j)$	Diffusion coefficient of CO_2 in soil air between the soil compartments i and j ($cm \cdot s^{-1}$)
d	Depth number of the soil compartments in the virtual soil column
$d_{D\text{-}ZFP}$	Depth number of the soil compartment at which the D-ZFP is found
h_C	Height of the inside space of the closed chamber (cm)
$J_a(i,j)$	Advective flux of CO_2 accompanied by the mass flow of soil air between the soil compartments i and j ($gCO_2 \cdot cm^{-2} \cdot s^{-1}$)
J_d	Diffusive flux of CO_2 in soil air
$J_d(i,j)$	Diffusive flux of CO_2 in soil air between the soil compartments i and j ($gCO_2 \cdot cm^{-2} \cdot$

s^{-1})

$J_{Mg}(i,j)$ Mass flow flux of soil air between the soil compartments i and j ($cm \cdot s^{-1}$)

$J_{Mw}(i,j)$ Flux of soil water between the soil compartments i and j ($cm \cdot s^{-1}$)

J_t' Sum of the absolute values of each flux of CO_2

$J_t(i,j)$ Total flux of CO_2 between the soil compartments i and j ($gCO_2 \cdot cm^{-2} \cdot s^{-1}$)

$J_w(i,j)$ Advective flux of dissolved CO_2 accompanied by the movement of soil water between the soil compartments i and j ($gCO_2 \cdot cm^{-2} \cdot s^{-1}$)

K_1, K_2 The first and the second acidity constant for the carbonate equilibrium

K_H Henry's law constant for the solubility of CO_2

k_n Empirical constants on the equilibrium of dissolved carbonate species, defined as $k_0 = -\log K_H$, $k_1 = -\log K_1$, $k_2 = -\log K_2$

l Thickness (cm)

l_i Thickness of the soil compartment i (cm)

M_C Total content of CO_2 in the closed chamber (gCO_2)

M_g Content of CO_2 in gaseous phase per unit volume of bulk soil ($gCO_2 \cdot cm^{-3}$ soil)

M_t Total content of CO_2 per unit volume of bulk soil ($gCO_2 \cdot cm^{-3}$ soil)

M_w Content of CO_2 dissolved in liquid phase per unit volume of bulk soil ($gCO_2 \cdot cm^{-3}$ soil)

m_{CO_2} Molecular weight of CO_2

n Empirical constant for the diffusion coefficient in free air

P Total pressure at the observation sites (hPa)

P_0 Total pressure at a standard state (hPa)

p_{CO_2} Partial pressure of CO_2 in soil air (atm)

R Gas constant for ideal gas ($hPa \cdot cm^3 \cdot mol^{-1} \cdot K^{-1}$)

T Temperature (K)

T_0 Temperature at a standard state (K)

T_C Air temperature in the closed chamber (K)

T_i, T_j Soil temperature at the soil compartments i and j (K)

T_t Soil temperature at a time of t (K)

t Time

V_i, V_j Volume of soil air at the soil compartments i and j

V_t	Volume of soil air at a time of t
z	Depth
z_i	Depth of the soil compartment i (cm)
α_i	Production rate of CO_2 at the soil compartment i ($gCO_2 \cdot cm^{-2} \cdot s^{-1}$)
ΔH	Difference in proton content in soil water between before and after degassing dissolved CO_2 ($mol \cdot dm^{-3}$)
ΔS_d	Change rate of CO_2 storage in the soil compartment d ($gCO_2 \cdot cm^{-2} \cdot s^{-1}$)
$\Delta S'_d$	Change rate of CO_2 storage per unit volume of bulk soil ($gCO_2 \cdot cm^{-3} \cdot day^{-1}$)
ΔV_{net}	Net change in the volume of gaseous phase
ΔV_T	Change in the volume of soil air
ΔV_{θ_g}	Change in the volume of gaseous phase
ΔV_{θ_w}	Change in the volume of liquid phase
θ_g	Air-filled porosity
$\theta_g(i,j)$	Air-filled porosity between the soil compartments i and j
$\theta_g(t)$	Air-filled porosity at a time of t
θ_t	Total porosity
$\theta_t(i,j)$	Total porosity between the soil compartments i and j
θ_w	Volumetric water content
$\theta_w(t)$	Volumetric water content at a time of t
$\xi(i,j)$	Relative diffusion coefficient between the soil compartments i and j

List of Abbreviations

Abbreviation	Definition
ERC	Environmental Research Center
C-ZFP	Convergent zero flux plane
D-ZFP	Divergent zero flux plane
GC	Gas chromatography
IPCC	Intergovernmental Panel on Climate Change
Max/Min	Ratio of the maximum value to the minimum value
RpH	Reserve pH, defined as the pH value eliminated the effect of volatile compounds
SC-F*n*	Sampling bores of soil core samples at the forest site (*n*=1 to 3)
SC-G*n*	Sampling bores of soil core samples at the grassland site (*n*=1 to 3)
SR-F*n*	Measuring spots for soil respiration rate at the forest site (*n*=1 or 2)
SR-G*n*	Measuring spots for soil respiration rate at the grassland site (*n*=1 or 2)
TCD	Thermal conductivity detector
TOC	Total organic carbon

Chapter 1

Introduction

1.1 Previous studies

1.1.1 Outline of the knowledge and importance of carbon dioxide in a soil

In general, carbon dioxide (CO_2) is continuously produced in a soil mainly due to the microbial decomposition of soil organic matter and the respiration of plant roots. By this reason, the concentration of CO_2 in soil air is usually higher than the concentration in the atmosphere (about 0.035% in vol.) and often becomes tens to hundreds times as high as in the atmosphere. Most of CO_2 produced in a soil is evolved into the atmosphere mainly by molecular diffusion, known as soil respiration. Hence the CO_2 produced in a soil is one of the important source of CO_2 in the atmosphere, so that the change in the rate of soil respiration will largely affect the concentration of CO_2 in the atmosphere.

According to the IPCC report in 1990, in the global scale, the amount of carbon stored in the soil is about 1500 Pg, equivalent to twofold of the amount in the atmosphere, one and a half in the surface ocean, and threefold in the terrestrial biomass. In addition, the carbon flux from the terrestrial biosphere into the atmosphere is estimated to 102 Pg per year. This carbon flux exceeds the flux between the surface ocean and the atmosphere by 10 Pg per year, and the half of the flux is occupied by the direct evolution of gaseous carbon from the soil, mostly soil respiration. On the other hand, the carbon fluxes into the atmosphere accompanied by burning of fossil fuels and deforestation are only 5 and 2 Pg per year, respectively. Thus in the determination of CO_2 concentration in the atmosphere, namely the determination of the intensity of greenhouse effect, the transport of CO_2 from a soil into the atmosphere is more important rather than the evolution of anthropogenic CO_2.

Because of high solubility of CO_2 into water, some of the CO_2 produced in a soil dissolves into soil water, and hydrates with the water to generate carbonic acid. A part of the carbonic acid

dissociates into bicarbonate ions and protons, and therefore lowering pH in the water. Thus the concentration of CO_2 in soil air is one of the important factors which determine the pH in soil water and groundwater, so that the effect of the dissolution of CO_2 on pH has increasingly attracted interests in relation to the acidification of soil caused by acid precipitation (e.g. Ohte et al., 1995; Hamada et al., 1996).

The CO_2 dissolved in soil water is brought into groundwater with the percolation of soil water. From the studies using isotopic composition of carbon, it is confirmed that the origin of dissolved carbonate species in many aquifers is not the carbonate minerals at depth of the ground, but the CO_2 biologically generated in soils (e.g. Wood and Petraitis, 1984; Mizutani and Yamamoto, 1993; Ishii et al., 1996). Nevertheless the magnitude of dissolved CO_2 flux transported into groundwater is usually much lower than that of CO_2 flux diffused into the atmosphere, the dissolved CO_2 flux is an important source of carbonate species in groundwater.

In addition, since the generation of CO_2 in a soil is essentially due to biological activity, the concentration of CO_2 in soil air indicates the extent of the activity. Some of the recent studies related to the remediation of pollution using indigenous soil microorganisms have attempted to use the concentration of CO_2 as an index of the in-situ microbial activity (e.g. Suchomel et al., 1990; Wood et al., 1993).

1.1.2 Previous methodology

The order of the behavior of CO_2 in a soil is as follows: First, CO_2 is biologically produced; secondly, CO_2 is transported by mainly molecular diffusion in soil air; thirdly, the profile of CO_2 concentration is formed as the result of the production and transport of CO_2. In spite of such an order, the majority of previous studies on CO_2 in soils have presented the distribution of CO_2 concentration only, because of the easiness of measuring the concentration and the difficulty in the determination of the production and transport fluxes.

Since the CO_2 produced in a soil is biogenic, and therefore the production rate is a function of soil temperature and soil moisture condition, CO_2 concentration in soil air generally distributes corresponding to the environmental conditions in the soil. By this reason, many of the previous studies have discussed about the direct relationships between the concentration and the environmental factors (e.g. Gunn and Trudgill, 1982; Buyanovsky and Wagner, 1983; Fernandez and Kosian, 1987; Castelle and Galloway, 1990; Kiefer, 1990; Hamada and Tanaka, 1997). For

example, Brook et al. (1983) established the empirical relationship between the concentration of CO_2 in soil air and actual evapotranspiration rate using the data presented in past literatures, and mapped the worldwide distribution of CO_2 concentration; actual evapotranspiration was used because the rate is a function of both temperature and soil moisture condition at the place. Despite these efforts, the relationships are physically and chemically indirect, and therefore empirical and site dependent. Because the concentration of CO_2 in soil air is determined not by the production rate of CO_2 only, but by the interaction of the production and transport of CO_2.

To elucidate the processes of the production and transport of CO_2 in a soil, several process-oriented studies have been carried out. Many of the studies assessed the processes using the following procedure (e.g. Bouten et al., 1984; Solomon and Cerling, 1987; Hendry et al., 1993; Kumagai, 1998): First, a numerical model which reproduces the transport processes of CO_2 in a soil profile was developed while the concentration profile was determined by field observation. Next, an arbitrary profile of the production rate of CO_2 was given to the process model, and then a profile of CO_2 concentration was obtained as the result of model calculation; this calculation was iterated many times and the CO_2 production profiles were given by trial and error. Finally, the profile of the production rate that had given the calculated concentration profile in the best agreement with the observed profile was regarded as the real profile. For such stochastic approaches to evaluate the production rate of CO_2, some problems have been pointed out. Solomon and Cerling (1987) illustrated that if different production profiles that had a common depth of the centroid of production were given, the calculated concentration profiles were little different. Kumagai (1998) suggested that some parameters which determine the profile of the production rate were interdependent, so that these parameters could not be determined uniquely.

On the other hand, another approaches, as it were deterministic approaches, have been attempted in some studies (e.g. de Jong and Schappert, 1972; Wood et al., 1993; Davidson and Trumbore, 1995). For example, de Jong and Schappert (1972) calculated CO_2 flux by diffusion in soil air for each depth from the observed concentration profile and the estimated diffusion coefficient, and then evaluated the production rate at the depth by the difference in fluxes between the upper and the lower depth. By the deterministic approach, the diffusive flux and the production rate of CO_2 can be quantified in turn from the measured values of CO_2 concentration in soil air. However, the reliability of the evaluation gradually lowers, so that some negative values were calculated as the production rate in de Jong and Schappert (1972).

1.2 Purpose of the study

Considering the essential uncertainty of the stochastic approaches, the deterministic approach was used in this study to clarify the processes of the production, transport, and formation of concentration profiles of CO_2 in soils. The outline of the procedure in this study is as described below:

First, as the base for the deterministic analysis, the temporal and spatial distributions of the concentration and content of CO_2 were determined by field observation. The concentration of CO_2 in soil air, the only directly measurable factor, was observed at several depths with related environmental conditions. Nevertheless the CO_2 dissolved in soil water is usually as important as CO_2 in soil air because of the dissolution equilibrium between both phases and the considerable volumetric proportion of liquid phase in soils, few studies have discussed on the dissolved CO_2 in soil water. In this study, dissolved CO_2 concentration was evaluated from the measured concentration in soil air and the environmental factors that affect the dissolution of CO_2 into soil water and the dissociation of carbonic acid in the water. At last, the actual content of CO_2 in bulk soil was evaluated from the measured concentration in soil air, the evaluated concentration dissolved in soil water, and the volumetric proportions of gaseous and liquid phases.

Next, using the distributions of the concentration and content of CO_2 obtained above, the transport fluxes of CO_2 were evaluated for each depth, and then the production rate of CO_2 was estimated by the difference of the fluxes at the depth. At first, to validate the whole production of CO_2 in soil profiles, soil respiration rate that is the only measurable flux of CO_2 was observed. As the most important flux of CO_2 in a soil profile, the diffusive flux of CO_2 in soil air was evaluated. The flux was calculated from the concentration gradient of CO_2 in soil air obtained from the field observation and the diffusion coefficient of CO_2 in soil air estimated by the known equation on the relative diffusion coefficient. The diffusion of CO_2 in soil water was not taken into consideration because the diffusion coefficient in water is about four orders of magnitude as small as that in air. As well as by diffusion, the CO_2 in a soil is also transported by advection accompanied by the movement of soil air and soil water. The advective flux of CO_2 accompanied by the mass flow of soil air has been intensively investigated by Romell (1922) and concluded to be negligible in general, but the quantitative evaluation of the flux has been seldom performed. The advective flux of CO_2 accompanied by the movement of soil water also has been rarely

examined, but the flux into groundwater is an important source of carbonate species in the groundwater. In this study, both advective fluxes were evaluated using the temporal variation of the volumetric proportions of gaseous and liquid phases in the soil. Using the evaluated fluxes for each depth, the production rate of CO_2 was calculated as the remainder of CO_2 mass balance, after evaluated the change rate of CO_2 storage in bulk soil.

In addition, to elucidate the response and feedback of the terrestrial ecosystems that have different vegetation to climate change, several intensive studies comparing the balances of water, energy and substances under different vegetation have been carried out recently. In the Amazon River basin, long-term meteorological observations were carried out at natural forest and artificially disturbed grassland to compare the fluxes and balances between the different vegetation (Gash et al., 1996). The comparative experiments by numerical models among the representative vegetations in the Northern Hemisphere were also performed (Breymeyer et al., 1996). For the CO_2 in a soil, several studies have compared the concentrations of CO_2 in soil air measured under different vegetation, but the effect of the difference in vegetation type on the production and transport processes of CO_2 has been hardly investigated. By this reason, field observation in this study was carried out at a forest and a grassland, which are representative vegetations in the temperate region. The grassland adjacent to the forest was selected to remove the difference in conditions other than vegetation. After that, the processes of the production and transport of CO_2 in the soils under both vegetations were assessed and the effect of the vegetation on the CO_2 processes was discussed.

Finally, the objectives of the present study are summarized as follows:

1) To determine the temporal and spatial distributions of the concentration and content of CO_2 in soils using the concentration of CO_2 in soil air and the environmental factors observed at a forest and an adjacent grassland.
2) To clarify the processes of the production and transport of CO_2 in soils by the deterministic approach using the distributions of the concentration and content of CO_2 in soils obtained above.

Chapter 2

Site description

2.1 General aspects of study area

For the field observation in this study, two sites were established in the Environmental Research Center (hereinafter referred to as ERC), University of Tsukuba. One is an artificial forest dominated by Red Pine; the other is a grassland, which was adjacent to the forest and created for meteorological observation. The location of ERC is mapped in Figure 2.1, and the detailed map and the locations of the observation sites in ERC are illustrated in Figure 2.2. The ERC is located at N36°7' E140°6' and an altitude of 27 m, in the campus of the University of Tsukuba, placed in Tsukuba City, Ibaraki Prefecture, about 50 km northeast from Tokyo.

According to the long term meteorological data of ERC, annual mean air temperature is 13.3°C and annual precipitation is in the range of 1200 to 1600 mm. The area is placed on a diluvial upland gradually descending toward the southeast. The top of the upland is covered by Kanto Loam by one to two meters in thickness, and 5-to-6-m thickness of Joso Clay layer is underlain (Inokuchi et al., 1977).

2.2 Observation sites

2.2.1 Forest site

The forest site was established at the middle of the artificial coniferous forest (Figure 2.2), which is placed at the southern part of ERC and dominated by Red Pine (*Pinus densiflora* Sieb. et Zucc.). The forest has an area of 0.017 km^2, tree ages of about thirty, 16.5 trees per 100 m^2, a mean tree height of 13.1 m, and a mean diameter at the breast height of 13.7 cm (Usami and Oikawa, 1993). Other than Red Pine, some species of Oak (*Quercus myrsinaefolia* Blume or *Quercus serrata* Thunb.) are found as shrubs. The soil of the forest is a typical light colored black soil, representative of the study area (Yasui and Oikawa, 1993). The profiles of the soil horizon have been surveyed by Sugita et al. (1986), and Yasui and Oikawa (1993). According to their studies, a soil layer from the surface to depths of 20 to 25 cm is A layer, and below those depths is B layer.

2.2.2 Grassland site

The grassland site was established near the southern edge of the heat balance and water balance observation field of ERC, adjacent to the Red Pine forest (Figure 2.2). The observation field is a flat, circular grassland that has a radius of 80 m and an area of 0.02 km^2, and was created in 1977 for the basic research on energy and water balances near the ground surface. After the creation, six species of pasture have been planted in 1978 and 1988, but recently creeping grasses and many other species of wild grass are found in the observation field.

The profile of soil horizon had not been observed at the observation field, so that a cross section of the soil, 1 m in width and 1 m in depth, was dug up and observed in September 1997 near the observation site. The result of the survey is summarized in Table 2.1. The profile was clearly different from that in the forest, and had a light brown colored clayey layer between depths of 10 and 25 cm and a dark brown colored silt layer between 40 and 80 cm. This stratigraphic sequence was upside down of that in natural soils such as the forest soil. This was due to the artificial disturbance by the creation of the observation field. Moreover, a gray or grayish blue colored clay layer was found between the inversely deposited layers. Such a clay layer has never been found in the Red Pine forest, so that the clay was probably dressed from other places to prevent the ground surface from subsiding by anthropogenic consolidation.

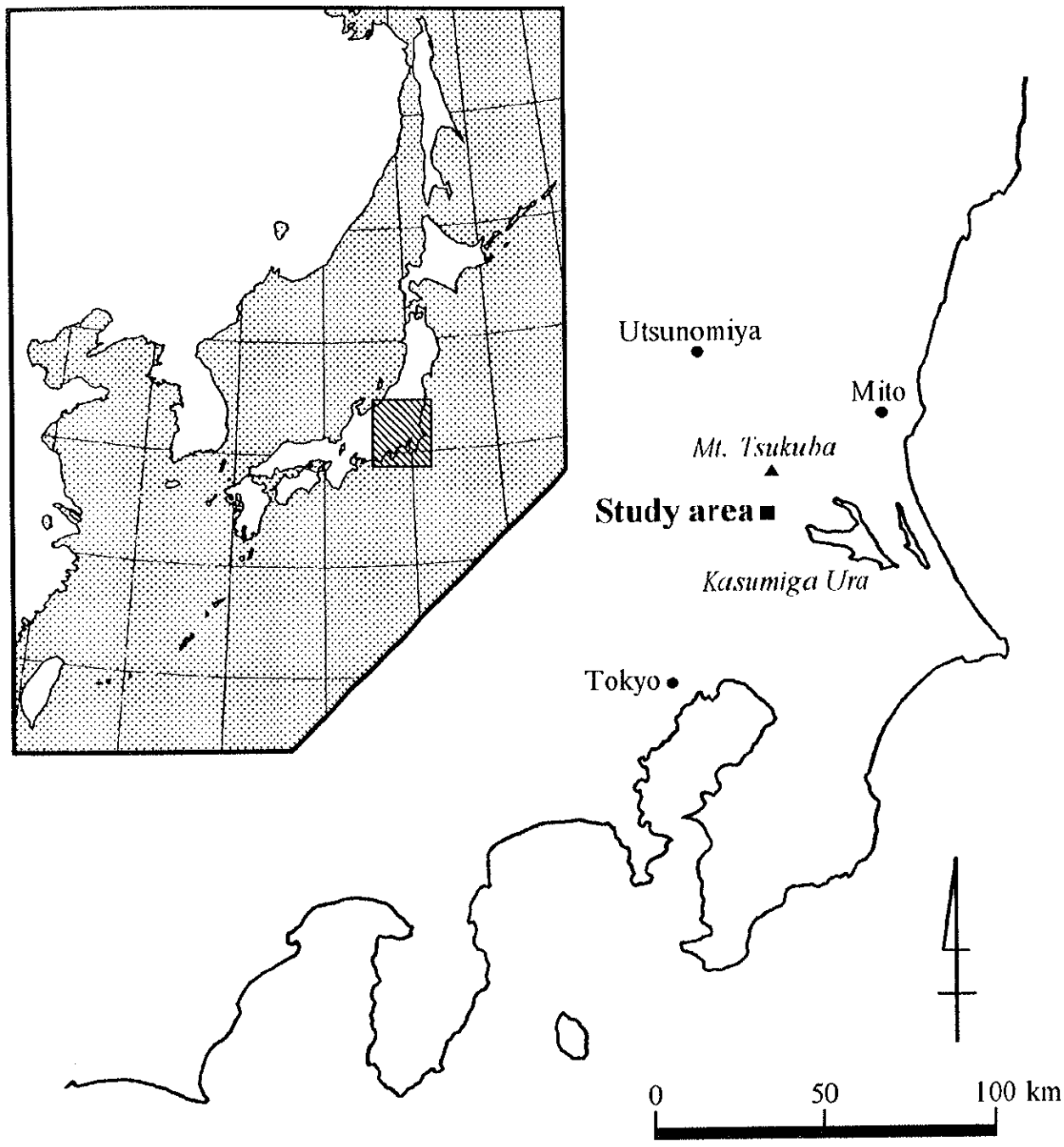

Figure 2.1. Location of the study area.

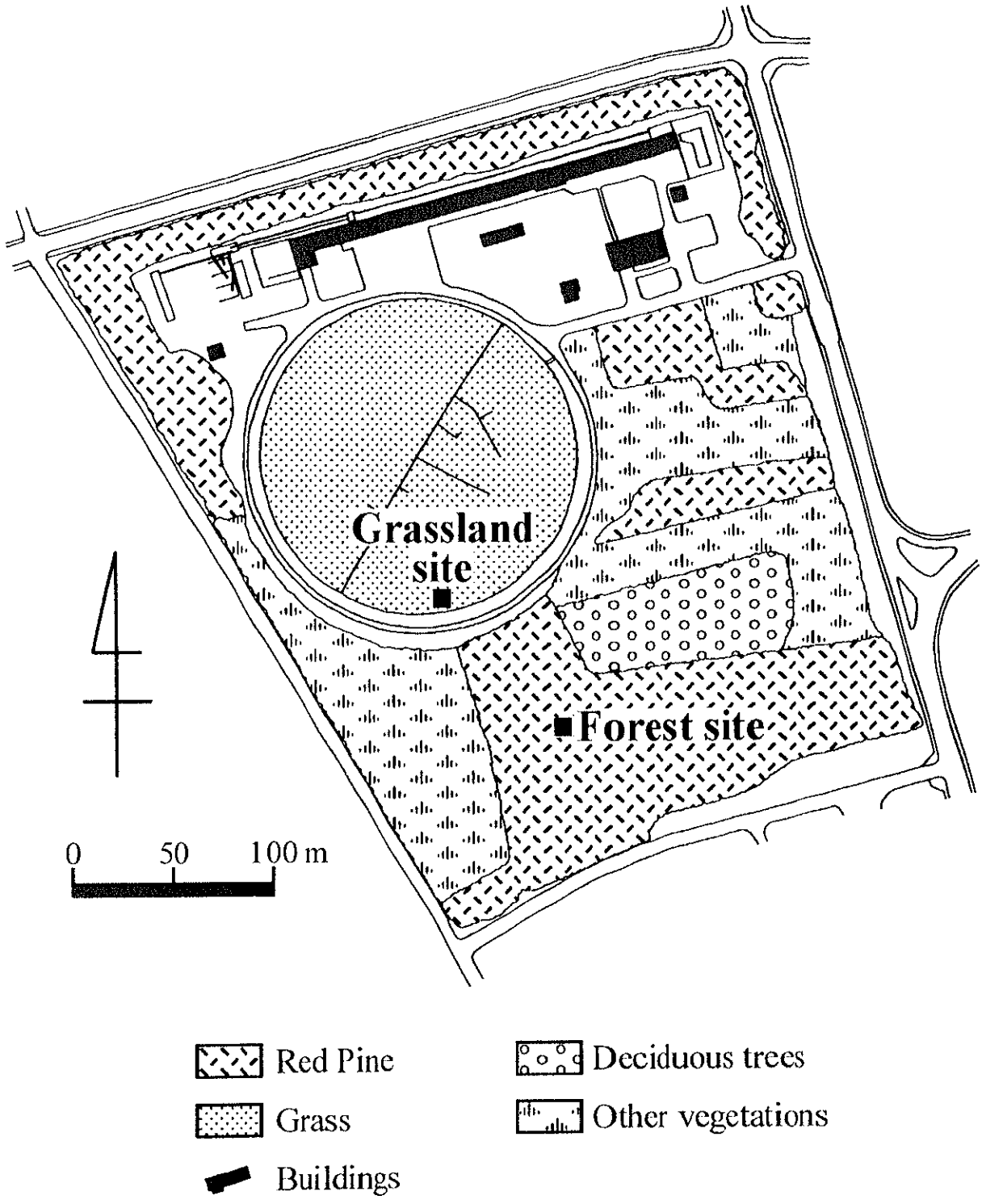

Figure 2.2. Map of the Environmental Research Center (ERC), University of Tsukuba, and the locations of the observation sites.

Table 2.1. Simple descriptions on the profile of soil horizon at the grassland site

Depth (cm)	Description
0 to 10	Aggregated, dark brown, intensive concentration of plant roots from 0 to 5 cm (typical surface soil)
10 to 25	Slightly clayey, dark red brown, a few roots, several dark brown clods of the size of about 5 cm
25 to 38-42	Clayey, gray or grayish blue, few roots (dressed clay)
38-42 to 57-60	Silty, dark brown, only a few roots
57-60 to 70	Silty, blackish brown, a few roots
70 to 80-85	Silty, dark brown, only a few roots
80-85 to 100<	Slightly clayey, dark red brown, few roots

Observed on September 11, 1997

Chapter 3

Characteristics of soils

3.1 Physical properties of soils

3.1.1 Method for data collection

For the Red Pine forest and the adjacent meteorological observation field in ERC, in which the field observation sites were established in this study, the collection of soil core samples and the examination on soil physical properties of the samples have been carried out for several times, and the results of the examination were summarized in Hamada et al. (1998). In this study, several sampling bores representative of the observation sites were selected for each site from the bores at which soil core samples had been collected, and soil physical properties indicated by the samples collected at the representative bores were applied.

Each soil core sample was collected into a metallic sampling cylinder that has an inner diameter of 5 cm and a capacity of 100 cm^3, without disturbance. Soils had been sampled every 10 cm depth, from the ground surface to a depth of 150 cm.

3.1.2 Three-phase distribution of soils

The three-phase distribution of a soil, namely the volumetric proportions of solid, liquid and gaseous phases in bulk soil, was determined for each depth at the forest and the grassland site. The profiles of the distribution at both sites are shown in Figures 3.1 and 3.2 with the profiles of soil horizon at the sites. The arithmetic mean values of total porosity and volumetric water content averaged among the values at the representative sampling bores are plotted with error bars which show the minimum and the maximum values.

At the forest site, total porosity was kept nearly constant values of 81 to 84% from the ground surface to a depth of 70 cm, and then decreased uniformly with depth to 63.2% at 150 cm. Volumetric water content largely increased from 34.4% near the surface to 57.6% at a depth of

50 cm, and gradually increased from 53.1% to 64.6% between depths of 50 and 100 cm with some fluctuations, and became constant below 100 cm, 62 to 64%. Consequently, air-filled porosity decreased with depth from 47.1% near the ground surface to 1.5% at a depth of 150 cm, mainly due to the increase in volumetric water content and partly due to the decrease in total porosity. In principle, the soil core samples have not been collected under extremely wet or dry conditions, so that the profile of the three-phase distribution shown in Figure 3.1 can be regarded as a typical profile after gravitational drainage at the forest site.

At the grassland site, as well as the profile of soil horizon, the three-phase distribution was highly different from that at the forest site. Total porosity was about 70% near the ground surface, but rapidly decreased to approximately 62% between depths of 10 and 40 cm, where the old subsoil and dressed clay were lain. Below these depths, total porosity increased to the maximum of about 77% at depths of 50 to 80 cm, then decreased again to 54.9% at 150 cm.

Near the ground surface, volumetric water content and air-filled porosity were 40-50% and 20-30%, respectively. Between depths of 10 and 40 cm, however, volumetric water content was nearly equal to total porosity, and therefore air-filled porosity was extremely small, 1.5 to 2.8%. Some of the soil core samples were completely saturated. From 40 to 80 cm in depth, volumetric water content increased with depth more gradually than total porosity, to about 70%. As a result, air-filled porosity also increased to 6-7%. Below those depths, volumetric water content decreased also more gradually than total porosity. Thus air-filled porosity also decreased, and the soil was almost saturated below a depth of 130 cm.

3.1.3 Soil water characteristic curves

Soil water characteristic curves, which show the relationship between free energy of soil water and volumetric water content, were determined for each depth at the forest and the grassland site. The curves were selected to reproduce the profiles of volumetric water content in the best agreement with the profiles shown in Figures 3.1 and 3.2. The curves selected for each depth at both sites are plotted in Figures 3.3 and 3.4.

At the forest site, from 10 to 70 cm in depth, the curves showed a common trend; little drainage of soil water from pF 0 to pF 1, rapid drainage from pF 1 to pF 2, and gradual drainage more than pF 2. The decrease in volumetric water content from pF 0 to pF 2.6 decreased with depth, from 47.8% at 10 cm to about 25% at 40-70 cm. At depths of 100 and 150 cm, on the

other hand, the total decreases in volumetric water content were only 6.8 and 2.6%, respectively. The drainage mainly occurred more than pF 1.5, and was more gradual than the above depths.

At the grassland, the trend of drainage similar to that in shallow soils at the forest site was found only at a depth of 10 cm. At this depth, the water was rapidly drained from pF 1 to pF 2, and the decrease in volumetric water content was 37.3% in total. In contrast, little water was drained at depths of 20 to 50 cm. The decreases in volumetric water content were 2.3 to 4.1% even in total, and the pF at which the water began to drain could not be determined. Below those depths, the total decreases in volumetric water content became slightly large, 5.5 to 10.0%, and much of the drainage occurred more than pF 2.0.

3.1.4 Saturated hydraulic conductivity

As an index of the permeability of the soils, the profiles of saturated hydraulic conductivity at the forest and the grassland site are shown in Figures 3.5 and 3.6, respectively. Each profile obtained at the sampling bores representative of both sites was plotted. Considering the viscosity of water, the values of the conductivity have been converted into the values at a temperature of 15°C.

At the forest site, saturated hydraulic conductivity exponentially decreased with depth in general. Taking the common logarithms, the conductivity decreased linearly, from about –2 near the ground surface to around –6 at depths below 100 cm. At depths of 40 to 50 cm, however, sudden decreases in the conductivity were observed at all the sampling bores. The sudden decreases probably suggest that some difference in the geometric structure of pore space of the soil to lower the permeability of substances is present at the depths, although total porosities and the soil water characteristic curves were not so different.

At the grassland site, saturated hydraulic conductivity ranged from –4 to –2 in common logarithms at a depth of 10 cm. In contrast, at depths of 10 to 40 cm, where the consolidated old subsoil and the dressed clay layer were lain (Figure 3.2), suddenly dropped to 2.3×10^{-7} cm·s^{-1} at the minimum. Taking the common logarithms, the conductivity slightly increased up to about –5 at depths of 50 to 100 cm, and then decreased again to –6 below 100 cm.

3.2 Distribution of plant roots

In the Red Pine forest of ERC, Sugita et al. (1986) has been examined the vertical distribution of plant roots, which is one of the important sources of CO_2 in a soil. The result of the investigation is shown in Figure 3.7, cited from Sugita et al. (1986). The roots of a Red Pine tree distributed from the ground surface to a depth of 140 cm, and the amount of the roots decreased with depth. Such a distribution of the roots is commonly observed among tree species. On the other hand, in the meteorological observation field of ERC, the distribution of plant roots has never been examined. In this study, therefore, the distribution of grass roots was investigated near the observation site in the observation field.

The investigation of the root distribution was carried out in September 1997, at the same time of the survey of the profile of soil horizon (see Section 2.2.2). As the method for investigation, the procedure described in Hamada et al. (1997) was applied after slightly simplified. After the soil cross section which had a depth of 1 m and a width of 1 m was dug up, a vertical section of 10 cm in width was sited on the cross section. Inside of the vertical section was divided into squares at an interval of 10 cm depth; only the top square was subdivided into 0-5 and 5-10 cm. After the division, the number of the roots exposed in each square was counted by eyes. These procedures for the vertical section were repeated for several times on the cross section of the soil.

The result of the investigation is shown in Figure 3.8. The data are expressed as root density, namely the number of plant roots that are exposed in a square centimeter of the soil cross section. Arithmetic mean values averaged for each depth were plotted with error bars that show the minimum and the maximum values obtained at the depth.

The plant roots at the grassland site extremely concentrated near the ground surface. From the surface to a depth of 20 cm, the root density rapidly decreased from 1.36 to 0.09 cm^{-2}. Then, the root density gradually decreased until 0.045 cm^{-2} at 40-50 cm. Between depths of 50 and 80 cm, where the old surface soil was deposited (Table 2.1), the root density showed relatively large values of about 0.1 cm^{-2}. It could not be determined whether the roots at these depths were the residues of the roots which had been contained in the old surface soil, or living roots which penetrated through the upper clayey soils. In both cases, the roots may act as a source of CO_2 in deep soils. Below a depth of 80 cm, the root density decreased again to 0.035 cm^{-2}.

3.3 Distribution of soil organic carbon

The distribution of soil organic carbon, which is the important source of CO_2 in a soil as well as plant roots, was determined for the soils at the forest and the grassland site. The soil core samples which had been collected at the representative bores of both observation sites were served for the analysis. After oven-dried, the samples were crushed into pieces in a porcelain mortar, and then sieved by 0.5 mm mesh to remove large pieces of soil organic matter. The amount of total organic carbon (hereinafter referred to as TOC) contained in the prepared soil samples were quantified by the C/N corder method after acid treatment. The chemical analysis was entrusted to the Geo-Science Laboratory Co. Ltd. The TOC quantified as gravimetric percentage was converted to the mass of carbon per unit volume of bulk soil by multiplied by the dry bulk density of the soil samples.

The results of the analysis are shown in Figure 3.9. The samples of the soil were gathered every 20 cm depth, and the samples ranged from the ground surface to 140 cm of the forest, and to 120 cm of the grassland, were served for the analysis.

At the forest site, the largest content of TOC was found near the ground surface. An average amount of TOC between depths of 0 and 20 cm was 1.93×10^{-2} gC·cm^{-3} soil. The content of TOC decreased with depth from the ground surface to depths between 40 and 60 cm, in which the TOC was 0.48×10^{-2} gC·cm^{-3} soil. Below 60 cm, although slightly large content of TOC was observed between depths of 80 and 100 cm, the content of TOC was kept less than 1.0×10^{-2} gC·cm^{-3} soil.

At the grassland site, a relatively high TOC content of 1.22×10^{-2} gC·cm^{-3} soil was found between the ground surface and a depth of 20 cm. Between 20 and 40 cm, where the old subsoil and the dressed clay layer were present (Table 2.1), the TOC decreased to 0.88×10^{-2} gC·cm^{-3} soil. The content of TOC between depths of 40 and 60 cm, in which the old surface soil was lain, however, increased rapidly and reached the maximum value of 2.60×10^{-2} gC·cm^{-3} soil. At these depths, the old surface soil was more or less consolidated and the old soil organic matter probably had not been highly decomposed, so that such a content of TOC higher than the content in the surface soil of the forest was observed. Below 60 cm, the content of TOC was relatively low, similar to the content at the same depths of the forest.

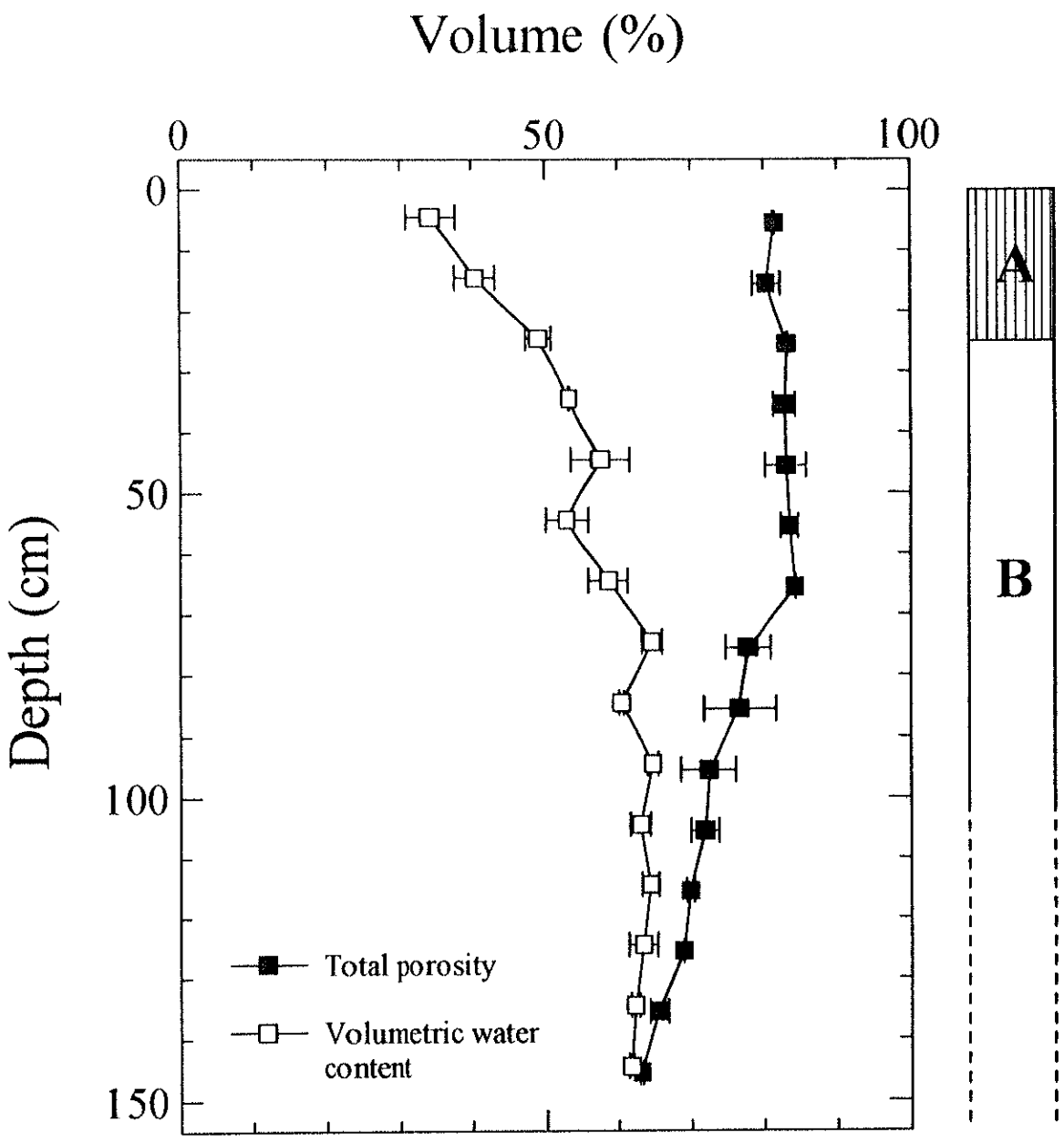

Figure 3.1. Profiles of the three-phase distribution of the soil and the soil horizon at the forest site.

Error bars show the minimum and the maximum values at each depth.

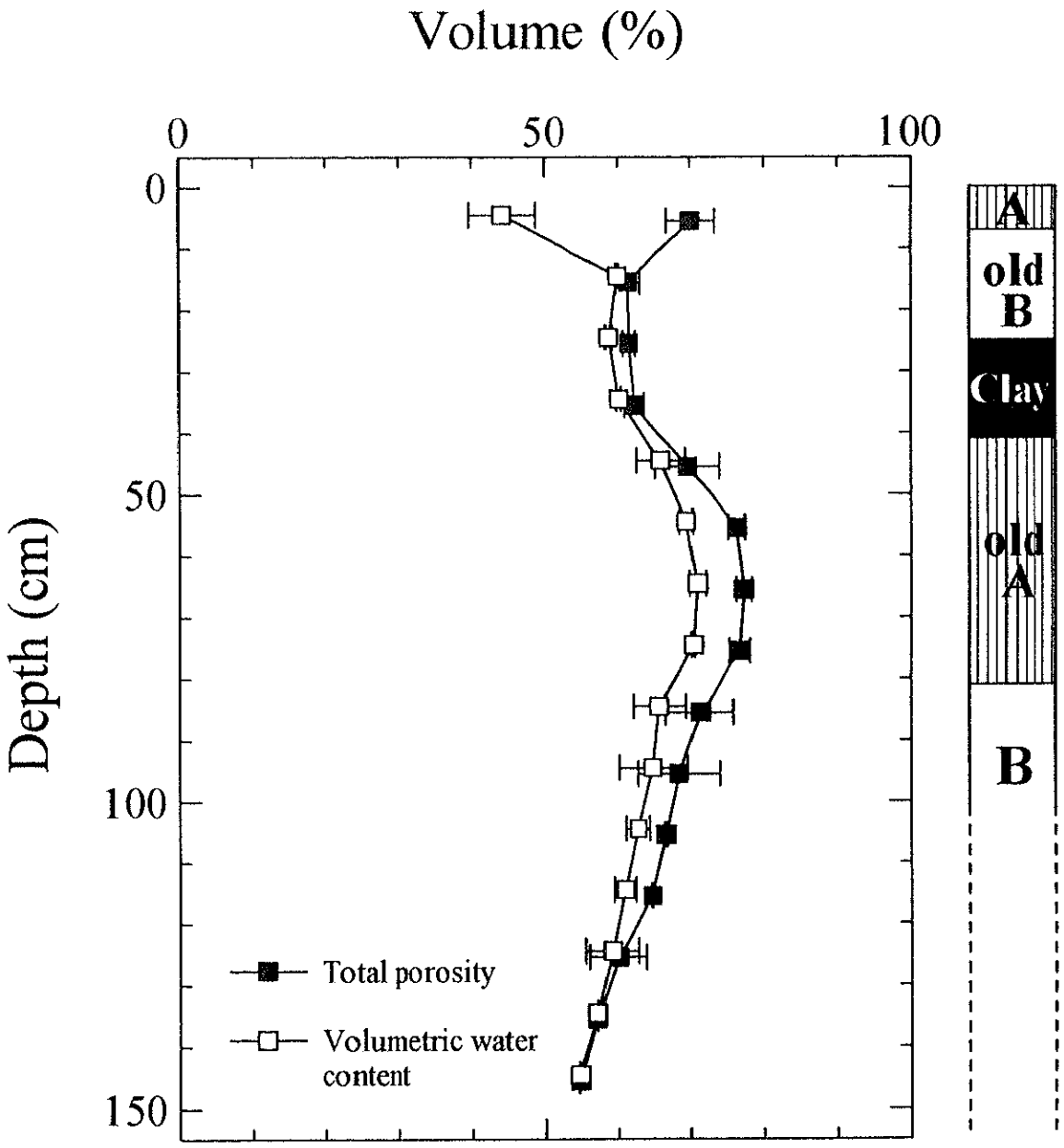

Figure 3.2. Profiles of the three-phase distribution of the soil and the soil horizon at the grassland site.

Error bars show the minimum and the maximum values at each depth.

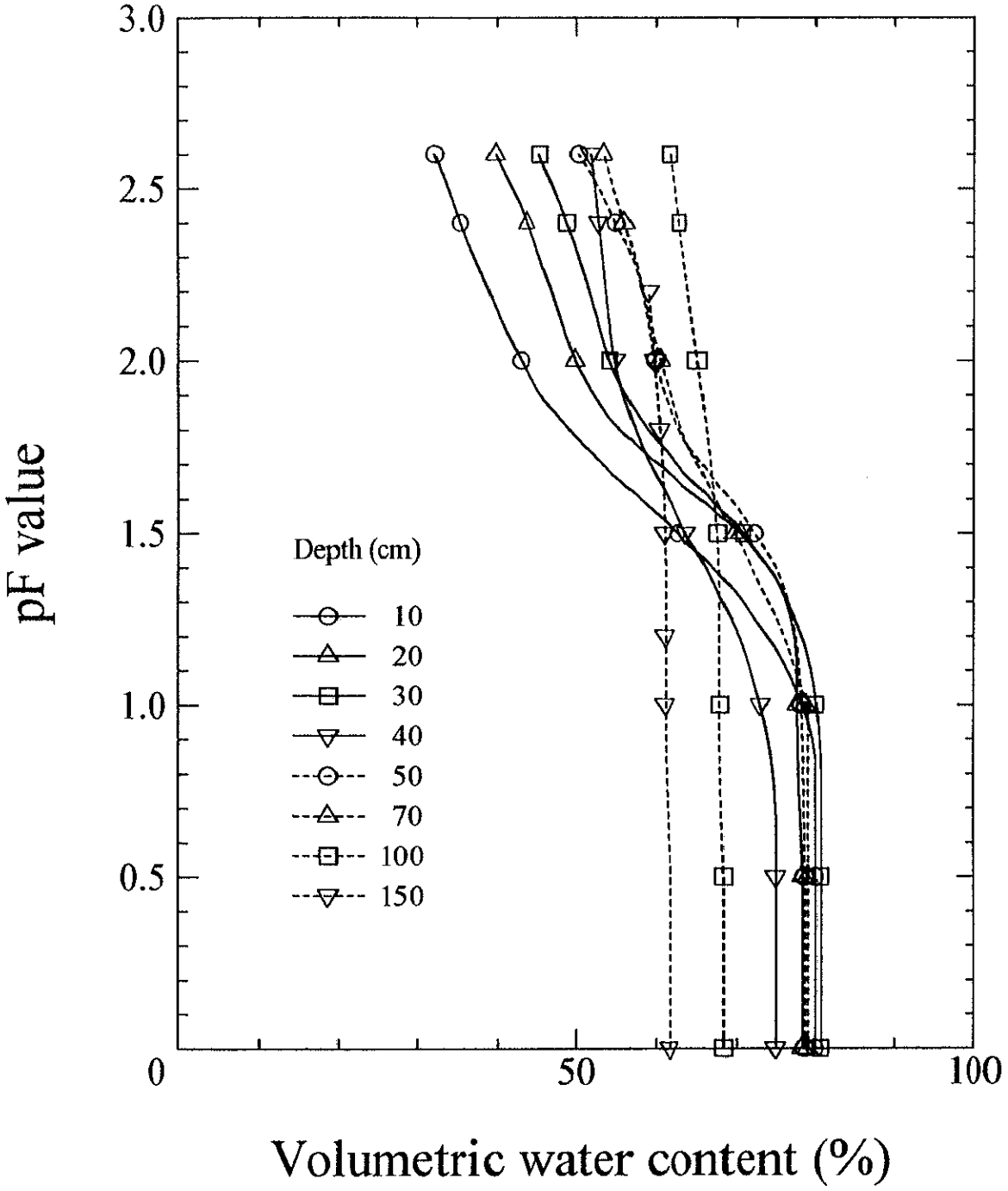

Figure 3.3. Soil water characteristic curves for each depth at the forest site.

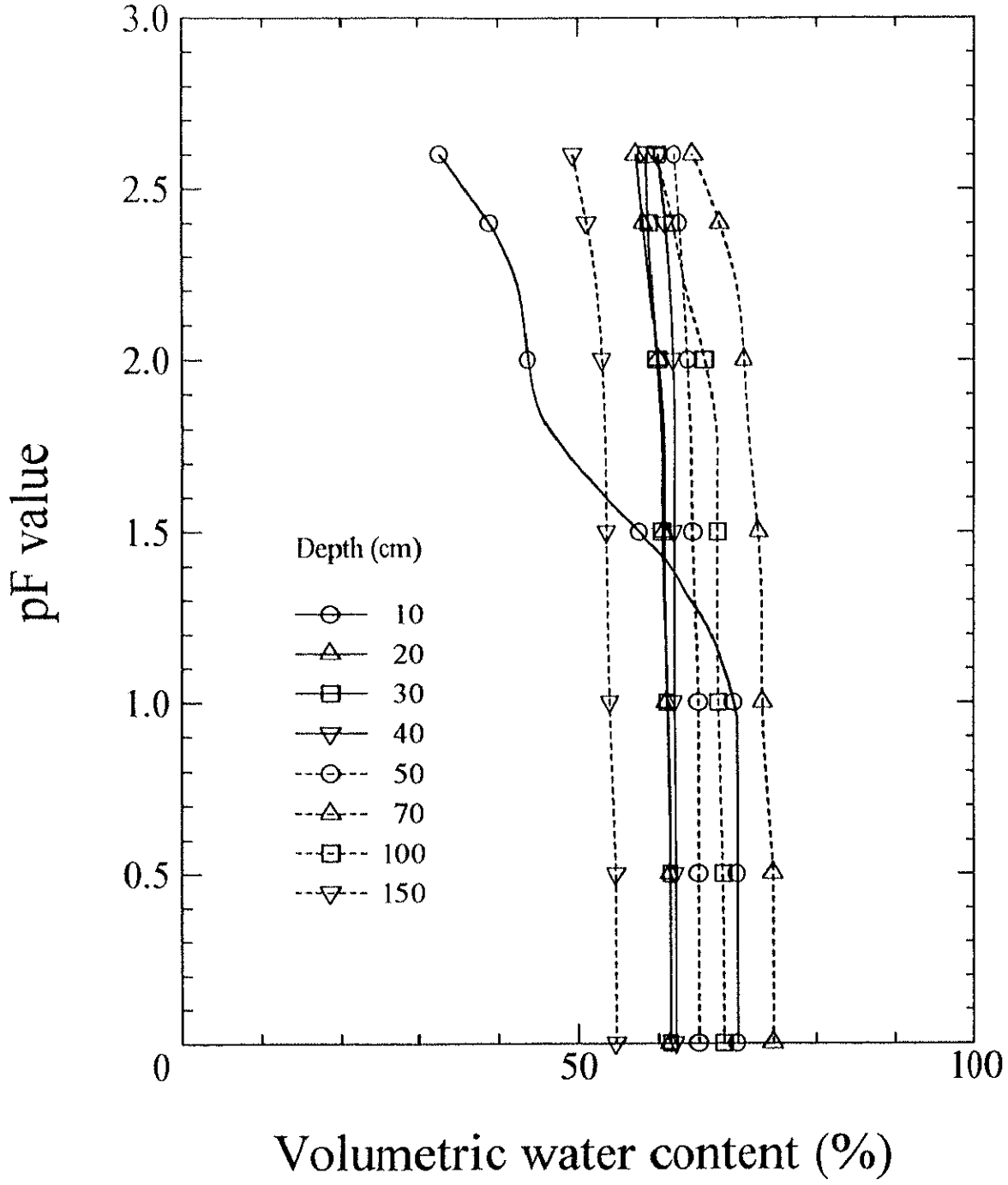

Figure 3.4. Soil water characteristic curves for each depth at the grassland site.

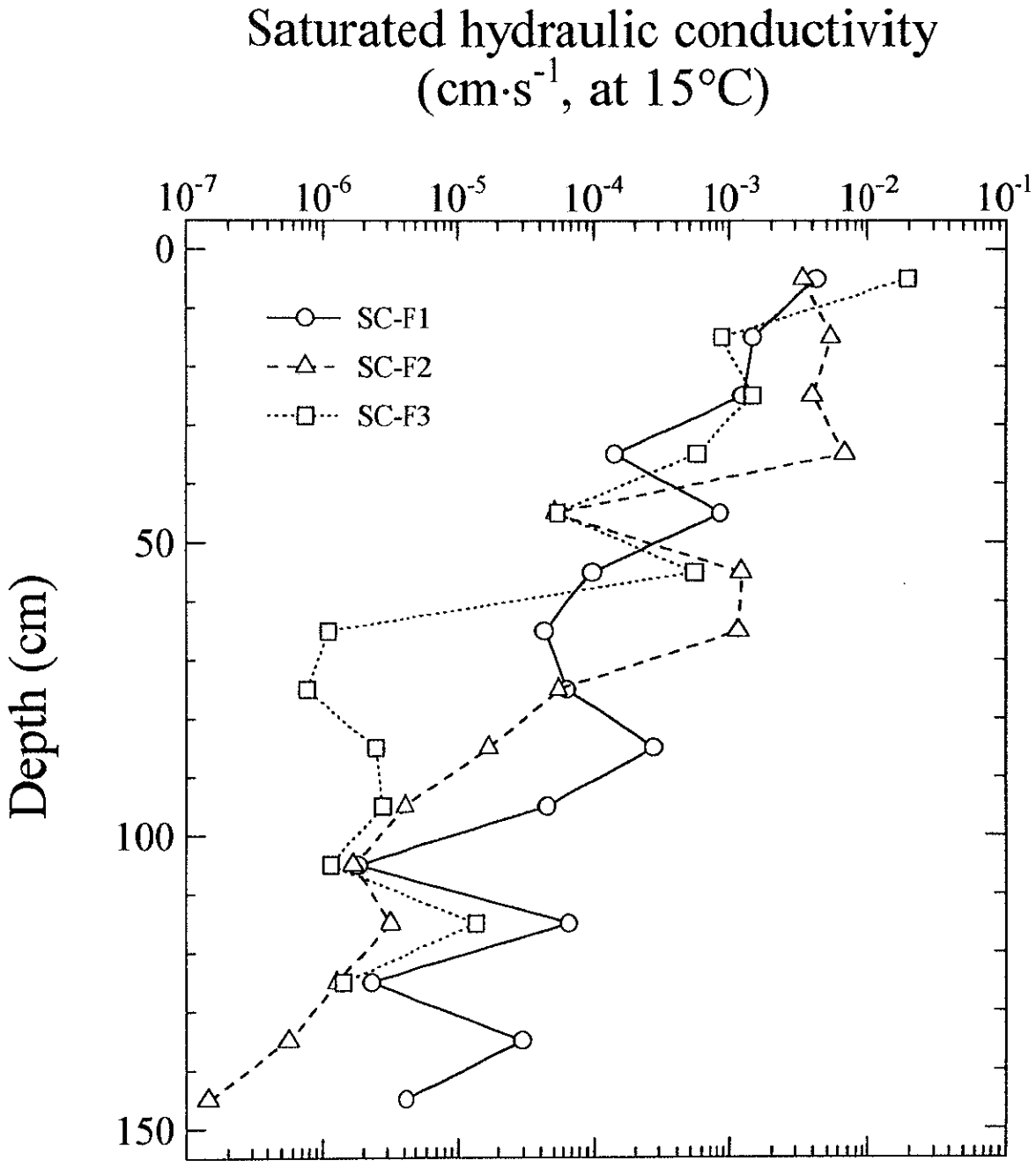

Figure 3.5. Profiles of saturated hydraulic conductivity at the forest site.

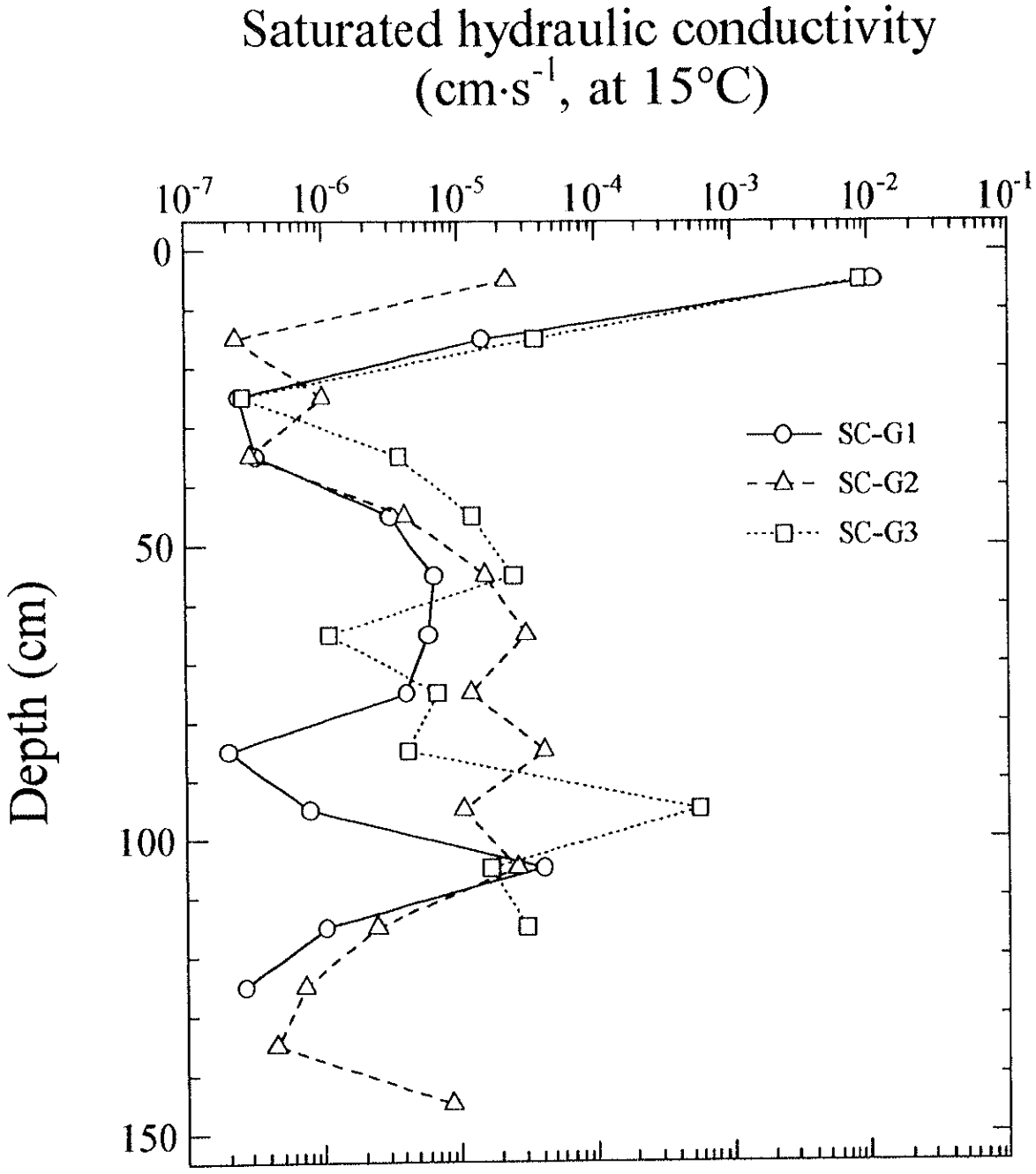

Figure 3.6. Profiles of saturated hydraulic conductivity at the grass-land site.

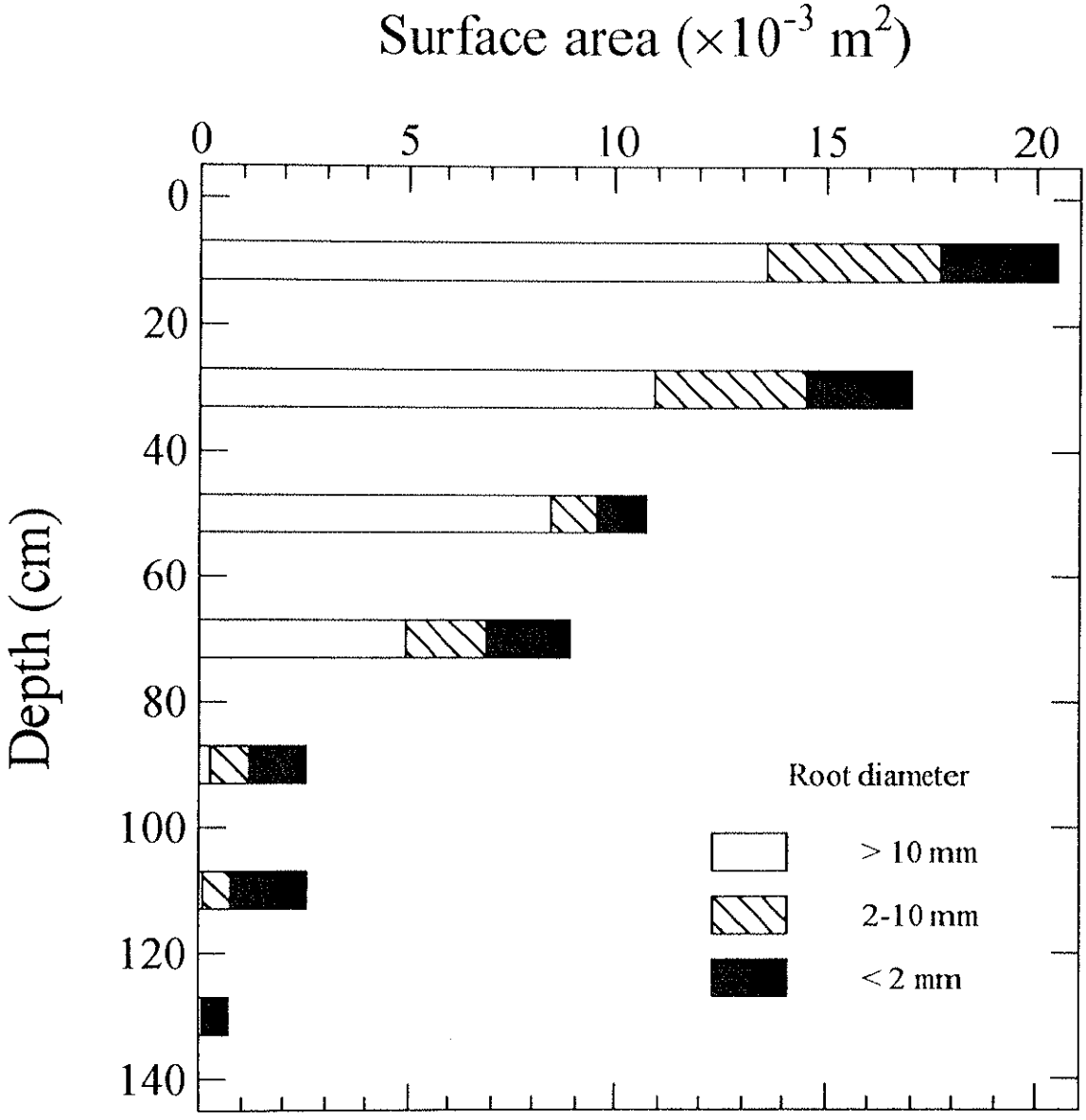

Figure 3.7. Profile of the surface area of plant roots in the Red Pine forest (cited from Sugita et al., 1986).

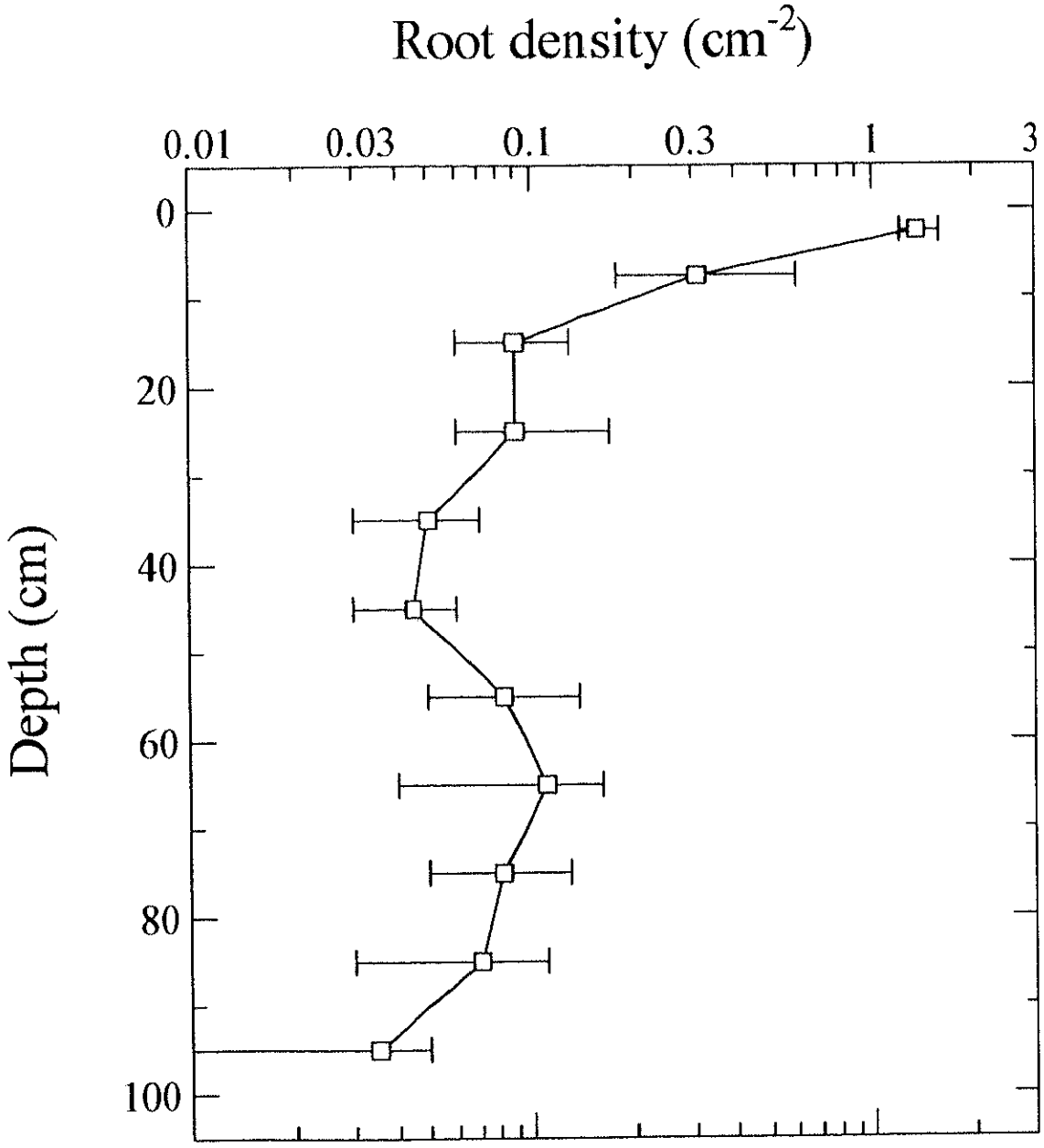

Figure 3.8. Profile of the number of plant roots per unit area of the soil cross section at the grassland site.

Error bars show the minimum and the maximum values at each depth.

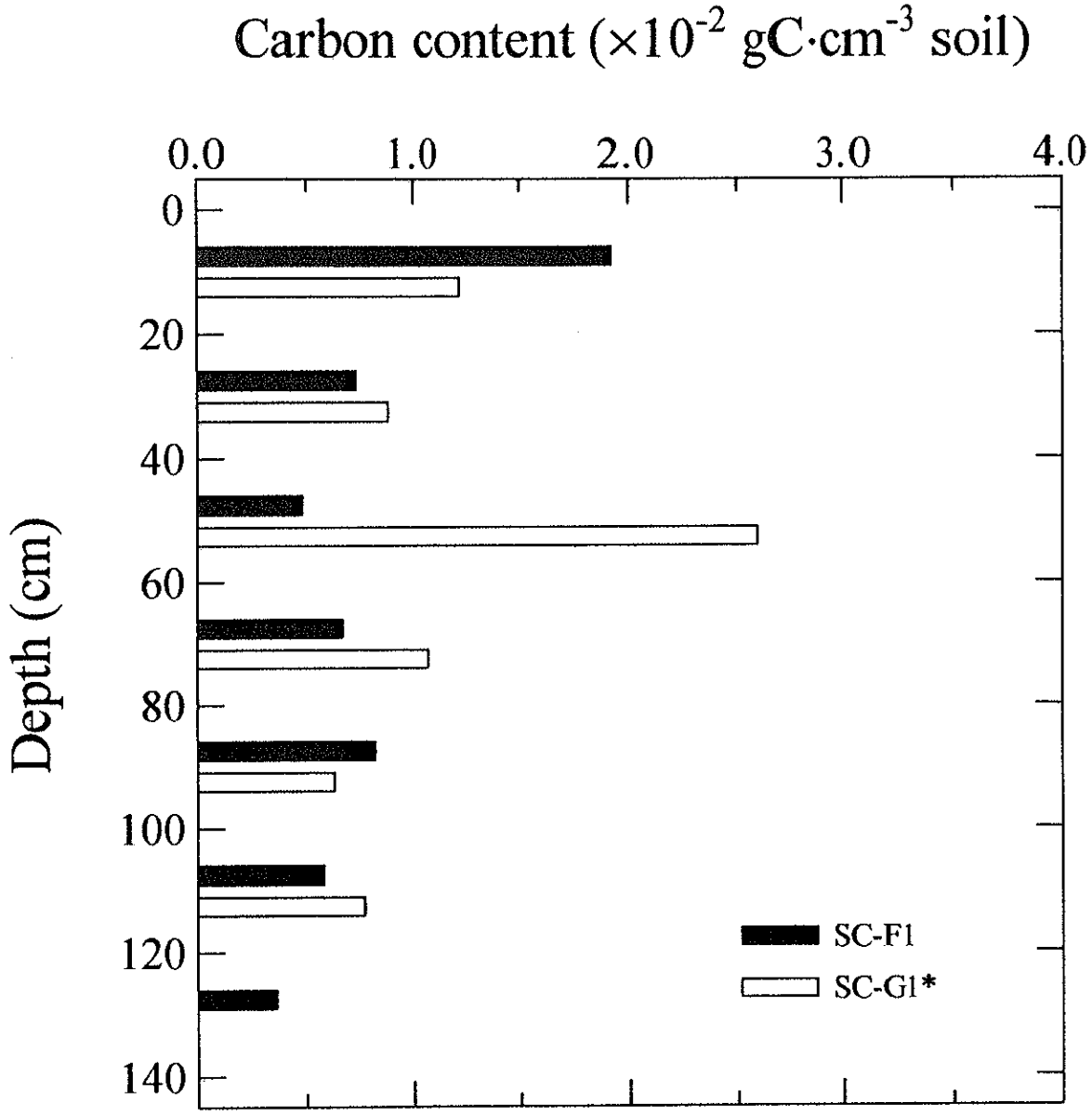

Figure 3.9. Profiles of the content of total organic carbon (TOC) in bulk soil at the forest and the grassland site.

* The datum of SC-G1 between depths of 120 and 140 cm is missing.

Chapter 4

Temporal and Spatial Distributions of Carbon Dioxide

4.1 Observation of the concentration of carbon dioxide in soil air and the environmental factors

4.1.1 Methods

(1) Concentration of carbon dioxide in soil air

The measurement of the concentration of CO_2 in soil air was carried out at the observation sites in the Red pine forest and the adjacent grassland, for whole two years from June 1996 to May 1998. The concentration of CO_2 was measured twice a month from the spring to the autumn and once a month in the winter. At both sites, groundwater tables are usually at depths of 1.5 to 2.5 m below the ground surface except for just after heavy rain, so that a soil layer ranged from the surface to 1.5 m was regarded as the unsaturated soil zone. Therefore, CO_2 concentration in soil air was measured at the ground surface and at depths of 5, 10, 20, 30, 40, 50, 70, 100 and 150 cm.

In advance of the observation, soil air collection probes were installed at both sites. The design and arrangement of the probe are illustrated in Figure 4.1. The tip of the probe was designed with reference to Allison et al. (1987). Soil air at a depth of 10 cm or below was drawn through the probes. The probes were installed at every depth for CO_2 measurement with horizontal intervals of more than 30 cm.

Two methods were employed for the determination of CO_2 concentration. In the first half of the observation period, namely a whole year from June 1996 to May 1997, gas detection tubes were used for the determination. The gas detection tube has been commonly used for the measurement of CO_2 concentration in soil air by many researchers (e.g. Miotke, 1974; Gunn and

Trudgill, 1982; Buyanovsky and Wagner, 1983; Fernandez and Kosian, 1987; Castelle and Galloway, 1990; Zabowski and Sletten, 1991; Fernandez et al., 1993; Hamada et al., 1996; Haibara et al., 1997).

As the CO_2 detection tube, GASTEC No. 2LL (for 300-5000 ppm) and No. 2L (for 0.25-3.0%) were mainly used; for extremely high concentrations, such as observed in deep soils at the grassland site (see below), No. 2H (for 1-10%) was used. The values indicated by No. 2L and No. 2LL tubes were corrected to the real values using the following equations given by Hamada and Tanaka (1995):

$$\begin{aligned} c_{CO_2} &= 0.849\, c_{TUBE} + 0.0513 \quad (c_{TUBE} \geq 0.1) \\ c_{CO_2} &= 1.36\ \ c_{TUBE} \qquad\qquad\ \ (c_{TUBE} < 0.1) \end{aligned} \tag{4.1}$$

where c_{CO_2} and c_{TUBE} are the corrected and the measured value of CO_2 concentration (% in vol.), respectively. The relationships indicated by Equation 4.1 have been established between the concentration measured with No. 2LL tube and that determined by neutralization titration, while the values indicated by No. 2L tube have been correlated to those by No. 2LL tube (Hamada and Tanaka, 1995). The range of CO_2 concentration for No. 2H tube is much higher than that for No. 2L and No. 2LL, so that the correction was not made for the values indicated by No. 2H tube.

In principle, the measurement was carried out according to the procedure presented by Hamada and Tanaka (1995). For a depth of 5 cm, where the soil air collection probe was not installed, the gas detection tube was penetrated to the depth and the soil air was drawn directly. The values of CO_2 concentration determined by the tubes were recorded in situ. Using this method, soil air must be extracted by 50 ml for the pre-extraction of resident air in the collection probe, and by 100 ml for the measurement of CO_2.

On the other hand, in the second half of the observation period, namely a whole year from June 1997 to May 1998, gas chromatography (hereinafter referred to as GC) was used for the determination of CO_2 concentration. The GC, as well as the gas detection tube, has been applied to the determination of CO_2 concentration in soil air in previous studies (e.g. De Jong and Schappert, 1972; Kiefer, 1990; Hendry et al., 1993; Wood et al., 1993). In contrast to the gas detection tube, GC cannot determine the concentration in situ, so that sampled soil air must be

brought back to the laboratory without mixing with the ambient air.

For the sampling and transportation of soil air, gas sampling glass tubes equipped with a vacuum valve and a rubber septum were designed. The designs of the glass tubes are illustrated in Figure 4.2. For the gas sampling, T-type (about 8.5 ml cap.) and L-type (about 16 ml cap.) of the glass tubes were used. Soil air was extracted by 15-25 ml through the collection probe into a plastic syringe equipped with an injection needle, after the resident air in the collection probe was drawn by about 10 ml. For a depth of 5 cm, an injection needle 5-cm long was penetrated to the depth, as the gas detection tube was done so, and then soil air was collected directly. The soil air collected in the syringe was immediately sampled into the glass tube, which had been evacuated previously, through its rubber septum. Between the septum and the vacuum valve, there is a dead volume that cannot be evacuated, but the volume is a hundred times smaller than the capacity of the T-type tube, hence the effect of the dead volume can be negligible. After sampling, the vacuum valve was turned off, and the sampled soil air was brought back to the laboratory for the determination of CO_2 concentration by GC.

For the determination of CO_2 concentration of the sample gas, GC-14B (Shimazu, Co. Ltd.), a GC system equipped with a thermal conductivity detector (hereinafter referred to as TCD) was employed. Helium was served as a carrier gas after dried and purified by passing through a short stainless steel column packed with Molecular Sieve 5A. A stainless steel column which has 3 mm i.d., 4 mm o.d. and 4-m-length and is full of Porapaq Q (50-80 mesh) as an adsorbent was used for separating CO_2 from other gases. The sample gas was measured out accurately by 1 ml from the glass tube using a gastight syringe, and then injected into the column through an injection port. The column was connected to the TCD, where CO_2 was detected by the change in voltage applied to a filament that was incorporated in the TCD. The change in voltage was indicated as peak-shaped on a recording chart. During the analysis, the temperature of the column was kept constant at 80°C in a thermostatic oven. The temperatures of TCD and the injection port were set at 150°C, and the current of the filament at 200 mA.

After the analysis, CO_2 concentration of the sample gas was determined by comparing its peak area with the areas for reference gases, which have known concentrations of CO_2; 0.1, 1.0 and 10% in vol. Reproducibility of duplicate gas analyses was about 0.5%.

For a comparison of the two methods, CO_2 concentrations in soil air at both sites were measured simultaneously by both methods. The procedure of the experiment was as follows:

First, the gas sample for GC was collected (hereinafter referred to as GC-1); second, the measurement of CO_2 using the gas detection tubes was carried out (as TUBE); third, the gas sample for GC was collected again (as GC-2). The concentration of CO_2 in soil air determined by both methods and the relationship between them were shown in Figures 4.3 and 4.4. In this section, CO_2 concentration is expressed as a percentage in volume.

For the measurement of CO_2 concentration in soil air, it is necessary for the gas detection tube to draw much more soil air than for GC. Therefore, it has been suggested that the compositions of soil air sampled by both methods are more or less different (Hamada and Tanaka, 1995). In fact, many of the measured values of GC-2 were smaller than those of GC-1. This suggests that the extraction of soil air by the gas detection tubes after the sampling for GC-1 might cause the inflow of soil air from other depths, mainly from the upper soil layer which would have lower CO_2 concentrations. Fortunately, little difference was found between GC-1 and TUBE, so that it was concluded that the difference in measured values due to the difference in methods was negligible for a single sampling for each depth.

(2) Environmental factors

In the same period for the measurement of CO_2 concentration, several related environmental factors were also observed at the forest and the grassland site.

At the forest site, air temperature and soil temperatures at several depths were automatically measured every two hours with platinum resistance thermometers and then recorded by a data-logging system. The soil temperatures were measured at depths of 5, 10, 20, 30, 50, 70, 100 and 225 cm. Actually, soil temperature at 225 cm was measured at the bottom of an observation well, where the level of groundwater was measured manually. On the other hand, at the grassland site, the heat balance and water balance observation system managed by ERC observes many micrometeorological factors every an hour. Selected data for this study were as follows: Air temperature at a height of 1.6 m; all the soil temperatures, namely at depths of 2, 10, 50 and 100 cm; groundwater level below the ground surface recorded at a 2.2-m-depth well; precipitation.

In addition, the potential of soil water was observed at both sites. Tensiometers equipped with a pressure sensor were installed at several depths, and the pressure head of soil water was automatically measured every thirty minutes. From June to November in 1996, the pressure heads were measured at depths of 10, 20, 30, 50, 70 and 100 cm by KADEC-UN system (Kona

System Co. Ltd.); after May 1997, at depths of 10, 20, 30, 40, 50, 70, 100 and 150 cm by UNSUC SK-5608D (Sankei Rika Co. Ltd.).

The depths for the measurement of CO_2 concentration in soil air and the environmental factors at both sites are summarized in Figure 4.5.

4.1.2 Results and discussion

(1) Seasonal variation of the environmental factors

Seasonal variations of monthly-mean air temperature, monthly precipitation and the groundwater levels at the forest and grassland sites are shown in Figure 4.6. The groundwater levels are plotted as the depths from the ground surface. Seasonal variations of soil temperature and the pressure head of soil water at the forest and the grassland site are also shown in Figures 4.7 and 4.8, respectively.

The air temperature averaged for the observation period is 12.1°C at the forest site and 13.8°C at the grassland site. In monthly-mean basis, air temperature at the grassland was always higher than that at the forest and the difference was usually more than 1°C, and reached up to 2.3°C in August 1997. At both sites, air temperature was at maximum in August and at minimum in January, and the ranges of the seasonal variation were 22-23°C.

On the soil temperature, the ranges of seasonal variation became narrower and the phases of the variation were increasingly delayed with depth. In annual-mean basis, however, soil temperatures were not so different among the depths and ranged from 12.5 to 13.1°C at the forest, and 14.5 to 15.7°C at the grassland, respectively. At both sites, soil temperatures averaged for each depth were about 1°C higher than the averaged air temperature, and like air temperature, soil temperatures at the grassland were about 2°C higher than those at the same depth of the forest. Soil temperatures at the grassland varied more widely than those at the forest, especially in deep soils. Comparing the soil temperatures at the same depth, the ranges of seasonal variation at depths of 10, 50 and 100 cm at the forest were about 21, 13 and 7°C, respectively; at the grassland were about 21, 16 and 11°C, respectively. There was no difference in the phases of the seasonal variation of soil temperature between both sites.

Total precipitation observed in the whole two years was 2308.3 mm, which included several days of missing measurement. The maximum daily precipitation was 172.7 mm and measured on September 22, 1996. The depths of the groundwater tables ranged from 1.5 to 2.0 m except

under extremely wet or dry conditions at both sites. The groundwater level averaged for the observation period was 1.796 m from the ground surface at the grassland site.

Patterns of the precipitation were quite different among seasons and years, so that the groundwater levels varied largely corresponding to the patterns. In the summer of 1996, it was extremely dry and only 0.6-mm rainfall was observed from August 1 to 27. Therefore, the groundwater tables increasingly lowered; at the grassland site, the depth of the groundwater table became lower than the depth of the observation well, thus the well was temporarily dried up. Some rainfall was observed in the late August, but the groundwater levels did not recover until September 22 when the maximum daily rainfall was observed. In contrast, in the October and November, rainfall was not so much but periodic, and the groundwater tables were kept relatively high.

In August 1997, in contrast to 1996, total precipitation reached 34.2 mm and no rainless period lasting more than seven days was observed, therefore the depressions of the groundwater tables were small. In the September, however, lack of such a heavy rain that observed on September 22, 1996 prevented the levels from recovering enough. In October and November 1997, also in contrast to 1996, less precipitation was observed; for example, only 3.2-mm rainfall was received from October 8 to November 12. In this period, the groundwater tables were depressed to the depths lower than those in the summer of the year due to the little rainfall as well as the small recovery of the levels in the September. In January 1998, heavy snowfall was observed for three times and the percolation of snowmelt water rapidly raised the groundwater table at the grassland site and rapidly decreased soil temperatures at both sites. A large amount of precipitation and relatively high groundwater levels were observed in April and May 1998.

Overall, the pressure head of soil water varied in response to the pattern of precipitation. In August 1996 and in October and November 1997, prolonged rainless period decreased the pressure heads down to –800 to –900 cmH_2O. In the summer of 1997, the depression in pressure head was smaller than that in the summer of 1996 because the rainless periods were relatively short. While in the autumn of 1996 and in the spring of 1998, the pressure heads showed larger values corresponding to the wet conditions. Especially when the groundwater table was at a depth above 150 cm, the pressure head at 150 cm showed a positive value.

In detail, however, several differences are found in the seasonal variations of the pressure head between both sites. In dry periods, the decrease in pressure head gradually progressed

toward deep soils at the forest; at the grassland, the pressure heads rapidly dropped at depths of 10 and 20 cm, whereas slowly decreased below the depths. This was typically observed in the autumn of 1997. The difference in vegetation between both sites, particularly in the distribution of plant roots might cause the discrepancy. At the forest site, the Red Pines and other tree species extend their roots into deep soils (Figure 3.7), so that pressure heads at the deep soils would decrease in response to soil water uptake by the roots. On the other hand, the roots of the grass are concentrated near the ground surface (Figure 3.8), therefore rapid decrease in the pressure head would be also limited within shallow soils at the grassland site. In the autumn of 1997, moreover, most of the grass had already withered in contrast to Red Pine, an evergreen conifer, and this might cause the larger difference between both sites.

(2) Seasonal variation of the concentration of carbon dioxide in soil air

The seasonal variation of CO_2 concentration in soil air at the forest site is shown in Figure 4.9. The concentration of CO_2 in soil air was always higher than that at the ground surface (about 0.05% in vol.) and showed more than 0.1% except at depths of 5 and 10 cm in winter months. The maximum of the concentration was 1.26% and observed at 100 cm in early August of 1997. The ranges of the seasonal variation of CO_2 concentration increased with depth; about 0.2% at depths of 5 and 10 cm, 0.3% at 20 to 50 cm, and more than 0.5% at 70 to 150 cm.

As a whole, CO_2 concentration in soil air increased from spring to summer and decreased from autumn to winter at all the depths, similar to the seasonal variation of soil temperature (Figure 4.7). In 1996, CO_2 concentration at depths of 5 to 50 cm began to rise in early June and peaked in mid-July. Although the concentrations decreased temporarily in the severely dry summer of 1996, they rose again in the late September and formed the second peaks that were lower than the first peaks. Then CO_2 concentrations began to fall again and were kept decreasing until the minimum values were observed in early February of 1997.

In the relatively moist summer of 1997, the variations of CO_2 concentration were relatively small except the temporarily high concentrations measured in the late June and the early August, and the concentrations at depths of 5 to 30 cm never exceeded those at the first peak in the summer of 1996. From October 1997 to January 1998, CO_2 concentrations decreased linearly and no second peak such as formed in 1996 was observed. In 1998, CO_2 concentration rapidly increased from March to May, especially in April when extremely wet conditions were observed.

The concentrations of CO_2 in soil air at depths of 70 to 150 cm also showed seasonal trends similar to those at 5 to 50 cm. Except for a depth of 150 cm, at which CO_2 measurement was often prevented by its nearly saturated condition, the maximum in the summer of 1996 and the minimum in the winter of 1997 were found a half or a whole month later than those in the above depths. In the summer of 1997, CO_2 concentrations kept increasing from June to July, and in August and September, they reached their maxima higher than those in 1996.

The seasonal variation of CO_2 concentration in soil air at the grassland site is shown in Figure 4.10. The concentrations of CO_2 at the grassland were almost always much higher than those at the forest, particularly in deep soils. The concentrations averaged for each depth at the grassland were 1.4 to 1.9 times as high as those at the forest at depths of 5 to 40 cm, whereas 4.4 to 8.3 times at 50 to 150 cm. The maximum of the measured concentrations was 9.89% at a depth of 70 cm in early September of 1997. The ranges of the seasonal variation of CO_2 concentration were also much larger; 0.5-1.3% at depths of 5 and 40 cm and 3-7% at 50 to 100 cm.

In spite of the difference in the magnitude of CO_2 concentration between both sites, the seasonal trend of the variation of the concentration at the grassland was similar to the trend at the forest. In 1996, CO_2 concentration at depths of 5 to 40 cm began to rise in early June and peaked in mid-July. Although the concentrations temporarily decreased after that, they rose again earlier than at the forest site and formed the second peaks in the early September. At this time, CO_2 concentrations at depths of 30 and 40 cm exceeded the concentrations observed in the mid-July and the concentration at 50 cm also increased rapidly. Then CO_2 concentrations decreased again until early February of 1997, except temporarily high values observed in October 1996.

In the summer of 1997, the variation of CO_2 concentration was relatively small from July to September. In the late June, when temporarily high concentrations of CO_2 were measured at the forest site, small peaks of the concentration were observed at depths of 10 and 20 cm, and the concentrations at 10 to 40 cm in the early August were heightened relative to the before and the after measurement. While in the mid-August, unlike at the forest site, a temporarily decrease in CO_2 concentration was observed at depths of 10 to 50 cm, and then maximum concentrations in 1997 were found at 20 to 50 cm in the September. Except for depths of 5 and 10 cm, CO_2 concentrations in the summer of 1997 were generally higher than those in the summer of 1996, also unlike at the forest site. After that, CO_2 concentrations decreased until January to March in 1998, then increased again.

The concentrations of CO_2 in soil air at depths of 70 to 150 cm also showed seasonal trends similar to the trends at the forest site. In the summer of 1996, CO_2 concentrations at depths of 70 and 100 cm reached their maximum in July to August. In the early September when the second peaks were observed at the above depths, the concentrations kept decreasing and increased temporarily in the October after a rapid rise of the groundwater table by which CO_2 measurement in deep soils was prevented. In 1997, CO_2 concentrations rose linearly from May to September and reached the maximum, nearly 10% at a depth of 70 cm. The concentration of CO_2 at a depth of 150 cm, where only a few measurements were carried out because of its nearly saturated condition, was also at the maximum in this period.

As described above, the concentration of CO_2 in soil air clearly showed a seasonal variation at all the depths at both sites. Much of the variation seems to be related to the variations of the environmental factors, especially soil temperature. Therefore, it is not surprising that the relationship between CO_2 concentration in soil air and soil temperature has been discussed in previous studies (e.g. Gunn and Trudgill, 1982; Buyanovsky and Wagner, 1983; Fernandez and Kosian, 1987; Castelle and Galloway, 1990; Hamada and Tanaka, 1997).

In spite of many studies, the relationships between CO_2 concentration and the environmental factors are essentially indirect, empirical and site specific, because the concentration is determined by two different processes; production and transport of CO_2. For example, the temporary decrease in CO_2 concentration in dry summer may be due to the reduction of CO_2 production caused by the inhibition of biological activities, but also may be due to the increase in CO_2 transport into the atmosphere by molecular diffusion. To understand the processes of determining the concentration of CO_2, investigations on the process of the production and transport of CO_2 are needed.

(3) Profiles of the concentration of carbon dioxide in soil air

The profiles of the concentration of CO_2 in soil air at the forest site in 1996, 1997 and 1998 are shown in Figures 4.11a, b and c, respectively; at the grassland site in Figures 4.12a, b and c, respectively. The seasonal variations of the concentration gradient of CO_2 between adjacent depths at both sites are also indicated in Figures 4.13 and 4.14. The upward gradients are shown in positive values. At both sites, CO_2 concentration was lowest near the ground surface and generally increased with depth. Such shapes of the profiles at each observation site were kept

almost constant throughout the observation period.

At the forest site, CO_2 concentration in soil air rose largely from the ground surface to a depth of 10 cm. The seasonal variations of the concentration gradient were also large in these depths, especially in the summer of 1997 and in the spring of 1998. At depths of 10 to 40 cm, the concentration increased gradually and uniformly with depth and the seasonal variations of the gradient were relatively small.

Between depths of 40 and 50 cm, however, little or even inverse gradients were found in most of the profiles. Below these depths, CO_2 concentration rapidly increased from 50 to 100 cm, and then decreased from 100 to 150 cm. Most of the maximum gradients in the profile were found between depths of 50 and 70 cm and the seasonal variation of the gradient was unclear below these depths. The maximum concentration of CO_2 in the profile was always observed at 100 cm.

For the Red Pine forest, Uchida (1995) has also observed the seasonal and vertical distributions of CO_2 concentration in soil air. According to his results, CO_2 concentration was also lowest near the ground surface and generally increased with depth up to 0.3-0.7% at a depth of 100 cm. In addition, little upward gradient or even downward gradients of CO_2 concentration, similar to the gradients obtained between depths of 40 and 50 cm in this study, were also observed between 20 and 40 cm. Therefore, it was suggested that such gradients were a common trend in the soil profiles of the Red Pine forest, rather than site specific profiles within the forest.

The profiles of CO_2 concentration in soil air at the grassland site were quite different from those at the forest site. The concentration of CO_2 gradually increased from the ground surface to a depth of 40 cm. In these depths, relatively large concentration gradients were found in summer but did not exceed $0.1\%\cdot cm^{-1}$. From 40 to 50 cm, CO_2 concentration sharply rose; because of the large difference in the concentrations between these depths, the concentration gradient between them varied mainly corresponding to the variation of the concentration at 50 cm.

The concentration of CO_2 jumped up to the maximum in the profile at a depth of 70 cm. Consequently, the concentration gradient between depths of 50 and 70 cm was largest in the profile and the difference in the concentrations between the depths was at least 2% and more than 6% at maximum. Below a depth of 70 cm, CO_2 concentrations gradually decreased and the seasonal variations of the gradient were small.

Nevertheless both plant roots and soil organic carbon, the major sources of CO_2 in a soil, concentrated near the ground surface (Figures 3.7 to 3.9), CO_2 concentration in soil air was

lowest around the surface and increased with depth. That is, CO_2 concentration at a certain depth cannot be determined directly by the rate of CO_2 production at the depth, because CO_2 transport into or out of the depth will occur. In the formation of the profile of CO_2 concentration, the transport of CO_2 among the depths is important.

4.2 Evaluation of the concentration of dissolved carbon dioxide in soil water

4.2.1 Methods

(1) Calculation of the concentration of dissolved carbon dioxide in soil water

In general, CO_2 in liquid phase (CO_2 (aq)) is in equilibrium with CO_2 in gaseous phase (CO_2 (g)):

$$CO_2\,(g) \leftrightarrow CO_2\,(aq)$$

A part of the CO_2 in liquid phase hydrates with the water to form carbonic acid:

$$CO_2\,(aq) + H_2O \leftrightarrow H_2CO_3$$

Some portion of the carbonic acid dissociate into bicarbonate ions, and then into carbonate ions:

$$H_2CO_3 \leftrightarrow HCO_3^- + H^+, \quad HCO_3^- \leftrightarrow CO_3^{2-} + H^+$$

Thus carbonate species dissolved in soil water consist of dissolved carbon dioxide (CO_2 (aq)), carbonic acid (H_2CO_3), bicarbonate ions (HCO_3^-) and carbonate ions (CO_3^{2-}). The dissolved carbon dioxide means only CO_2 (aq) in a narrow sense; in this study it represents all the carbonate species listed above, namely:

$$C'_w = [H_2CO_3^*] + [HCO_3^-] + [CO_3^{2-}] \tag{4.2}$$

where C'_w and carbonate species parenthesized by brackets are the molar concentrations of dissolved CO_2 and each carbonate species ($mol \cdot dm^{-3}$) in soil water, respectively. Dissolved carbon dioxide in a narrow sense cannot be analytically distinguished from carbonic acid, so that the sum of their concentrations is shown as $[H_2CO_3^*]$.

If the molar concentrations of the species can be used instead of their activities, each term in the right side of Equation 4.2 is given as follows (Bolt and Bruggenwert, 1978):

$$\log[H_2CO_3^*] = \log p_{CO_2} - k_0 \quad (4.3)$$

$$\log[HCO_3^-] = \log p_{CO_2} - (k_0 + k_1) + \mathrm{pH} \quad (4.4)$$

$$\log[CO_3^{2-}] = \log p_{CO_2} - (k_0 + k_1 + k_2) + 2\mathrm{pH} \quad (4.5)$$

where p_{CO_2} is the partial pressure of CO_2 in soil air (atm), given by the following equation:

$$p_{CO_2} = c_{CO_2} \times P / P_0 \times 10^{-2} \quad (4.6)$$

where P and P_0 are the total pressures at the observation sites and at a standard state (hPa), respectively; therefore P/P_0 gives the atmospheric pressure at the sites in the unit of atm. In practice, a constant value of 1.0 was applied to P/P_0 because the altitude of both sites (27 m, see Chapter 2) is nearly equal to the sea level, while the total pressure in soil air usually equals the atmospheric pressure.

On the other hand, k_n is defined as follows:

$$k_0 = -\log K_H, \quad k_1 = -\log K_1, \quad k_2 = -\log K_2$$

$$K_H = \frac{[H_2CO_3^*]}{p_{CO_2}}, \quad K_1 = \frac{[H^+][HCO_3^-]}{[H_2CO_3^*]}, \quad K_2 = \frac{[H^+][CO_3^{2-}]}{[HCO_3^-]}$$

where K_H is Henry's law constant for the solubility of CO_2, and K_1 and K_2 are the first and the second acidity constant for carbonate equilibrium, respectively.

The k_n depends on temperature, therefore in this study k_n was determined as a function of soil temperature using the relationships between k_n and temperature summarized by Stumm and Morgan (1981). If in need, soil temperature was estimated by linear interpolation using the measured values. For a depth of 150 cm at the grassland site, the soil temperature at 100 cm was applied. The pH in Equations 4.4 and 4.5 is given by the value of pH in soil water and the method for the measurement is described below.

The C_w' was given by substituting Equations 4.3-4.5 into 4.2, then converted into C_w, the mass of CO_2 dissolved in a unit volume of soil water ($gCO_2 \cdot cm^{-3}$), by the following equation:

$$C_w = m_{CO_2} \cdot C_w' \times 10^{-3} \quad (4.7)$$

where m_{CO_2} is the molecular weight of CO_2, equivalent to 44.01.

(2) Measurement of pH in soil water

As described above, pH in soil water is one of the factors that determine the concentration of dissolved CO_2 in the water. At the same time, the value of pH in soil water is affected by the dissolved CO_2 concentration. Therefore, reserve pH (hereinafter referred to as RpH), the pH value eliminated the effect of the volatile compounds, mainly CO_2, was also measured in addition to pH. The comparison of pH and RpH in soil water expresses clearly the effect of the dissolution of CO_2 into soil water on its pH.

The pressure of soil water is usually lower than the atmospheric pressure, so that negative pressures must be applied to extract the water. In previous studies, due to the relatively simple installation and the negligible disturbance of the soil profile, a suction-cup method has been used widely (Grossman and Udluft, 1991). For the method, however, it is suggested to cause degassing of dissolved CO_2 and the corresponding upward shift of pH (Suarez, 1986; 1987; Grossman and Udluft, 1991). To know the real values of pH in soil water, a new method for measuring pH in soil water without CO_2 degassing was developed.

For the measurement of pH in soil water, the tensiometer that was used since May 1997 was employed. Diagram of the structure of the tensiometer and the operation of water sampling are illustrated in Figure 4.15. The tip of the tensiometer has a water pool (about 30 ml cap.), which is surrounded by a cylindrical porous ceramic wall and connected to the ground surface by two access tubes, one is used for supplying water to the pool and the other draining water from the pool. The water inside of the pool is hydraulically connected with the surrounding soil water through the ceramic wall. Except for compounds adsorbed in the wall, a sufficiently long period would change the chemical composition in the pooled water into the same as that in the surrounding soil water. In this study, it was assumed that the composition in the pooled water represents that in the soil water at the same depth and therefore the pH in soil water can be determined by the measurement of pH in the pooled water. Considering the time for the chemical equilibrium, the pH measurements were not carried out until at least a week had passed since the last supply of water to the pool.

In the normal operation, the resident air in the water pool is drawn from the water-drain valve with a syringe, and then the pool is filled with distilled water supplied through the another valve

without leaving bubbles. To collect the pooled water, the operation was performed reversely: After opening the water-drain valve, all the water in the pool was extracted from the water-supply valve. Collection of the water was carried out carefully not to form bubbles and degas dissolved CO_2. Immediately after the sampling, the pH in the water was measured using a glass-electrode pH meter. Subsequently, sampled water was shaken and aerated enough to degas the dissolved CO_2 sufficiently. After that pH of the water was measured again and recorded as the value of RpH.

In the Red Pine forest of ERC, soil water has been collected by a suction-cup method and analyzed its chemical composition in 1990. The result of the comparison of the concentrations of anions in the pooled water of the tensiometer at the forest site and those in the soil water collected in 1990 is shown in Figure 4.16. The concentrations of Cl^-, SO_4^{2-} and NO_3^- were determined by a capillary electrophoresis analyzing system. The concentrations of HCO_3^- in the soil water had been measured by titration, while the concentration in the pooled water was evaluated from Equation 4.4. The concentration of anions is plotted in the unit of equivalent concentration ($mol \cdot dm^{-1}$).

The profiles of anion concentrations in the pooled water were generally similar to those in the soil water. The Cl^- concentrations were relatively high whereas the concentrations of SO_4^{2-} and NO_3^- were low and decreased with depth. The concentrations of HCO_3^- in the soil water were lower than those in the pooled water, suggesting the CO_2 degassing during the water collection. Although the soil water had been collected in 1990 at another sites in the forest, the result of the comparison would support that the chemical composition in the pooled water sufficiently reflects that in the surrounding soil water.

According to the method mentioned above, the measurement of pH and RpH in soil water was carried out for seven times from July 1997 to June 1998 at the forest and the grassland site. Because of the less frequent measurements of pH relative to the measurement of CO_2 concentration in soil air, the pH on the date of CO_2 measurement was linearly interpolated using the last and the next measured value of pH for the second half of the CO_2 observation period. At a depth of 5 cm, where the tensiometer was not installed, the values of pH at 10 cm were applied.

On the other hand, the values of pH were not obtained for the first half of the observation period. Then, to examine whether or not the mean values of pH for each depth could be applied to the dissolved CO_2 calculation instead of the interpolated values, application of different types

of pH value to the calculation was attempted: The one is estimated by linear interpolation using measured values and seasonally variable, the other is a simply arithmetic-averaged value for each depth and kept constant during the observation period. The relationship between the concentration of dissolved CO_2 calculated using the seasonally variable pH and the constant pH is shown in Figure 4.17. As indicated in the graph, the ratio of them was almost 1:1. This suggests that the effect of the seasonal variation of pH on the dissolved CO_2 concentration is less important. Therefore, for the first half of the period for CO_2 measurement, from June 1996 to May 1997, the seasonally constant pH given by the arithmetic mean value was applied to the calculation.

4.2.2 Results and discussion

(1) pH and RpH in soil water

The seasonal variations of pH and RpH in soil water at the forest and the grassland site are shown in Figures 4.18 and 4.19, respectively. The profiles of them at both sites are also shown in Figures 4.20 and 4.21; for each depth, the arithmetic-averaged values are plotted and the maximum and the minimum values are indicated by error bars.

The pH in soil water at the forest site ranged from 5.5 to 6.5, showing weak acidity. The value of pH averaged for all the depths was 6.03. The pH in soil water showed relatively small seasonal variation. At many depths, the maximum values of pH were observed in July 1997 and the minimum values were found in October 1997 or June 1998, but the seasonal trend was unclear. In contrast, the vertical trend was apparent. The pH in soil water decreased with depth, from 6.07-6.54 at 10 cm to 5.64-6.11 at 150 cm, except for 20 cm where the pH values were kept relatively small. This trend in the profile was always found during the observation period.

The values of RpH in soil water were about a pH unit larger than those of pH and generally ranged from 6.5 to 7.5 at the forest site. The seasonal trend in RpH was not so evident as well as that in pH. The difference in RpH among the depths was small, and the RpH below 30 cm showed almost similar values of about 6.9 in the arithmetic mean, exhibiting nearly neutrality. The mean value of RpH at 20 cm was 6.49 and smallest in the profile, suggesting the effect of some acids other than CO_2 at the depth.

At the grassland, the pH in soil water was generally lower than that at the forest. For all the depths, the minimum, maximum and averaged values were 5.23, 6.80 and 5.71, respectively. At

most of the depths, the values of pH were at the minima in August 1997 and then increased up to the maxima in March 1998, but the seasonal variations were as small as those at the forest site. The values of pH in soil water increased with depth from 10 to 70 cm and decreased below the depths. The pH at a depth of 70 cm was always lowest in the profile.

The RpH in soil water ranged from 7.0 to 7.5, showing neutrality to weak alkalinity, except at a depth of 10 cm. The difference in RpH among the depths was smaller than that in pH, as well as at the forest site, and almost common values ranged from 7.1 to 7.4 were observed except at 10 cm, where some acids other than CO_2 might play a role in the determination of pH and RpH.

As mentioned previously, the difference between pH and RpH in soil water reflects the effect of CO_2 dissolution in the water. For this reason, ΔH, the difference in proton content in soil water between before and after degassing dissolved CO_2 ($mol \cdot dm^{-3}$) was defined as:

$$\Delta H = 10^{-pH} - 10^{-RpH} \tag{4.8}$$

All the measured profiles of ΔH at the forest and the grassland site are plotted in Figures 4.22 and 4.23, respectively.

Except for a depth of 20 cm, ΔH at the forest site increased with depth, corresponding to the profiles of CO_2 concentration in soil air (Figure 4.11). The large values of ΔH at 20 cm, reached 2.32×10^{-6} $mol \cdot dm^{-3}$ at the maximum, implies the presence of some volatile acids except CO_2, such as some kind of organic acids. The ΔH also showed the following clear seasonal variation: The ΔH increased from July to October in 1997, after that decreased until March 1998, and then increased again.

At the grassland, ΔH was generally higher than at the forest, and the shapes of the profile were quite similar to those of CO_2 concentration in soil air at the site (Figure 4.12). The values of ΔH increased with depth from 10 to 70 cm, and then decreased with depth. As well as CO_2 concentration at the depth, ΔH at 70 cm was always highest in the profile and reached 5.80×10^{-6} $mol \cdot dm^{-3}$ at the maximum. At the most of the depths, ΔH was at maximum in August or September in 1997 and at minimum in March 1998, and the ranges of the seasonal variation were relatively large.

The good agreement on the shapes of the profile between ΔH and CO_2 concentration in soil air observed at both sites indicates the importance of CO_2 dissolution on the determination of pH

in soil water. Because of the small fluctuation in RpH in the profile, the difference in pH among the depths depends mainly on the difference in CO_2 concentration. On the other hand, the seasonal variations of ΔH did not completely correspond to those of CO_2 concentration, partly this might be caused by temperature dependence of the measured values of pH. Between both sites, the larger values of ΔH were observed at the grassland where CO_2 concentration was also much higher than at the forest, suggesting the larger effect on pH in soil water due to the higher CO_2 concentrations. Paradoxically, these results would prove that the values of pH and RpH obtained in this study reflect the real values in soil water rather well.

(2) Concentration of dissolved carbon dioxide in soil water

The seasonal variations of dissolved CO_2 concentration in soil water at the forest and the grassland site are shown in Figures 4.24 and 4.25, respectively. Overall, dissolved CO_2 concentration varied seasonally and vertically in response to the variations of CO_2 concentration in soil air.

At the forest site, dissolved CO_2 concentration was at maximum in August 1996 and June 1997, and at minimum in February 1997 and March 1998. At all the depths, the Max/Min values, defined as the ratios of the maximum value to the minimum value observed at each depth or in each profile, were about two, slightly smaller than the ratios in CO_2 concentration in soil air ranged from two to three. The peaks of dissolved CO_2 concentration in June 1997 did not coincide with those of the concentration in soil air (Figure 4.9). This was due to the relatively high pH in this period (Figure 4.18), because high pH in soil water promotes the dissociation of carbonic acid and the corresponding generation of bicarbonate ions in the water.

The difference in dissolved CO_2 concentration among the depths was similar to that in CO_2 concentration in soil air except at a depth of 20 cm, where the dissolved CO_2 concentration was generally less than that at 10 cm because of the low pH values. The profile of pH decreasing with depths (Figure 4.20) also influenced the concentrations of dissolved CO_2 at another depths: Although CO_2 concentration in soil air at a depth of 50 cm was similar to that at 40 cm (Figure 4.11), dissolved CO_2 concentration at the former was lower than that at the latter. Nevertheless the concentrations in soil air were higher at 150 cm than at 70 cm in many cases, the concentrations in soil water were similar. As well as in soil air, however, the maximum value of dissolved CO_2 concentration in soil water was always found at a depth of 100 cm and reached

3.85×10^{-5} $gCO_2 \cdot cm^{-3}$ in July 1997. The values of dissolved CO_2 concentration at 100 cm ranged from 3.3 to 7.3 times as high as those at 5cm, where the least concentration in the profile was found; for CO_2 concentration in soil air, the values of Max/Min in the profile were 4 to 10.

At the grassland site, due to the much higher concentration in soil air, dissolved CO_2 concentrations in soil water were much higher than those at the forest site except near the ground surface. The seasonal variation of dissolved CO_2 concentration was almost similar to that of CO_2 concentration in soil air, and the effect of the seasonal variation of pH was found little. The values of Max/Min at each depth were three to five in shallow soils and about two in deep soils, whereas for CO_2 concentration in soil air, the ratios were about six in shallow soils and more than three in deep soils (Figure 4.10), larger than those for dissolved CO_2 concentration.

The profiles of dissolved CO_2 concentration were slightly different from those of the concentration in soil air (Figure 4.12). In July and August 1996 and from June to September in 1997, dissolved CO_2 concentrations at a depth of 100 cm exceeded those at 70 cm and were highest in the profile, while CO_2 concentrations in soil air were always highest at 70 cm. The soil water at a depth of 70 cm had the smallest values of pH in the profile (Figure 4.21) and the dissociation of carbonic acid was most strongly inhibited. In addition, soil temperatures in the periods at 70 cm were higher than the temperatures at 100 cm (Figure 4.8). As the temperature rises, the solubility of CO_2 into soil water is reduced and the dissociation of carbonic acid and bicarbonates are promoted. In the range of pH observed at the grassland site, a large portion of the carbonate species in soil water is occupied by dissolved CO_2 in a narrow sense, namely CO_2 (aq), so that the former influence will appear more remarkably. Consequently, in these periods, the dissolved CO_2 concentrations at a depth of 70 cm became lower than those at 100 cm. The maximum value of dissolved CO_2 concentration in soil water was, therefore, observed at a depth of 100 cm in September 1997, and was as high as 17.6×10^{-5} $gCO_2 \cdot cm^{-3}$. The values of Max/Min of dissolved CO_2 concentration in the profile ranged from 10 to 30, while for CO_2 concentration in soil air, the ratios ranged from 15 to 35 and also larger than those for dissolved CO_2 concentration.

(3) Relationship between carbon dioxide concentrations in soil air and dissolved in soil water

As described above, seasonal and vertical distributions of dissolved CO_2 concentration in soil water generally corresponded to the distributions of CO_2 concentration in soil air. Thus, to

examine the relationship between CO_2 concentrations in soil air and dissolved in soil water more precisely, the measured values of CO_2 concentration in soil air (c_{CO_2}, % in vol.) were converted into the mass of CO_2 in a unit volume of soil air (C_g, in $gCO_2 \cdot cm^{-3}$), the same unit as the dissolved CO_2 concentration, by the following equation:

$$C_g = \frac{m_{CO_2} \cdot P}{R \cdot T} \times c_{CO_2} \times 10^{-2} \tag{4.9}$$

where T is soil temperature (K) measured at the depth, and R is a gas constant for ideal gas ($hPa \cdot cm^3 \cdot mol^{-1} \cdot K^{-1}$) and takes a value of 83128.18 in Equation 4.9. A constant value of 1013 was applied to P as the atmospheric pressure at both sites. Hereinafter CO_2 concentration in soil air is expressed in $gCO_2 \cdot cm^{-3}$ in principle.

Using the measured values of CO_2 concentration in soil air and soil temperature, C_g was calculated from Equation 4.9. Then the C_w/C_g values, which is the ratio of CO_2 concentration dissolved in soil water to that in soil air, were calculated at the forest and the grassland site and plotted in Figures 4.26 and 4.27, respectively. A value of C_w/C_g more than 1.0 means that the CO_2 concentration dissolved in soil water is higher than that in soil air.

The C_w/C_g at the forest site was always more than 1.0 at all the depths and generally ranged from 1.5 to 2.5, that is, CO_2 concentrations dissolved in soil water were 1.5 to 2.5 times as high as those in soil air. The C_w/C_g was varied seasonally in an opposite way to the soil temperatures (Figure 4.7), low in the summer and high in the winter. This is mainly due to the CO_2 solubility into water which decreases in response to the increasing temperature, and therefore the range of seasonal variation of C_w/C_g was relatively large in shallow soils and the phases of the variation were delayed in deep soils (cf. Figure 4.7). Except for June and July in 1997, when relatively high pH in soil water was observed (Figure 4.18), the effect of pH on the seasonal variation of C_w/C_g was smaller than the effect of soil temperature.

The C_w/C_g decreased with depth throughout the observation period except for a depth of 20 cm. The profiles of pH (Figure 4.20) were similar to those of C_w/C_g, whereas annually averaged soil temperatures were not so different among the depths. Under low pH conditions, the dissociation of carbonic acid into bicarbonates and the corresponding increase in dissolved carbonate species are inhibited, thus such C_w/C_g profiles would be caused by lowering pH with

depth. In the same manner, relatively small values of C_w/C_g at a depth of 20 cm was due to the exceptionally low pH at the depth.

Overall, the values of C_w/C_g at the grassland were low relative to those at the forest, partly due to the higher averaged soil temperature (see Section 4.1) and partly due to the lower pH in soil water. The C_w/C_g approximately ranged from 1.0 to 2.0 except at depths of 5 and 10 cm. In the summer of 1997, the values of C_w/C_g at depths of 30 to 70 cm were less than 1.0, namely CO_2 concentrations in soil air exceeded those dissolved in soil air. The seasonal variation of C_w/C_g showed a pattern opposite to the variation of soil temperature (Figure 4.8) other than at depths of 5 and 10 cm in the spring of 1998, when exceptionally high pH values were obtained at these depths (Figure 4.19).

Like at the forest, the profiles of C_w/C_g were in good agreement with those of pH at the grassland (Figure 4.21). In many cases, the C_w/C_g was largest at a depth of 10 cm, and then decreased with depth until 70 cm, at which the smallest value in the profile was observed. The C_w/C_g values less than 1.0 found at depths of 30 to 70 cm in the summer of 1997 are partly due to the low pH values at these depths, as well as the high temperatures in this period.

The relationship between CO_2 concentrations in soil air and dissolved in soil water at both sites is summarized as follows: In response to the seasonal variation of soil temperature, CO_2 concentration in soil air rose from spring to summer and fell from autumn to winter, while the solubility of CO_2 into soil water varied reversely. Consequently, the ranges of the seasonal variation of CO_2 concentration dissolved in soil water became smaller than the ranges of the variation in soil air. Therefore, the Max/Min of CO_2 concentration observed for each depth was less in soil water than in soil air. On the other hand, CO_2 concentration in soil air generally increased with depth. In contrast, pH in soil water decreased with depth. Because of the little difference in RpH among the depths, the profile of pH would be considerably affected by the profile of CO_2 concentration itself. Consequently, the difference in CO_2 concentration dissolved in soil water among the depths became smaller than the difference in soil air. Therefore, the Max/Min of CO_2 concentration observed in each profile was less in soil water than in soil air.

Namely, owing to such a dependence of dissolved CO_2 concentration on temperature and pH, the dissolution of CO_2 in soil air into soil water would reduce the temporal and spatial differences in CO_2 within the soil profile at both sites.

4.3 Evaluation of the content of carbon dioxide in bulk soil

4.3.1 Methods

The content of CO_2 in a unit volume of bulk soil was calculated from the measured values of the concentration of CO_2 in soil air and the pressure head of soil water (Section 4.1) and the evaluated values of dissolved CO_2 concentration in soil water (Section 4.2). First, the pressure head at each depth was converted to volumetric water content, θ_w, using the soil water characteristic curve of the depth at both sites (Figures 3.3 and 3.4). Hysteresis in the curve was not considered. Next, air-filled porosity, θ_g, at each depth was given by the difference between total porosity, θ_t, and volumetric water content at the same depth, namely:

$$\theta_g = \theta_t - \theta_w \tag{4.10}$$

At a depth of 5 cm, where the pressure head was not measured, it was assumed that the volumetric water content had the same value as that at 10 cm. In 1996, the pressure heads were not measured at depths of 40 and 150 cm. Therefore, using the values measured in 1997 and 1998, the relationships on volumetric water content between at 40 cm and at 30 and 50 cm, and between at 150 cm and at 100 cm, were established by the regression analyses between the values at the depths. The relationships were sufficiently expressed by the regression curves and the values of volumetric water content at depths of 40 and 150 cm were estimated using the curves. From January to April in 1998, the values of pressure head at a depth of 10 cm at the grassland site were given by the values at 20 cm due to the failure of tensiometer at 10 cm. Because of the lack of data on the pressure head, CO_2 contents were not evaluated from December 1996 to May 1997.

From the volumetric ratio in the soil obtained above and the concentrations of CO_2 in soil air and dissolved in soil water, the contents of CO_2 in gaseous phase, M_g, and in liquid phase, M_w, per unit volume of bulk soil ($gCO_2 \cdot cm^{-3}$ soil) were given as follows:

$$M_g = C_g \cdot \theta_g \tag{4.11}$$

$$M_w = C_w \cdot \theta_w \tag{4.12}$$

Finally, M_t, the total content of CO_2 per unit volume of bulk soil was obtained:

$$M_t = M_g + M_w \tag{4.13}$$

4.3.2 Results and discussion

(1) Content of carbon dioxide in the gaseous phase of bulk soil

The seasonal variations of the content of CO_2 in gaseous phase per unit volume of bulk soil, given by Equation 4.11, at the forest and the grassland site are shown in Figures 4.28 and 4.29, respectively.

At the forest site, CO_2 content in the gaseous phase increased from spring to summer and decreased from autumn to winter, corresponding to the seasonal variation of CO_2 concentration in soil air (Figure 4.9). The Max/Min in the CO_2 content found at each depth ranged from 2.8 to 4.6 and exceeded the Max/Min in the CO_2 concentration, ranged from 1.9 to 4.0, at all the depths. This suggests that the seasonal variation of CO_2 content was enhanced more largely than the variation of CO_2 concentration, due to the increase in air-filled porosity in summer months, when CO_2 concentration was also high.

The profiles of CO_2 content in the gaseous phase were slightly different from those of CO_2 concentration (Figure 4.11); the CO_2 content gradually increased with depth to a depth of 70 cm and then rapidly decreased. At a depth of 70 cm, CO_2 concentration was highest next to at depths of 100 and 150 cm, and air-filled porosity showed relatively high values of 0.2 to 0.3 (Figure 3.1). Consequently CO_2 content in the gaseous phase was always highest at 70 cm in the profile and reached the maximum value of 5.14×10^{-6} $gCO_2 \cdot cm^{-3}$ soil in September 1997. While at 100 cm, where the highest concentration of CO_2 in the profile was always found, CO_2 content in the gaseous phase was as low as that at depths of 5 to 20 cm and less than the half of the content at 70 cm, due to the low air-filled porosity of 0.05 to 0.1. At a depth of 150 cm, air-filled porosity was lowest in the profile, so that the CO_2 content was also smallest.

Due to the extremely low air-filled porosity, CO_2 content in the gaseous phase at the grassland was similar to or even lower than that at the forest except at a depth of 70 cm, although CO_2 concentration in soil air was much higher than at the forest. The Max/Min in CO_2 concentration at each depth ranged from 3.2 to 8.1, whereas the Max/Min in CO_2 content ranged from 13 to 14 near the ground surface, 5 to 6 at depths of 50 and 70 cm, and 23 to 27 at the other depths. Such

high values of the ratio like 23-27 were mainly due to the small values of the minimum CO_2 contents caused by the extremely low air-filled porosities (Figure 3.2), and actually the CO_2 content was little at these depths.

The difference in the characteristic on CO_2 content among the depths was evident at the grassland site. Near the ground surface, air-filled porosity largely varied in the range of 0.08 to 0.48 and increased in summer to extend the seasonal variation of CO_2 content more widely than the variation of CO_2 concentration. As a result, CO_2 content at depths of 5 and 10 cm was relatively large and ranged from 0.5 to 3.0×10^{-6} $gCO_2 \cdot cm^{-3}$ soil. At depths of 20 to 40 cm, in contrast, little CO_2 was found in the gaseous phase due to the extremely low air-filled porosities (0.01 to 0.05 at the maxima for each depth, Figure 3.2) and CO_2 content rarely exceeded 0.5×10^{-6} $gCO_2 \cdot cm^{-3}$ soil. At depths of 50 and 70 cm, much higher concentrations of CO_2 (Figure 4.12) and relatively large values of air-filled porosity kept CO_2 contents high; the maximum values at these depths were observed in the extremely dry summer of 1996 and reached 4.15 and 16.8×10^{-6} $gCO_2 \cdot cm^{-3}$ soil, respectively. At depths of 100 and 150 cm, where CO_2 concentrations were comparable to those at 70 cm, the low air-filled porosities kept CO_2 contents lower except in the summer of 1996.

(2) Content of carbon dioxide dissolved in the liquid phase of bulk soil

The seasonal variations of the content of CO_2 dissolved in liquid phase per unit volume of bulk soil, given by Equation 4.12, at the forest and the grassland site are shown in Figures 4.30 and 4.31, respectively.

At the forest site, the seasonal variation of the content of CO_2 dissolved in the liquid phase was similar to the variation of dissolved CO_2 concentration (Figure 4.24). The content of CO_2 was larger than that in the gaseous phase at the same depth and time except in some dry periods, because CO_2 concentration dissolved in soil water was about 1.5 to 2.5 times as high as that in soil air (Figure 4.26) and volumetric water content was larger than air-filled porosity at most of the depths (Figure 3.1). The CO_2 content at a depth of 100 cm was always largest in the profile, as well as dissolved CO_2 concentration at the depth, and reached the maximum of 2.55×10^{-5} $gCO_2 \cdot cm^{-3}$ soil in July 1997. The Max/Min in CO_2 content in the liquid phase observed at each depth ranged from 1.7 to 2.7 and was similar to the Max/Min in dissolved CO_2 concentration, ranged from 1.8 to 2.8. In dry periods, however, especially from late July to early September in

1996, the decrease in volumetric water content reached a depth of 100 cm caused the depression in CO_2 content larger than the depression in dissolved CO_2 concentration.

Overall, the effect of the variation of volumetric water content on the content of CO_2 dissolved in the liquid phase was smaller than the effect of the variation of air-filled porosity on the content in the gaseous phase at the forest site. This was due to the general distribution of the gaseous and liquid phases in the soil profile (Figure 3.1). For air-filled porosity, the Max/Min at each depth ranged from 1.4 to 3.9 and the Max/Min in the profile reached more than thirty. For volumetric water content, in contrast, the Max/Min at each depth ranged only from 1.1 to 1.7, and the Max/Min in the profile was less than two. In addition, volumetric water content generally increased with depth, as well as dissolved CO_2 concentration. Consequently, the temporal and spatial distributions of the content of CO_2 dissolved in the liquid phase highly depended on the distributions of dissolved CO_2 concentration.

Mainly due to the large volume of liquid phase (Figure 3.2) and partly due to the dissolved CO_2 concentration in soil water higher than CO_2 concentration in soil air (Figure 4.27), CO_2 content dissolved in the liquid phase was about an order of magnitude as large as the content in the gaseous phase at the grassland site, except near the ground surface. The maximum value was 12.6×10^{-5} $gCO_2 \cdot cm^{-3}$ soil, observed at a depth of 70 cm in October 1997. While the Max/Min in dissolved CO_2 concentration at each depth ranged from 1.5 to 5.4, the Max/Min in CO_2 content was relatively large near the ground surface, 6.3 at 5 cm and 9.0 at 10 cm, but nearly equal to the Max/Min in the concentration below these depths, ranged from 1.5 to 4.7.

At the grassland, the effect of the variation of volumetric water content on the content of CO_2 dissolved in the liquid phase was smaller than at the forest, because as indicated by the soil water characteristic curves (Figure 3.4), the change in volumetric water content in response to the change in pressure head was small except near the ground surface. From 70 to 150 cm, however, the CO_2 content decreased with depth nevertheless dissolved CO_2 concentrations among these depths were similar. This was due to the decrease in volumetric water content according to the decrease in total porosity.

(3) Total content of carbon dioxide in bulk soil

The seasonal variations of the total content of CO_2 per unit volume of bulk soil, given by Equation 4.13, at the forest and the grassland site are shown in Figures 4.32 and 4.33,

respectively. Due to the common seasonal trends of CO_2 content in the gaseous and liquid phases, inevitably total CO_2 content given by the sum of both CO_2 contents showed similar seasonal variation. Then, to compare the contribution of both CO_2 contents to the total content, the proportion of the CO_2 content in the liquid phase to the total content, M_w/M_t, at both sites is plotted in Figures 4.34 and 4.35.

By the magnitude of total CO_2 content, the forest soil was classified into three layers; at depths of 5 to 20 cm, 30 to 50 cm, and 70 to 150 cm. First, at depths of 5 to 20 cm, total CO_2 contents were relatively small and ranged from 0.2 to 0.7×10^{-5} $gCO_2 \cdot cm^{-3}$ soil, and increased with depth. In addition, the M_w/M_t approximately ranged from 50 to 70%, and became less than 50% in dry periods. As a result, it was suggested that CO_2 contents in the gaseous and liquid phases almost equally contributed to the total CO_2 content at depths of 5 to 20 cm.

Secondly, at depths of 30 to 50 cm, total CO_2 contents ranged from 0.6 to 1.2×10^{-5} $gCO_2 \cdot cm^{-3}$ soil, but were not so different among the depths. The M_w/M_t was about 80% and higher than that in the upper layer, therefore it was shown that the total CO_2 content was mainly determined by the content in the liquid phase. Exceptionally, for dry periods in the summer and from October to November in 1997, the increase in CO_2 content in the gaseous phase accompanied by the increase in air-filled porosity offset the decrease in CO_2 content in the liquid phase to some extent, and then the reduction in the total CO_2 content became small.

Thirdly, at depths of 70 to 150 cm, the largest values of total CO_2 content in the profile were always observed at 100 cm, where the contents generally ranged from 1.5 to 2.5×10^{-5} $gCO_2 \cdot cm^{-3}$ soil and reached 2.69×10^{-5} $gCO_2 \cdot cm^{-3}$ soil at the maximum in July 1997. At depths of 100 and 150 cm, the M_w/M_t usually exceeded 90% and therefore total CO_2 content at these depths was dominated by the content in the liquid phase, whereas the values of M_w/M_t ranged from 70 to 85% at 70 cm and were similar to those at 30 to 50 cm. Furthermore CO_2 content in the gaseous phase at a depth of 70 cm was much larger than the content at any other depths (Figure 4.28), so that total CO_2 contents at 70 cm were higher than those at 150 cm nevertheless CO_2 content in the liquid phase was often less than that at 150 cm (Figure 4.30).

At the grassland site, total CO_2 content of bulk soil was almost equal to the content in the liquid phase, because of the extremely low air-filled porosity throughout the profile (Figure 3.2). Exceptionally, at depths of 5 and 10 cm, the M_w/M_t ranged widely from 35 to 95% and the total CO_2 content reached up to 1.5-2 times as large as the content in the liquid phase in dry periods.

Besides these depths, at depths of 70 and 100 cm, air-filled porosities were relatively high and the values of M_w/M_t were about 5 to 10 %. The CO_2 content in the gaseous phase at 70 cm was much larger than that at 100 cm (Figure 4.29), while CO_2 content in the liquid phase at 70 cm was similar to that at 100 cm (Figure 4.31). Therefore, total CO_2 contents at a depth of 70 cm were larger than those at 100 cm and reached 13.6×10^{-5} $gCO_2 \cdot cm^{-3}$ soil at the maximum in October 1997. Except for these depths, the values of M_w/M_t were usually more than 95% and the contribution of CO_2 content in the gaseous phase was little.

Comparing the contribution of the content of CO_2 in the gaseous and liquid phases of the soil to the total content of CO_2, the importance of the liquid phase as a reservoir of CO_2 in soils was indicated at both observation sites. Some of the previous studies have also presented the amount of CO_2 contained in soil profiles (e.g. Kirita, 1971; Haibara et al., 1997), but most of them estimated the content only in the gaseous phase. In general, CO_2 in soil air is in equilibrium with the CO_2 dissolved in soil water, so that the content in the liquid phase must be taken into consideration to clarify the dynamics and storage of CO_2 in soil profiles.

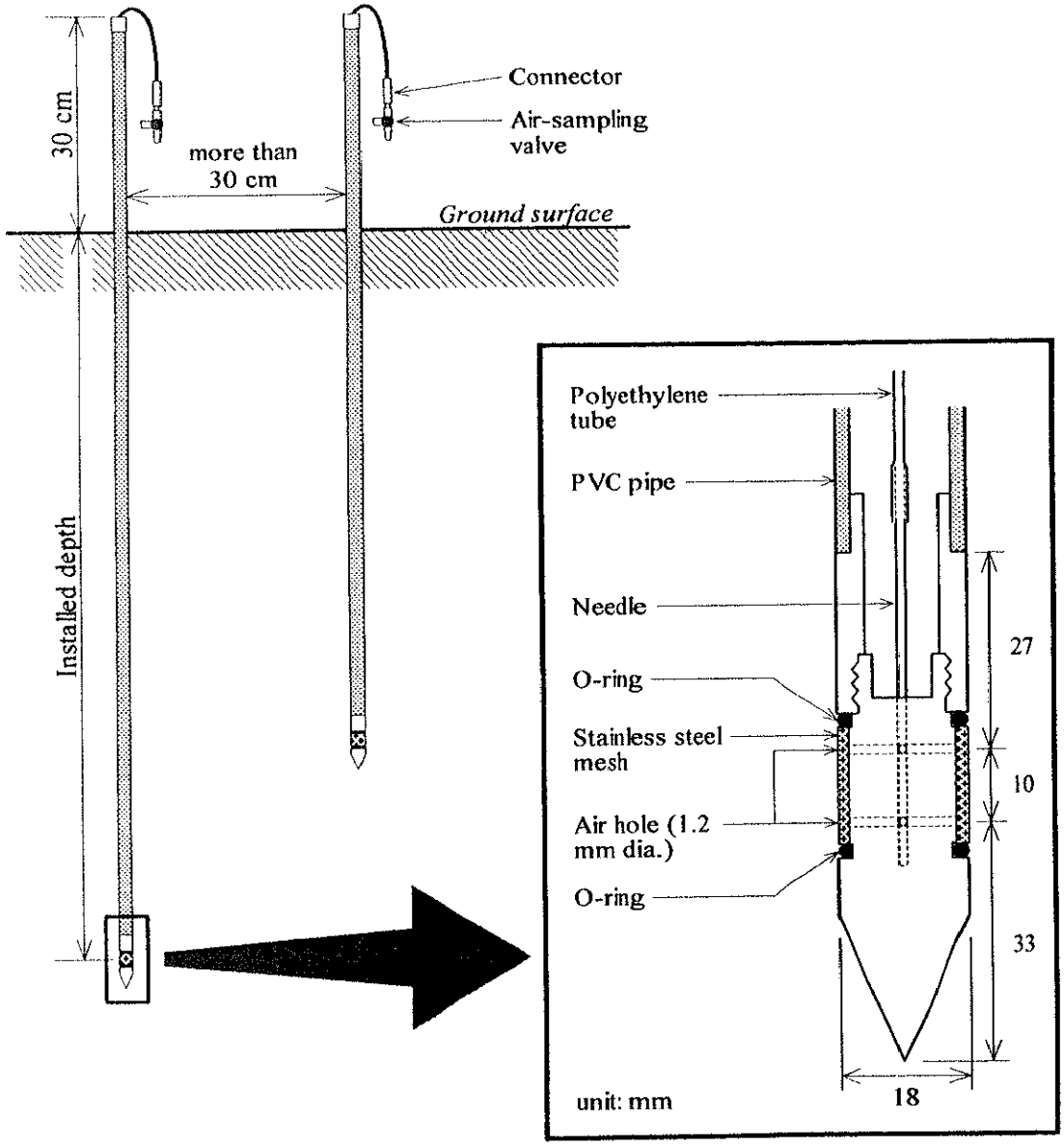

Figure 4.1. Design and arrangement of the soil air collection probe.

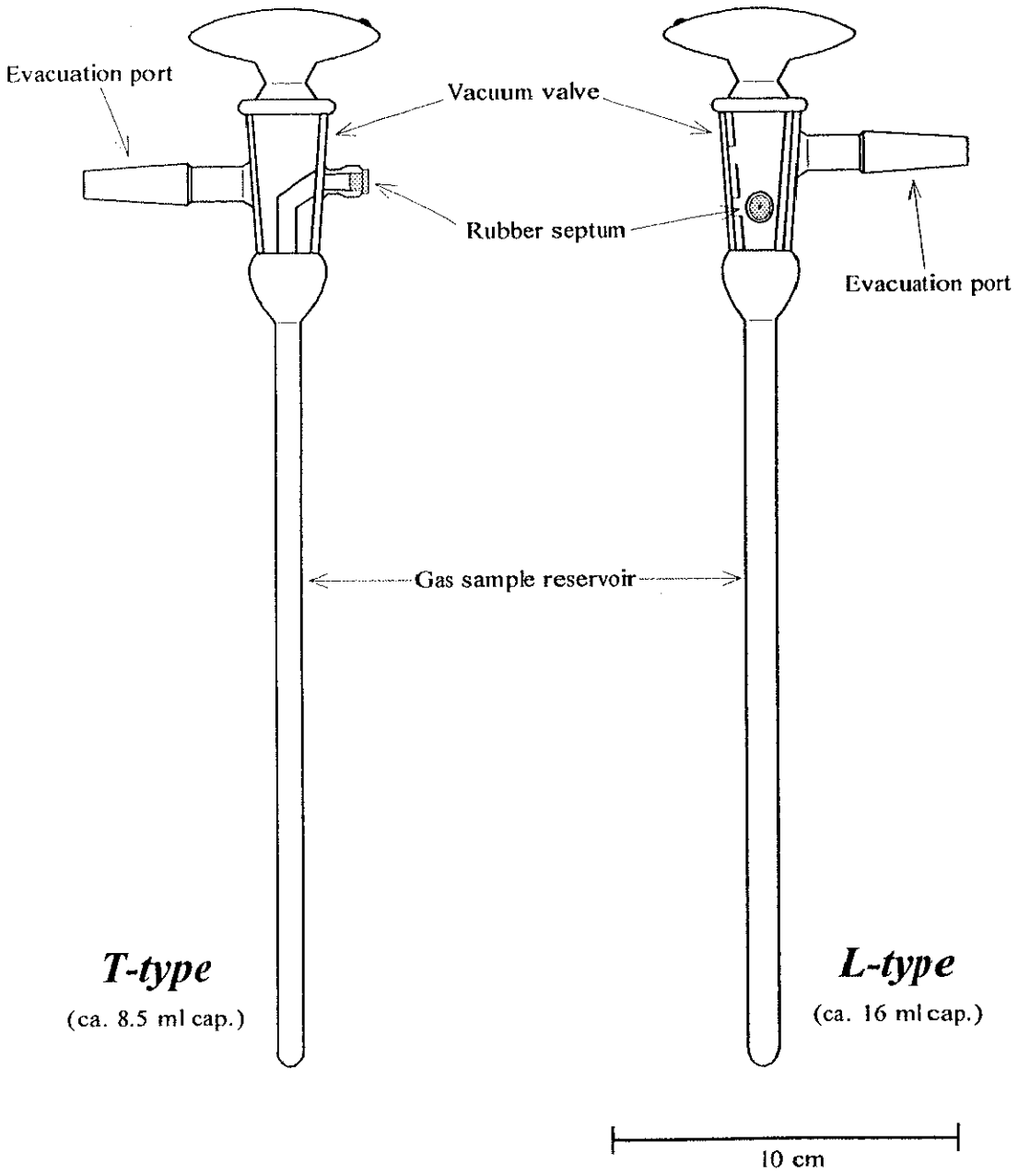

Figure 4.2. Designs of the gas sampling glass tubes.

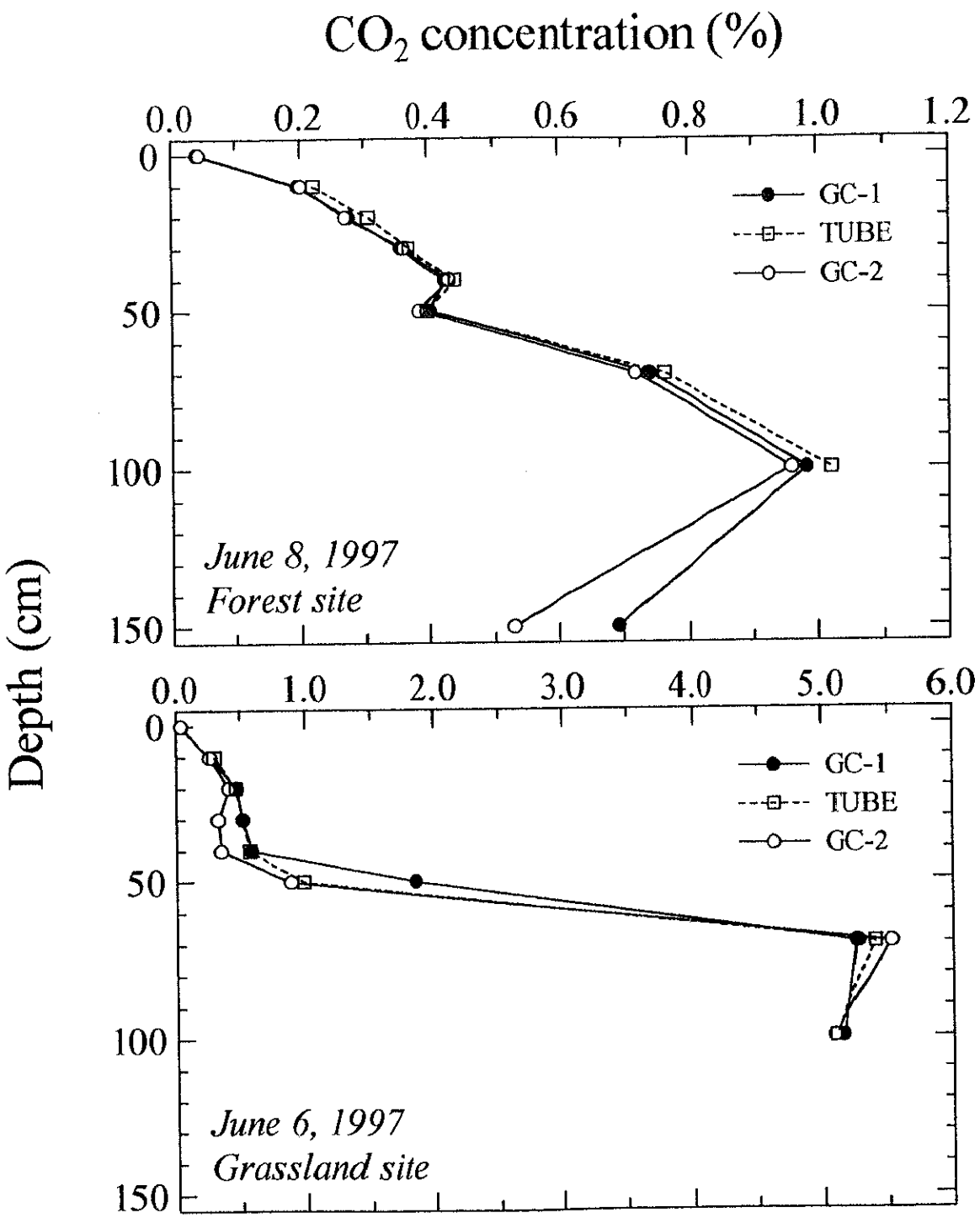

Figure 4.3. Comparison of the profiles of CO_2 concentration in soil air determined with the gas detection tubes (TUBE) and by gas chromatography (GC-1 and 2) at the forest and the grassland site.

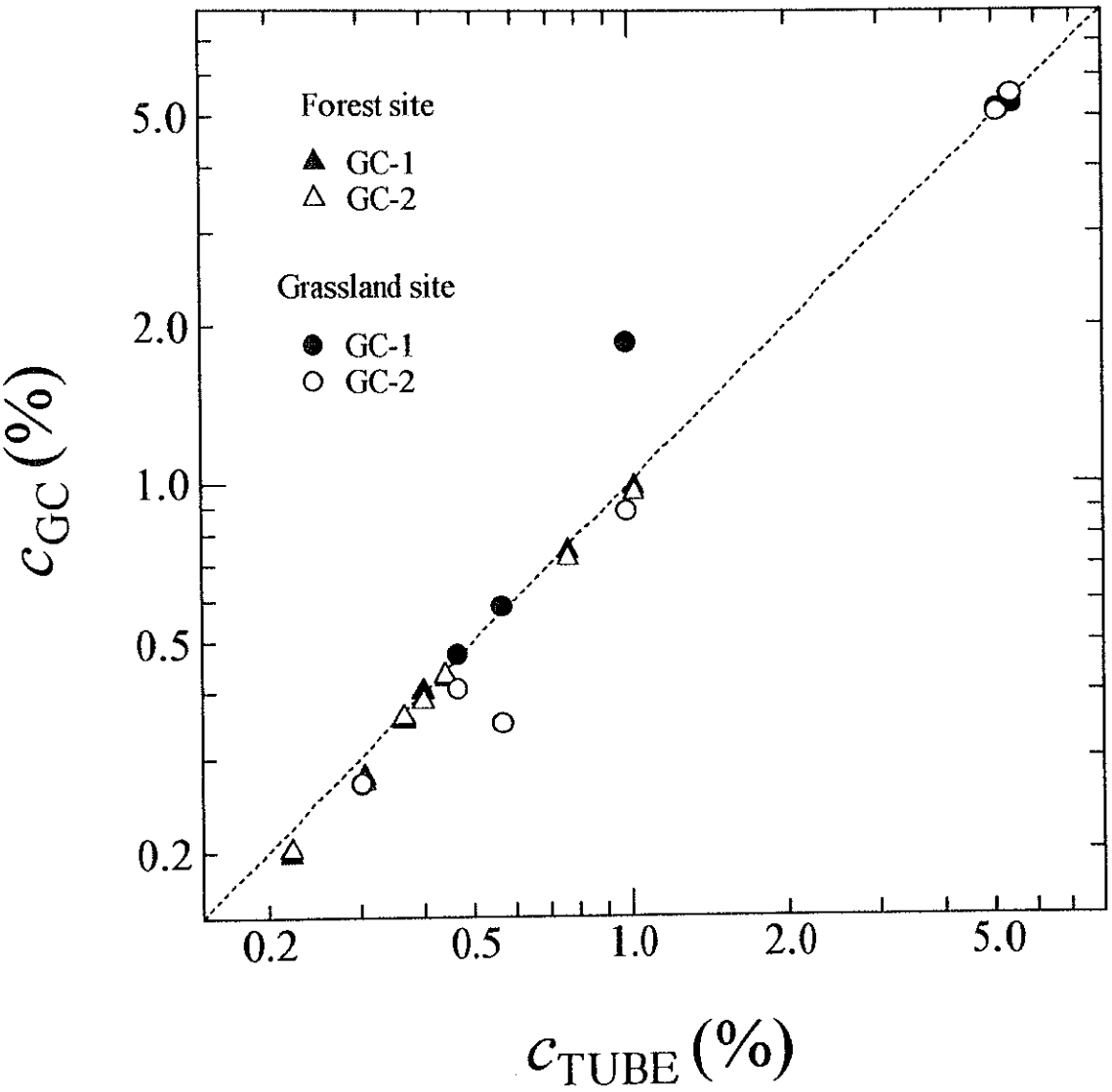

Figure 4.4. Relationship between CO_2 concentration in soil air measured with the gas detection tubes (c_{TUBE}) and that determined by gas chromatography (c_{GC}).

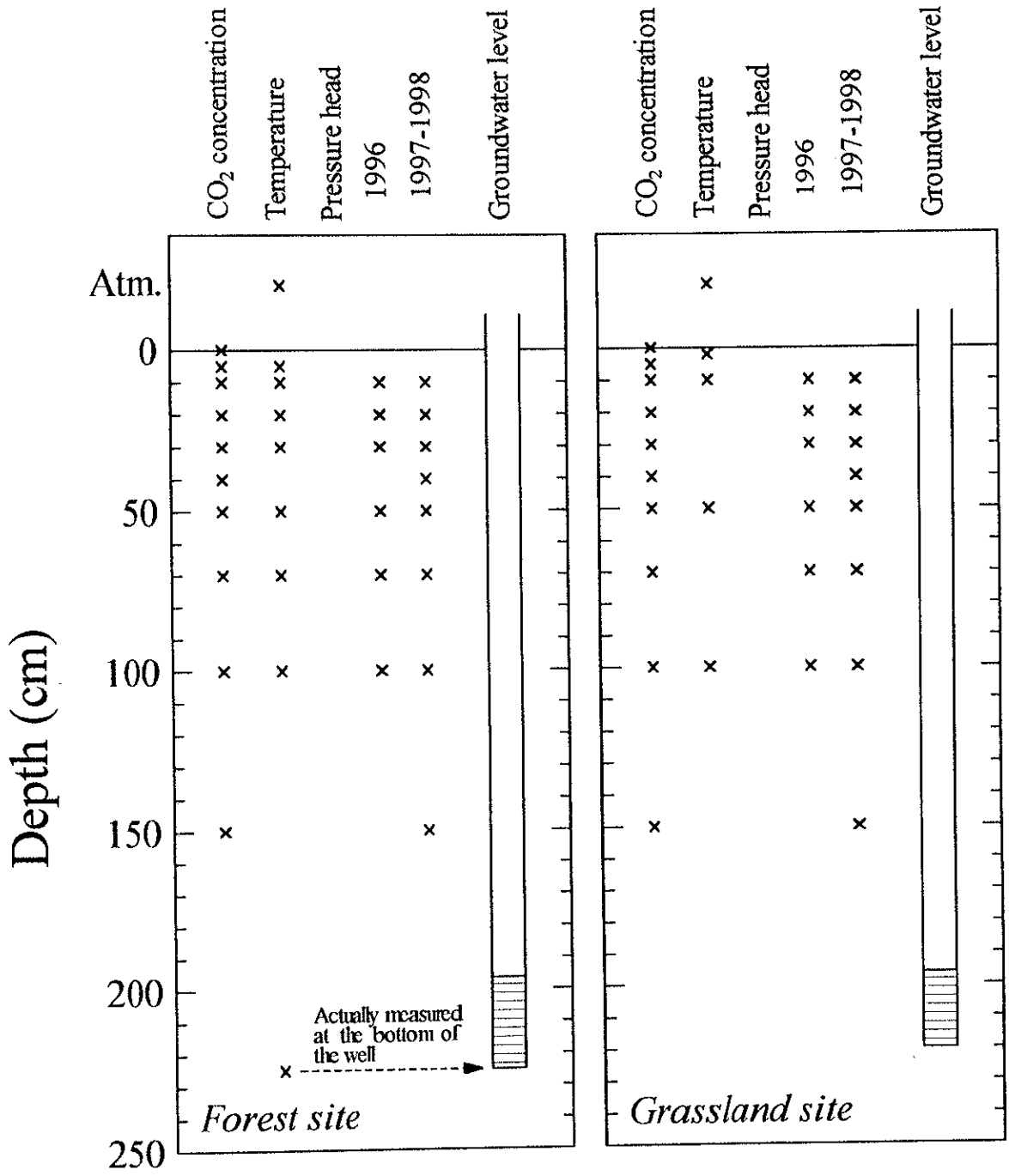

Figure 4.5. Summary of the depths for the measurement of CO_2 concentration in soil air and the environmental factors at the forest and the grassland site.

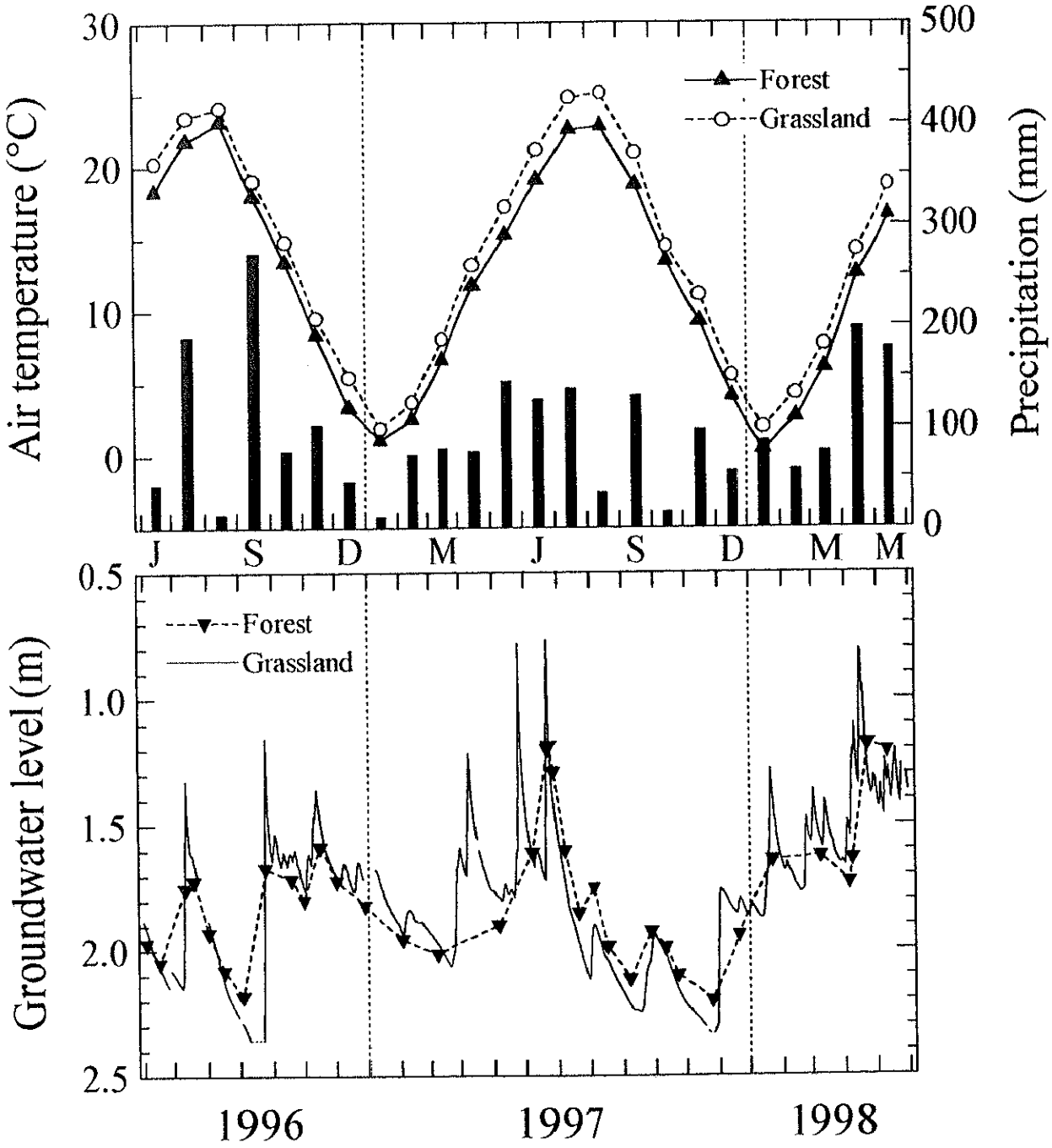

Figure 4.6. Seasonal variations of monthly-mean air temperature, monthly precipitation and the groundwater levels at the forest and the grassland site.

The groundwater levels are shown as the depth from the ground surface.

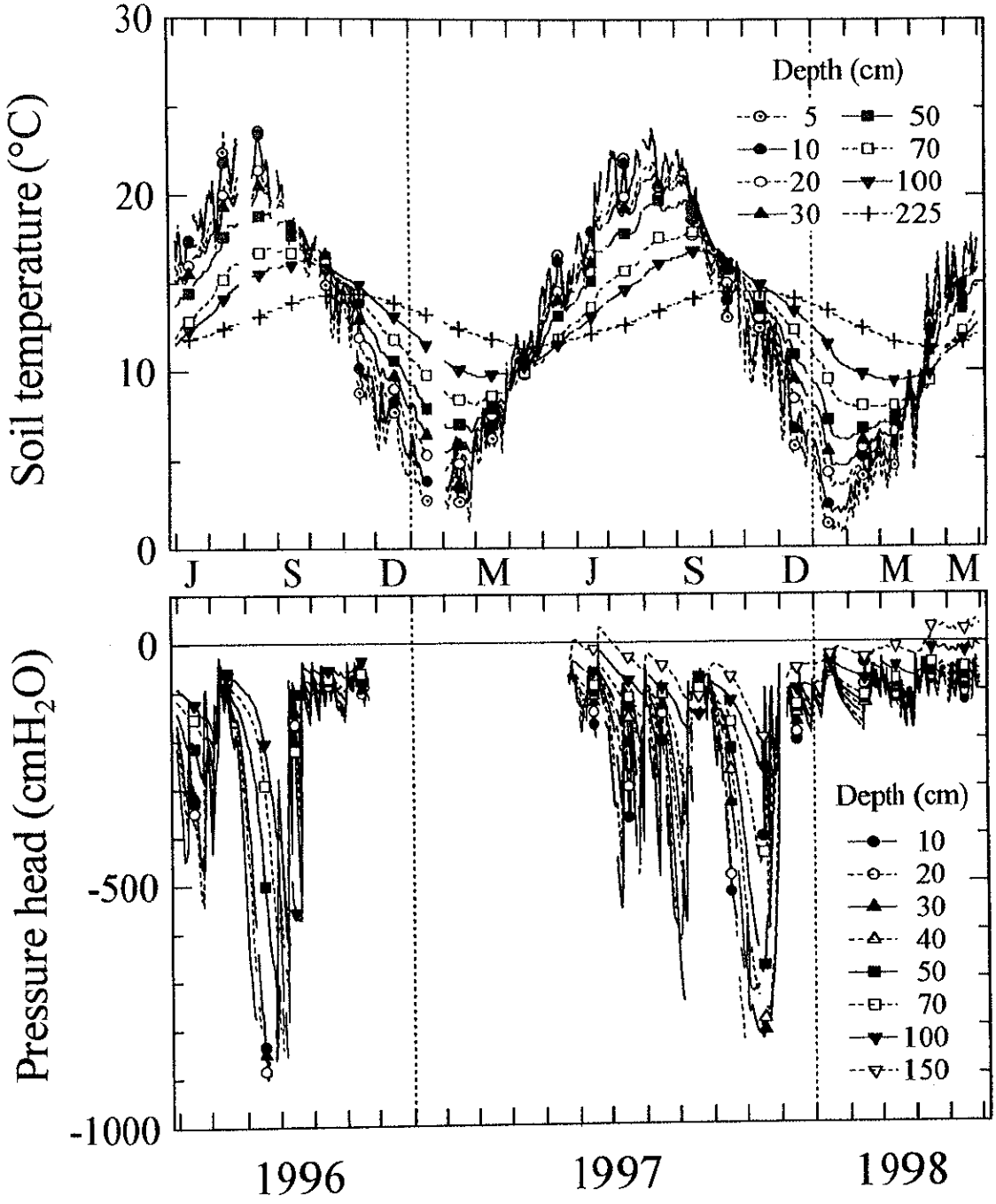

Figure 4.7. Seasonal variations of soil temperature and the pressure head of soil water at the forest site.

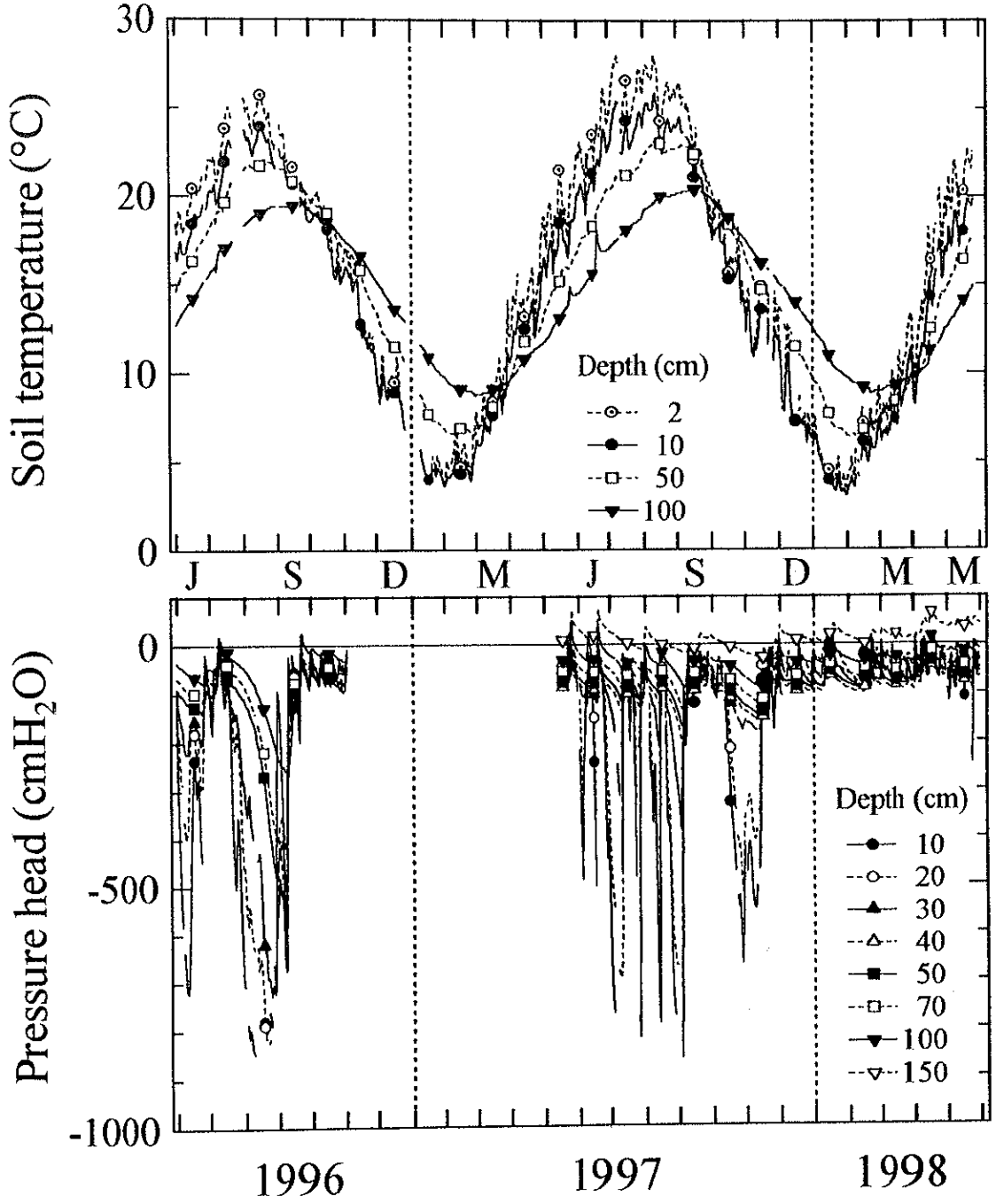

Figure 4.8. Seasonal variations of soil temperature and the pressure head of soil water at the grassland site.

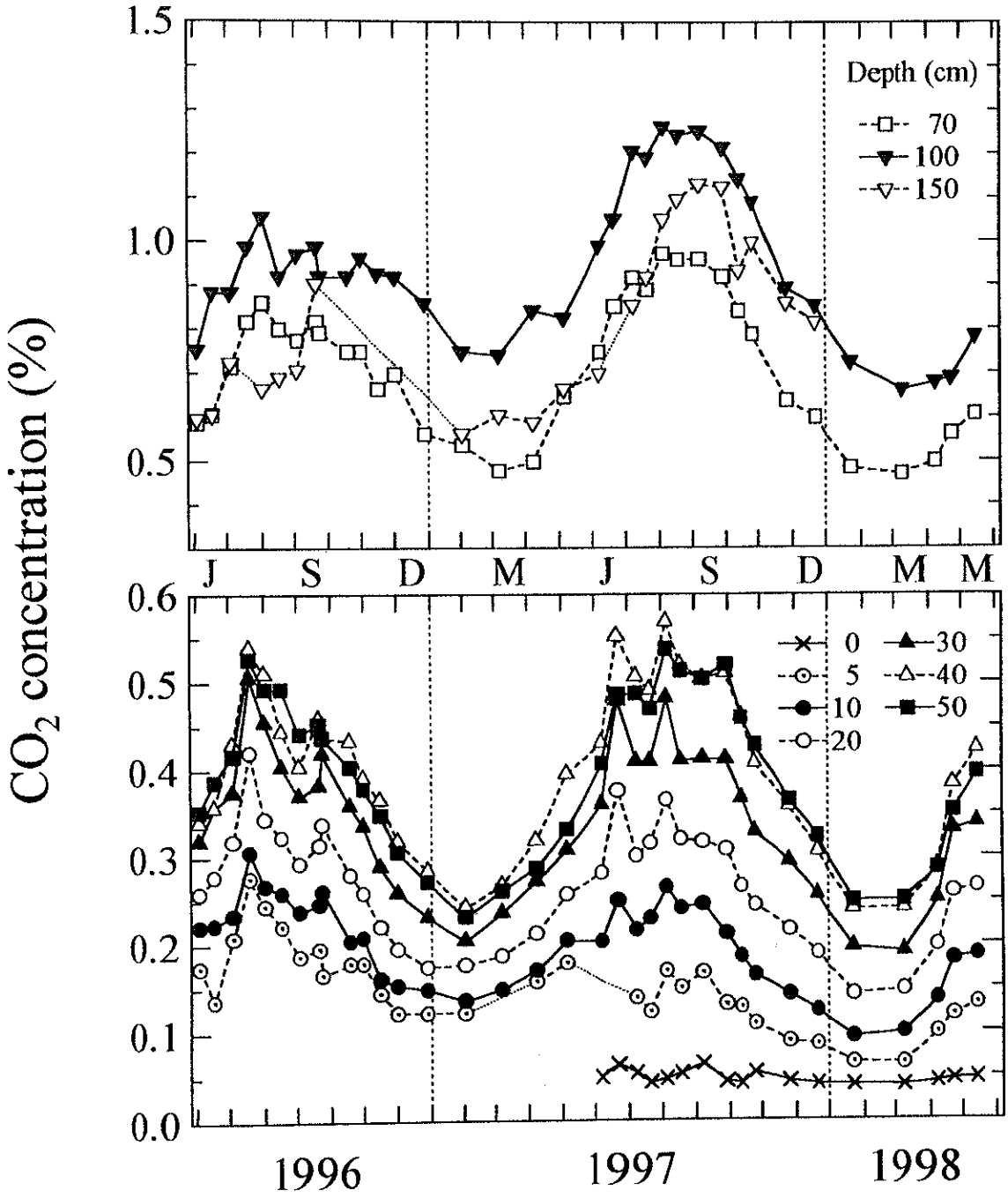

Figure 4.9. Seasonal variation of CO_2 concentration in soil air at the forest site.

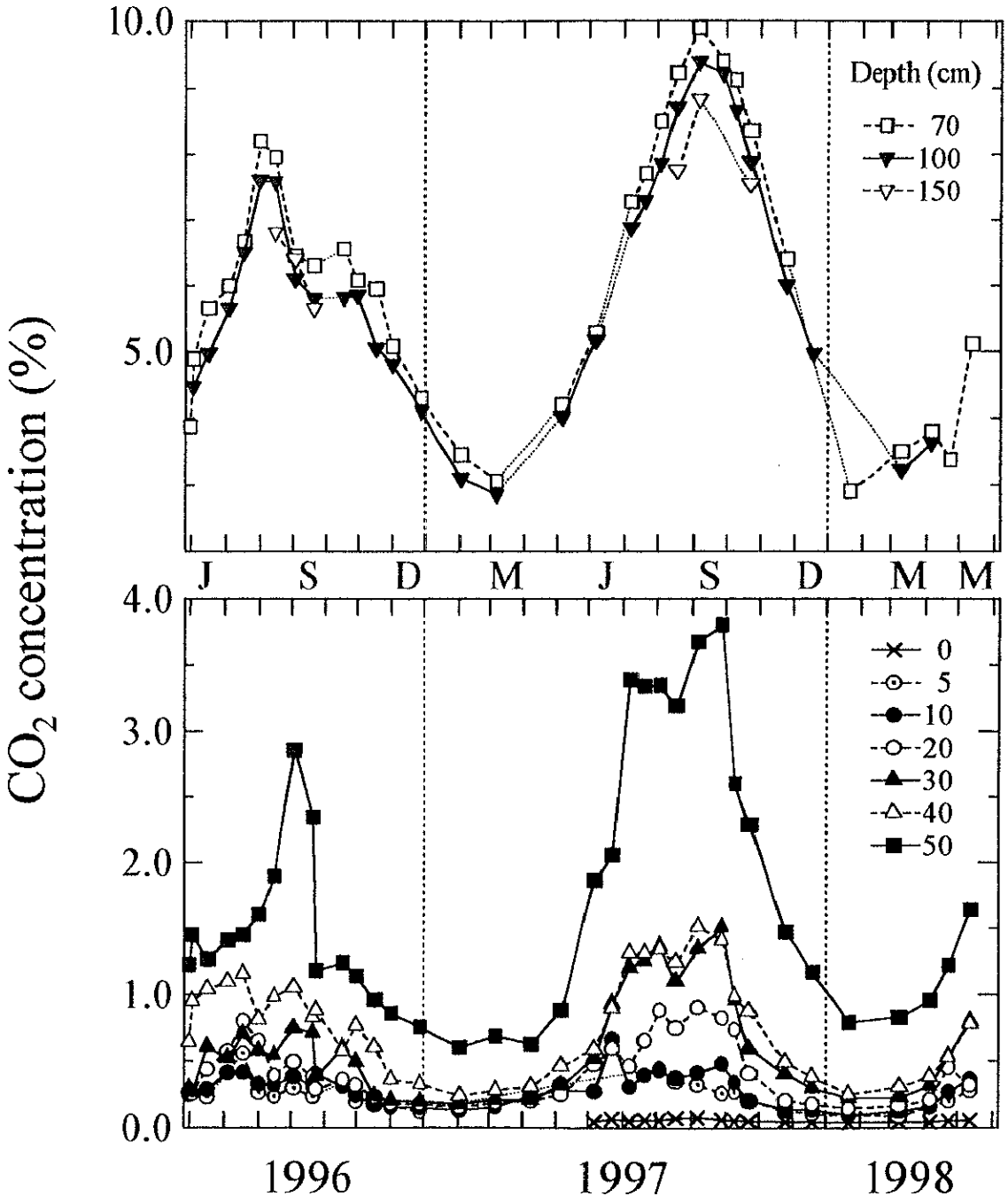

Figure 4.10. Seasonal variation of CO_2 concentration in soil air at the grassland site.

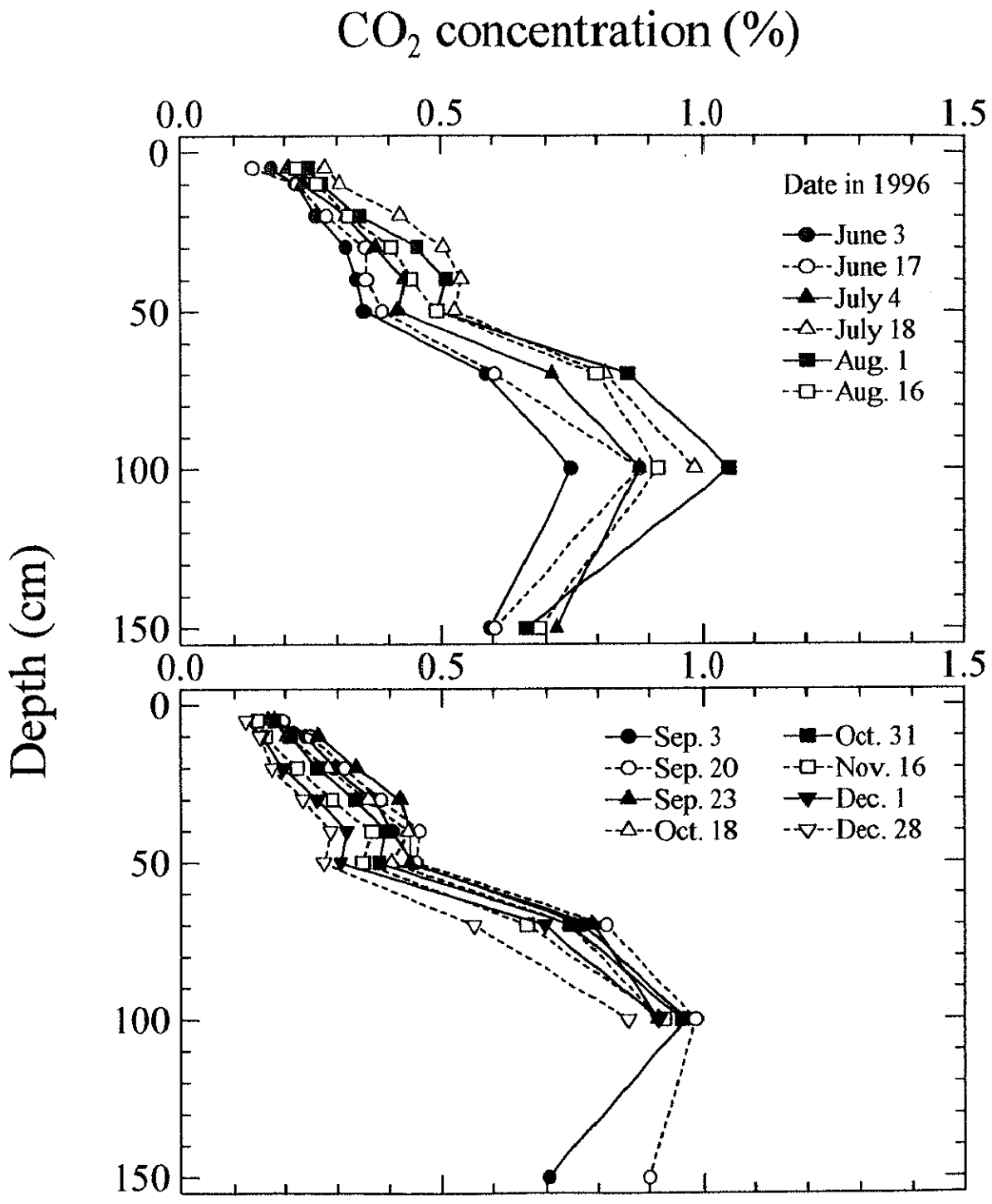

Figure 4.11a. Profiles of CO_2 concentration in soil air at the forest site in 1996.

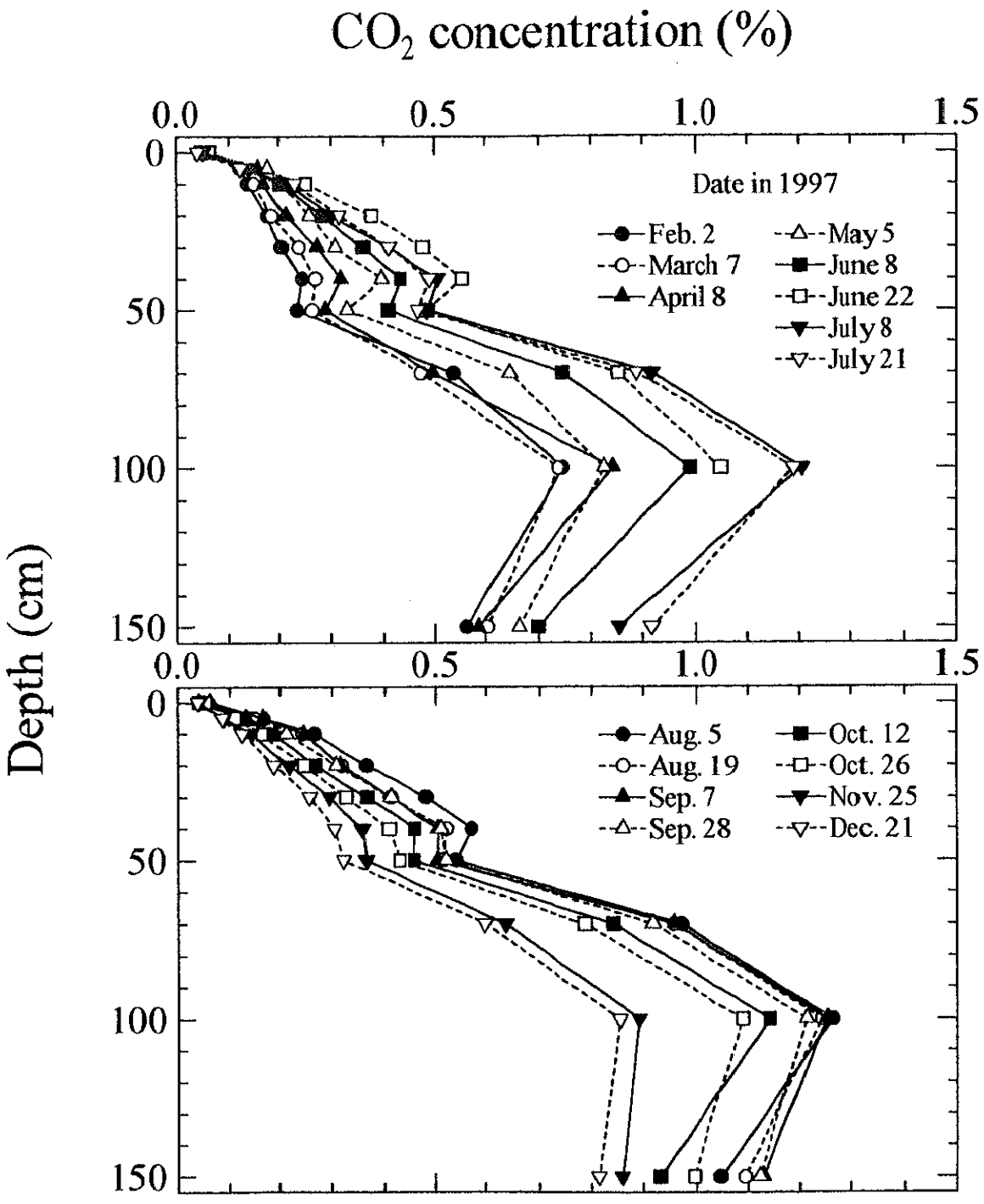

Figure 4.11b. Profiles of CO_2 concentration in soil air at the forest site in 1997.

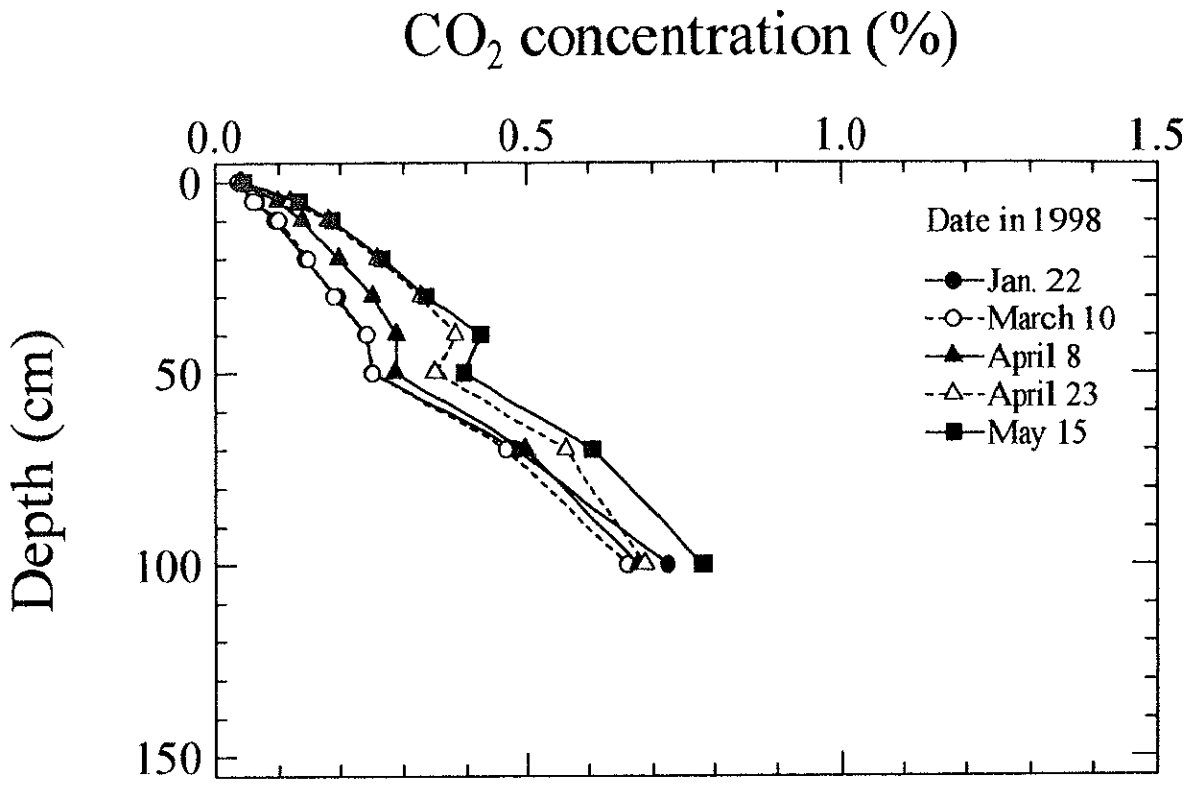

Figure 4.11c. Profiles of CO_2 concentration in soil air at the forest site in 1998.

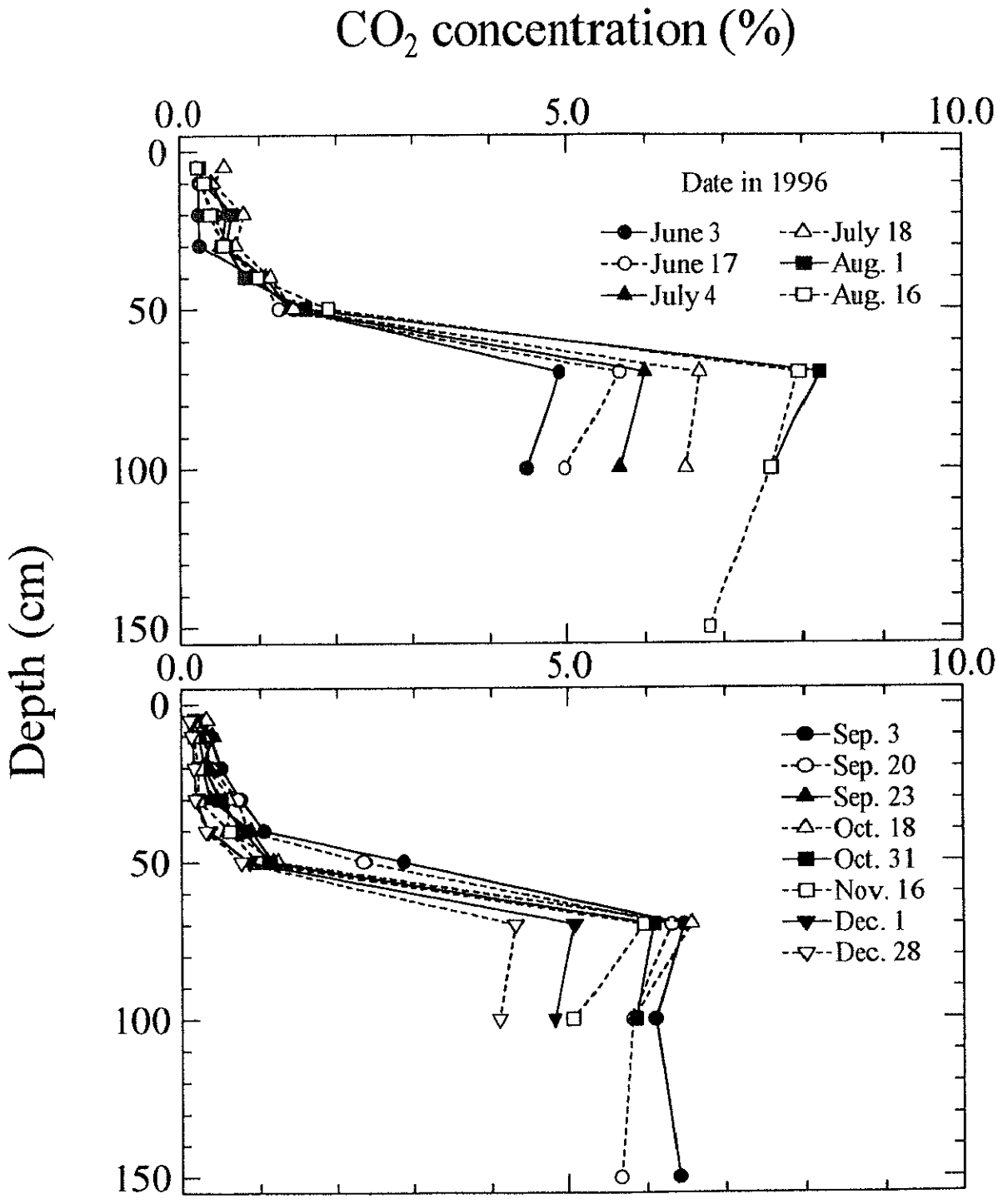

Figure 4.12a. Profiles of CO_2 concentration in soil air at the grassland site in 1996.

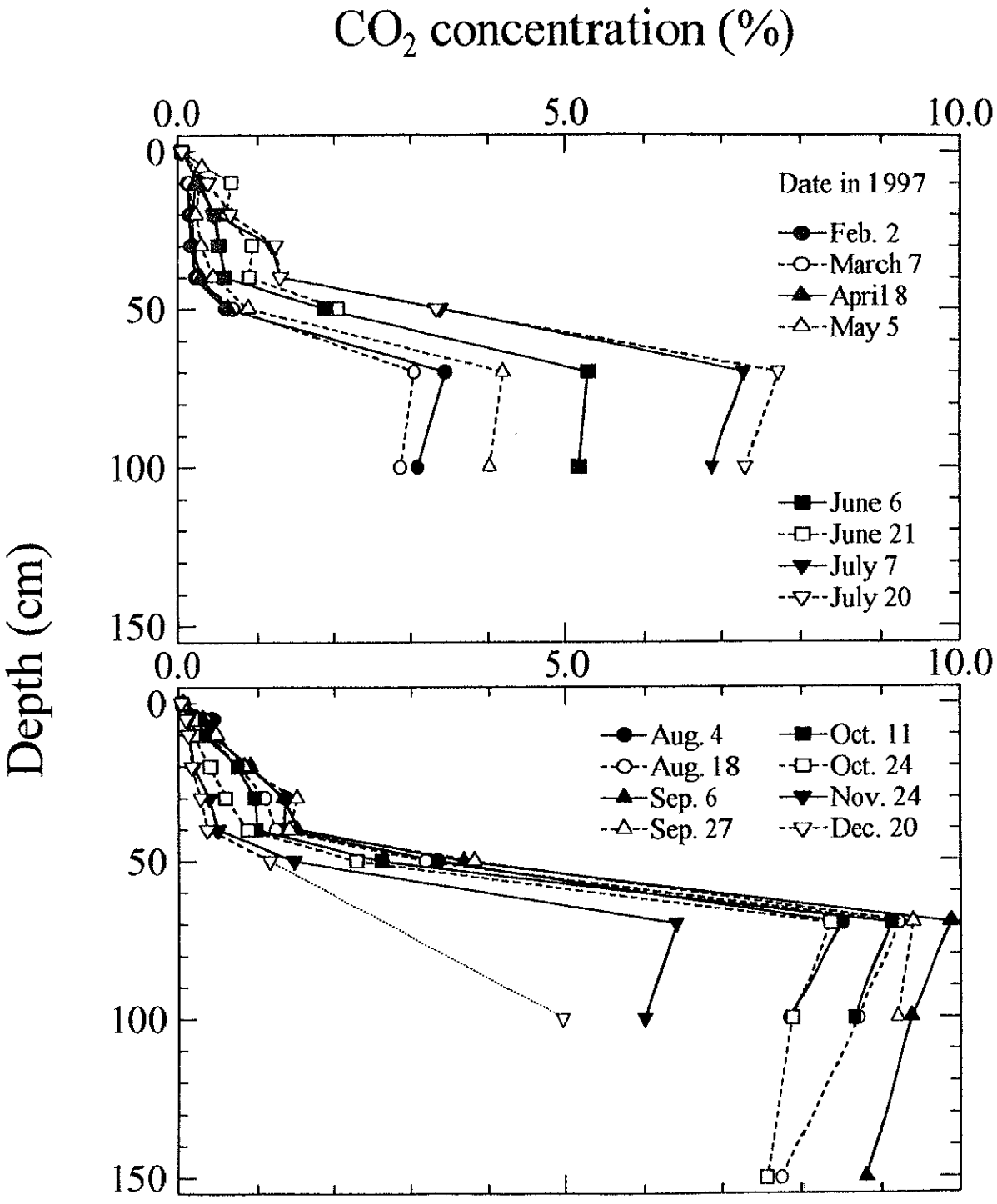

Figure 4.12b. Profiles of CO_2 concentration in soil air at the grassland site in 1997.

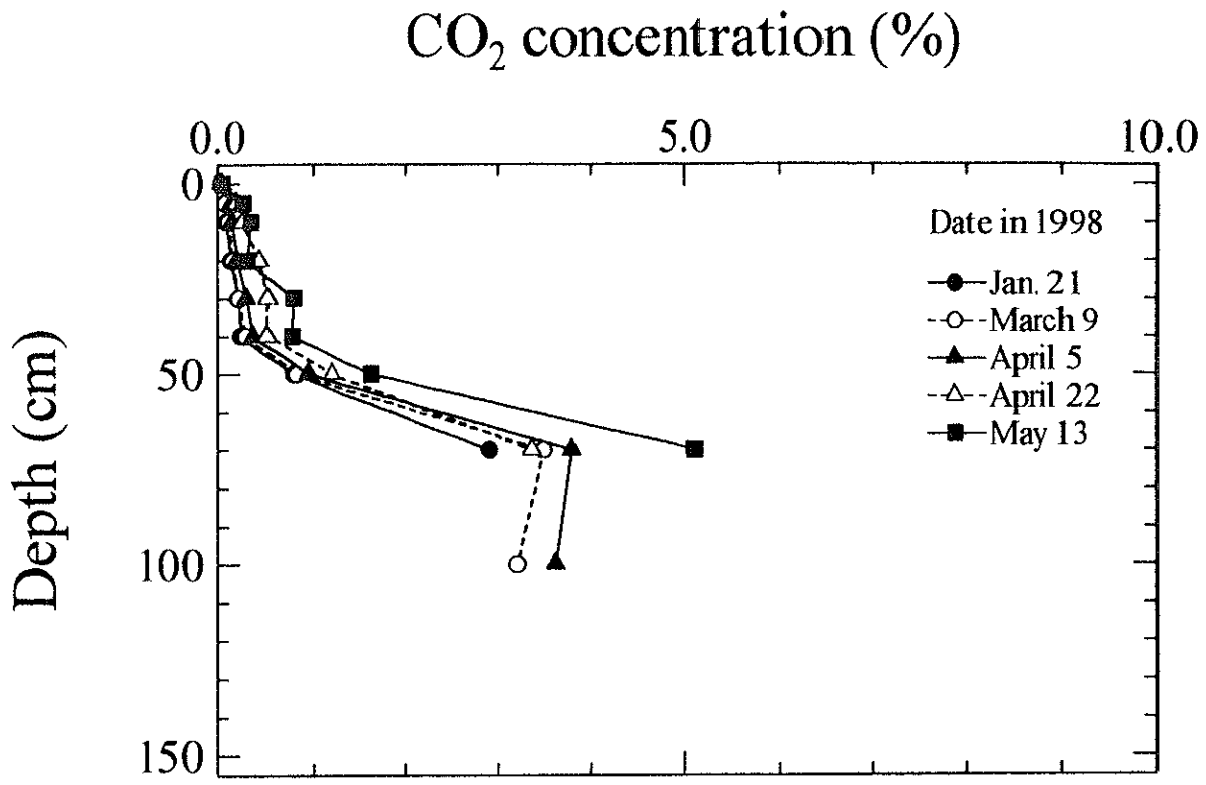

Figure 4.12c. Profiles of CO_2 concentration in soil air at the grassland site in 1998.

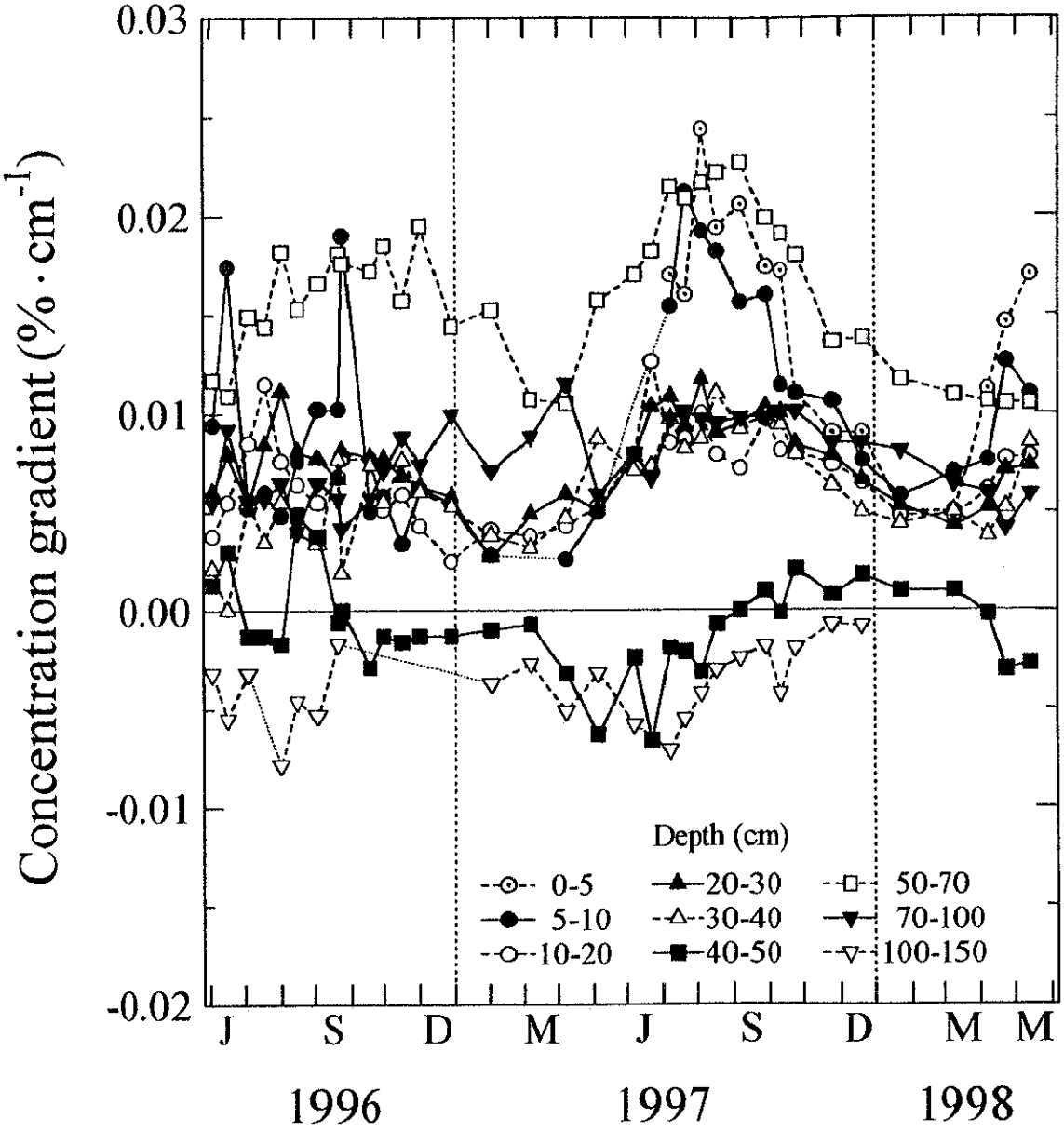

Figure 4.13. Seasonal variation of the concentration gradient of CO_2 in soil air at the forest site.

Upward gradients are shown in positive values.

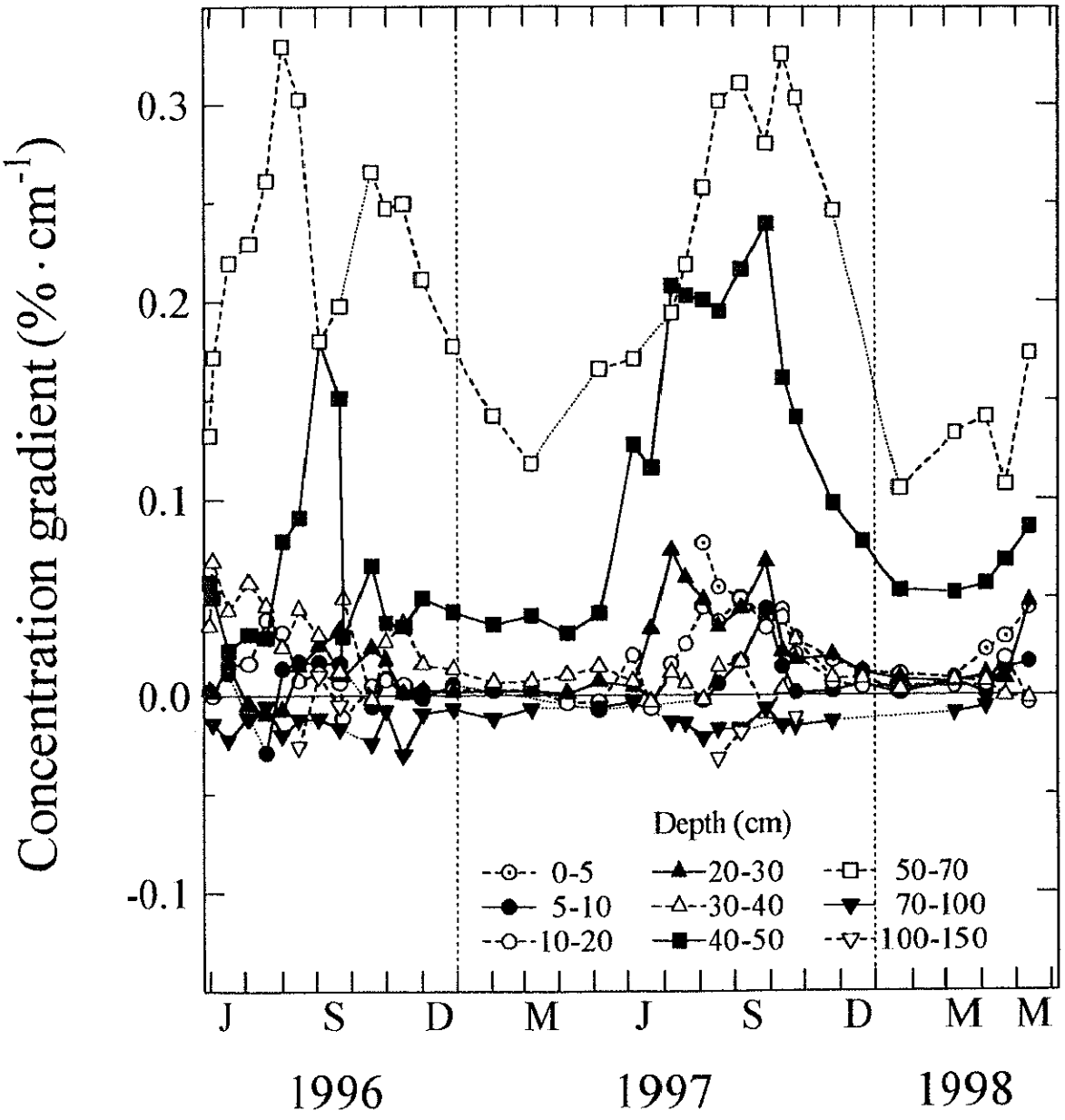

Figure 4.14. Seasonal variation of the concentration gradient of CO_2 in soil air at the grassland site.

Upward gradients are shown in positive values.

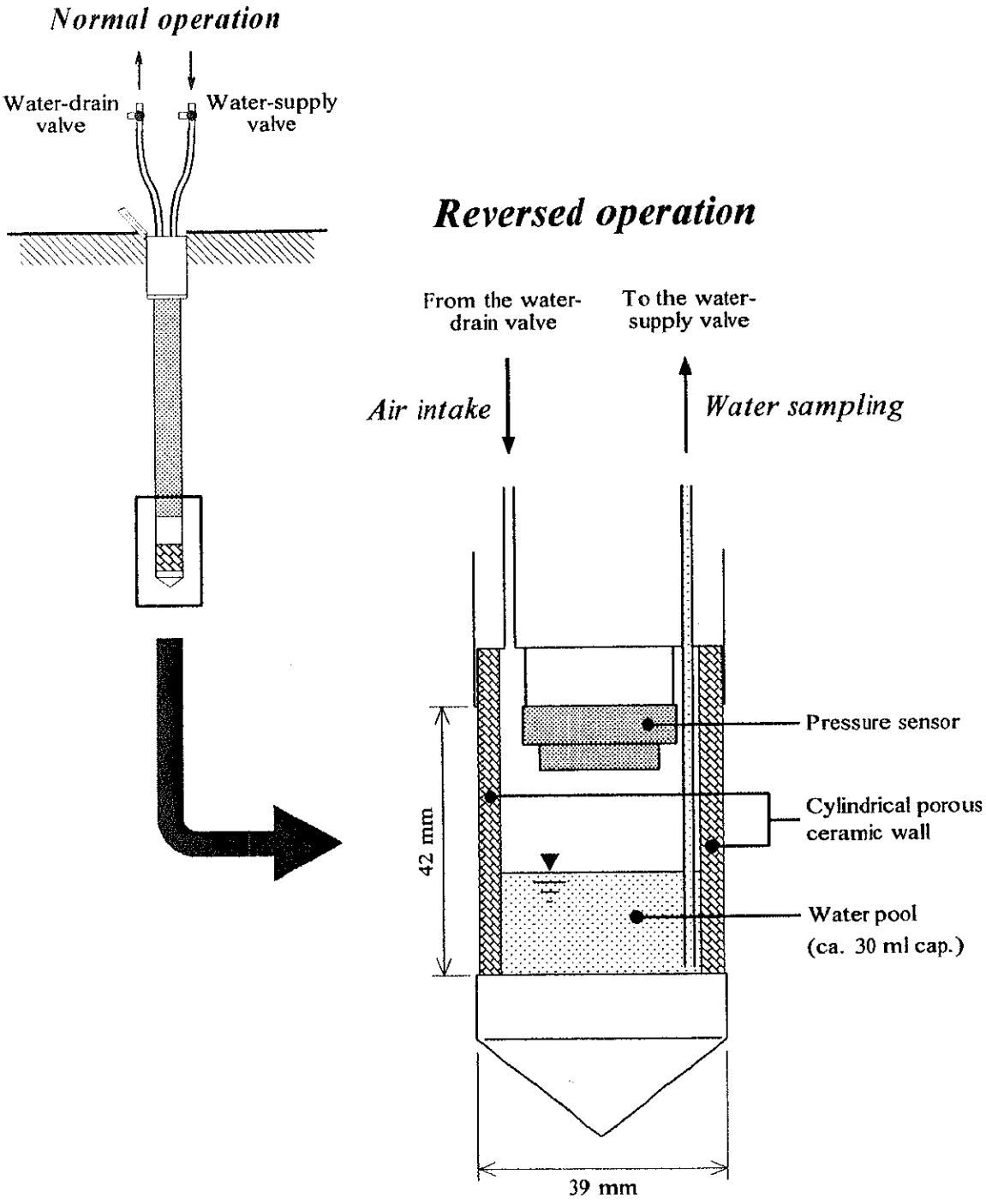

Figure 4.15. Diagram of the structure of the tensiometer (SK-5500E, Sankei Rika Co. Ltd.) used for the determination of pH in soil water and the operation of water sampling.

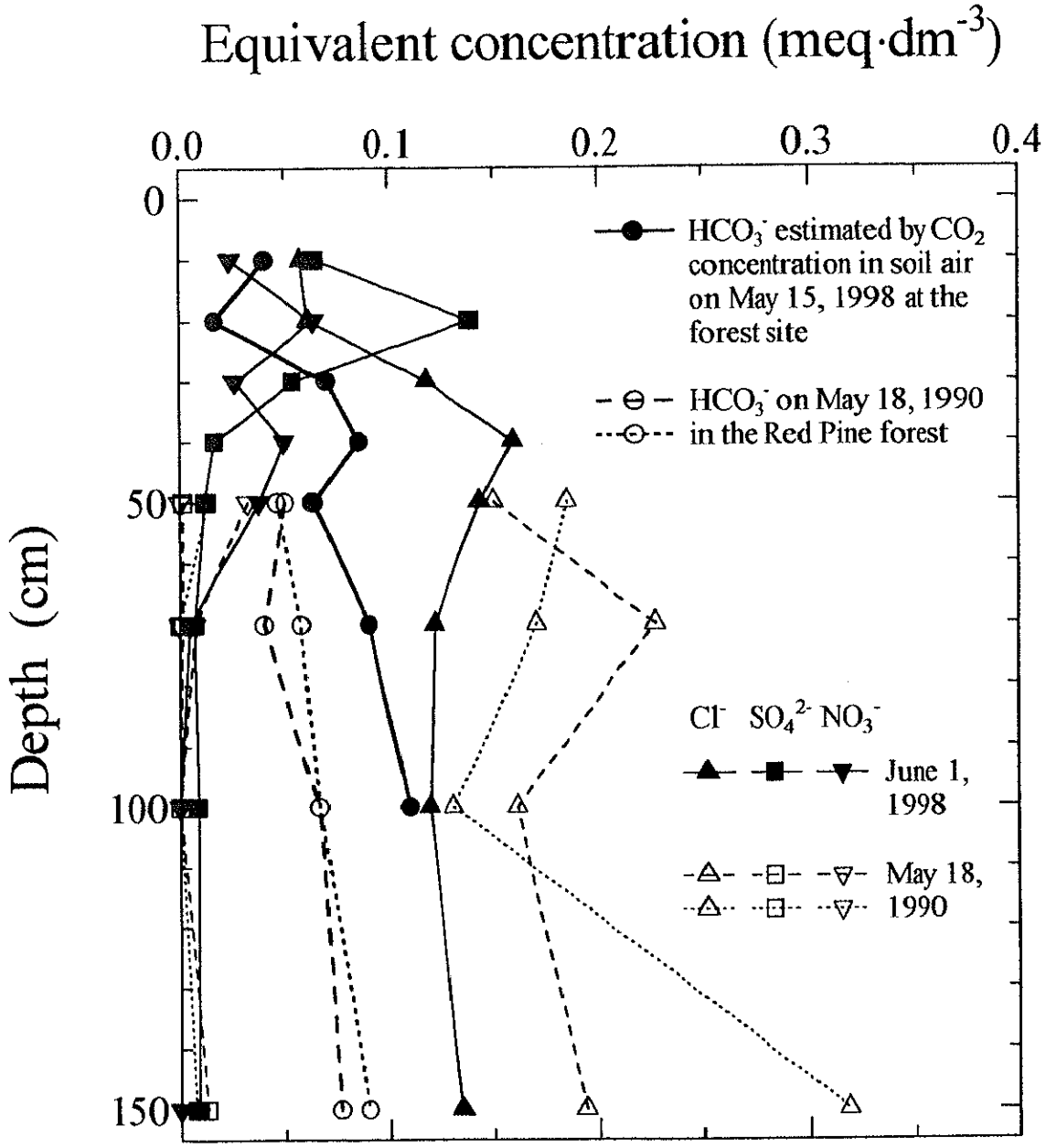

Figure 4.16. Comparison of the profiles of anion concentrations in the pooled water of the tensiometer at the forest site and those in soil water of the Red Pine forest.

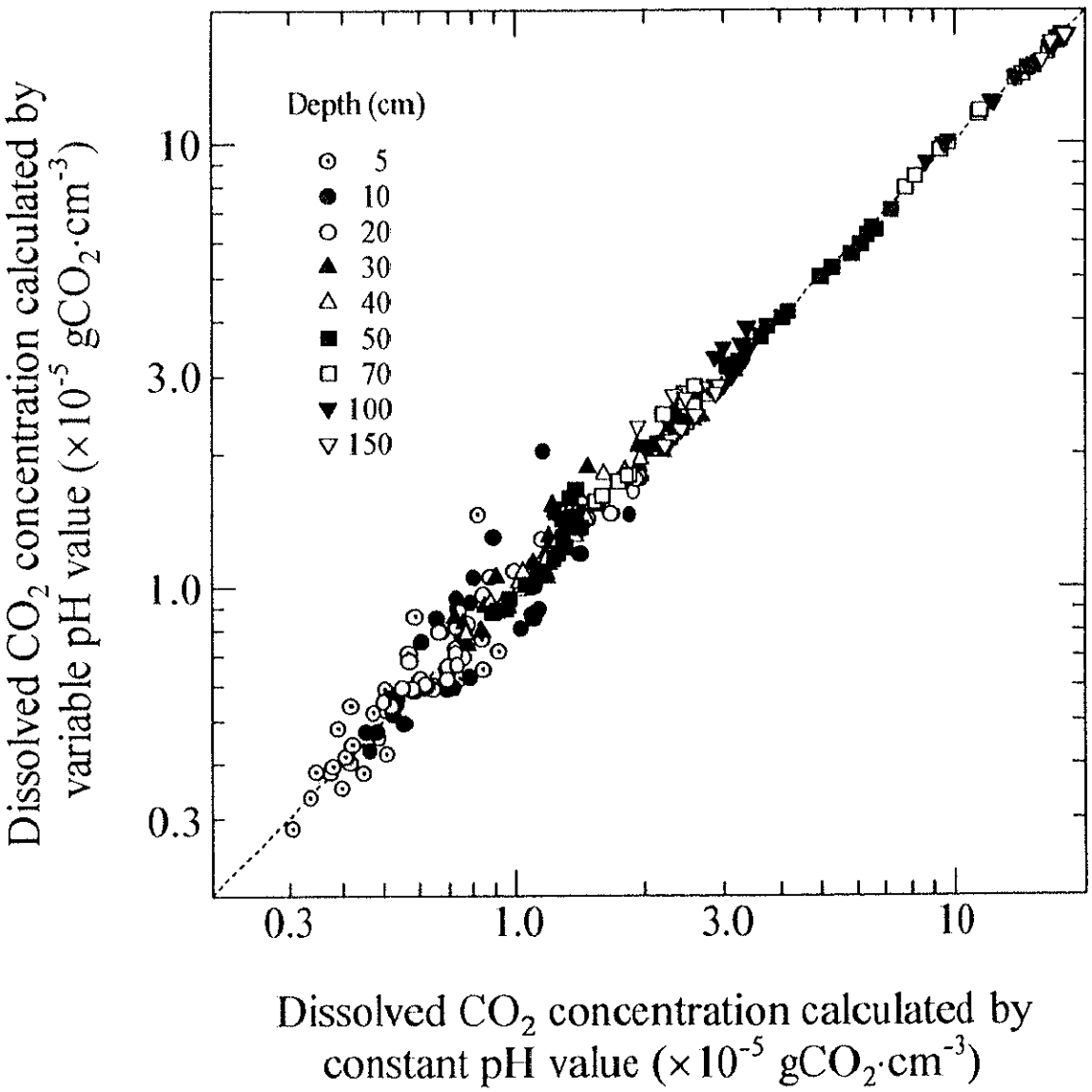

Figure 4.17. Comparison of dissolved CO_2 concentrations in soil water calculated by constant pH values averaged for each depth and those by seasonally variable pH values.

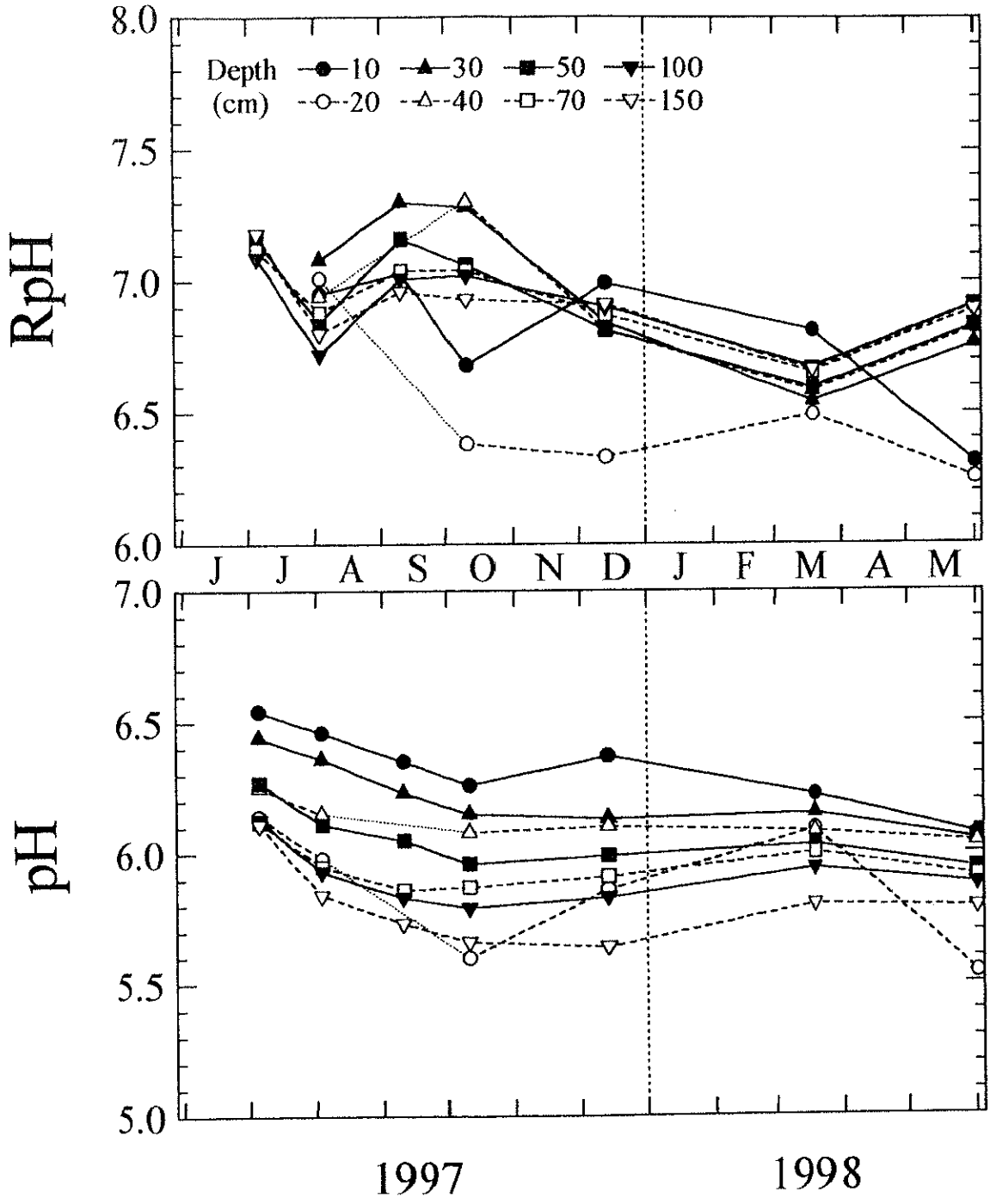

Figure 4.18. Seasonal variations of pH and RpH in soil water at the forest site.

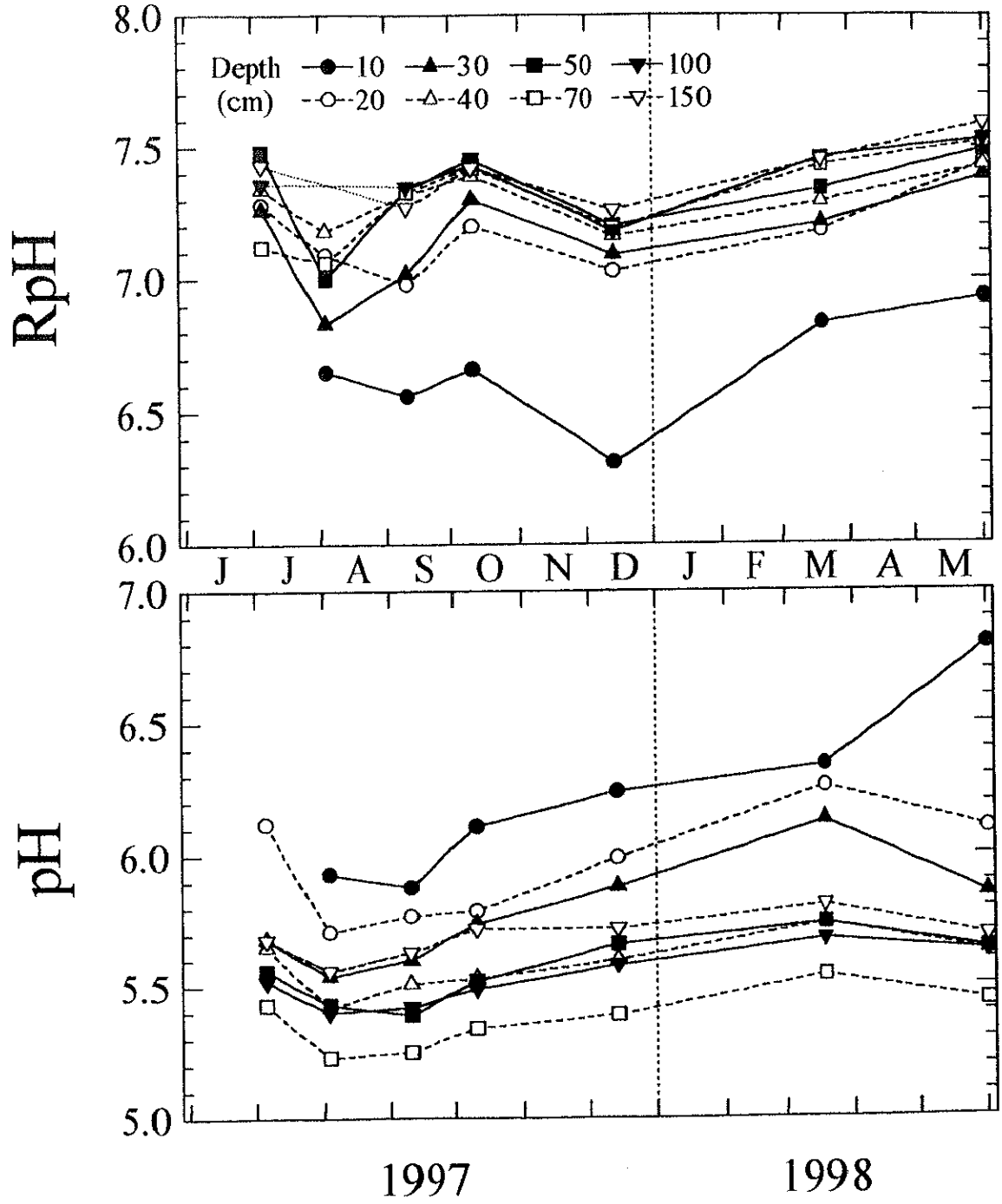

Figure 4.19. Seasonal variations of pH and RpH in soil water at the grassland site.

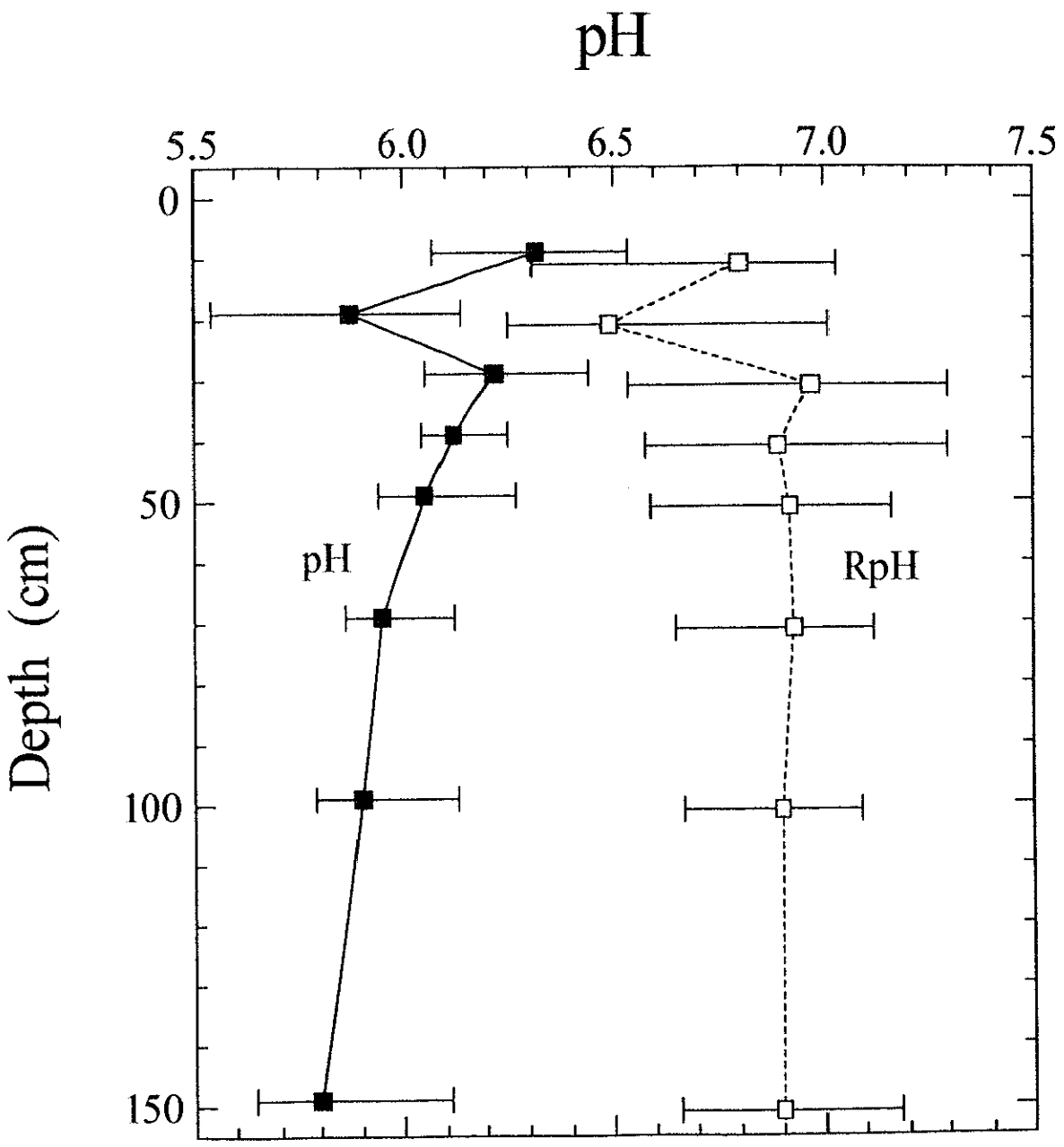

Figure 4.20. Profiles of the arithmetic mean values of pH and RpH in soil water at the forest site.

Error bars show the minimum and the maximum values at each depth.

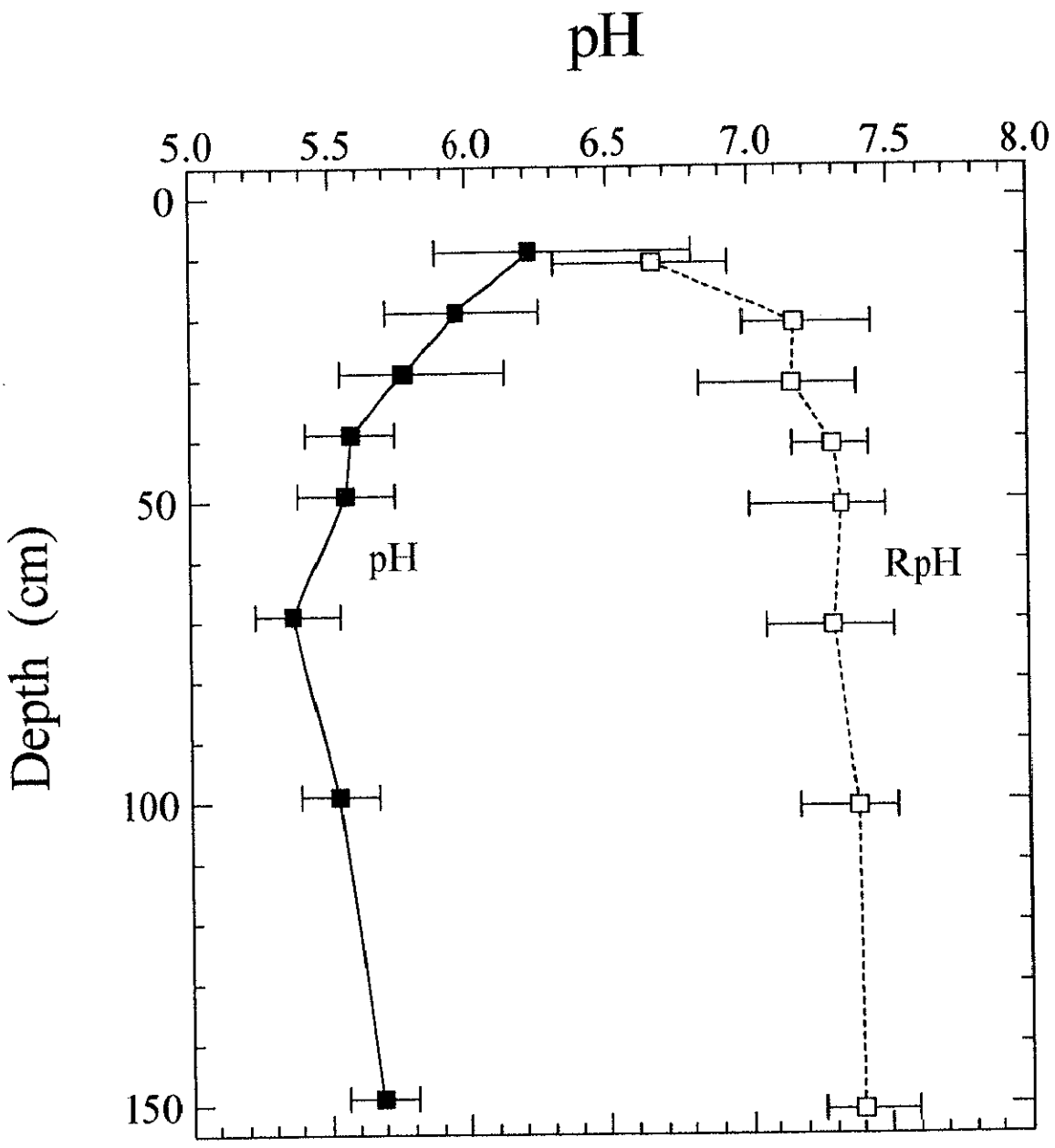

Figure 4.21. Profiles of the arithmetic mean values of pH and RpH in soil water at the grassland site.

Error bars show the minimum and the maximum values at each depth.

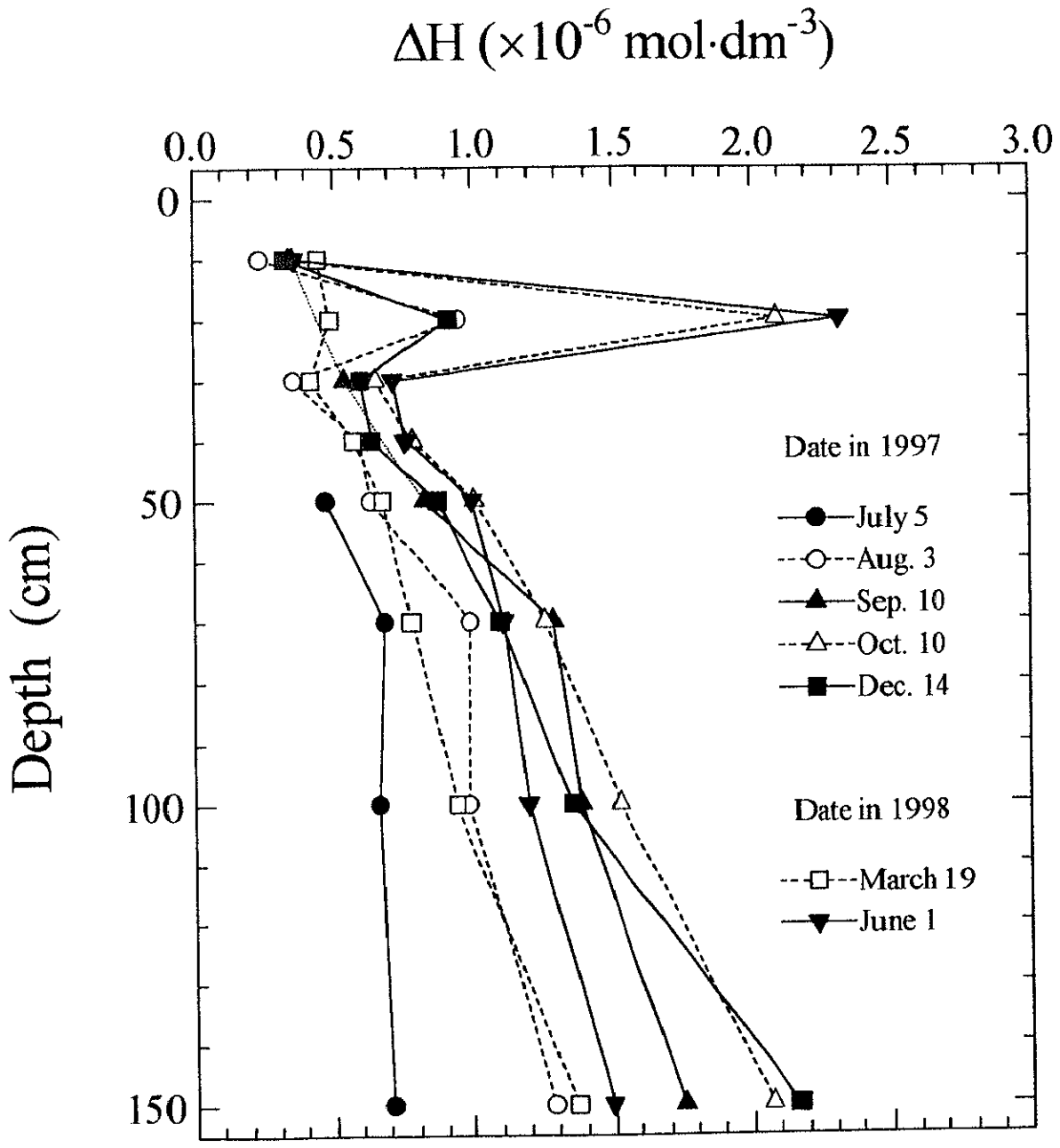

Figure 4.22. Profiles of the difference in proton content in soil water between before and after degassing dissolved CO_2 (ΔH) at the forest site.

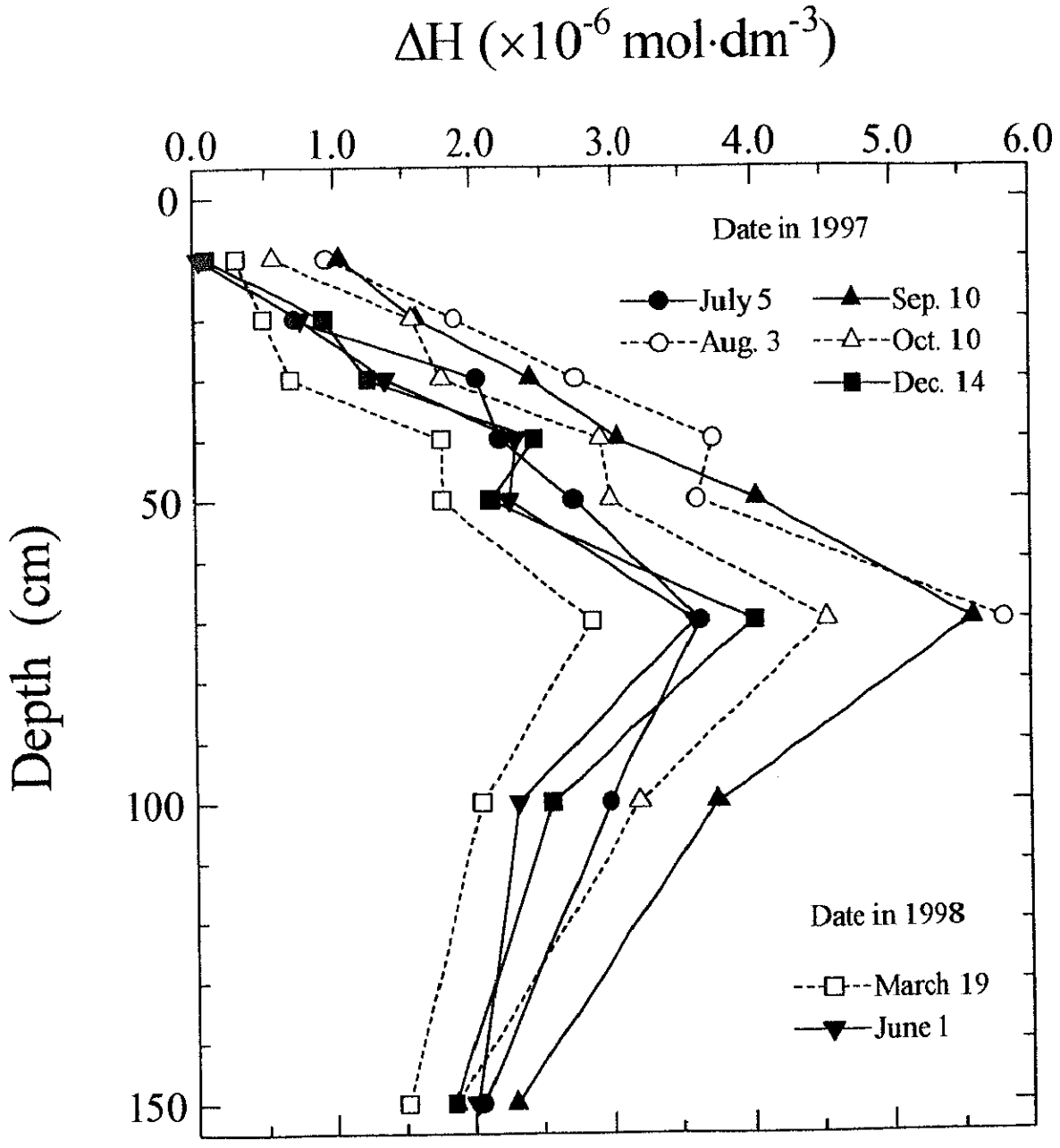

Figure 4.23. Profiles of the difference in proton content in soil water between before and after degassing dissolved CO_2 (ΔH) at the grassland site.

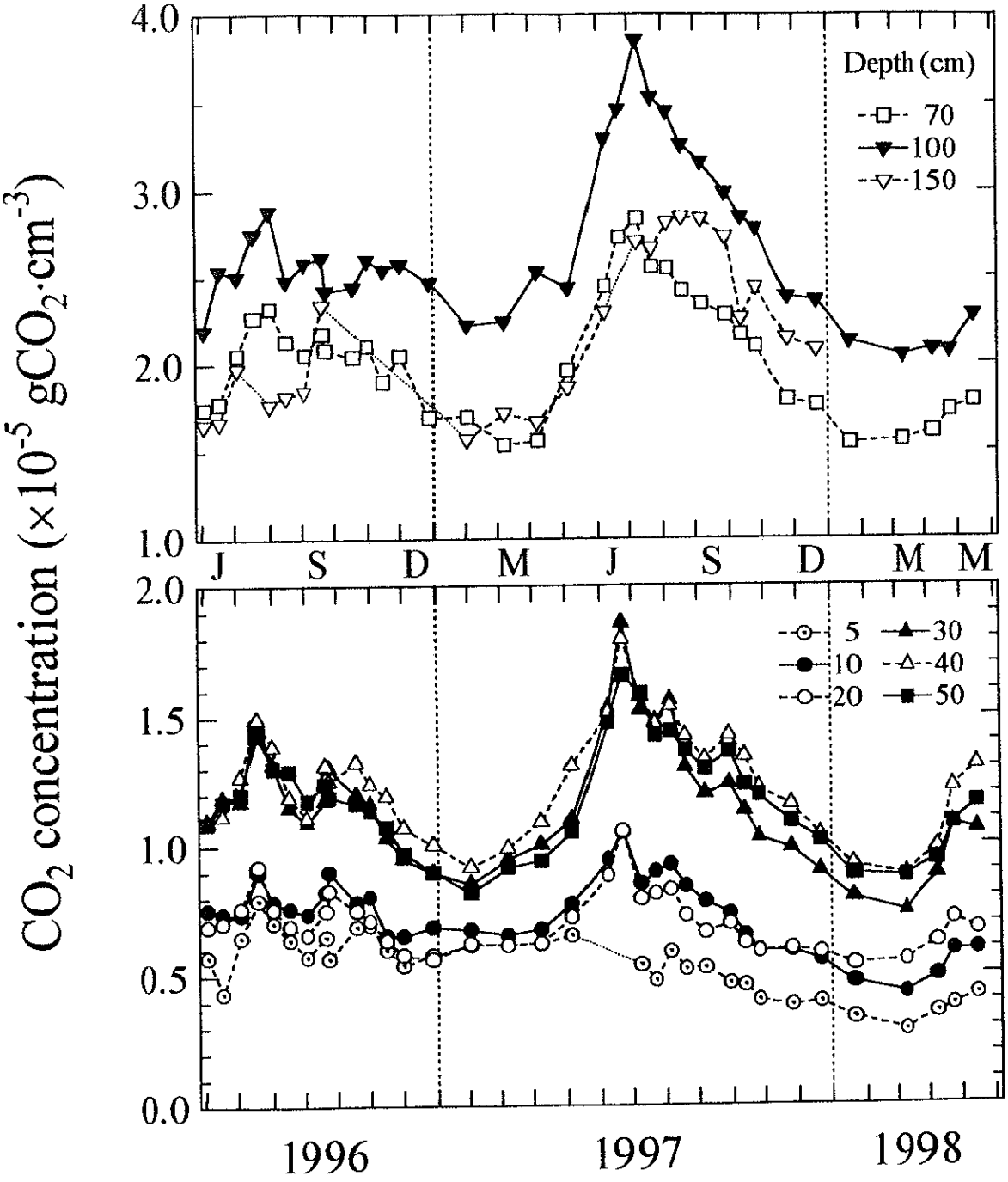

Figure 4.24. Seasonal variation of dissolved CO_2 concentration in soil water at the forest site.

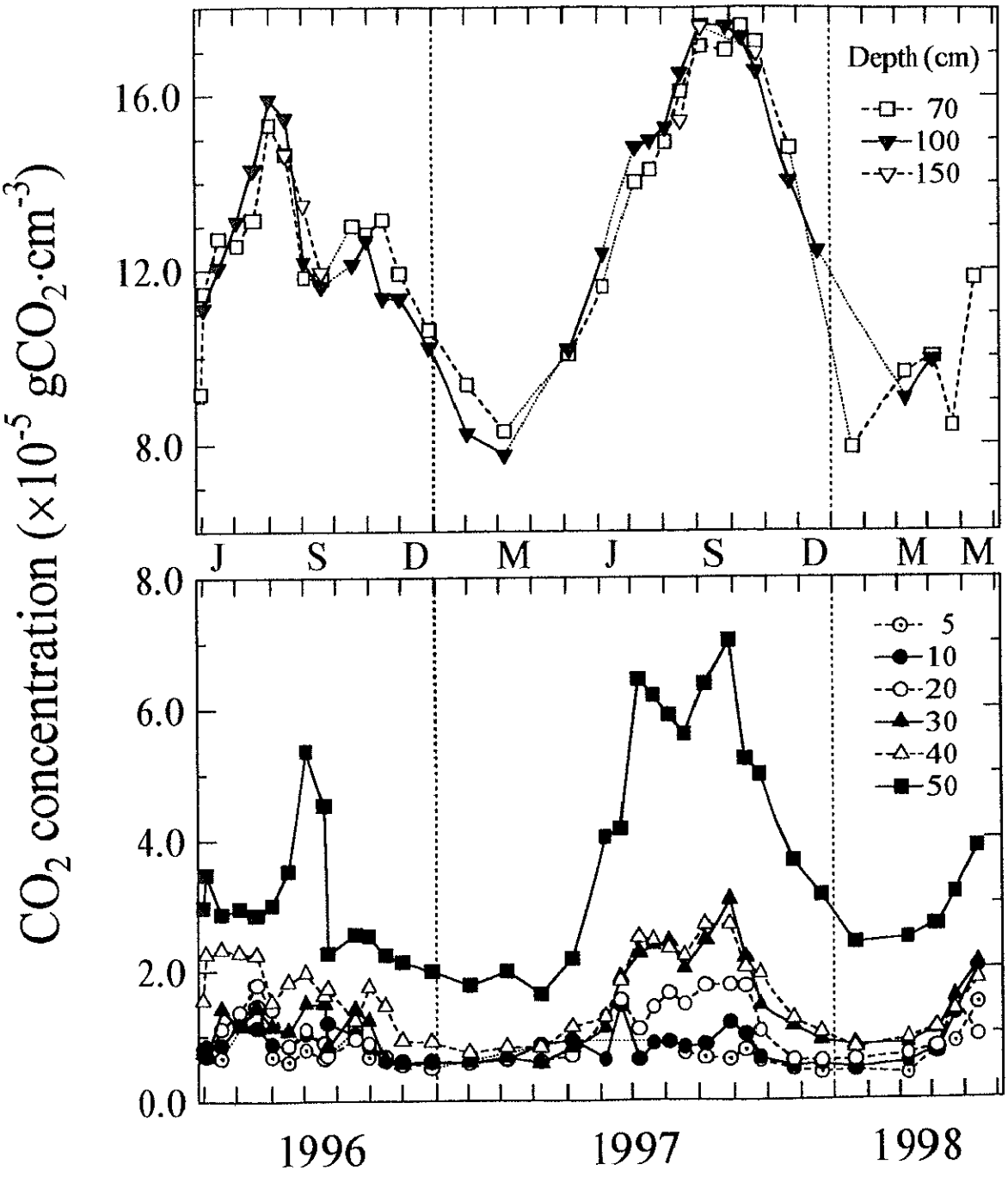

Figure 4.25. Seasonal variation of dissolved CO_2 concentration in soil water at the grassland site.

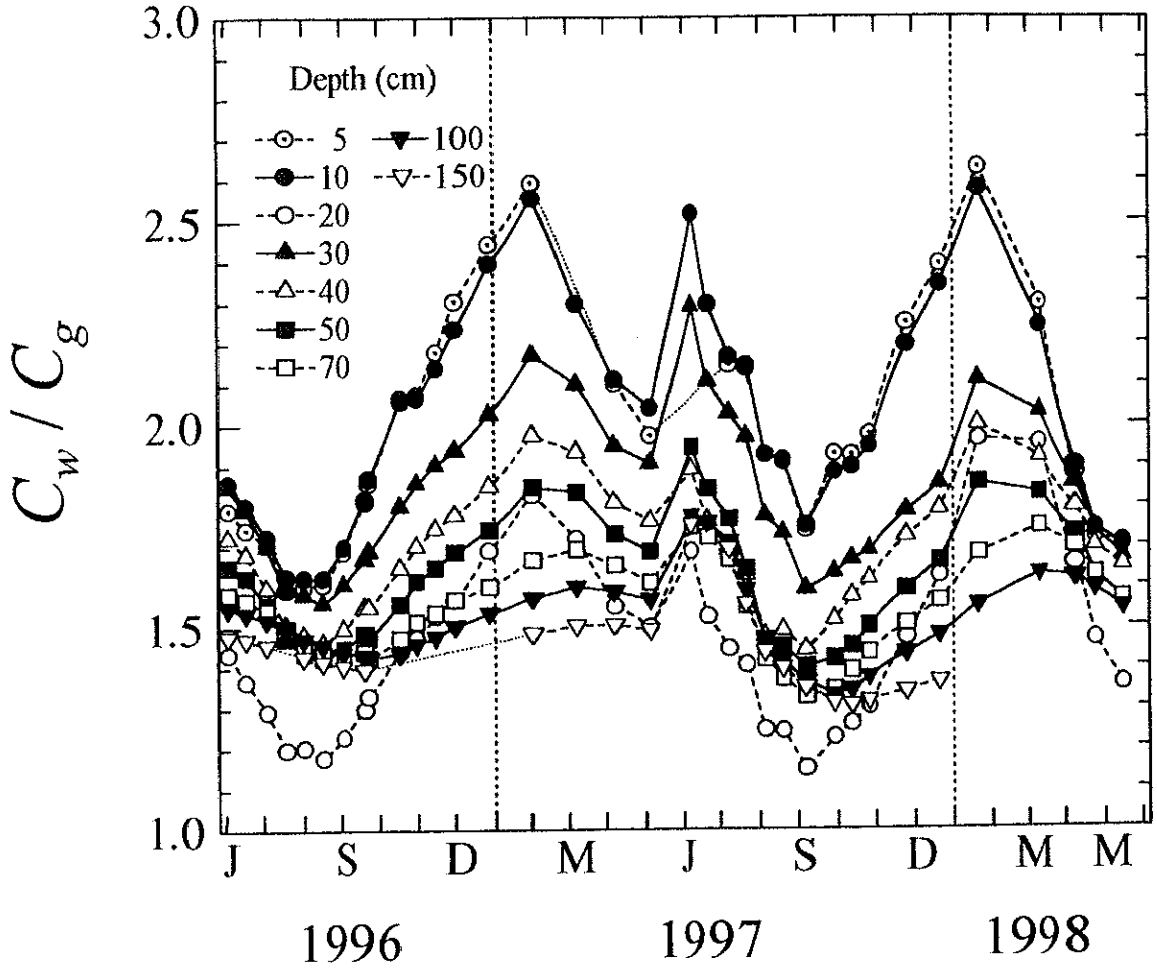

Figure 4.26. Seasonal variation of the ratio of CO_2 concentration dissolved in soil water (C_w) to that in soil air (C_g) at the forest site.

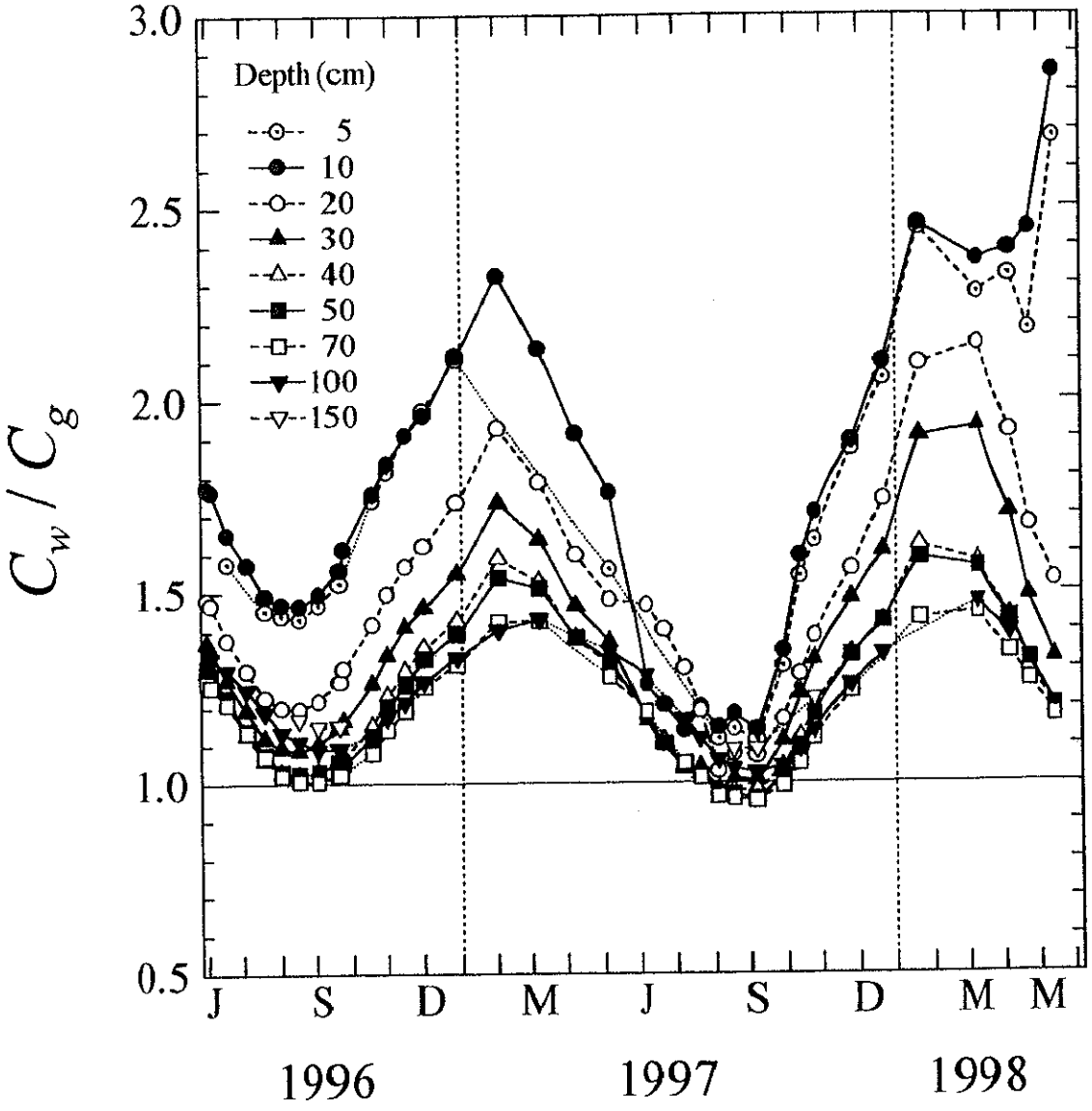

Figure 4.27. Seasonal variation of the ratio of CO_2 concentration dissolved in soil water (C_w) to that in soil air (C_g) at the grassland site.

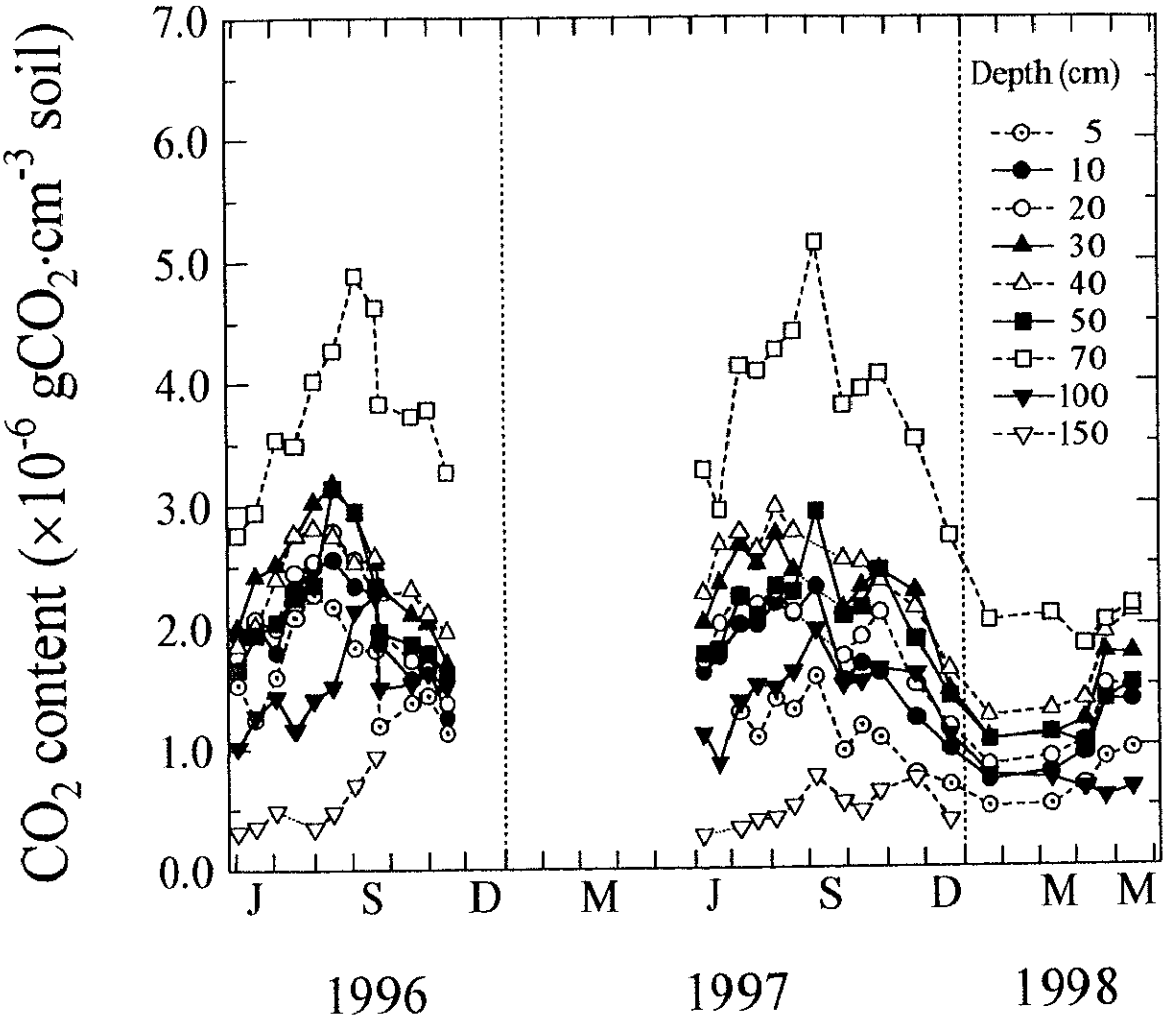

Figure 4.28. Seasonal variation of CO_2 content in gaseous phase per unit volume of bulk soil at the forest site.

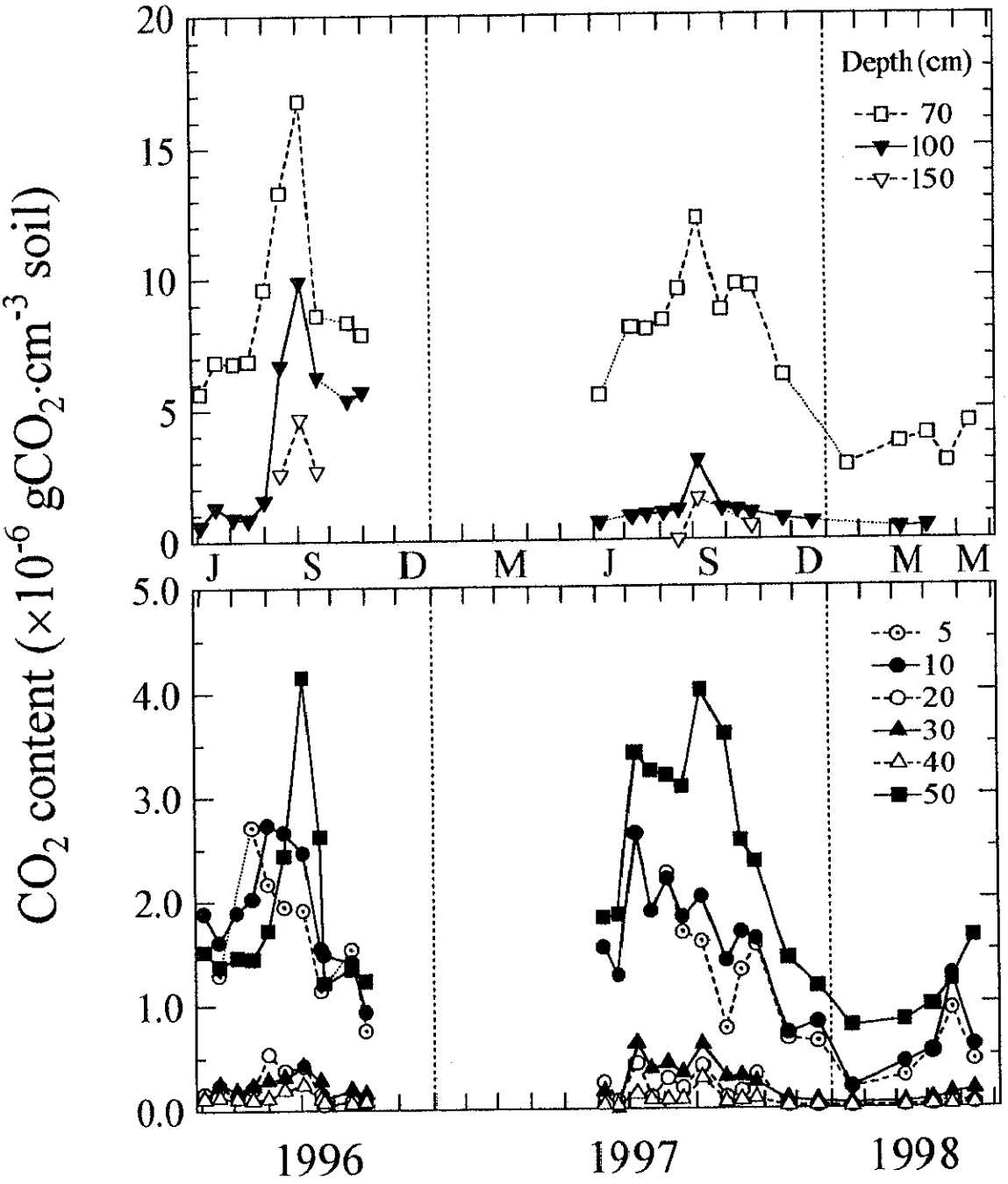

Figure 4.29. Seasonal variation of CO_2 content in gaseous phase per unit volume of bulk soil at the grassland site.

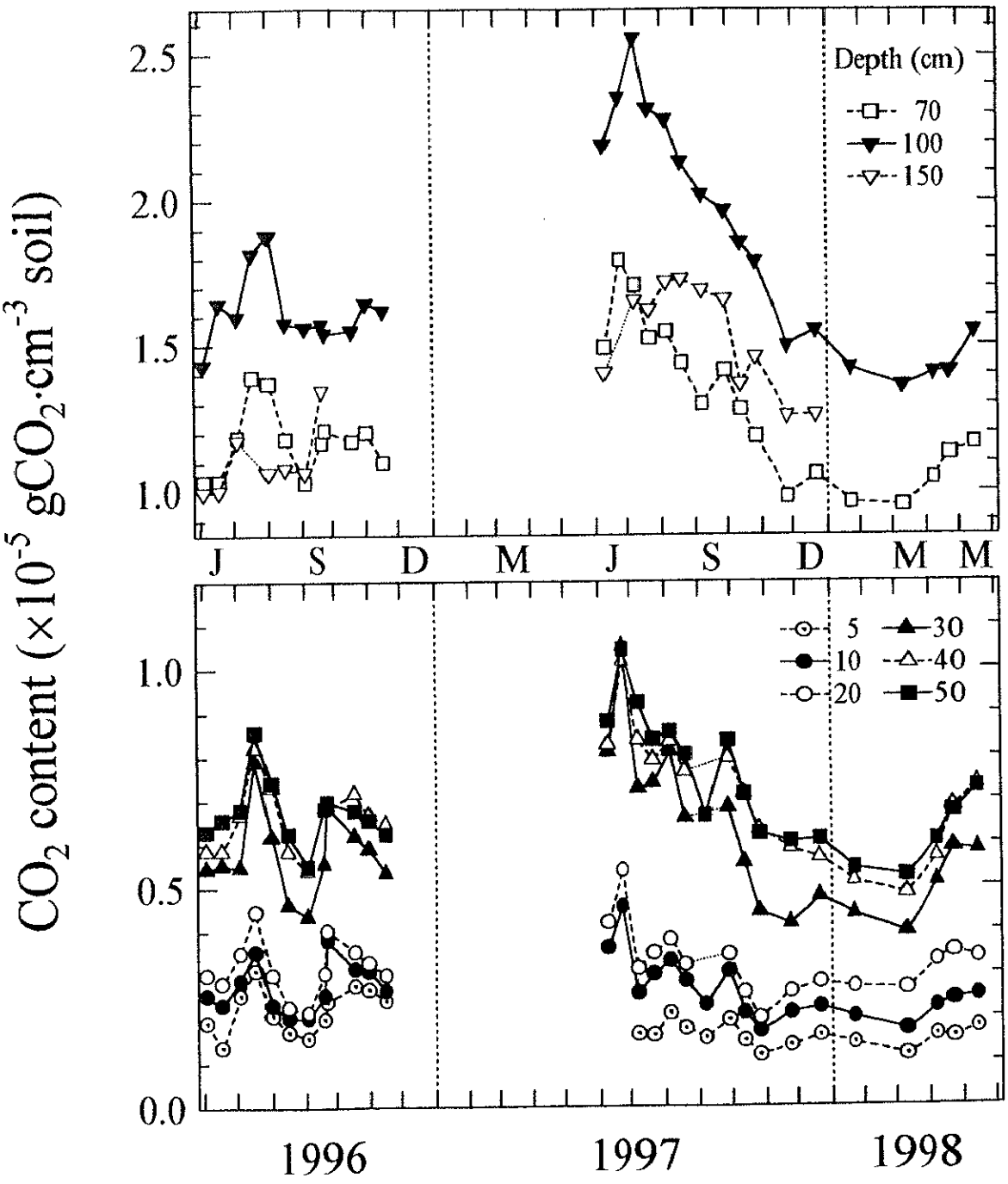

Figure 4.30. Seasonal variation of CO_2 content dissolved in liquid phase per unit volume of bulk soil at the forest site.

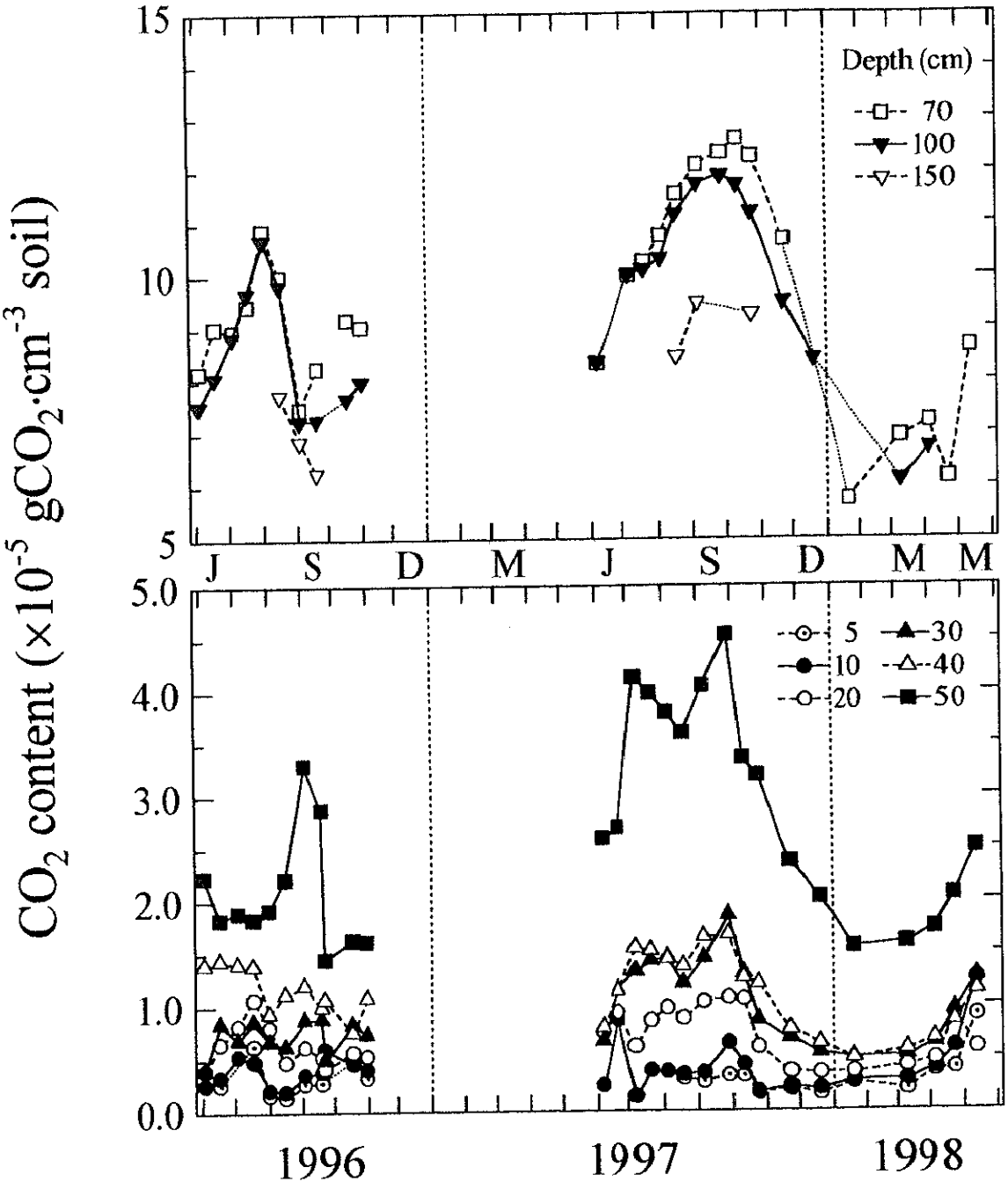

Figure 4.31. Seasonal variation of CO_2 content dissolved in liquid phase per unit volume of bulk soil at the grassland site.

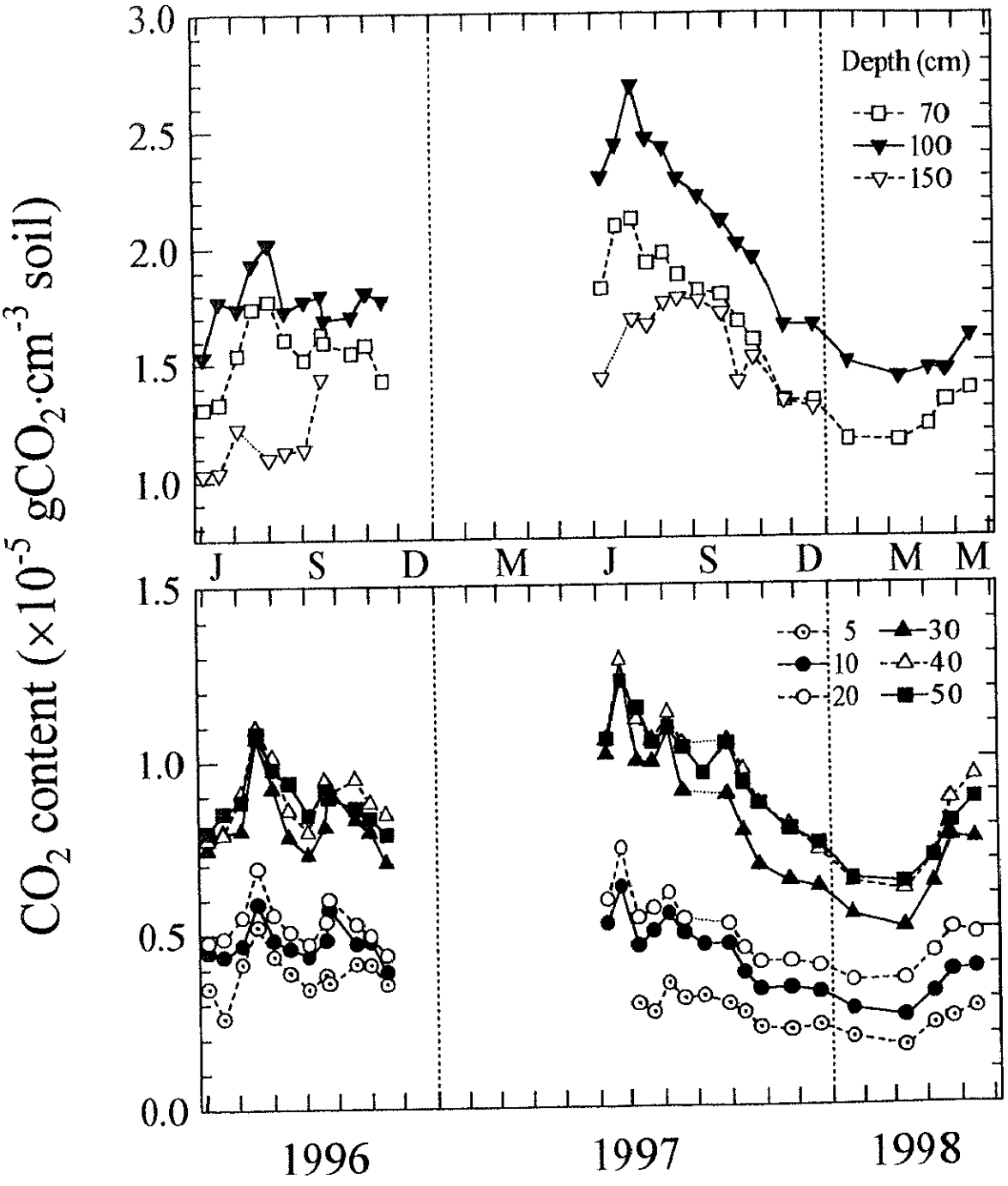

Figure 4.32. Seasonal variation of the total content of CO_2 per unit volume of bulk soil at the forest site.

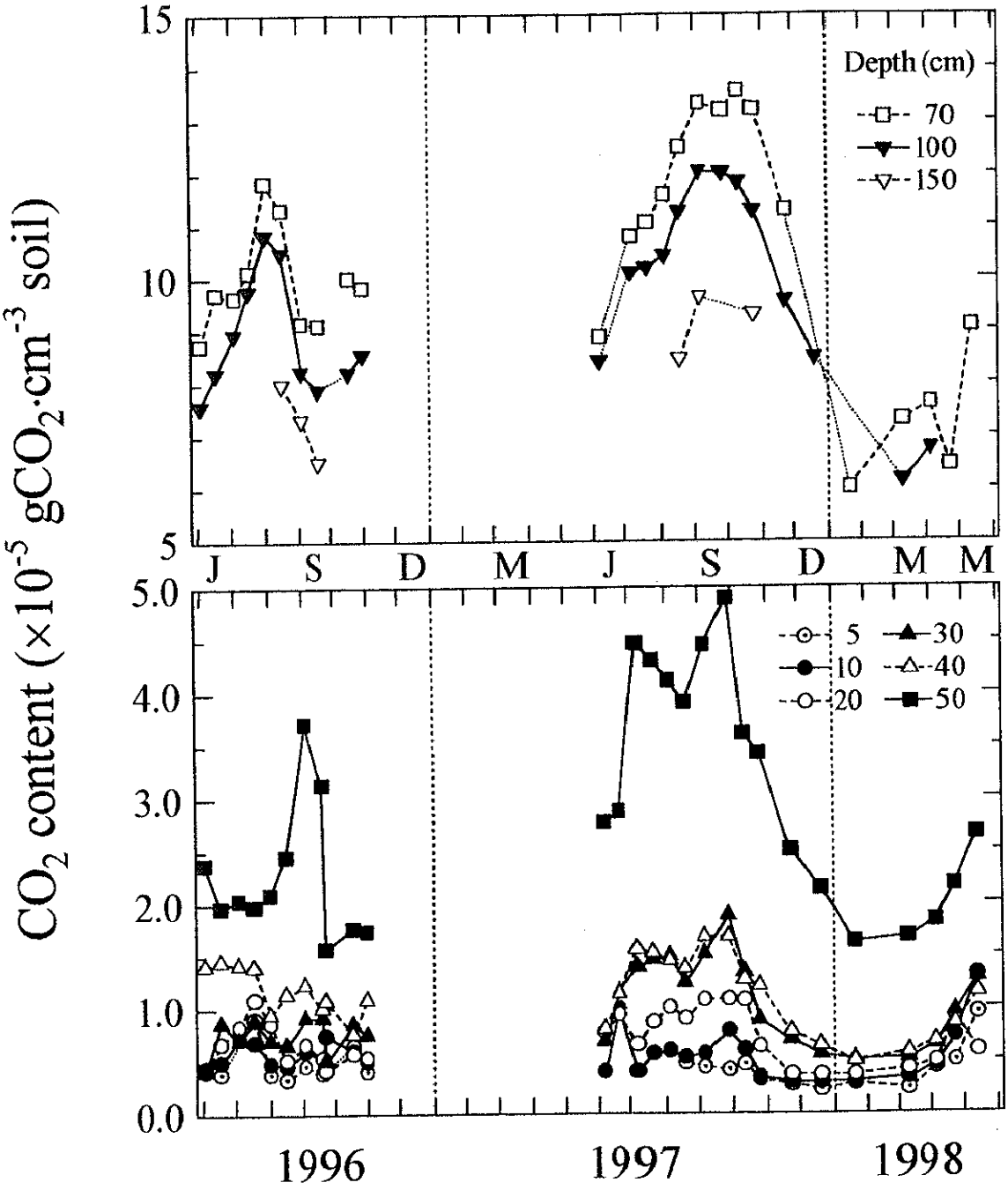

Figure 4.33. Seasonal variation of the total content of CO_2 per unit volume of bulk soil at the grassland site.

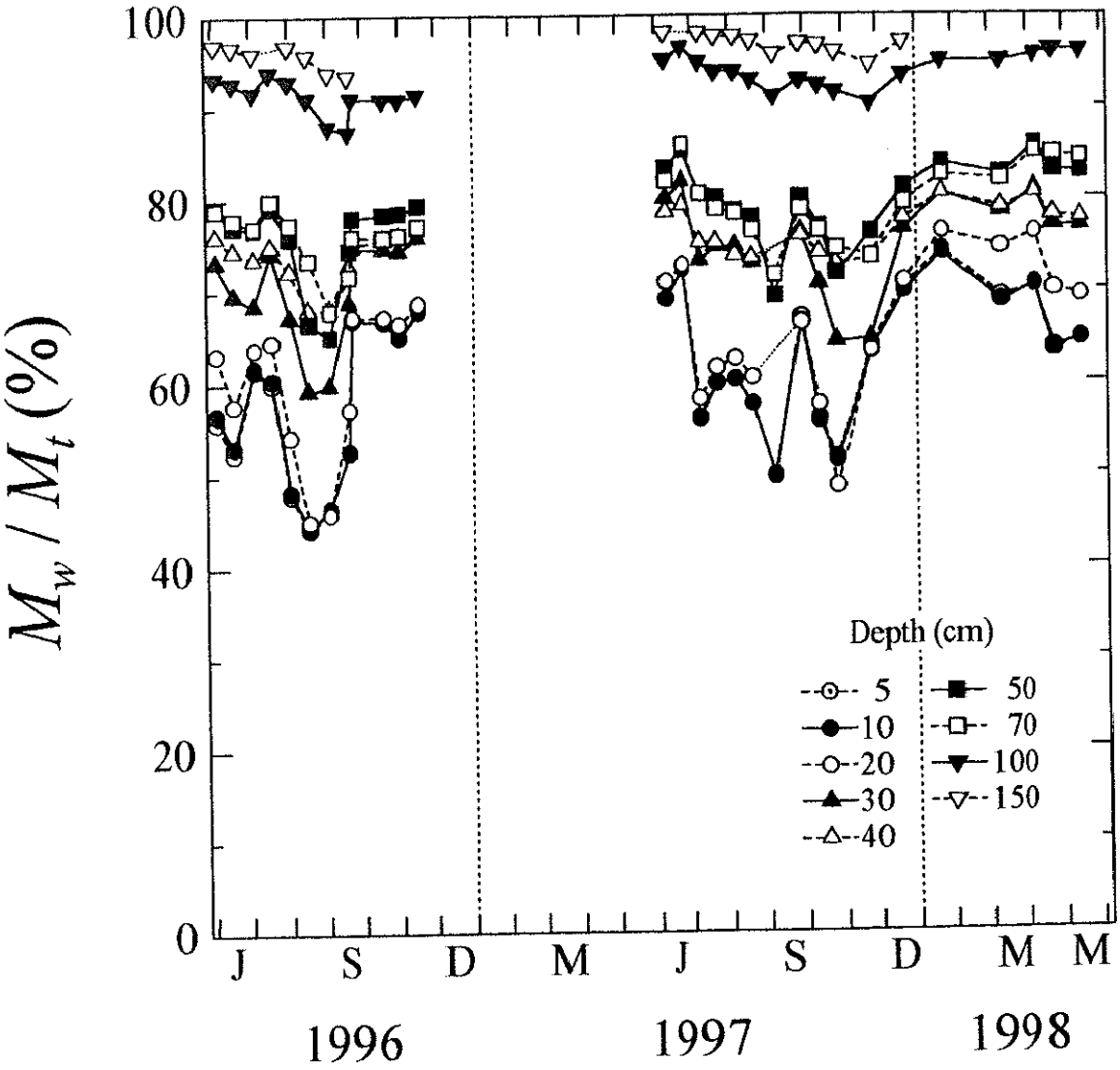

Figure 4.34. Seasonal variation of the proportion of CO_2 content in the liquid phase (M_w) to the total content (M_t) per unit volume of bulk soil at the forest site.

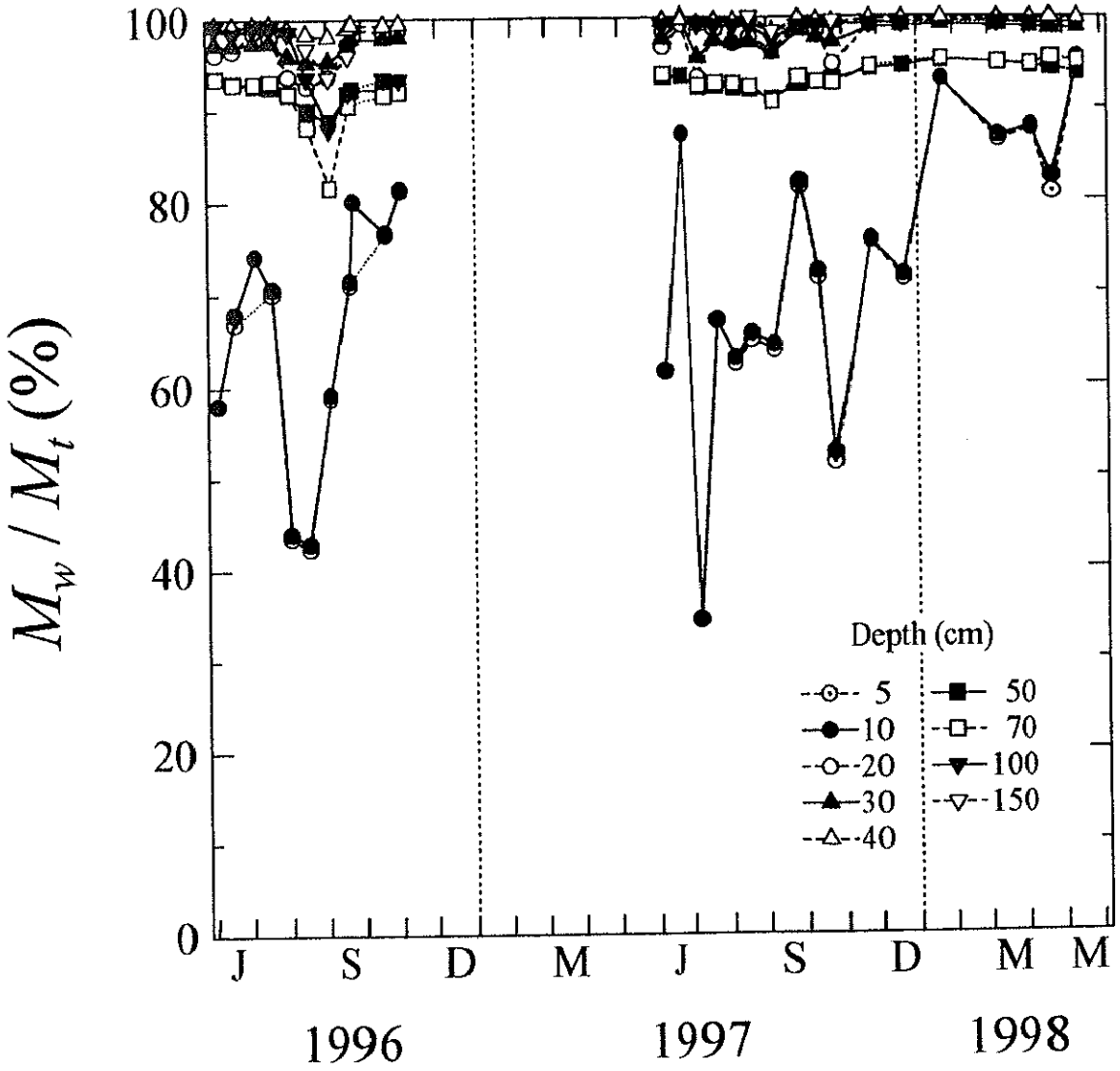

Figure 4.35. Seasonal variation of the proportion of CO_2 content in the liquid phase (M_w) to the total content (M_t) per unit volume of bulk soil at the grassland site.

Chapter 5

Production and Transport of Carbon Dioxide

5.1 Measurement of soil respiration rate

5.1.1 Methods

The rate of soil respiration, namely the amount of CO_2 which is transferred from the soil into the atmosphere across a unit area of the ground surface within a unit time, was observed for a whole year from June 1997 to May 1998. Two spots for measuring soil respiration rate were placed at each observation site. At the forest site, the one was placed at midmost among the Red Pine trees (hereinafter referred to as SR-F1) and the other at the foot of a Red Pine tree which had a diameter of 16.9 cm at the breast height (SR-F2). At the grassland site, a small space in a closed community of grass (SR-G1) and nearly bare soil surface (SR-G1) were selected as the measuring spots for soil respiration rate.

The rate of soil respiration was measured by a closed chamber method. A cylindrical closed chamber (21 cm in dia. and about 14 cm in height) equipped with a gas sampling port and a digital thermometer was used for the measurement. The design of and the schematic operation on the chamber are illustrated in Figure 5.1.

In advance of the measurement, the chamber was laid on its side adjacent to the measuring spot for two or three minutes and the air inside the chamber was mixed with the ambient air. At the beginning of measurement, the chamber was turned on the spot and immediately pushed into the soil by about 1 cm depth. After that, the air inside the chamber was collected from the gas sampling port with a syringe, for several times at intervals of two to three minutes. Before each sampling, some amount of the inside air was pulled out and pushed in using the syringe for several times to disturb and homogenize the inside air. At the same time, air temperature in the chamber was measured with the digital thermometer. The air collected into the syringe was immediately sampled into the T-type gas sampling glass tube (Figure 4.3) which had been

evacuated previously. After the sampling, CO_2 concentration in sampled air was determined by GC (see Section 4.1.1).

The concentration of CO_2 in the chamber, C_C ($gCO_2 \cdot cm^{-3}$), was calculated from CO_2 concentration in the sampled air (c_C, % in vol.) and temperature inside the chamber (T_C, K), by analogy with Equation 4.9:

$$C_C = \frac{m_{CO_2} \cdot P}{R \cdot T_C} \times c_C \times 10^{-2} \tag{5.1}$$

Then the total content of CO_2 in the chamber (M_C, gCO_2) was given as follows:

$$M_C = h_C \cdot A_C \cdot C_C \tag{5.2}$$

where h_C and A_C are the height (cm) and the bottom area (cm^2) of the inside of the chamber, respectively. For the chamber used in this study, they were 13.0 cm and 346.6 cm^2.

The amount of CO_2 contained in the chamber per unit area of the ground surface, namely M_C/A_C, was plotted against the time for sampling. For example, the result of the plot obtained for June 1, 1997 is shown in Figure 5.2. As indicated in the graph, the slope of the linear regression curve was regarded as the soil respiration rate ($gCO_2 \cdot cm^{-2} \cdot s^{-1}$).

It has been suggested that the closed chamber method have some possibilities for both overestimating and underestimating soil respiration rate. The rise in CO_2 concentration inside the chamber will inhibit the diffusive transport of CO_2 out of the soil. In addition, particularly at the grassland spots, air temperature inside the chamber was likely to increase with time; this might cause the increase in the inside air pressure and the corresponding mass flow of the air into the soil. These phenomena could act as the cause of underestimate of soil respiration rate. In fact, in the result shown in Figure 5.2, the increase in CO_2 concentration of SR-G2 was inhibited after six minutes from the beginning of the measurement. The effect of these phenomena becomes increasingly large with time, so that the measurement was usually completed within six minutes in this study.

On the other hand, sampling of air inside the chamber will reduce the inside air pressure, and then draw soil air into the chamber compulsorily. In turn, this could be a cause of overestimate of

soil respiration rate. Betsumiya (1992) reported on the effect of air sampling on the measured value of the rate. According to her result, the measured values by a closed chamber were in good agreement with those by a flow-through chamber, provided that each volume of the sampled air was less than 0.2% of the capacity of the chamber. If the sampling volume was more than 0.6% of the capacity, the closed chamber method overestimated soil respiration rate by 20%. In this study, the sampling volume of air inside the chamber was about 15 cm^3, equivalent to 0.33% of the capacity of the closed chamber of 4500 cm^3, therefore some overestimate might be occur.

In practice, these effects of the phenomena on the measured values of soil respiration rate depend on the magnitude of soil respiration itself, and micrometeorological factors such as wind speed and surface temperature. Moreover, the effects for overestimating and for underestimating the rate might more or less offset each other. The detailed discussion on the improvement and development of the method for measuring soil respiration rate deviates from the objective in this study, so this issue is no more discussed below.

5.1.2 Results and discussion

(1) Seasonal variation of soil respiration rate

The seasonal variations of soil respiration rate at the measuring spots in the forest and the grassland are shown in Figures 5.3 and 5.4, respectively. The values of the rate are expressed in the unit of daily mass flux of CO_2 per one square meter of the ground surface. Soil temperatures, measured at a depth of 5 cm in the forest and at 2 cm in the grassland, are also plotted.

At the forest site, soil respiration rates measured at both spots were high in the summer and low in the winter, corresponding to the soil temperature at a depth of 5 cm. The maximum rates were obtained in late June and early July of 1997 and reached 18.1 and 17.3 $gCO_2 \cdot m^{-2} \cdot day^{-1}$ at SR-F1 and SR-F2, respectively. The minimum rates were recorded in January 1998 at both spots and were 0.24 at SR-F1 and 0.22 at SR-F2. Thus, the difference in the soil respiration rates between both spots was not significant.

In the Red pine forest, Yasui and Oikawa (1993) have measured soil respiration rate using a flow-through chamber method. According to their results, the rate ranged from 0.5 to 12.1 $gCO_2 \cdot m^{-2} \cdot day^{-1}$ and showed large values in the summer and small values in the winter, similar to the soil respiration rate observed in this study. Although the maximum rate presented by Yasui and Oikawa (1993) was relatively lower than those obtained in this study, this was probably due

to the lack of measurement from mid-July to mid-August in their observation, when soil respiration rates higher than the measured maximum rate might have been observed because of the high temperatures in the period, rather than due to the difference in methodology.

At the grassland, the maximum values of soil respiration rate were obtained about a month later than those at the forest and reached 27.2 and 11.3 $gCO_2 \cdot m^{-2} \cdot day^{-1}$ at SR-G1 and SR-G2, respectively. In January 1998, the minimum rate of 0.13 $gCO_2 \cdot m^{-2} \cdot day^{-1}$ was obtained at SR-G1, but a negative value was evaluated at SR-G2, so that the rate was regarded as zero. The soil respiration rates observed at SR-G1 was about 1.5 to 4.5 times as high as those at SR-G2, and the values were equal to or larger than those at SR-F1 and SR-F2. Therefore, the rate measured at SR-G2 was always lower than the rates at the forest spots. Relative to the forest spots, soil respiration rates showed sensitive fluctuations in response to the change in micrometeorological conditions at the grassland spots.

(2) Relationship between soil respiration rate and soil temperature

As shown in Figures 5.3 and 5.4, the seasonal variations of soil respiration rate at the forest and the grassland spots were almost similar to the variations of soil temperature near the ground surface. Thus the relationships between soil respiration rate and soil temperature at both sites are plotted in Figures 5.5 and 5.6. As expected from the seasonal variation, the soil respiration rates generally increased with the soil temperatures. At the forest site, soil respiration rates measured at both spots similarly increased corresponding to rising soil temperature. On the other hand, the response of soil respiration rate observed at SR-G2 to the rise in soil temperature was more gradual than the response at SR-G1.

The results of the regression analysis on the relationships are listed in Table 5.1. The regression curves obtained from the analysis are also plotted in Figures 5.5 and 5.6. The soil respiration rates were well expressed as exponential functions of the soil temperature. The regression analyses using linear and parabolic functions were also carried out, but the correlation was less significant. The coefficients of determination at the forest spots were 0.90 and 0.88, indicating high correlation between the soil respiration rate and the soil temperature. At the grassland spots, the coefficients of determination were 0.87 and 0.47, lower than those at the forest spots.

5.2 Evaluation of the fluxes of carbon dioxide in a soil profile

5.2.1 Methods

(1) Definition of a virtual soil column

In contrast to CO_2 flux across the ground surface, which is given as soil respiration rate, the rate of CO_2 transport at any depths in a soil profile cannot be measured directly. The fluxes of CO_2 in a soil profile, therefore, were evaluated from the analysis of CO_2 transport processes in the profile using the soil physical properties given in Chapter 3, and the concentrations and contents of CO_2 and the environmental factors obtained in Chapter 4. For the analysis, a horizontally homogeneous soil was assumed for the observation sites and only vertical CO_2 transport was considered.

As a framework for the analysis of the fluxes and mass balance of CO_2, a virtual soil column was defined, with reference to the similar framework applied in de Jong and Schappert (1972). The diagram of the column is illustrated in Figure 5.7. The column has a unit bottom area and consists of several soil compartments, and each compartment has a depth number d which ranges from 0 to N. Physical or chemical variables of the compartment d are represented by the values determined at a depth of z_d, which is placed in the center of the compartment. The soil compartment d is divided from the upper (d–1) and the lower (d+1) compartment at the middle depth of z_{d-1} and z_d and the middle depth of z_d and z_{d+1}, respectively. By way of exceptions, the depths of the upper division of the compartment 0 and the lower division of the compartment N are defined as z_0 and z_N, respectively. The thickness of the compartment d, l_d, is given by the difference between the depths of the upper and lower divisions of the compartment.

The values of the parameters of the virtual soil column applied to the analysis are listed in Table 5.2. All the depths at which CO_2 concentration in soil air was measured were given as z_d, from the ground surface to a depth of 150 cm. In addition, the divisions of the compartments were partly modified to conform with the real conditions: The soil compartment 0 represents the ground surface, has no thickness, and gives the upper boundary condition of the virtual soil column; the soil compartment 1 ranges from the surface to a depth of 7.5 cm and reflects the values determined for a depth of 5cm. Using the virtual soil column, the analysis of the fluxes and mass balance of CO_2 was carried out for the whole year from June 1997 to May 1998, namely the second half of the observation period in this study, because of the continuous

measurements of the pressure head of soil water (Section 4.1) and soil respiration rate (Section 5.1) in the second-half period.

(2) Diffusive flux of carbon dioxide in soil air

In principle, the flux of molecular diffusion in gaseous phase obeys Fick's first law. Thus the vertical diffusive flux of CO_2 in soil air, J_d ($gCO_2 \cdot cm^{-2} \cdot s^{-1}$), is described as follows:

$$J_d = -D_s \frac{dC_g}{dz} \tag{5.3}$$

where D_s is the diffusion coefficient of CO_2 in soil air ($cm \cdot s^{-1}$), C_g is the concentration of CO_2 in soil air ($gCO_2 \cdot cm^{-3}$) and z is depth (cm). The negative sign in the right side of Equation 5.3 indicates that the CO_2 will diffuse from the depths of the higher concentrations to the depths of the lower. The diffusion coefficient in soil air is a function of the coefficient in free air, D_a, which is given by:

$$D_a = D_0 \frac{P_0}{P}\left(\frac{T}{T_0}\right)^n \tag{5.4}$$

where P and T are the total pressure (hPa) and temperature (K) of the air, and the subscript 0 refers to the standard state, namely P_0 and T_0 are 1013 hPa and 273.16 K (equivalent to 0°C), respectively. The D_0 is the diffusion coefficient of CO_2 at the standard state and n is an empirical constant, and both of them have characteristic values for CO_2.

The diffusive flux of CO_2 in soil profiles were evaluated by applying Equation 5.3 to the soil sections which consist of couples of the soil compartments adjacent to each other in the virtual soil column. The diffusive transport of CO_2 between the compartments d–1 and d was given by the mean diffusive flux in the soil section between depths of z_{d-1} and z_d. The diffusive flux was calculated from the difference in CO_2 concentration and the averaged diffusion coefficient between these depths. Therefore, the diffusive flux of CO_2 in soil air between the soil compartments d–1 and d, $J_d(d\text{–}1, d)$, was obtained by rearranging Equations 5.3 and 5.4 as follows:

$$J_d(d-1,d) = -D_s(d-1,d)\frac{C_g(d)-C_g(d-1)}{z_d - z_{d-1}} = -\xi(d-1,d)\,D_a(d-1,d)\frac{C_g(d)-C_g(d-1)}{z_d - z_{d-1}} \tag{5.5}$$

$$D_a(d-1,d) = D_0\frac{P_0}{P}\left(\frac{T_{d-1}+T_d}{2T_0}\right)^n \tag{5.6}$$

where $C_g(i)$ and T_i are the concentration of CO_2 in soil air and the soil temperature at a depth of z_i; $D_s(i,j)$, $D_a(i,j)$ and $\xi(i,j)$ represent the diffusion coefficients of CO_2 in soil air and in free air, and the relative diffusion coefficient, respectively. Referred to Nakano (1991), the values of 0.135 cm·s^{-1} and 1.71 were applied to D_0 and n, respectively. The relative diffusion coefficient is defined as the ratio of the diffusion coefficient in soil air to that in free air, namely D_s/D_a, and described below.

(3) Determination of the relative diffusion coefficient

The diffusion coefficient in soil air is smaller than that in free air, since soil particles and soil water will cut off and lengthen the pathways for diffusion in soil air. Thus the relationships between the relative diffusion coefficient, D_s/D_a, and soil physical properties such as air-filled porosity and total porosity have been investigated in many studies.

For example, Penman (1940) showed a simple relationship between D_s/D_a and air-filled porosity (θ_g):

$$D_s / D_a = 0.66\,\theta_g \tag{5.7}$$

On the other hand, Millington and Quirk proposed more complex relationships, expressed as functions of air-filled porosity and total porosity, θ_t (Millington, 1959; Millington and Quirk, 1961):

$$D_s / D_a = \frac{\theta_g^{10/3}}{\theta_t^2} \tag{5.8}$$

$$D_s / D_a = \frac{\theta_g^2}{\theta_t^{2/3}} \tag{5.9}$$

Other relationships between D_s/D_a and θ_g and/or θ_t similar to these equations have been presented by many researchers (e.g. Blake and Page, 1948; van Bavel, 1952; Marshall, 1959; Currie, 1960; 1961), but the relationships which have been mainly used for estimating D_s/D_a are the three equations mentioned above. Hereinafter, these equations are referred to as the Penman (Equation 5.7), and M-Q 1 (Equation 5.8) and M-Q 2 (Equation 5.9) equations, from the names of proposers. The relationships between D_s/D_a and the air-filled porosity and total porosity of the soil are shown in Figure 5.8.

To select the equation used for estimating the diffusion coefficient in soil air in this study, the utility of the three equations was examined. The averaged diffusive fluxes of CO_2 between the ground surface and a depth of 5 cm were calculated from Equations 5.5 and 5.6, using the relative diffusion coefficients estimated by each equation, and then compared with the rates of soil respiration obtained in Section 5.1, because the soil respiration is mostly caused by the diffusive transport of CO_2. The results of the comparison at the forest and the grassland site are indicated in Figures 5.9 and 5.10, respectively. The diffusive fluxes are plotted after converted to the same unit of the soil respiration rate ($gCO_2 \cdot m^{-2} \cdot day^{-1}$).

During the period for the comparison, the largest value of the diffusion coefficient in soil air was always estimated by the Penman equation, the next by M-Q 2, and the least by M-Q 1. At the forest site, the evaluated diffusive fluxes of CO_2 using the Penman equation were in good agreement with the measured rates of soil respiration, but sometimes exceeded the rates. The values of the flux evaluated by the M-Q 2 equation were slightly less than the measured values of soil respiration rate, in contrast to those by the Penman. For the M-Q 1 equation, the evaluated fluxes were nearly equal to or even lower than the half of the soil respiration rates. At the grassland site, in many cases, the diffusive fluxes of CO_2 evaluated by the Penman were higher than the soil respiration rates measured at SR-G1, while the fluxes evaluated by the M-Q 1 were lower than the rates measured at SR-G2. For the M-Q 2, the evaluated fluxes were similar to the measured rates at either of the spots or intermediate between the rates at both spots.

Soil respiration rate is a CO_2 flux at the ground surface. On the other hand, the diffusive flux of CO_2 evaluated for the soil section between depths of 0 and 5 cm represents the averaged flux

for these depths. In practice, the production of CO_2 would occur between these depths, so that the CO_2 flux at the ground surface became larger than the averaged flux by the amount of CO_2 produced between these depths. Considering the CO_2 production, it was suggested that the diffusive flux of CO_2 evaluated by the M-Q 2 equation best agreed with the real flux.

Actually at both sites, the differences between the evaluated flux by the M-Q 2 and the measured rates of soil respiration were relatively large from spring to summer in 1997, when the soil temperatures near the ground surface were higher than those in deep soils (Figures 4.7 and 4.8), and were small from autumn to winter. This can be explained as follows: From spring to summer, the production rates of CO_2 at depths between the ground surface to 5 cm were high due to the high temperatures, so that the difference between the soil respiration rate and the averaged CO_2 flux between 0 and 5 cm became large; from autumn to winter, the production rates are low due to the low temperatures, so that the difference between them became small. In addition, Jin and Jury (1996) also compared the D_s/D_a estimated by the same three equations with the experimentally determined values of D_s/D_a, and found that the estimated values by the M-Q 2 equation provided significantly better agreement with the measured values. According to these results, the M-Q 2 equation was used for estimating the diffusion coefficient in soil air in this study.

Consequently, $\xi(d-1, d)$ in Equation 5.5 was given by:

$$\xi(d-1,d) = \frac{\theta_g(d-1,d)^2}{\theta_t(d-1,d)^{2/3}} \tag{5.10}$$

where $\theta_g(i, j)$ and $\theta_t(i, j)$ represent air-filled porosity and total porosity averaged for the adjacent depths of z_i and z_j. At depths of 0 and 5 cm, the values of air-filled porosity and total porosity are assumed to be equal to the values at 10 cm.

Finally, by substituting all the related equations into Equation 5.5, the diffusive flux of CO_2 in soil air at the soil section between depths of z_{d-1} and z_d was obtained by the following equation:

$$J_d(d-1,d) = -\frac{[(\theta_g(d-1)+\theta_g(d))/2]^2}{[(\theta_t(d-1)+\theta_t(d))/2]^{2/3}} D_0 \frac{P_0}{P}\left(\frac{T(d-1)+T(d)}{2T_0}\right)^n \frac{C_g(d)-C_g(d-1)}{z_d - z_{d-1}} \tag{5.11}$$

(4) Advective flux of carbon dioxide accompanied by the mass flow of soil air

Essentially, the mass flow flux of soil air is given as the product of the total pressure gradient and the aeration coefficient. Because of the little difference in total pressure in a soil profile, however, it is difficult to evaluate the mass flow flux precisely using this method.

On the other hand, temporal and spatial distributions of air-filled porosity was obtained in this study using soil water characteristic curves (Figures 3.3 and 3.4) and the measured values of the pressure head of soil water (Figures 4.7 and 4.8), and showed fairly large variations in response to the patterns of precipitation and evapotranspiration. These variations of air-filled porosity will cause the mass flow of soil air. Furthermore, soil temperatures at all the depths also varied largely, so that the expansion and shrinking of soil air corresponding to the change in soil temperature might cause the mass flow. Thus, in this study, the advective flux of CO_2 accompanied by the mass flow of soil air caused by the changes in air-filled porosity and soil temperature was evaluated.

In the case of the passage of a front, however, rapid temporal change in the atmospheric pressure would occur and might cause relatively large mass flow of soil air by the total pressure gradient. In this study, however, most of the measurements of CO_2 were carried out on fine days, so that the effect of the change in the atmospheric pressure was probably small. The convective flow of soil air due to the temperature gradient in the soil profiles and the turbulent flow caused by wind were also not taken into consideration because of the difficulty of quantitative analysis of them. In the cases that these effects on the mass flow of soil air became important, the advective flux of CO_2 evaluated in this study becomes less reliable.

To evaluate the mass flow flux of soil air and the accompanied advective flux of CO_2 in soil profiles, the virtual soil column defined above was applied as the framework for analysis. If a soil compartment which has a thickness l shows the values of air-filled porosity of $\theta_g(t_1)$ at a time of t_1 and $\theta_g(t_2)$ at a time of t_2, the change in the volume of gaseous phase in the compartment between t_1 and t_2 is given by:

$$\Delta V_{\theta_g} = l \cdot \theta_g(t_2) - l \cdot \theta_g(t_1) \tag{5.12}$$

On the other hand, the volume of soil air itself initially contained in the compartment also changes in response to the change in soil temperature, provided that the total pressure of the air

is kept constant. Therefore, for the same compartment, if the soil temperature and the volume of soil air changed from T_{t_1} and V_{t_1} to T_{t_2} and V_{t_2} between t_1 and t_2, the volumetric change of soil air itself is given by:

$$\Delta V_T = V_{t_2} - V_{t_1} = l \cdot \theta_g(t_1) \times \left(\frac{T_{t_2}}{T_{t_1}} - 1 \right) \tag{5.13}$$

From Equations 5.12 and 5.13, the net change in the volume of gaseous phase in the compartment between t_1 and t_2 is obtained:

$$\Delta V_{\text{net}} = \Delta V_T - \Delta V_{\theta_g} = l \left[\theta_g(t_1) \frac{T_{t_2}}{T_{t_1}} - \theta_g(t_2) \right] \tag{5.14}$$

By this net volumetric change, the total pressure of soil air will change unless the net inflow or outflow of soil air on the soil compartment occurs, whereas the total pressure gradient of soil air is negligible under conditions without remarkable source or sink of a gas, wetting front and redistribution of soil water (Nakano, 1991). To keep the total pressure of soil air constant, the mass flow into or out of a soil compartment must occur by the amount equivalent to the net decrease ($\Delta V_{\text{net}} < 0$) or increase ($\Delta V_{\text{net}} > 0$) of the volume of gaseous phase in the compartment. For example, if the volumetric increase of gaseous phase according to the increase in air-filled porosity exceeds the volumetric increase of soil air itself in response to the rise in soil temperature, the remainder must be replenished by the inflow of equivalent volume of soil air from the upper and lower compartments.

The mass flow flux of soil air between each pair of the soil compartments in the virtual soil column was calculated by accumulating the net change in the volume of gaseous phase at each compartment. The lower boundary of the column is placed at a depth of 150 cm, where the soil was nearly saturated and the volume of gaseous phase was little (Figures 3.1 and 3.2); so that it was assumed that the mass flow flux of soil air across the lower boundary of the column was not occurred. According to the assumption, the net increase or decrease in the volume of gaseous phase in the soil compartment N, the bottom of the column, causes the mass flow of soil air out of or into the upper compartment N–1. Therefore, the mass flow flux of soil air between the

compartments d–1 and d was given by the accumulation of the net change in the volume of gaseous phase in the compartments from d to N.

In addition, the soil air which moves among the compartments changes its volume in response to the difference in soil temperature. If the compartments i and j have soil temperatures of T_i and T_j, and if the soil air at the compartment j has a volume of V_j, the volume of the same soil air at the compartment i, V_i, is given by:

$$V_j = V_i \frac{T_j}{T_i} \tag{5.15}$$

From Equations 5.14 and 5.15, the mass flow flux of soil air at the soil section of d–1 and d, $J_{Mg}(d\text{–}1, d)$, was expressed as follows:

$$J_{Mg}(d-1,d) = T' \sum \Delta V_g(d) \tag{5.16}$$

$$\sum \Delta V_g(d) = \sum_{i=d}^{N} (\Delta V_{\text{net}}(i)/T_i) \tag{5.17}$$

where T' is the soil temperature at the compartment d–1 or d, which determines the volume of the moving soil air at the compartment.

At last, the advective flux of CO_2 accompanied by the mass flow of soil air was given as the product of the mass flow flux obtained above and the concentration of CO_2 in soil air (Section 4.1). The soil air moving upward between soil compartments d–1 and d has a CO_2 concentration of $C_g(d)$ at a temperature of T_d in the compartment d; the soil air moving downward has the concentration $C_g(d\text{–}1)$ at $T_{d\text{-}1}$ in the compartment d–1. So that the advective flux of CO_2 between the compartments d–1 and d, $J_a(d\text{–}1, d)$ was given by the following equations:

$$J_a(d-1,d) = \begin{cases} \sum \Delta V_g(d) \cdot T_d \cdot C_g(d) & (J_{Mg}(d-1,d) > 0) \\ 0 & (J_{Mg}(d-1,d) = 0) \\ \sum \Delta V_g(d) \cdot T_{d-1} \cdot C_g(d-1) & (J_{Mg}(d-1,d) < 0) \end{cases} \tag{5.18}$$

In the actual calculation, for the change rates in air-filled porosity and soil temperature, the

averaged change rates for the three-day period, which consists of the day of CO_2 measurement and before and after the day, were applied. If significant precipitation was observed only on the third day of the period, the change rates were given by the changes between the first and the second day of the period, because the decrease in air-filled porosity from the second to the third day due to the precipitation do not match the drainage process of soil water observed on the second day. The depths at which CO_2 concentration in soil air was failed to measure were regarded as missing data, but regarded as zero if the mass flow of soil air itself did not occur.

(5) Advective flux of dissolved carbon dioxide accompanied by the movement of soil water

Essentially, similar to the mass flow flux of soil air, the flux of soil water is given as the product of the hydraulic gradient and unsaturated hydraulic conductivity. Mainly due to the variability of the unsaturated conductivity in response to the change in soil water potential, however, it is difficult to evaluate the soil water flux precisely using this method.

On the other hand, using the observed profiles of the pressure head of soil water (Figures 4.7 and 4.8) and the soil water characteristic curves (Figures 3.3 and 3.4), the profiles of the hydraulic gradient, which determines the direction of soil water movement, and the profiles of volumetric water content were obtained. Different from soil air, the change in the volume of soil water corresponding to the change in soil temperature can be negligible. Thus, in this study, the advective flux of CO_2 accompanied by the movement of soil water caused by the variation of volumetric water content was evaluated by analogy with the advective flux accompanied by the mass flow of soil air.

As the framework for analysis, the virtual soil column defined above was also applied to evaluate the flux of soil water and the accompanied advective flux of CO_2 in soil profiles. If a soil compartment which has a thickness l shows the values of volumetric water content of $\theta_w(t_1)$ at a time of t_1 and $\theta_w(t_2)$ at a time of t_2, the change in the volume of liquid phase in the compartment between t_1 and t_2 is given by analogy with Equation 5.12:

$$\Delta V_{\theta_w} = l \cdot \theta_w(t_2) - l \cdot \theta_w(t_1) \tag{5.19}$$

On the other hand, the direction of the flux is determined by the hydraulic gradient in the profile. For the soil compartments d–1, d and d+1, which are arranged continuously in the virtual

soil column, combinations of the directions of soil water movement among these compartments are the following four patterns: 1) consistently downward flow from the compartment d–1, through d, to d+1; 2) consistently upward flow from the compartment d+1, through d, to d–1; 3) divergent flow from the compartment d to d–1 and d+1; 4) convergent flow from the compartments d–1 and d+1 to d. The increase or decrease in the volume of liquid phase in a soil compartment will cause the inflow or outflow of the equivalent volume of soil water from the upper and lower compartments, in the case of the absence of any sources or sinks of the water in the compartment. Then in the cases of 1) and 2), the soil water fluxes are calculated in the same manner of the mass flow flux of soil air.

In the case of 1), the flux of soil water between the compartments d–1 and d, $J_{Mw}(d-1, d)$, was given by the accumulation of the volumetric change of liquid phase in the compartments from $d_{\text{D-ZFP}}$, at which the divergent zero flux plane (hereinafter referred to as D-ZFP) is found at first above d–1, to d–1:

$$J_{Mw}(d-1,d) = \sum_{i=d_{\text{D-ZFP}}+1}^{d-1} \Delta V_{\theta_w}(i) + J_{Mw}(d_{\text{D-ZFP}}, d_{\text{D-ZFP}}+1) \tag{5.20a}$$

In the case of 2), inversely:

$$J_{Mw}(d-1,d) = -\left(\sum_{i=d}^{d_{\text{D-ZFP}}-1} \Delta V_{\theta_w}(i) + J_{Mw}(d_{\text{D-ZFP}}-1, d_{\text{D-ZFP}}) \right) \tag{5.20b}$$

In the case of 3), the D-ZFP lies at the compartment d, so that the decrease in the volume of liquid phase at d was simply divided into the half and served as the upward (soil compartment d to d–1) and downward (d to d+1) fluxes of soil water, that is:

$$J_{Mw}(d-1,d) = -\frac{1}{2}\Delta V_{\theta_w}(d), \quad J_{Mw}(d,d+1) = \frac{1}{2}\Delta V_{\theta_w}(d) \tag{5.20c}$$

If the volume of liquid phase at the compartment d increased, the fluxes toward both directions were regarded as zero.

In the case of 4), in contrast to 3), the convergent zero flux plane (hereinafter referred to as C-ZFP) lies at the compartment d, the soil water fluxes were given by Equation 5.20a for the downward flow from the compartment d–1 to d, and given by Equation 5.20b for the upward flow from the compartment d+1 to d, respectively. If the volume of liquid phase at the compartment d decreases or do not increase enough to account for the amount of the inflow of soil water, the presence of a sink of the water is needed. The sink was not taken into consideration for the calculation because the sink within a soil compartment did not contribute to the soil water flux between adjacent soil compartments.

At last, the advective flux of dissolved CO_2 accompanied by the movement of soil water was given as the product of soil water flux obtained above and the concentration of CO_2 dissolved in soil water (Section 4.2). The soil water moving upward between soil compartments d–1 and d has a dissolved CO_2 concentration of $C_w(d)$ in the compartment d; the soil water moving downward has the concentration $C_w(d-1)$ in the compartment d–1. So that the advective flux of dissolved CO_2 between the compartments d–1 and d, $J_w(d-1, d)$ was given by the following equations:

$$J_w(d-1,d) = \begin{cases} J_{Mw}(d-1,d)\cdot C_w(d) & (J_{Mw}(d-1,d) > 0) \\ 0 & (J_{Mw}(d-1,d) = 0) \\ J_{Mw}(d-1,d)\cdot C_w(d-1) & (J_{Mw}(d-1,d) < 0) \end{cases} \tag{5.21}$$

In the actual calculation, the averaged change rate in volumetric water content for the same three-day period used for evaluating the advective flux of CO_2 accompanied by the mass flow of soil air was applied. To obtain the hydraulic gradients, the profile of the pressure head of soil water observed at the time for CO_2 measurement was used after converted to the total head. If significant precipitation was observed only on the third day of the period, the change rate was given by the change between the first and the second day of the period; the increase in volumetric water content from the second to the third day due to the precipitation do not match the drainage process of soil water and the hydraulic gradient observed on the second day.

The hydraulic gradient between the ground surface and a depth of 10 cm was regarded as upward in principle, because most of CO_2 measurement was carried out on rainless days. Only in the case that the supply of soil water from the depths above 10 cm was required to account for

the increase in the volume of liquid phase in the soil compartments below 10 cm, the equivalent downward fluxes were given.

For the soil water flux across the lower boundary of the virtual soil column, only in the case that the supply of soil water below a depth of 150 cm was required to account for the increase in the volume of liquid phase in the compartments above 150 cm, the equivalent upward fluxes were given. Except for the case, even the upward gradient was observed between depths of 100 and 150 cm, the flux across the lower boundary was considered as zero, because of the low saturated hydraulic conductivity in deep soils (Figures 3.5 and 3.6) and relatively small hydraulic gradients between these depths. The soil water flux across the lower boundary is hereinafter referred to as groundwater recharge or capillary rise from groundwater.

5.2.2 Results and discussion

(1) Diffusion coefficient of carbon dioxide in soil air

As described above, the diffusion coefficient of CO_2 in soil air at the soil sections of the virtual soil column is given as the product of the diffusion coefficient in free air (Equation 5.6) and the relative diffusion coefficient (Equation 5.10). The diffusion coefficient in free air is a function of the temperature at the soil section, but the seasonal and vertical variations were little. The values of Max/Min of the diffusion coefficient in free air at each depth were almost equal to one and fluctuated only slightly, from 1.04 to 1.16 at the forest site and from 1.07 to 1.17 at the grassland site, although the changes were found to be relatively large near the ground surface, where soil temperatures varied largely. In contrast, the values of Max/Min of the diffusion coefficient in soil air ranged from 2.10 to 6.01 at the forest; at the grassland, the difference in Max/Min among the depths was large, and the ratios ranged from 1.96 to more than a hundred and reached 318 at the soil section of 30-40 cm. Therefore, the temporal and spatial variations of the diffusion coefficient in soil air were determined almost only by the variations in the relative diffusion coefficient.

The seasonal variations of the diffusion coefficient of CO_2 in soil air at the forest and the grassland site are shown in Figures 5.11 and 5.12, respectively. At the forest site, the diffusion coefficient was largest near the ground surface and decreased with depth, corresponding to the decrease in air-filled porosity (Figure 3.1). The effect of the change in total porosity was relatively small because of its nearly constant profile. The maximum values of the diffusion

coefficient in the profile were always observed at the soil section of 0-5 cm and reached 4.80×10^{-2} cm·s^{-1} in September 1997. The reason for the agreement in the diffusion coefficient at the soil sections of 0-5 and 5-10 cm was that the same values of air-filled porosity and total porosity were applied to both sections; the difference in the diffusion coefficient between both sections were caused only by the difference in soil temperature.

As expected from the soil water characteristic curves at the forest (Figure 3.3), the air-filled porosities varied largely, particularly in shallow soils, in response to the seasonal variations of precipitation and evapotranspiration. Consequently, the diffusion coefficient in soil air also varied with air-filled porosity. During short dry periods in the summer of 1997, such as the early July and the early September, and the long rainless period observed in the late October, the diffusion coefficients became high. In contrast, in August 1997, when the rainless periods were relatively short, and after heavy rain such as the late June, the late September, and early April of 1998, the diffusion coefficients were low. These seasonal variations were evident from the ground surface to the soil section of 50-70 cm, and were also found to some extent at 70-100 cm. At 100-150 cm, the values of the diffusion coefficient itself were small, ranged from 1.60 to 9.60×10^{-4} cm·s^{-1}, and the seasonal trend was unclear.

In contrast to the forest site, as a result of the low air-filled porosity (Figure 3.2) and the high water retention properties (Figure 3.4) except near the ground surface, the diffusion coefficient of CO_2 in soil air was much lower and seasonally varied little at the grassland site. At the soil section of 50-70 cm, however, slightly larger values of the diffusion coefficient were found due to the relatively large air-filled porosities at these depths, but the values were only $3.40\text{-}7.80\times10^{-4}$ cm·s^{-1}, as low as the values at the soil section of 100-150 cm of the forest. Except this section and near the ground surface, the diffusion coefficient mostly ranged from 0.02 to 2×10^{-4} cm·s^{-1} and reached only 3.47×10^{-4} cm·s^{-1} at the maximum.

On the other hand, the diffusion coefficients in soil air near the ground surface at the grassland compared with those at the forest. The maximum values of the diffusion coefficient in the profile were also always observed at the soil section of 0-5 cm and reached 4.68×10^{-2} cm·s^{-1} in July 1997. At the soil section of 10-20 cm, the values of the diffusion coefficient were nearly one-third of the values at the sections of 0-5 and 5-10 cm. At these sections, the diffusion coefficients varied in response to the variation of micrometeorological conditions, as well as at the forest site. The diffusion coefficients were extremely high in dry periods such as early July

and late October in 1997, and extremely low in wet periods such as the late June and the late September. The variations of the diffusion coefficient at these soil sections were much larger and much more rapid than the variations at the sections of the forest, because of the sensitivity of soil moisture condition to the micrometeorological conditions at the grassland, similar to the soil respiration rate (Section 5.1).

(2) Diffusive flux of carbon dioxide in soil air

The seasonal variations of the diffusive flux of CO_2 in soil air at the forest and the grassland site are shown in Figures 5.13 and 5.14, respectively. All the profiles of the diffusive flux observed at each site are also indicated in Figures 5.15a and b for the forest, and Figures 5.16a and b for the grassland. The diffusive flux of CO_2 in soil air at the soil sections of the virtual soil column was given by Equation 5.11, as the product of the concentration gradient of CO_2 in soil air (Figures 4.13 and 4.14) and the diffusion coefficient in soil air (Figures 5.11 and 5.12). Therefore, the temporal and spatial variations of the diffusive flux reflected the effects of the variations of both variables.

At the forest site, the seasonal variation of the diffusive flux in soil air generally reflected the variation of the concentration gradient of CO_2. The effect of the seasonal variation of the diffusion coefficient was remarkably found, provided that large concentration gradients were observed during the periods or at the soil sections. From the ground surface to a depth of 40 cm, and at the soil section of 50-70 cm, the diffusive fluxes increased in early July, early September and late October in 1997, and decreased in the late September. For these periods, the variations of the concentration gradient at these sections were relatively small, so that the variations of the diffusion coefficient mainly affected the fluxes.

On the other hand, the diffusive flux in soil air generally decreased with depth, similar to air-filled porosity (Figure 3.1) and then similar to the diffusion coefficient, except for the soil sections of 40-50 and 50-70 cm. At the soil sections of 0-5 and 5-10 cm, the largest flux in the profile was always observed. Especially in the summer of 1997, mainly due to the large concentration gradients during the period and partly due to the largest diffusion coefficients in the profiles, the diffusive fluxes at these sections were much larger than any other soil sections. The maximum value of the flux was 1.80×10^{-8} $gCO_2 \cdot cm^{-2} \cdot s^{-1}$, observed at the soil section of 0-5 cm in early September of 1997. Comparing the two uppermost soil sections, because of almost

the same values of the diffusion coefficient, the diffusive flux at the upper section exceeded that at the lower section in the summer of 1997 and the spring of 1998, when the concentration gradient at the upper was larger than at the lower.

At the soil sections between 10 and 40 cm, the diffusive fluxes were largest next to those at the above sections and were about 0.3-0.6×10^{-8} $gCO_2 \cdot cm^{-2} \cdot s^{-1}$ in the summer and 0.1-0.2×10^{-8} $gCO_2 \cdot cm^{-2} \cdot s^{-1}$ in the winter. Among the soil sections, the diffusion coefficients decreased with depth whereas the difference in the concentration gradient was little, consequently the diffusive flux decreased with depth. At the soil section of 40-50 cm, the absolute values of the diffusive flux were extremely small and rarely exceeded 0.1×10^{-8} $gCO_2 \cdot cm^{-2} \cdot s^{-1}$. During the period for analysis, the direction of the flux was downward in the spring and summer, and upward in the autumn and winter. The magnitude and direction of the diffusive flux observed at the soil section were mainly due to the specific trend in the concentration gradient.

At the soil section of 50-70 cm, in contrast to the upper section, the diffusive fluxes similar to those found between 10 to 40 cm were evaluated, because the concentration gradient at the section was usually largest in the profile. At 70-100 cm, the low diffusion coefficients kept the diffusive flux less than 0.1×10^{-8} $gCO_2 \cdot cm^{-2} \cdot s^{-1}$ in most cases, nevertheless the concentration gradient was also large and nearly equal to the gradients at the soil sections between 10 and 40 cm. At the deepest section, 100-150 cm, the smallest values of the diffusion coefficient in the profile inhibited the diffusive flux almost completely.

At the grassland site, different from the forest site, the diffusive flux of CO_2 in soil air was mainly determined by the diffusion coefficient in soil air. Except for the winter months, nevertheless the concentration gradients of CO_2 at all the soil sections of the grassland were much higher than the gradients at the same depths of the forest, the diffusive fluxes were much lower due to the extremely low diffusion coefficients caused by the low air-filled porosity (Figure 3.2), except near the ground surface and the soil section of 50-70 cm.

At the soil section of 0-5 cm, the diffusive flux was almost always much larger than at any other soil sections. The maximum value of the flux was 2.26×10^{-8} $gCO_2 \cdot cm^{-2} \cdot s^{-1}$, observed in early August of 1997. At the soil section of 5-10 cm, in contrast, the diffusion coefficient was almost equal to that at the upper section but the concentration gradient was much smaller, so that the diffusive flux became much lower, too. The exceptionally large values of the flux evaluated in June and July of 1997 were obtained, because CO_2 concentrations in soil air at a depth of 5 cm

were failed to measure during the period and then given by the averaged concentration measured at the ground surface and at 10 cm. Except for the period, the diffusive flux at the soil section never exceeded 0.5×10^{-8} $gCO_2 \cdot cm^{-2} \cdot s^{-1}$. The low concentration gradients found at the section might be due to the difference in the method for sampling soil air for the determination of CO_2 concentration between these depths; at a depth of 5 cm, soil air was directly sampled through a penetrated injection needle into a syringe; at 10 cm, soil air was collected from the soil air collection probe, which was permanently installed at the observation sites (Section 4.1.1).

At the soil section of 10-20 cm, the concentration gradient was usually larger than that at the upper section, but the diffusion coefficient was always much lower. Consequently, the diffusive flux at the section became slightly lower than at 5-10 cm in many cases.

At the soil sections between 20 and 40 cm, due to the diffusion coefficients much lower than those at the above sections, the diffusive fluxes were almost inhibited. At 20-30 cm, even by the large upward concentration gradients observed in summer of 1997, the flux never exceeded 0.05×10^{-8} $gCO_2 \cdot cm^{-2} \cdot s^{-1}$. At 30-40 cm, as well as at 40-50 cm at the forest site, the downward flux of CO_2 was sometimes obtained also in the spring and summer; namely, late June, early August and late September of 1997, and mid-May of 1998.

At the soil sections of 40-50 cm and 50-70 cm, the concentration gradients were extremely large and the diffusion coefficients were slightly large relative to at the upper and lower sections. As a result, especially at 50-70 cm, the diffusive fluxes much larger than those at the adjacent sections were evaluated. At the soil sections between 70 and 150 cm, different from other sections, the concentration gradients were downward throughout the period for analysis, but the absolute values were much smaller than those at 40-50 and 70-100 cm. Due to the small values of the gradients and the diffusion coefficients, practically no diffusive fluxes was observed at these sections.

As indicated in Figures 5.15 and 5.16, the diffusive flux of CO_2 in soil air evaluated at the soil section of 50-70 cm was much larger than the flux at the upper section, namely 40-50 cm, throughout the period for analysis at both observation sites. This might cause some troubles; to keep such a profile of diffusive flux, the presence of a net CO_2 sink must be assumed at a depth of 50 cm, unless the diffusive flux is offset by other fluxes. Such a large flux evaluated at the soil section of 50-70 cm probably suggests that the diffusive flux at the section would be overestimated. The relative diffusion coefficient estimated by Equation 5.10 was validated by the

comparison of the measured values of soil respiration rate and the diffusive fluxes evaluated using the relative diffusion coefficient at the soil section of 0-5 cm only, so that it is possible that the estimated values of the diffusion coefficient of CO_2 in soil air were more or less different from the real values other than at 0-5 cm. For example, Haibara et al. (1997) showed the difference in the relationship between the relative diffusion coefficient and air-filled porosity among the depths.

There is evidence supporting the overestimate of the diffusion coefficient at the soil section of 50-70 cm at the forest site. As shown in Figure 3.5, the saturated hydraulic conductivity at the soil core sampling bores representing the observation site showed rapid decreases around a depth of 50 cm in the profiles. Especially for SC-F3, the conductivity around 70 cm was also extremely low. Although little or no relationship has been established between the diffusion coefficient in soil air and the hydraulic conductivity, both parameters indicate the permeability of substances in the soil and are determined essentially by the geometric structure of pore space in the soil. The sudden decrease in the saturated hydraulic conductivity at a depth of 50 cm would imply that the soil around the depth has a structure of pore space that inhibits the transport of substances more intensively than the structure at the upper and lower depths, and that such a difference in the structure is not always reflected in the three-phase distribution (Figure 3.1).

Such a specific structure of pore space at a depth of 50 cm around the forest site might cause the overestimate of the diffusion coefficient at the soil sections of 40-50 cm and 50-70 cm using Equation 5.10. Fortunately, the absolute values of the concentration gradient of CO_2 in soil air were extremely small at 40-50 cm, so that the effect of the overestimate would be small. In contrast, the concentration gradient at 50-70 cm was usually largest in the profile, thus the values of the diffusive flux probably much larger than the real values were evaluated.

In the Red Pine forest of ERC, Uchida (1995) also has been observed the concentration of CO_2 in soil air and the similar trend in the profiles that showed little or even inverse gradient between depths of 20 and 40 cm. To avoid the presence of a net CO_2 sink caused by the convergent fluxes of CO_2 calculated from the gradients, he obtained an averaged distribution of CO_2 concentration shown as an exponential curve from the regression analysis between the concentration and the depth. Using the averaged distributions, he inevitably obtained the profiles of the production rate of CO_2 exponentially decreased with depth. However, no scientific evidence is present supporting the exponential concentration profiles and the neglect of the little

or inverse gradients between depths of 20 and 40 cm.

Because of the less amount of plant roots (Figure 3.7) and soil organic carbon (Figure 3.9) below a depth of 50 cm relative to the above depths, paradoxically, the large upper gradients of CO_2 concentration at the soil sections below 50 cm would result from the inhibition of CO_2 diffusion caused by the specific geometric structure of soil pores around 50 cm. Thus, the transport processes of CO_2 in soil air were probably more or less different between above and below a depth of 50 cm, so that separating the profile into several soil layers would be more appropriate for the analysis of CO_2 transport rather than simply giving an exponential distribution throughout the profile.

On the other hand, at the grassland site, the effect of the soil structure on the diffusion coefficient is more apparent. As mentioned in Chapter 2, the grassland soil was largely disturbed and a dressed clay layer was lain between depths of 25 and 40 cm (Table 2.1). Around the depths, the saturated hydraulic conductivity also much lower than the other depths (Figure 3.6).

From these evidences, it is readily expected that the real values of the diffusion coefficient at these depths would be smaller than the values estimated by Equation 5.10. Due to the much larger concentration gradient than any other soil sections, the diffusive flux was highly overestimated at the section of 50-70 cm, as well as at the same depths of the forest site, while the diffusive flux at 40-50 cm was not overestimated so much. At the grassland site, the large upward gradient of CO_2 concentration at the soil sections below 40 cm might be partly due to the presence of soil organic carbon contained in the old surface soil (Figure 3.9), but was probably due to the inhibition of CO_2 diffusion caused by the highly compacted clay layer.

(3) Advective flux of carbon dioxide accompanied by the mass flow of soil air

The seasonal variations of the advective flux of carbon dioxide accompanied by the mass flow of soil air at the forest and the grassland site are shown in Figures 5.17 and 5.18, respectively. Because the measurements of CO_2 concentration were carried out on rainless days in principle, the downward flow of soil air caused by increasing air-filled porosity during the drainage process was dominant. By way of exception, after rainfall such as late November of 1997 and early April of 1998, upward flow of soil air caused by decreasing air-filled porosity was observed.

As shown in Figures 4.11 and 4.12, CO_2 concentration in soil air generally increased with

depth at both observation sites. On the other hand, when the downward flux of soil air was found at all the soil sections, the downward flux decreased with depth because the increase in the volume of gaseous phase was accumulated from the bottom of the virtual soil column to the upper soil sections. The advective flux of CO_2 accompanied by the mass flow of soil air, obtained as the product of these contrarily distributed variables, resulted in relatively complex profiles at both sites.

At the forest site, the mass flow flux of soil air decreased linearly with depth except late November of 1997 and early April of 1998 when the upward fluxes were dominant. The downward flux at the soil section of 0-5 cm, which represents the inflow of air from the atmosphere into the soil, reached about 1 $cm \cdot day^{-1}$ at the maximum. In contrast, at the lowest section, 100-150 cm, little flux of the mass flow was observed.

Consequently, the advective flux of CO_2 was relatively high at the soil sections between 10 and 50 cm and relatively low at the above and below sections. At the soil sections between 10 and 50 cm, the advective fluxes were about -0.2×10^{-10} $gCO_2 \cdot cm^{-2} \cdot s^{-1}$ from July to November in 1997, and the maximum downward flux of -0.45×10^{-10} $gCO_2 \cdot cm^{-2} \cdot s^{-1}$ was observed at 20-30 cm in late June of 1997. The absolute values of the advective flux found at these sections were, however, two orders of magnitude as low as the values of the diffusive flux in soil air at the sections of the same depth.

At the soil sections between 0 and 10 cm, the downward fluxes of mass flow were always larger than the fluxes at the below sections while CO_2 concentrations in soil air were lower. As a result, the advective fluxes were relatively small. Especially at 0-5 cm, the soil air which moved downward had low CO_2 concentrations equivalent to those at the ground surface, so that the advective flux was lowest in the profile next to at 100-150 cm and limited to about -0.05×10^{-10} $gCO_2 \cdot cm^{-2} \cdot s^{-1}$. In contrast, at the soil sections below 40 cm, the downward fluxes of mass flow were smaller than the fluxes at the above sections whereas CO_2 concentrations in soil air were higher. Consequently, the advective fluxes were also relatively small. In many cases, the linear decrease in the downward advective flux was observed from the soil section of 40-50 cm to that of 100-150 cm.

The downward advective flux of CO_2 was generally high in the summer and low in the winter. This resulted from the higher concentrations of CO_2 and the higher change rates in the volume of gaseous phase corresponding to the higher rates of evapotranspiration in the summer relative to

those in the winter.

In late November of 1997 and early April of 1998, some rainfall was observed a few days before the CO_2 measurements. The upward fluxes of mass flow observed in the periods were therefore caused by the decrease in air-filled porosity in response to the redistribution of soil water after the rainfall. Especially in the late November, the soil was extremely dry after the almost rainless period lasting about a month, so that much of the rainfall was consumed for the recovery of volumetric water content and little water was served as groundwater recharge. In both periods, however, the decrease in gaseous volume in deep soils was almost offset by the increase in the volume in shallow soils, as a result the outflow of soil air across the ground surface was small.

On the other hand, in late June and late September of 1997, some rainfall also observed several days before the measurements contrarily resulted in the large downward fluxes of the mass flow. This can be explained that the air-filled porosity that had been decreased by the rainfall rapidly increased again in the drainage process. Such a difference in the effect of rainfall might be partly due to the difference in the season. In late June and late September of 1997, relative high rates of evapotranspiration would rapidly increase air-filled porosity. In late November of 1997 and early April of 1998, inversely, relatively low rates of evapotranspiration might retard air-filled porosity from increasing.

As naturally expected from the soil water characteristic curves (Figure 3.4), little change was found in the volume of gaseous phase at the grassland site, except near the ground surface. The mass flow flux of soil air was usually largest at the soil section of 0-5 cm in the profile and the upward and downward maximum fluxes were both observed in April 1998, 5.76 and −14.87 $mm \cdot day^{-1}$, respectively. Because of the failure of tensiometer at 10 cm, however, the values of pressure head at the soil section were given by the measured values at 20 cm in this period, and therefore the estimated air-filled porosity was less reliable. Excepting the period, the observed maximum values of the upward and downward fluxes were 4.97 and −5.80 $mm \cdot day^{-1}$, respectively. At the soil section of 5-10 cm, the flux of mass flow was about the half of the flux at the upper section, and most of the fluxes were less than 1 $mm \cdot day^{-1}$ below 10 cm.

Consequently, the advective flux of CO_2 accompanied by the mass flow of soil air was high at the soil sections of 5-10 and 50-70 cm relative to the other sections. Mainly, the former was due to the large flux of mass flow and the latter was due to the extremely high concentration of CO_2

in soil air. At these sections, the advective fluxes generally ranged from 0.2 to -0.4×10^{-10} $gCO_2 \cdot cm^{-2} \cdot s^{-1}$ and were relatively high in the summer and low in the winter, mainly corresponding to the seasonal variations of CO_2 concentration and partly the variations of the mass flow flux. At 50-70 cm, in particular, exceptionally high values of the advective flux were observed several times. The maximum values of the upward and downward fluxes reached 0.901 and -0.587×10^{-10} $gCO_2 \cdot cm^{-2} \cdot s^{-1}$, but the orders of magnitude were lower than those of the diffusive fluxes near the ground surface by two orders.

At the soil section of 0-5 cm at the grassland, as well as at the same depths of the forest, the lowest concentration of CO_2 in the profile inhibited the advective flux, which showed the values similar to those at the forest. At the soil sections between 10 and 50 cm, the combination of the mass flow fluxes smaller than the upper section and the CO_2 concentrations lower than the lower section caused the advective fluxes to be relatively small. At the soil sections of 70-100 and 100-150 cm, little flux of the mass flow of soil air almost inhibited the advective fluxes, nevertheless CO_2 concentrations were much higher than those at the above sections. Once some mass flow was generated, however, extremely large values of the advective flux were obtained as well as at 50-70 cm. The maximum values of the upward and downward fluxes at 70-100 cm reached 1.69 and -0.539×10^{-10} $gCO_2 \cdot cm^{-2} \cdot s^{-1}$, respectively.

In contrast to air-filled porosity, the effect of the temporal and spatial variations of soil temperature was little. In principle, increasing soil temperature will cause the expansion of soil air and the following outflow of soil air into the atmosphere, and decreasing soil temperature will cause the inverse processes. In addition, under the condition of decreasing temperature with depth, the volume of soil air which moves downward decreases and then additional soil air must move downward by the amount equivalent to the shrinkage; the volume of soil air moving upward inversely increases and then additional movement must occur by the amount equivalent to the expansion; therefore, the mass flow of soil air will be enhanced at both upward and downward directions under the condition. In contrast, under the condition of increasing temperature with depth, the mass flow will be weakened.

In practice, however, no effect of the variations of soil temperature was found in the advective flux of CO_2. The terms of the temperature effects, T_i/T_j, in Equations 5.13-5.15 showed almost constant values of 0.99-1.01 at both sites, though the seasonal trends in the effect were in agreement with the principle described above. As a result, the fluxes of the mass flow of soil air,

and therefore the following advection of CO_2 were determined as a function of almost only air-filled porosity.

(4) Advective flux of dissolved carbon dioxide accompanied by the movement of soil water

The seasonal variations of the advective flux of dissolved CO_2 accompanied by the movement of soil water at the forest and the grassland site are shown in Figures 5.19 and 5.20, respectively. As described above, first, the hydraulic gradient at each soil section was determined by the profile of the total head of soil water derived from the measured values of the pressure head (Figures 4.7 and 4.8); next, the soil water flux accompanied by the volumetric change of liquid phase was estimated using Equations 5.20a, b and c, by analogy with the mass flow flux of soil air; finally, as the product of the soil water flux and dissolved CO_2 concentration in soil water (Figures 4.24 and 4.25), the dissolved CO_2 flux was calculated from Equation 5.21. Therefore, at both sites, the dissolved CO_2 flux reflected the temporal and spatial variations of both the soil water flux and the concentration of dissolved CO_2.

At the forest site, the soil increasingly dried from the ground surface to relatively deep soils in response to evapotranspiration. In the summer of 1997, the D-ZFP was found at a depth of 40 or 50 cm. The C-ZFP was also observed at 70 cm sometimes, but the hydraulic gradients at the upper and lower soil sections were small, so that the downward flow of soil water was expected to be dominant below a depth of 50 cm during the period. In the dry periods of early July, early September and late October of 1997, although upward hydraulic gradients were observed throughout the profile, the supply of water from the groundwater to the soil profile by capillary rise was probably small due to the small gradient at the soil section of 100-150 cm. In the winter months and the wet periods of the late June and the late September, in contrast, downward hydraulic gradients were large from the ground surface to a depth of 70 cm, and were little below the depth.

By such profiles of the hydraulic gradient, the upward fluxes of soil water were obtained between the ground surface and a depth of 50 cm during the dry periods. Because the flux was calculated by accumulating the decrease in volume of the liquid phase from the D-ZFP to the ground surface, it became larger with approaching the surface and reached the maximum at the soil section of 0-5 cm. The maximum value of the flux observed at the section was about 5 $mm \cdot day^{-1}$. In practice, however, particularly near the ground surface, vaporization of soil water

and water uptake by plant roots also reduce the volume of liquid phase, as well as the movement of soil water into another depths. Such reduction of the water will act as the sink of soil water within the soil compartments, not considered in the calculation. As a result, the upward fluxes of soil water near the ground surface were more or less overestimated. Below 50 cm, downward flux of soil water was usually dominant; although some upward fluxes were observed, the values were not so large.

On the other hand, in the winter and the wet periods, the soil sections that had downward fluxes of soil water were dominant. In late June and late September of 1997, the downward fluxes occurred below a depth of 30 cm and reached the maxima of about 3 $mm \cdot day^{-1}$ at the section of 50-70 cm. Such large downward fluxes suggested the presence of intensive sink of soil water at 70 cm, but the sink was not taken into account in the calculation. The sink was partly due to the overestimate of soil water flux by the amount equivalent to the decrease in volume of the liquid phase caused by the uptake of soil water in shallow soils, but might be partly due to the systematic error on the total head at 70 cm, because of the small hydraulic gradients found at the upper and lower soil sections. In the winter months, the volumetric change of liquid phase was generally small, so that the flux of soil water was also small except for January 1998, when consistently downward flux and the groundwater recharge of 3.8 $mm \cdot day^{-1}$ were obtained due to the infiltration of snowmelt water.

By way of exception, in early April of 1998, continuous rainfall was observed during the three-day period for the analysis and reached the total amount of 70 mm, and downward hydraulic gradients were found throughout the soil profile. So that the throughfall of 23.25 $mm \cdot day^{-1}$, given by 90 % of the total rainfall (Indra, 1997), was served as a source of soil water from the ground surface; the loss of water by evapotranspiration was neglected. Consequently, the supply of water resulted in the groundwater recharge of 24.6 $mm \cdot day^{-1}$. Only 1.38 mm was contributed to the recharge by the volumetric decrease in liquid phase, namely the water that had been stored in the soil profile by the preliminary rainfall. In addition, relatively high saturated hydraulic conductivity at the forest site (Figure 3.5) would indicate that the saturated water flux ranged from 1 to 10 $cm \cdot day^{-1}$ can occur even in deep soils. These results suggest the important role of heavy rain and the corresponding soil water movement without the volumetric change in liquid phase.

As given above, the absolute values of upward flux of soil water found in shallow soils were

generally larger than the values of downward flux in deep soils. On the other hand, CO_2 concentration dissolved in soil water was increased with depth (Figure 4.24). As a result, the advective fluxes of dissolved CO_2 accompanied by the movement of soil water showed similar values for both upward and downward directions. The dissolved CO_2 fluxes reached about $\pm 0.5\times10^{-10}$ $gCO_2 \cdot cm^{-2} \cdot s^{-1}$ at the maxima, similar to the maximum values of advective flux of CO_2 accompanied by the mass flow of soil air, and two orders of magnitude as small as the diffusive flux of CO_2 in soil air at the soil sections of the same depth.

The maximum upward flux of dissolved CO_2 was usually found at the soil section of 5-10 cm or 20-30 cm. The former was due to the higher dissolved CO_2 concentration at 10 cm than at 5 cm where the upward flux of soil water was larger, and the latter was due to the larger soil water flux at 20-30 cm than the fluxes at the sections of 30-40 and 40-50 cm, because dissolved CO_2 concentrations among the depths were almost similar. However, the dissolved CO_2 fluxes obtained at these sections were probably overestimated due to the overestimate of soil water flux.

On the other hand, the downward flux of dissolved CO_2 was usually largest at the soil section of 100-150 cm, where dissolved CO_2 concentration was highest in the profile. This section was usually placed below the lowest D-ZFP and therefore not affected by the sinks of soil water caused by vaporization and the uptake by plant roots, and the sinks within the section were also expected to be negligible. Thus, the dissolved CO_2 flux would be correctly evaluated at the soil section relative to near the ground surface.

In early April of 1998, because of the heavy rain and the corresponding specific operation on the evaluation of soil water flux, exceptionally large downward fluxes of dissolved CO_2 were obtained throughout the profile. The maximum downward flux of -5.99×10^{-10} $gCO_2 \cdot cm^{-2} \cdot s^{-1}$ was observed at the soil section of 100-150 cm. Because of the missing of measured value of CO_2 concentration, the dissolved CO_2 flux across a depth of 150 cm into the groundwater was not evaluated and plotted in the figures. However, if the dissolved concentration at 100 cm is applied, the flux results in -5.94×10^{-10} $gCO_2 \cdot cm^{-2} \cdot s^{-1}$.

In the winter months, the small downward fluxes of soil water and the low concentrations of dissolved CO_2 caused little advective fluxes of dissolved CO_2 except for January 1998, when the dissolved CO_2 flux reached up to -0.93×10^{-10} $gCO_2 \cdot cm^{-2} \cdot s^{-1}$ at the soil section of 100-150 cm, due to the infiltration of snowmelt water and the following consistently downward flux of soil water.

As shown in Figure 4.8, the decrease in the pressure head of soil water corresponding to dry

conditions did not tend to advance into deep soils at the grassland site. Thus the hydraulic gradient was not formed clearly below a depth of 40 cm except for early September of 1997, when the effect of evapotranspiration during the summer was accumulated. Relatively dry conditions were also observed in the early July and the late October, but remarkable upward gradients were limited between the ground surface and a depth of 40 cm. In relatively wet periods, directions of the hydraulic gradients were generally upward at the soil section of 10-20 cm, downward at the sections of 20-30 and 30-40 cm, and also little below 40 cm. As the result of the profiles of hydraulic gradient, the D-ZFP was found at 20 cm in the wet periods and at 70 or 100 cm in the dry periods. Although the D-ZFP at a depth of 70 or 100 cm was sometimes observed under wet conditions, the soil water flux around the depth would be little in practice because of the small hydraulic gradients at the upper and lower soil sections. In addition, the C-ZFP was frequently found between 30 and 50 cm, but the gradient at the lower section was almost equal to zero, so that the convergent movement of soil water to the C-ZFP probably occurred little.

Due to the high water retention properties as shown in Figure 3.4 and the profiles of hydraulic gradient described above, the flux of soil water movement evaluated by the volumetric change of liquid phase was extremely small except near the ground surface. The soil water flux was usually largest at the soil section of 0-5 cm in the profile and the upward and downward maximum fluxes were both observed in April 1998, 13.6 and -6.05 mm·day^{-1}, respectively. As mentioned previously, however, because of the failure of tensiometer at 10 cm, the values of the pressure head at the soil section were given by the measured values at 20 cm in this period, and therefore the estimated volumetric water content was more or less different. Excepting the period, the observed maximum values of the upward and downward fluxes were 7.50 and -4.52 mm·day^{-1}, respectively. At the soil section of 5-10 cm, as well as the mass flow of soil air, the soil water flux was about the half of the flux at the upper section. In practice, however, the evaluated fluxes at these sections were probably overestimated because of the presence of the sink of soil water. Below 10 cm, most of the fluxes were less than 1 mm·day^{-1}, though the effect of the sink was relatively small. Such small fluxes were in good agreement with the saturated hydraulic conductivity between depths of 10 and 40 cm, which showed the values of less than 1 mm·day^{-1} (Figure 3.6).

At the grassland, such a heavy rain continued during the three-day period for the analysis,

similar to the rainfall observed in early April of 1998 at the forest, was never observed. Although some rainfall was received in the three-day period for several times, the infiltration of the rainfall was not considered because of the extremely low saturated hydraulic conductivity in shallow soils. In practice, however, the depth of groundwater table at the observation field of ERC tended to rise rapidly in response to heavy rain. This may suggest the importance of horizontally heterogeneous phenomena, such as preferential flow of soil water downward into the groundwater through macropores or the spots that have relatively high hydraulic conductivity.

The advective flux of dissolved CO_2 accompanied by the movement of soil water was given as the product of the soil water flux presented above and the dissolved CO_2 concentration in soil water (Figure 4.25); the flux mainly depended on the latter. Most of the case, the maximum upward flux of dissolved CO_2 in the profile was obtained at the soil section of 50-70 cm, and the maximum downward flux was found at 70-100 and 100-150 cm. These fluxes had the dissolved CO_2 concentrations at depths of 70 and 100 cm, where the largest values of the concentration in the profile were observed. The upward and downward maximum fluxes at these sections were both observed in late September of 1997, 0.71 and -0.74×10^{-10} $gCO_2 \cdot cm^{-2} \cdot s^{-1}$, respectively. At another soil sections, relatively large upward fluxes were evaluated at 0-5 and 5-10 cm, where the soil water flux was largest in the profile but probably overestimated.

In spite of the much higher dissolved CO_2 concentration, the magnitude of the advective flux of dissolved CO_2 at the grassland was generally similar to the magnitude at the forest due to the lower fluxes of soil water caused by the smaller volumetric changes in liquid phase of the grassland soils. As a result, the dissolved CO_2 flux at the grassland site was two orders of magnitude as low as the diffusive fluxes near the ground surface. During the heavy rain, however, preferential downward flow of soil water might cause the large downward flux of dissolved CO_2, removing the accumulated CO_2 in deep soils into the groundwater.

(5) Total flux of carbon dioxide and the proportions of each flux

As the sum of the three types of CO_2 flux discussed previously, that is, the diffusive flux in soil air and the advective fluxes accompanied by the movement of soil air and soil water, the total flux of CO_2 was obtained. Due to the extremely large values of the diffusive flux of CO_2 near the ground surface at both sites, however, the temporal and spatial distributions of total CO_2 flux were almost similar to the distributions of the diffusive flux. Then, to examine the

contributions of each flux to the total flux, the sum of the absolute values of each flux, J_t', defined as:

$$J_t' = |J_d| + |J_a| + |J_w| \tag{5.22}$$

and the proportions of each value to the total value at the forest and the grassland site are plotted in Figures 5.21 and 5.22, respectively. The arithmetic mean values averaged for each depth during the period for analysis, at the depth and time at which all the three fluxes had been obtained, were plotted.

At the forest site, the total value of the absolute values of each flux generally decreased with depth, as well as the diffusive flux in soil air (Figure 5.15). The total flux was largest near the ground surface, 0.90 and 0.82×10^{-8} $gCO_2 \cdot cm^{-2} \cdot s^{-1}$ at the soil sections of 0-5 and 5-10 cm, respectively. At the sections between 10 and 40 cm, the total flux gradually decreased with depth, from 0.4 to 0.2×10^{-8} $gCO_2 \cdot cm^{-2} \cdot s^{-1}$. Then the total flux rapidly decreased to 0.04×10^{-8} $gCO_2 \cdot cm^{-2} \cdot s^{-1}$ at the soil section of 40-50 cm, at which downward flux was often observed due to the inverse gradient of CO_2 concentration in soil air frequently obtained at the section (Figure 4.11). At the soil section of 50-70 cm, the total flux suddenly increased to 0.31×10^{-8} $gCO_2 \cdot cm^{-2} \cdot s^{-1}$, probably due to the overestimate of the diffusive flux. Because a sink of CO_2 must be present at 50 cm if such an averaged profile were actually obtained. Thus, in fact, the total flux of CO_2 at the soil section would be much smaller. Below the soil section, the total flux decreased again and became less than 0.01×10^{-8} $gCO_2 \cdot cm^{-2} \cdot s^{-1}$ at 100-150 cm, where downward flux was usually observed.

On the proportions of each flux of CO_2 to the total flux, the diffusive flux in soil air was dominant at most of the depths. The proportion of the diffusive flux was particularly large in shallow soils and was never less than 99% of the total flux at the soil sections between the ground surface and 20 cm, except for early April of 1998, when large advective flux of dissolved CO_2 was evaluated (Figure 5.19). Except for the period, the proportion of the diffusive flux was more than 98% at the sections of 20-30 and 30-40 cm. Even at 40-50 cm, the proportion was usually more than 80% of the total flux; only in the early April of 1998, it dropped to 7.8%. At the soil section of 50-70 cm, the proportion of the diffusive flux to the total flux ranged from 78.3 to 99.9% and averaged 97.8%, but was probably much lower in practice because of the

overestimate of the diffusive flux. Below the section, the proportion decreased with depth as well as the total flux. At the lowest soil section, 100-150 cm, the proportion of the diffusive flux varied in the range of 20 to 80 % and averaged 55.3%.

The proportions of the advective flux of CO_2 accompanied by the mass flow of soil air were small throughout the profile. The proportion of the advective flux averaged for all the depth and time was only 1.52% of the total flux. At the soil section of 40-50 cm, exceptionally, the proportion ranged from 0.78 to 32.3% and averaged 6.63%. Also at 100-150 cm, the maximum value of 14.6% and the mean value of 4.81% were obtained. Except for these soil sections, the proportion of the advective flux was usually less than 1.0% and never exceeded 3.0%.

The proportions of the advective flux of dissolved CO_2 accompanied by the movement of soil water was also generally small. By way of exception, during heavy rain observed in the early April of 1998, the proportion of the advective flux of dissolved CO_2 exceeded 10% below 20 cm, and reached the maximum of 88.8% at the soil section of 40-50 cm. Except for the period, the proportion was less than 1.0% at the sections between the ground surface to 40 cm. In deep soils, however, the proportion of the dissolved CO_2 flux increased with depth; in average, 1.71% at 50-70 cm, 5.8% at 70-100 cm, and 39.9% at 100-150 cm where the proportion ranged from 9.01 to 76.0%.

In general, the profiles of the total flux of CO_2 and the proportions of each flux to the total flux at the grassland site were similar to the profiles at the forest site. At the soil sections between the ground surface and 20 cm, the total flux rapidly decreased with depth, from 0.85×10^{-8} $gCO_2\cdot cm^{-2}\cdot s^{-1}$ at 0-5 cm to 0.17×10^{-8} $gCO_2\cdot cm^{-2}\cdot s^{-1}$ at 10-20 cm. The proportion of the diffusive flux in soil air was dominant at these sections, more than 99% in many cases. Sometimes relatively large proportions of both advective fluxes were found, but usually the fluxes were less than 1%. In contrast, at the sections between 20 and 40 cm, where the dressed clay layer was present (Table 2.1), the absolute values of the total flux became extremely small, less than 0.01×10^{-8} $gCO_2\cdot cm^{-2}\cdot s^{-1}$. Because of the nearly saturated conditions (Figure 3.2), the diffusive fluxes at these sections were two or three orders of magnitude as small as the fluxes at the above sections, and the proportion was also small. As a result, the proportions of both advective fluxes became relatively large. The proportions of the advective flux accompanied by the mass flow of soil air were 22.9% at 20-30 cm and 43.1% at 30-40 cm in average; for the advective flux of dissolved CO_2, 10.8 and 26.2%, respectively. Particularly at the soil section of

30-40 cm, downward fluxes of advection by the movement of soil air and soil water were found to completely offset the upward flux of diffusion for several times.

At the soil sections between 40 and 70 cm, the diffusive flux in soil air was evaluated to be relatively large due to the large concentration gradients of CO_2 in soil air (Figure 4.14). Consequently, the proportion of the diffusive flux, as well as the total flux, became large again. By the reason discussed previously, however, the diffusive fluxes at these sections were probably overestimated, and the observed large concentration gradients would result from the inhibition of the upward diffusion of CO_2 caused by the dressed clay layer presented above. So that in practice, the proportion of the diffusive flux would be relatively small and the proportions of the advective fluxes would be relatively large.

Below a depth of 70 cm, the total flux was kept extremely small. The proportion of the diffusive flux decreased with depth, while the proportion of the advective flux of dissolved CO_2 increased with depth. At the soil section of 70-100 cm, the proportion of the dissolved CO_2 flux widely ranged from 3.87 to 80.4 %, except for the case when no change in the volume of liquid phase of the soil was observed. At 100-150 cm, where only three data were obtained, the proportions were 0.0, 48.6 and 90.3 %. On the other hand, the advective flux accompanied by the mass flow of soil air was small at these sections, usually less than 1.0% except for the large values more than 10% obtained for several times.

The total flux of CO_2 at the grassland site was concentrated closer to the ground surface than that at the forest site. Most of the upward flux was observed between the surface and a depth of 40 cm at the forest, between the surface and 20 cm at the grassland. At both sites, the diffusive flux in soil air was dominant generally throughout the profiles. The small proportions of the diffusive flux usually corresponded to the small values of the total flux, and did not mean the large flux of the advective fluxes accompanied by the movement of soil air and soil water. In deep soils, however, the advective flux of dissolved CO_2 increased with depth, suggesting the importance of the dissolved CO_2 flux on the transport of CO_2 generated in soil into groundwater. On the other hand, the advective flux accompanied by the mass flow of soil air was usually kept little.

5.3 Evaluation of the production rate of carbon dioxide

5.3.1 Methods

(1) Calculation of the production rate of carbon dioxide using a mass balance equation

A mass balance of a substance on a unit volume of soil is expressed by the following three terms if the source or sink of the substance is not present in the volume; the input of the substance into the volume, the output out of the volume and the temporal change rate in the storage of the substance within the volume. Generally, soils have the sources of CO_2, which can be given as the remainder of the three terms in the mass balance equation for CO_2. Therefore, the production rate of CO_2 on a soil compartment d in the virtual soil column, α_d, was evaluated by the following equation:

$$\alpha_d = J_t(d-1,d) - J_t(d,d+1) + \Delta S_d \tag{5.23}$$

where $J_t(i, j)$ is the total CO_2 flux between the compartments i and j ($gCO_2 \cdot cm^{-2} \cdot s^{-1}$), and ΔS_d is the change rate of CO_2 storage in the compartment d.

The mass balance of CO_2 on the soil compartment d is illustrated in Figure 5.23. The total flux of CO_2 were given by the sum of the three types of the flux evaluated in Section 5.2; the diffusive flux in soil air and the advective fluxes accompanied by the movement of soil air and soil water. On the other hand, the change rate of the storage was evaluated using the total content of CO_2 per unit volume of bulk soil, obtained in Section 4.3, as described below.

(2) Evaluation of the change rate of the storage of carbon dioxide

The change rate of the storage of CO_2 in a soil compartment of the virtual soil column was evaluated from temporally continuous data sets on the total content of CO_2 per unit volume of bulk soil, shown in Figures 4.32 and 4.33.

An example for the evaluation is illustrated in Figure 5.24. First, the total content of CO_2 and the day of CO_2 measurement were applied to the vertical and horizontal axes, respectively, and then the total contents on the day of the measurement, as well as those on the days of the last and next measurements, were plotted. Next, a linear regression for the three plotted data was carried out and the slope determined by the regression was defined as the averaged change in the total

CO_2 content with time. Finally, the change rate of CO_2 content given by the slope, $\Delta S'_d$, which is expressed per unit volume of bulk soil per day, was converted into the change rate in the soil compartment d per second, ΔS_d, as follows:

$$\Delta S_d = l_d \cdot \Delta S'_d \div (60 \times 60 \times 24) \tag{5.24}$$

If one of the three data was missing, the remainder was served for the regression, as the case for a depth of 150 cm illustrated in Figure 5.24. If more than two of the three data were missing, the change rate was not evaluated.

5.3.2 Results and discussion

(1) Change rate of the storage of carbon dioxide

The seasonal variations of the change rate of CO_2 storage in the soil compartments at the forest and the grassland site are shown in Figures 5.25 and 5.26, respectively. The change rates of CO_2 storage generally indicated positive values from spring to summer, when the total content of CO_2 per unit volume of bulk soil was increasing (Figures 4.32 and 4.33), and showed negative values from autumn to winter inversely. The ranges of the seasonal variation were relatively large in deep soils, where the total content was also large.

At the forest site, the total content of CO_2 peaked in the early part of the summer of 1997 at all the depths and then decreased, so that the maximum increasing rates of CO_2 storage were observed in the June. After that, the values of the change rate were generally kept negative until January 1998, showing several large decreasing rates from July to October 1997. The change rates turned into positive in March and April 1998 in response to increasing total CO_2 content.

As a whole, the ranges of seasonal variation of the change rate of CO_2 storage increased with depth and largest at a depth of 100 cm in the profile, at which the total content of CO_2 was also largest. The maximum values of the increasing and the decreasing rate at 100 cm were 6.10 and -4.32×10^{-11} $gCO_2 \cdot cm^{-2} \cdot s^{-1}$, respectively. Such a significant difference among the depth, however, highly depended on the difference in the thickness of the soil compartments (Table 5.2). For the change rates per unit volume of bulk soil, the difference among the depths was much smaller, and the maximum values of the increasing and decreasing rates were 2.25 and -1.51×10^{-12} $gCO_2 \cdot cm^{-3} \cdot s^{-1}$, both of them were found at a depth of 30 cm.

Similar to at the forest site, the maximum increasing rate of CO_2 storage was observed in June 1997 at many of the depths at the grassland site. However, the following decrease in the total content of CO_2 after that was not so apparent, even some of the increases were found in deep soils, therefore the decreasing rates were not so large. From the August to the September, large increasing rates of CO_2 storage was observed again corresponding to the recovery of the total CO_2 content. After that, the values of the change rate largely turned to negative in the October and returned to positive during March and April 1998.

As well as at the forest, the ranges of seasonal variation of the change rate of CO_2 storage generally increased with depth at the grassland. The maximum values of the increasing and decreasing rates were 3.64 and -2.64×10^{-10} $gCO_2 \cdot cm^{-2} \cdot s^{-1}$, both of them were observed at a depth of 70 cm. The large difference among the depths was also mainly due to the thickness of the soil compartments. Especially, the reason for the similar ranges of the seasonal variation at depths of 70 and 100 cm, nevertheless the total content of CO_2 was always larger at 70 cm than at 100 cm, was that the thickness of these compartments were 25 and 40 cm, respectively (Table 5.2). Like at the forest site, the difference among the depths in the change rates per unit volume of bulk soil was much smaller, but the maximum values of the increasing and decreasing rates were also found at a depth of 70 cm, due to the total content of CO_2 much larger than any other depths, and reached 1.45 and -1.05×10^{-11} $gCO_2 \cdot cm^{-3} \cdot s^{-1}$, respectively.

Because of the much larger content of CO_2, the absolute values of the change rate of CO_2 storage at the grassland site were generally larger than the values at the forest site. The values of the change rate at both sites, however, were two or three orders of magnitude as small as the values of the diffusive flux of CO_2 in soil air and therefore as the values of the total CO_2 flux in the soil profile. Consequently, the significance of the term on the change of storage in Equation 5.23, ΔS_d, was relatively small.

(2) Temporal and spatial distributions of the production rate of carbon dioxide

The seasonal variations of the production rate of CO_2 at each soil compartment of the virtual soil column, which was evaluated as the remainder of CO_2 mass balance using Equation 5.23, at the forest and the grassland site are shown in Figures 5.27 and 5.28, respectively. All the profiles of the production rate are also plotted in Figures 5.29a, b and c for the forest, in Figures 5.30a, b and c for the grassland. The production rate in the profile was plotted after converted into the

rates per unit volume, divided by the thickness of each soil compartment. That is, the area surrounded by the base line and each line plotted as a solid or broken or dotted line is equivalent to the production rate. Because of the large proportion of the diffusive flux of CO_2 in soil air to the mass balance of CO_2, the production rate was strongly affected by the seasonal variation and the difference among the soil sections in the diffusive flux.

At the forest site, the production rate of CO_2 generally showed large values in the summer and small values in the winter, similar to the seasonal variation of the diffusive flux in soil air (Figure 5.13). In many cases, the largest production rates in the profile were observed at a depth of 10 cm. The maximum value was obtained in late July of 1997, when the maximum value of the diffusive flux at the soil section of 5-10 cm was observed, and reached 1.40×10^{-9} $gCO_2 \cdot cm^{-3} \cdot s^{-1}$. The proportion of the production rate at a depth of 10 cm to the total production rate in the whole profile ranged from 25.3 to 86.8% and averaged 47.4%. That is, about a half of the CO_2 production in the soil of the forest site concentrated between depths of 7.5 and 15 cm, according to the depths of division on the soil compartment (Table 5.2).

At a depth of 5 cm, in contrast, the production rate of CO_2 was much smaller and often showed negative values. This was due to the diffusive flux in soil air at the soil section of 0-5 cm, which was similar to or even less than the diffusive flux at 5-10 cm. However, the evaluated flux at the section of 0-5 cm indicated the averaged flux between these depths, and therefore the CO_2 produced between the depths was not included. As mentioned in Section 5.2.1 (3), the diffusive fluxes evaluated by the M-Q 2 equation at the soil section of 0-5 cm at the forest site were lower than the measured fluxes of soil respiration, especially from spring to summer (Figure 5.9). Consequently, in practice, the production rate of CO_2 at a depth of 5 cm was probably much higher, and therefore the total production rate and the proportion of the production rate at 5 cm to the total were relatively larger.

At the soil compartments between 20 and 40 cm, relatively large production rates were observed. The averaged proportions of the production rate at each depth to the total production rate were 13.5, 11.1 and 28.1%, respectively, except for negative values obtained at 30 cm for several times. These relatively similar values of the production rate resulted from the similar diffusive fluxes at these soil sections. The relatively large production rate at 40 cm was due to the extremely low flux at the section of 40-50 cm.

At depths of 50 and 70 cm, large negative and positive values of the production rate of CO_2

were kept throughout the period for analysis, respectively. The production rates evaluated for these depths would be affected by the overestimate of the diffusive flux between both depths (see Section 5.2.2 (2)), because the production rates at these depths changed complementarily and were considerably offset each other. On the other hand, the uptake of dissolved CO_2 in soil water by plant roots might play a role as the sink of CO_2. Although the sink was not considered in the evaluation of soil water flux among the soil compartments, some sinks of soil water were actually obtained at the depth of C-ZFP. However, most of the sinks were found at depths of 20 and 70 cm, and the sum of the sinks in each profile ranged from 1.42×10^{-13} to 3.85×10^{-12} $gCO_2\cdot cm^{-3}\cdot s^{-1}$, much smaller than the averaged sink of 2.01×10^{-10} $gCO_2\cdot cm^{-3}\cdot s^{-1}$, evaluated at 50 cm. Moreover, biologically active roots probably act as a source of CO_2 by their respiration rather than as a sink by their water uptake. So that the uptake by plant roots cannot explain the sink of CO_2 at a depth of 50 cm. Therefore, the net sink of CO_2 at a depth of 50 cm would not be present actually and the production rate at 70 cm must be much lower. Because of the small total flux, the production rates of CO_2 at depths of 100 and 150 cm were kept extremely low.

At the grassland site, the seasonal variations of the production rate of CO_2 were almost similar to the variations of the diffusive flux in soil air, showing large values and fluctuations in the summer of 1997. The largest value of the production rate in the profile was mostly obtained at a depth of 5 cm. The maximum value reached 3.11×10^{-9} $gCO_2\cdot cm^{-3}\cdot s^{-1}$ in early August of 1997, when the diffusive flux at the soil section of 0-5 cm was also at maximum. At a depth of 10 cm, in contrast, the production rate showed generally small values or even negative values frequently. The large values observed in June and July 1997 resulted from the exceptional treatment corresponding to the missing of the measured values of CO_2 concentration in soil air at 5 cm. Such a difference in the production rate between these depths was due to the diffusive flux at the soil section of 5-10 cm much smaller than at 0-5cm; as discussed previously, this difference in the diffusive flux might be caused by the specific method for measuring CO_2 concentration at 5 cm. Usually, exceptionally large values of the production rate at a depth of 5 cm accompanied relatively large negative values of the rate at 10 cm. As a result, the sum of the production rate at these depths became relatively stable, and the proportion of the summed rate to the total production rate in the whole profile ranged from 67.7 to 97.6% and averaged 79.5%. That is, the four-fifths of the CO_2 generated in the soil of the grassland site concentrated between the ground surface and a depth of 15 cm.

At a depth of 20 cm, relatively large production rates of CO_2 were observed. The proportion of the rate to the total production rate ranged from 6.0 to 28.8% and averaged 18.2%, but the rate was always lower than the rate at either of the above depths and never exceeded 0.5×10^{-9} $gCO_2 \cdot cm^{-3} \cdot s^{-1}$. At a depth of 30 cm, in contrast, extremely low production rates were kept due to the little diffusive flux in soil air. The evaluated negative values were only a few, but the proportion of the production rate reached up to 2.16% and was usually less than 1.0%.

At depths of 40 and 50 cm, negative values were consistently evaluated as the production rate of CO_2. The reason for the negative values at 40 cm was that the total flux of CO_2 was little at the soil section of 30-40 cm while the relatively large upward flux of diffusion was obtained at 40-50 cm, and for 50 cm was that the larger upward flux was estimated at 50-70 cm than the flux at 40-50 cm. On the other hand, relatively large production rates were found at 70 cm. Such positive and negative values of the production rate evaluated at these depths were almost completely offset. Such production rates would be due to the overestimate of the diffusion flux in soil air at the soil sections of 40-50 and 50-70 cm, similar to at the forest site. As well as at the forest site, some sinks of dissolved CO_2 in soil water were obtained, but the rate was similar to that at the forest, much smaller than the evaluated sinks by the mass balance. Hence the net sinks of CO_2 at depths of 40 and 50 cm were actually absent, and the production rate at 70 cm was probably much lower. At a depth of 100 cm, the extremely small total flux was usually kept the production rate little. At 150 cm, where few data were obtained because of the missing of CO_2 measurement, the evaluated values of the production rate were also little.

The difference in the total production rate of CO_2 between both observation sites was small. At the grassland site, however, the CO_2 production was concentrated closer to the ground surface than the production at the forest site. Except for the depths affected by the overestimate of the diffusive flux at both sites, the soil layer in which CO_2 was mainly produced ranged from the surface to a depth of 45 cm at the forest, and to 25 cm at the grassland. The profiles of the production rate were corresponding to the distribution of plant roots at both sites; namely, both CO_2 production and plant roots were found in deeper soils at the forest than at the grassland (Figures 3.7 and 3.8). This agreement of the distribution between the production rate and the plant roots would support the reliability of the deterministic approach used for evaluating CO_2 production rate in this study.

At both sites, the negative production rate, namely the net sink of CO_2 was obtained around a

depth of 50 cm. Such negative values have been also obtained previous studies that used similar approaches. For example, de Jong and Schappert (1972) divided the soil profile into every 15-20 cm depth interval and estimated the production rate of CO_2 as the difference in the diffusive flux of CO_2 among the depths. They attributed the obtained negative activities to the low reliability of soil moisture profiles determined with a neutron moisture probe as well as the variation of the relationship between the relative diffusion coefficient and air-filled porosity. On the other hand, Wood et al. (1993) and Davidson and Trumbore (1995) divided the soil profiles into soil layers which had at least 1 m in thickness to avoid the problem. Instead, the detailed processes within the thick soil layers could not be examined. In this study, the soils around the depth at which the negative production rates were evaluated showed relatively low saturated hydraulic conductivity (Figures 3.5 and 3.6), so that it was suggested that the diffusion coefficient of CO_2 in soil air estimated by the M-Q 2 equation, which was validated only near the ground surface, would be overestimated especially around the depth.

(3) Relationship between the production rate of carbon dioxide and soil temperature

The relationships between the production rate of CO_2 per unit volume of bulk soil and the soil temperature at the same depth of the forest and the grassland site are shown in Figures 5.31 and 5.32, respectively. The relationship was plotted for the depths in shallow soils at which significant production of CO_2 was observed; from the ground surface to a depth of 40 cm for the forest, from the surface to 20 cm for the grassland. The production rate of CO_2 generally increased in response to the rise in soil temperature.

At the forest site, the production rate of CO_2 exponentially increased with rising soil temperature. From the regression analysis on the relationships excepting the negative values of the production rate, at depths of 10 and 40 cm, where relatively high production rates were observed, the production rates were well expressed as exponential functions of the soil temperature, as well as the relationship between soil respiration rate and soil temperature near the ground surface (Figure 5.5), and showing the coefficients of determination of more than 0.85. The mean values of the production rate averaged for the soil compartments between depths of 5 and 40 cm also exponentially increased with the averaged soil temperatures weighted by the thickness of the compartments at these depths. The coefficient of determination of the relationship was 0.939.

At the grassland site, high production rates of CO_2 were also found under high temperature conditions, but the amount of scatter was large. The averaged production rate between 5 and 40 cm distributed widely against the weighted mean values of soil temperature at these depths. The correlation between them was lower than that at the forest site, showing the coefficient of determination of 0.551. The difference in the correlation of the relationship between the forest and the grassland, which was also obtained relative to soil respiration rate (cf Figures 5.5 and 5.6), was probably due to the high variability of the micrometeorological conditions other than soil temperature, such as soil moisture condition at the grassland site.

The relationship that the production rate of CO_2 exponentially increases in response to the linearly rising soil temperature has been presented in previous studies using the collected soil samples by laboratory experiment (e.g. Seto et al., 1978; Howard and Howard, 1993). Therefore, the relationships between the production rate and soil temperature obtained in this study would be suggest that the production rate given as the remainder of CO_2 mass balance (Equation 5.23) was evaluated reasonably.

(4) Mean residence time of carbon dioxide

The residence time of a substance, namely the time in which the substance is stored within a reservoir, is given by the turnover time that is calculated by dividing the amount of the stored substance by the input or output fluxes of the substance, if the system is under steady-state and the substance is completely mixed in the reservoir (Yamamoto, 1986). In this study, for the soil compartments in shallow soils of both sites showing significant CO_2 production, the change rate of the storage of CO_2 in the compartment was much lower than the production rate and the diffusive flux in soil air, so that the system of CO_2 movement in the shallow soils can be regarded as almost steady-state. Thus, for the soil compartments at these depths, the mean residence time was estimated simply by dividing the storage of CO_2 in the compartment by the total flux out of the compartment. The results of the estimate at the forest and the grassland site are shown in Figures 5.33 and 5.34, respectively. The mean residence time was not estimated for the depth and time at which negative values of the production rate were obtained.

In general, at both sites, the total content of CO_2 per unit volume of bulk soil increased with depth (Figures 4.32 and 4.33), whereas the total flux of CO_2 decreased with depth (Figures 5.21 and 5.22). As a result, inevitably, the mean residence time of CO_2 was shortest near the ground

surface and increased with depth. At the forest site, the mean residence time at a depth of 5 cm was within an hour at maximum and less than thirty minutes at minimum. The mean residence time increased gradually with depth, but even at 40 cm, the time ranged from 8 to 24 hours and was rarely more than a day.

At the grassland, in contrast, the mean residence time of CO_2 was much longer than at the forest, due to the higher total content and the lower total flux except near the grouund surface. At a depth of 5 cm, the mean residence time reached more than half a day at maximum, though the time became less than half an hour at minimum. At depths of 10 and 20 cm, the values of the mean residence time at minimum were also similar to the time at the same depths of the forest site, but the values at maximum became extremely large. The largest values of the mean residence time obtained at both depths were 58.9 and 190 hours, respectively.

The mean residence time of CO_2 also varied seasonally, short in the summer and long in the winter. This seasonal trend suggests that the increasing rate of the total flux of CO_2 was higher than the rate of the total content of CO_2 in the summer, and the decreasing rate of the flux was higher than the rate of the content in the winter.

The mean residence time of CO_2 in a soil has been estimated by Kirita (1971). He estimated roughly the residence time in the shallow soil layer ranged from the ground surface to a depth of 60 cm, using the measured values of soil respiration rate and the concentration of CO_2 in soil air at a warm-temperate evergreen broadleaf forest in the Southwestern Japan. According to his results, the mean residence times were about two to three hours. In Kirita (1971), the air-filled porosity was assumed as a constant value of 50%, and the CO_2 dissolved in liquid phase of the soil was not considered. In addition, Kirita (1971) determined the soil respiration rate by alkali adsorption method, which has been suggested to be likely to overestimate the rate. Considering these aspects, the estimated values of the residence time by Kirita (1971) was probably underestimated, and the residence time actually might be similar to the time obtained in this study. The reasonably estimated mean residence time of CO_2 in the soils is one of the factors that suggest the reliability of the deterministic approach used in this study for assessing quantitatively the production and transport processes of CO_2 in soil profiles.

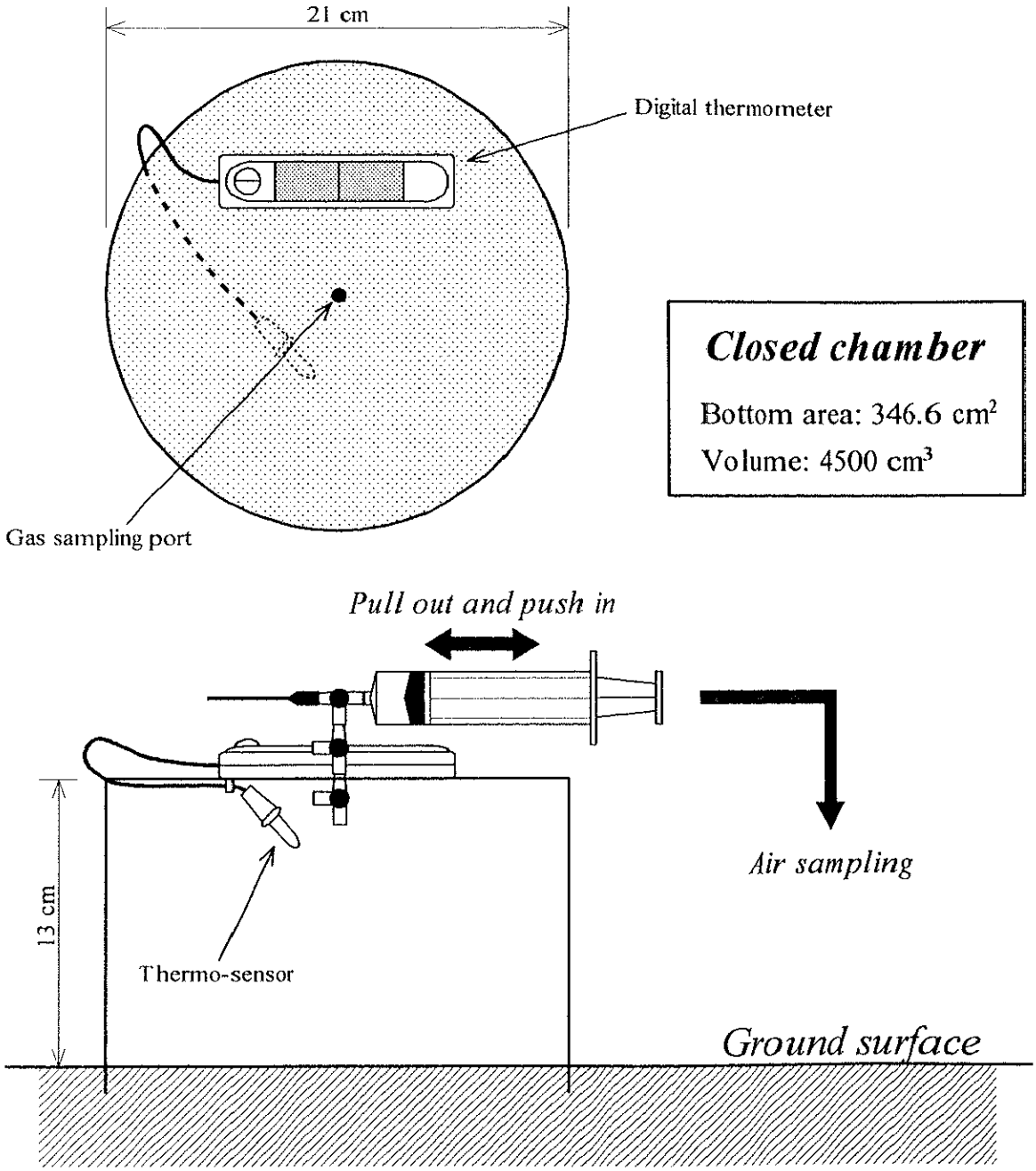

Figure 5.1. Design of and schematic operation on the closed chamber used for measuring soil respiration rate.

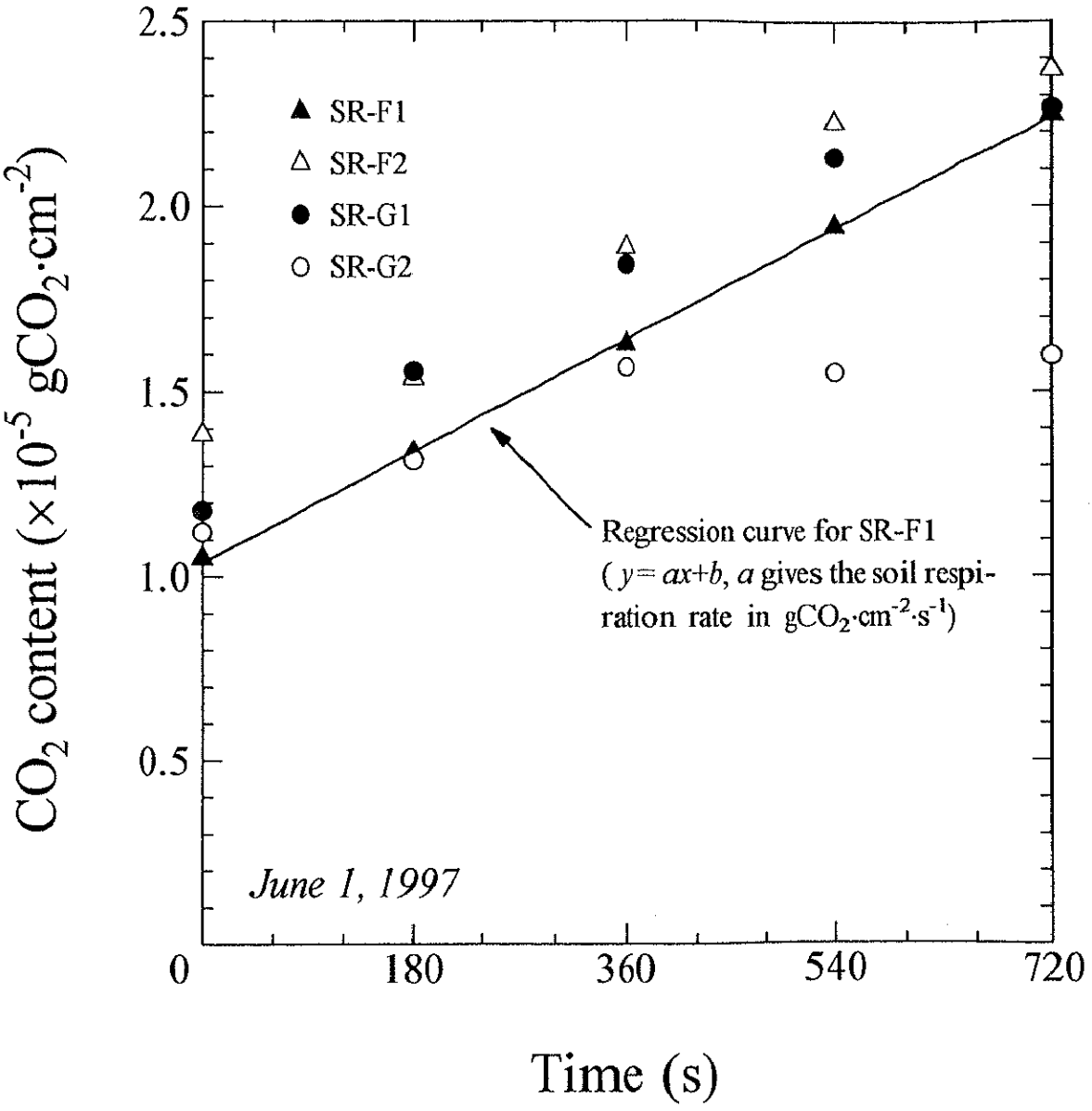

Figure 5.2. Temporal variation of CO_2 content in the closed chamber at the forest and the grassland site on June 1, 1997.

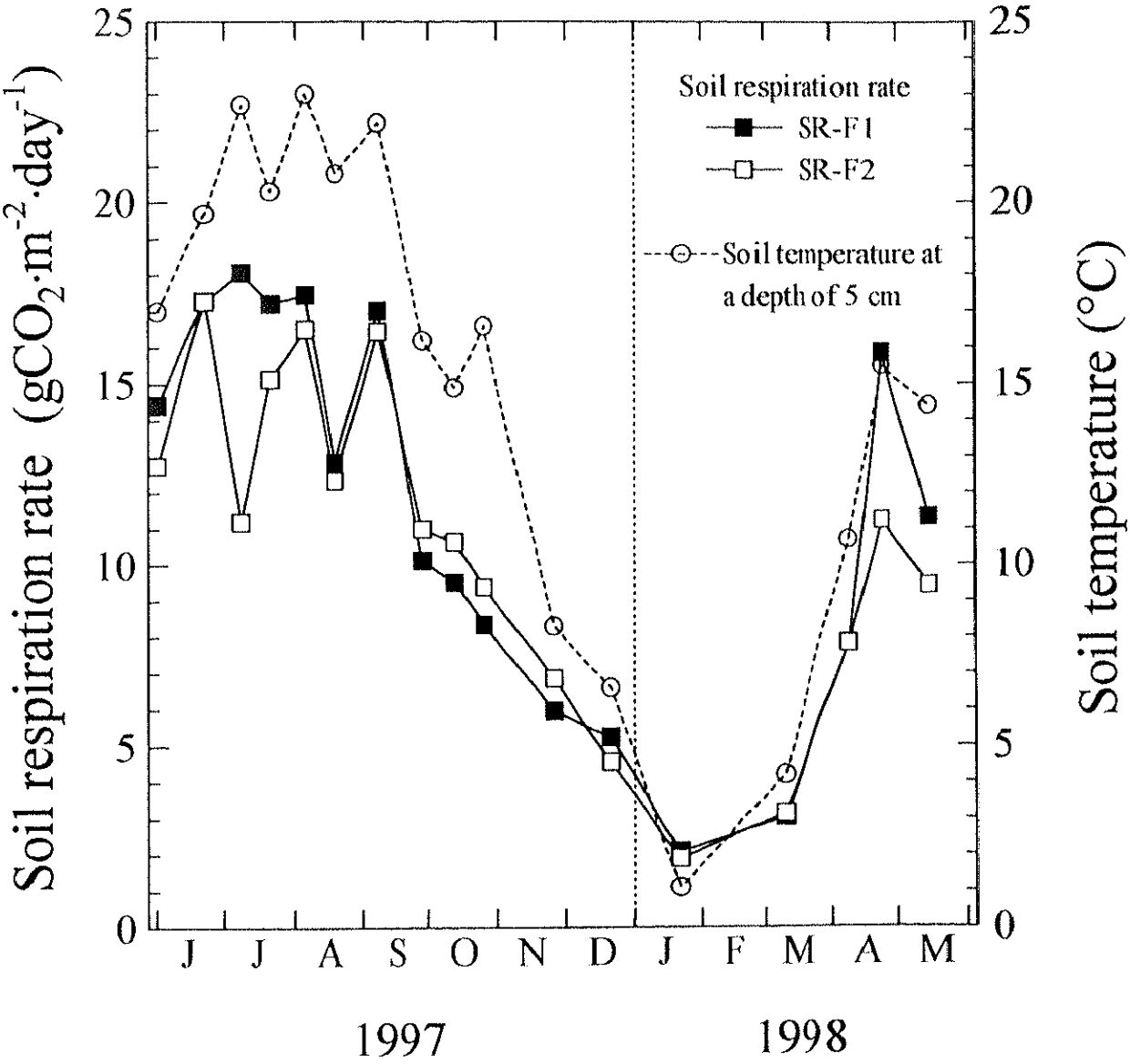

Figure 5.3. Seasonal variations of soil respiration rate and the soil temperature at a depth of 5 cm at the forest site.

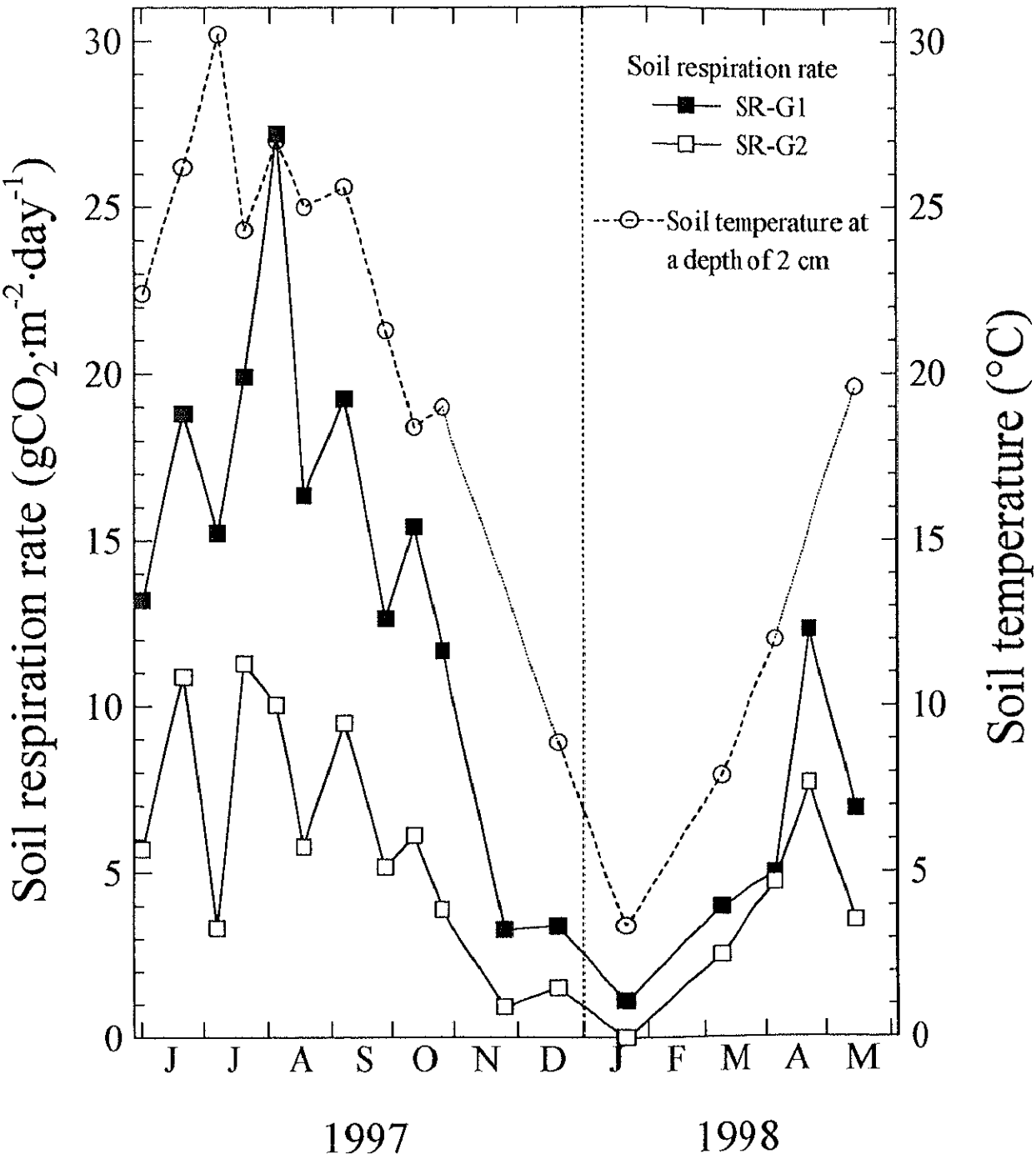

Figure 5.4. Seasonal variations of soil respiration rate and the soil temperature at a depth of 2 cm at the grassland site.

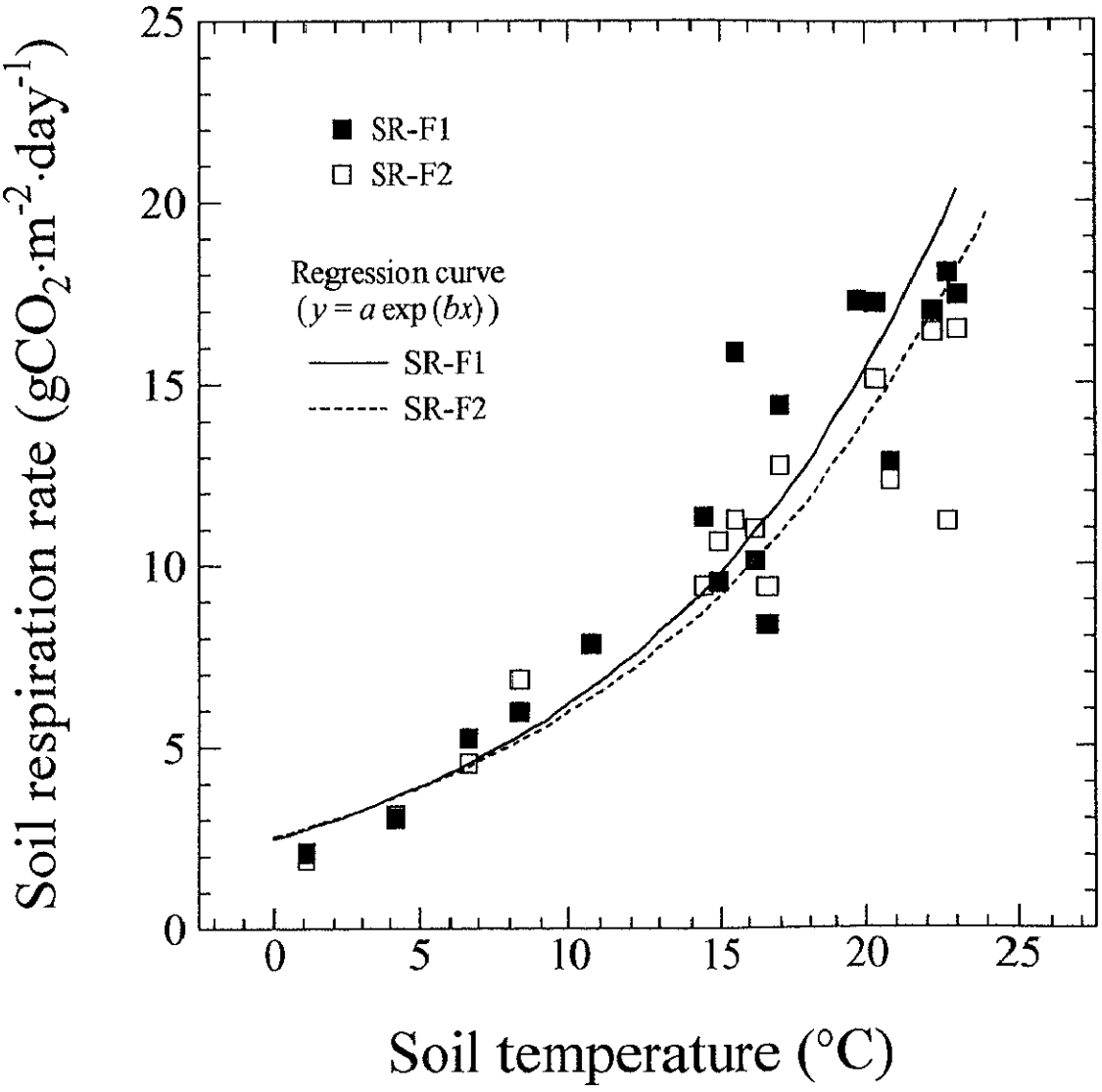

Figure 5.5. Relationship between soil respiration rate and the soil temperature at a depth of 5 cm at the forest site.

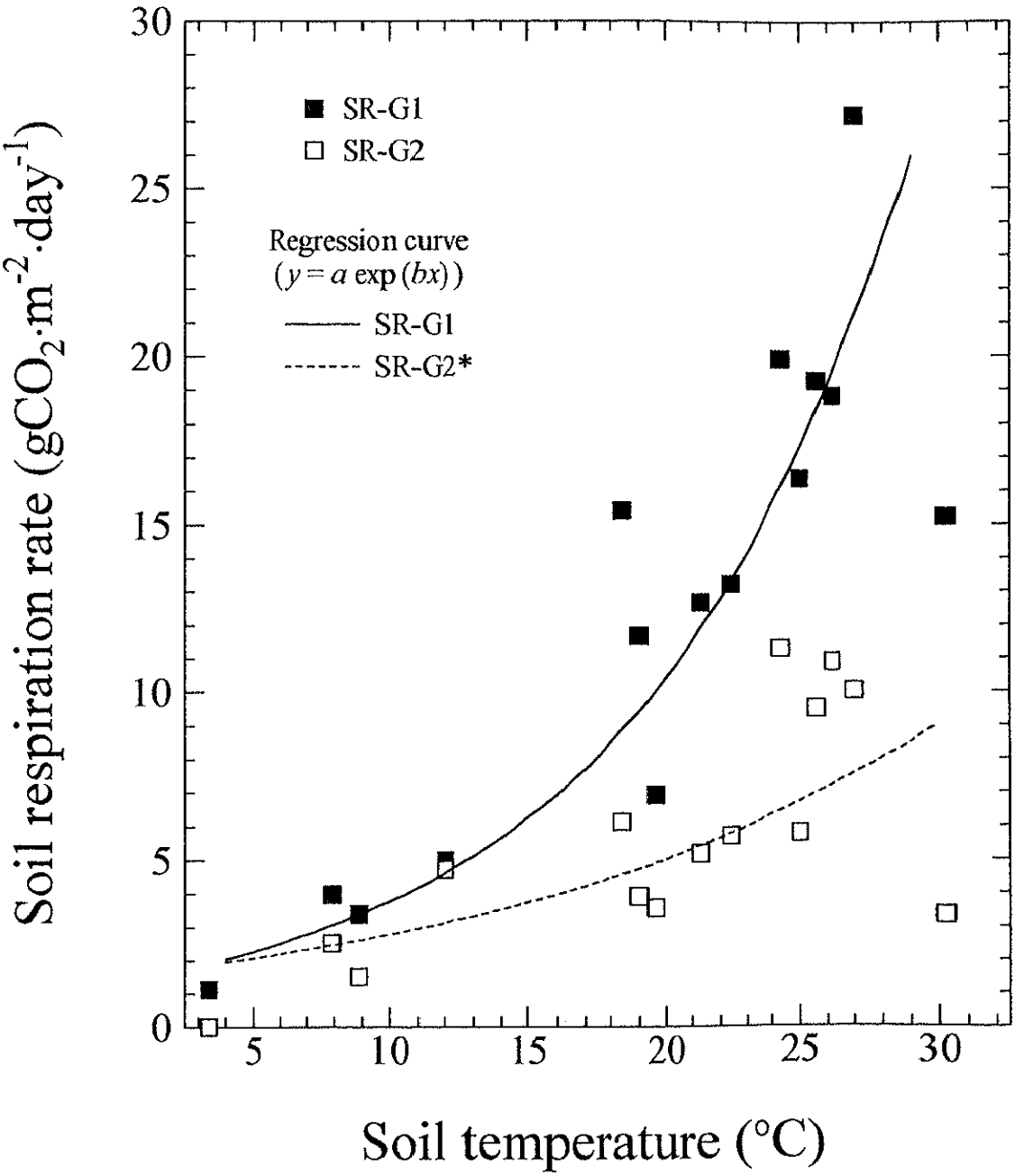

Figure 5.6. Relationship between soil respiration rate and the soil temperature at a depth of 2 cm at the grassland site.

* Data which showed zero as the value of soil respiration rate was omitted from the regression analysis.

Table 5.1. Results of the regression analysis between the soil temperature at a depth of 5 cm or 2 cm (x, °C) and soil respiration rate (y, $gCO_2 \cdot m^{-2} \cdot day^{-1}$) at the forest and the grassland site. Regression curves are expressed as $y = a \exp(bx)$, and the number of the samples and the coefficient of determination are shown as n and R^2, respectively.

Spot	n	a	b	R^2
SR-F1	17	2.494	0.09125	0.897
SR-F2	17	2.545	0.08543	0.880
SR-G1	15	1.369	0.1015	0.866
SR-G2	14	1.548	0.05874	0.467

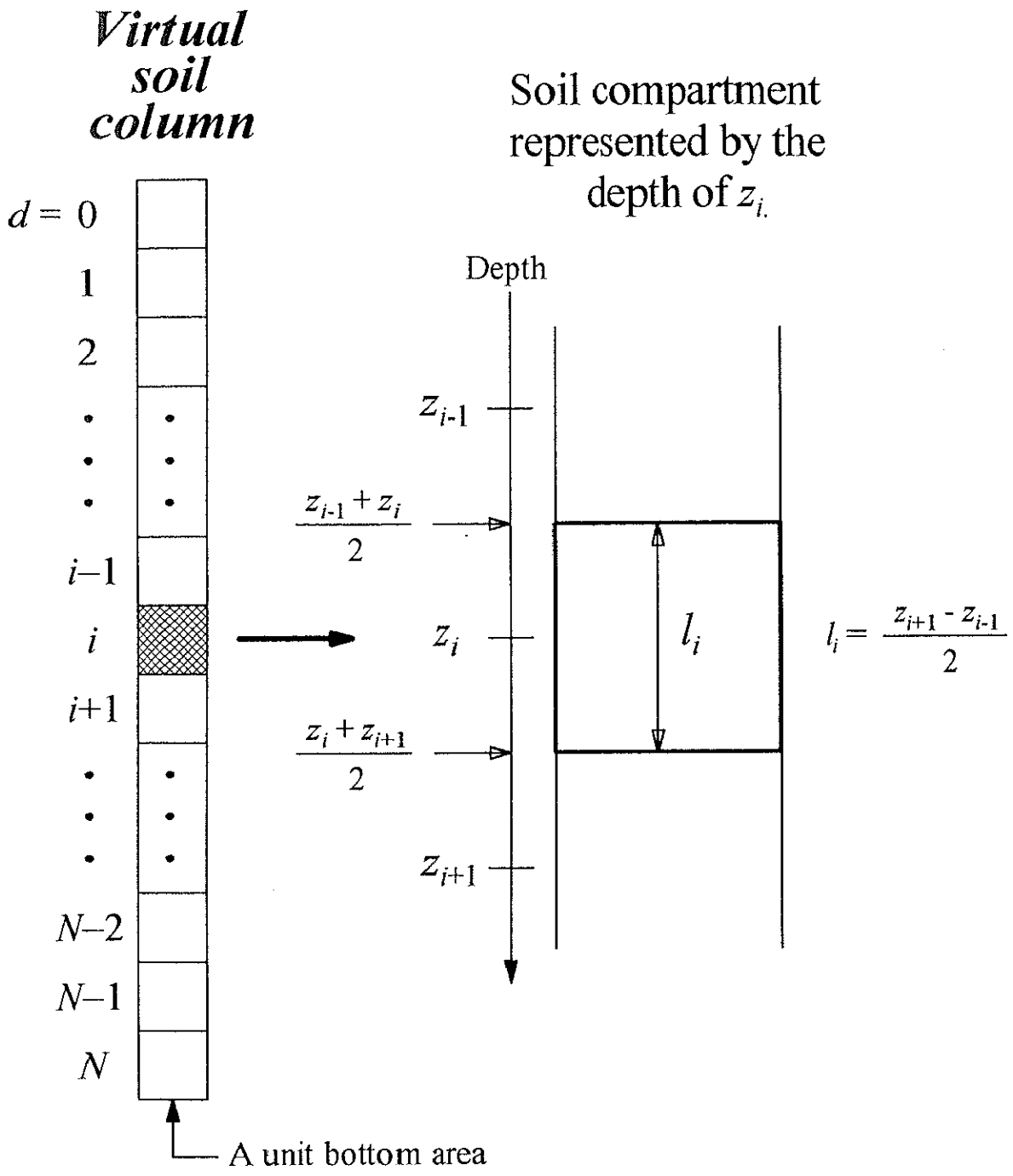

Figure 5.7. Diagram of the virtual soil column applied to the analysis of the fluxes and mass balance of CO_2.

Table 5.2. List of the values applied to the parameters of the virtual soil column to analyze the fluxes and mass balance of CO_2. Depth number of the soil compartment are shown as d, and the depth and the thickness of the compartment d are shown as z_d and l_d, respectively.

d	z_d (cm)	Depth of division (cm)	l_d (cm)
0	0		—
		0	
1	5		7.5
		7.5	
2	10		7.5
		15	
3	20		10
		25	
4	30		10
		35	
5	40		10
		45	
6	50		15
		60	
7	70		25
		85	
8	100		40
		125	
9	150		25
		150	

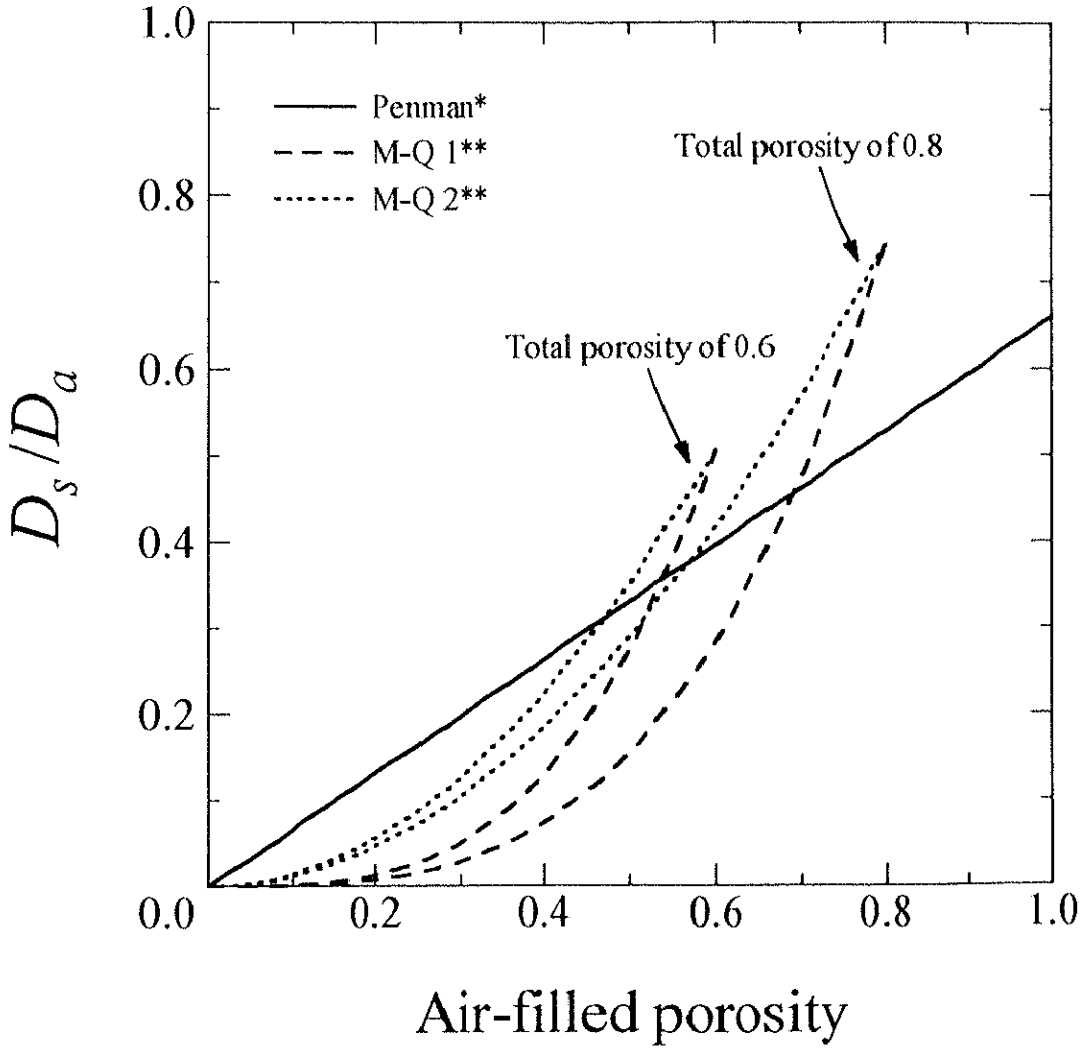

Figure 5.8. Relationship between the relative diffusion coefficient (D_s/D_a) estimated by each equation (Penman, M-Q 1 and 2) and the air-filled porosity and total porosity.

* Cited from Penman (1940).
** Cited from Millington (1959) and Millington and Quirk (1961).

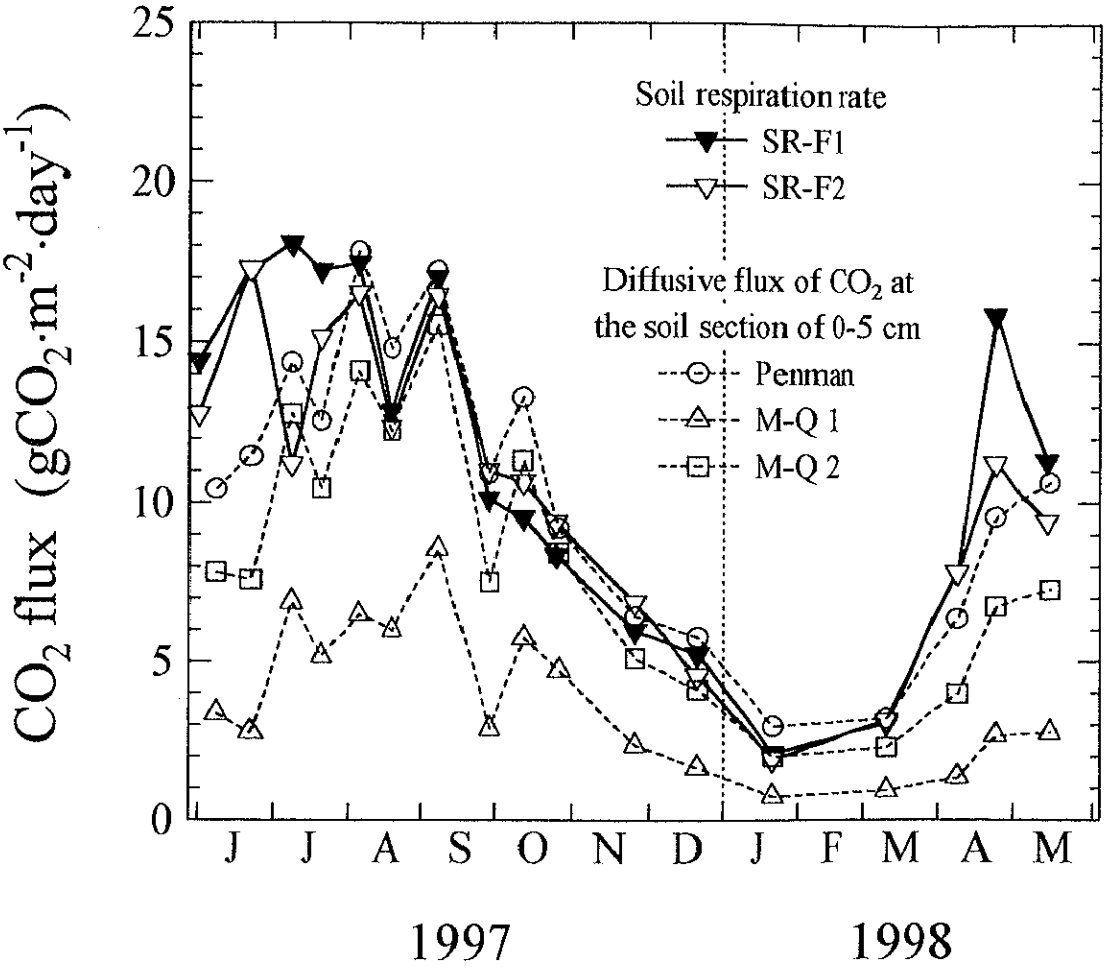

Figure 5.9. Comparison of the measured soil respiration rate and the evaluated diffusive flux of CO_2 in soil air at the soil section of 0-5 cm using each equation at the forest site.

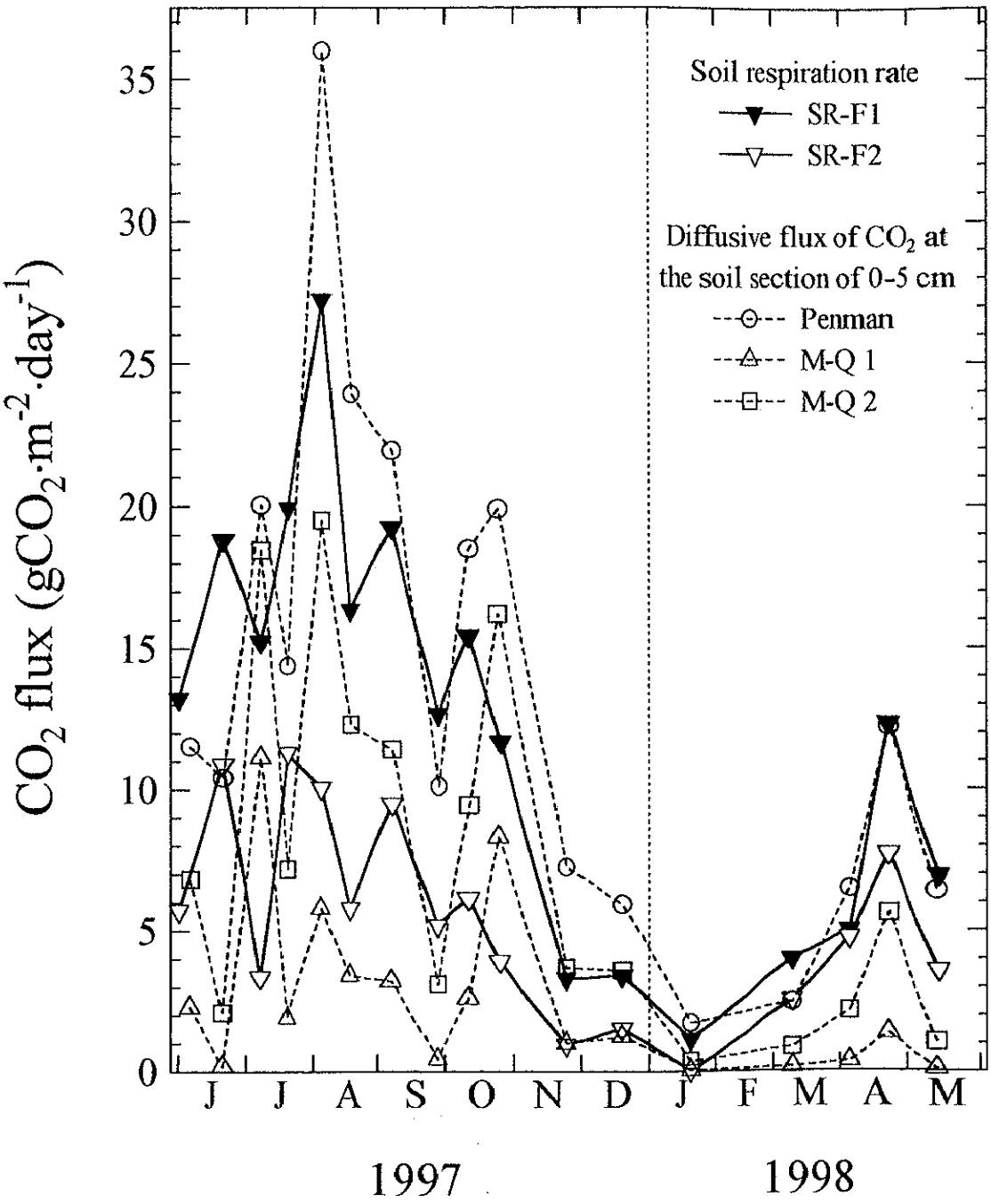

Figure 5.10. Comparison of the measured soil respiration rate and the evaluated diffusive flux of CO_2 in soil air at the soil section of 0-5 cm using each equation at the grassland site.

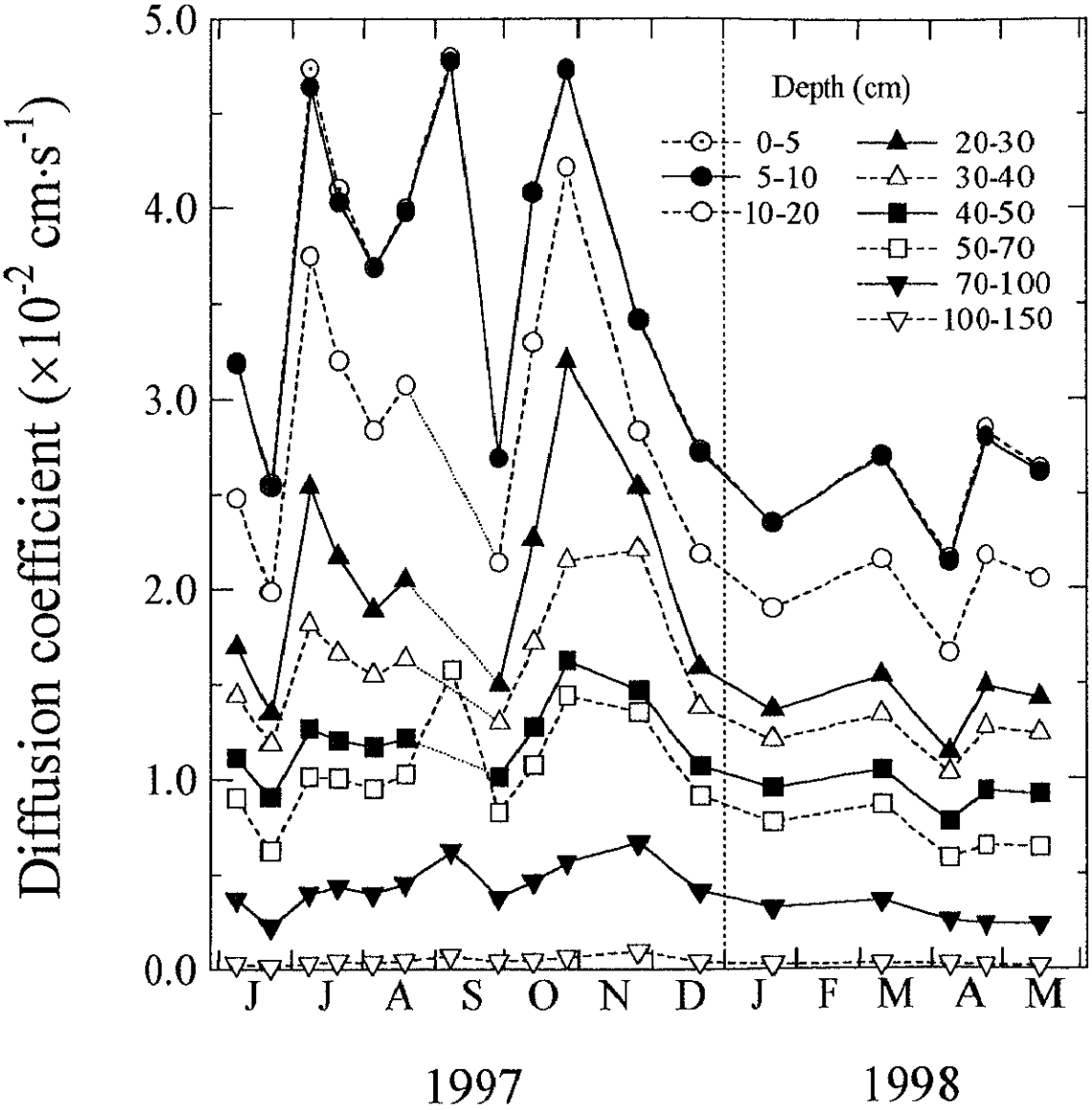

Figure 5.11. Seasonal variation of the diffusion coefficient of CO_2 in soil air at the forest site.

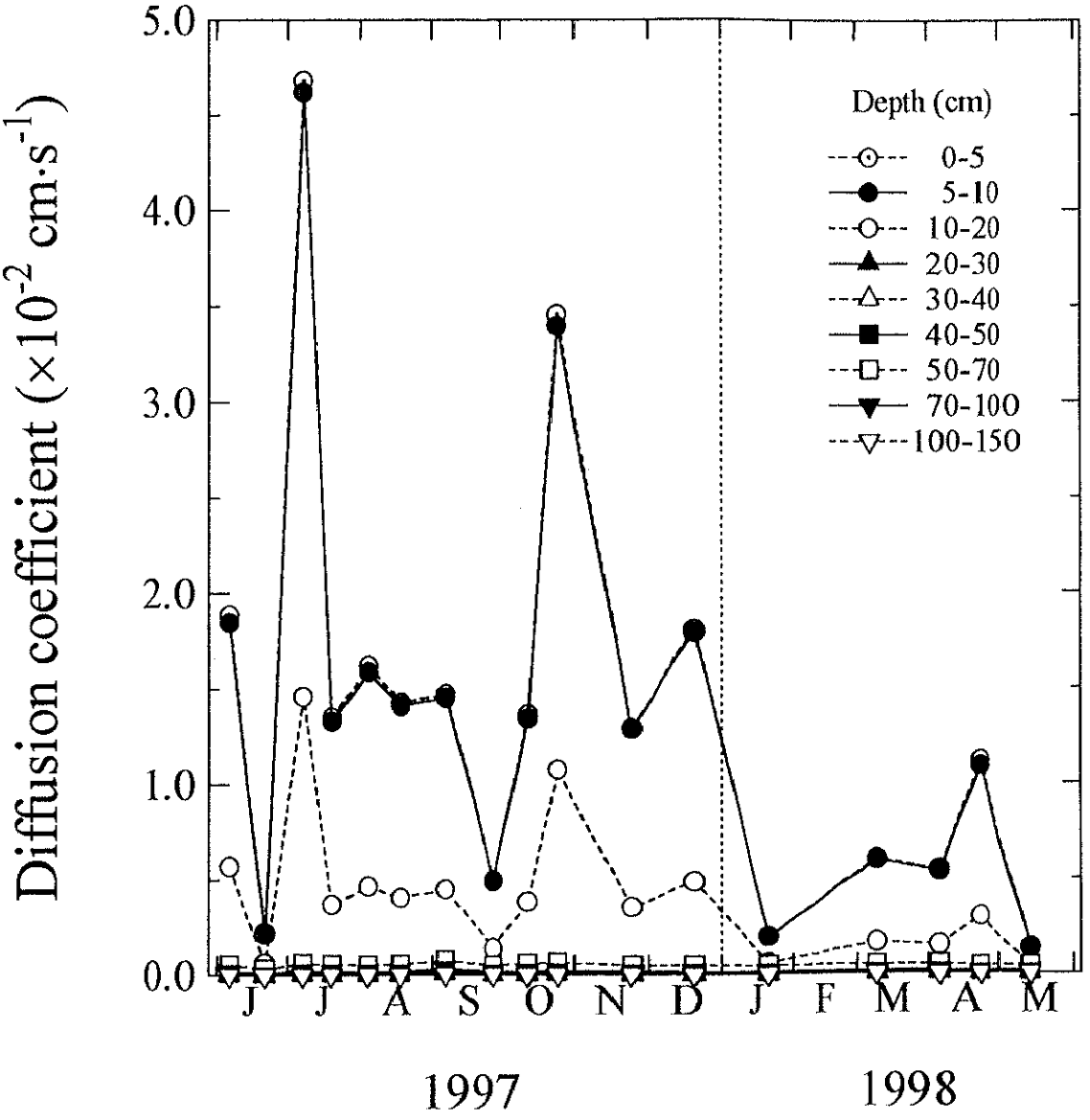

Figure 5.12. Seasonal variation of the diffusion coefficient of CO_2 in soil air at the grassland site.

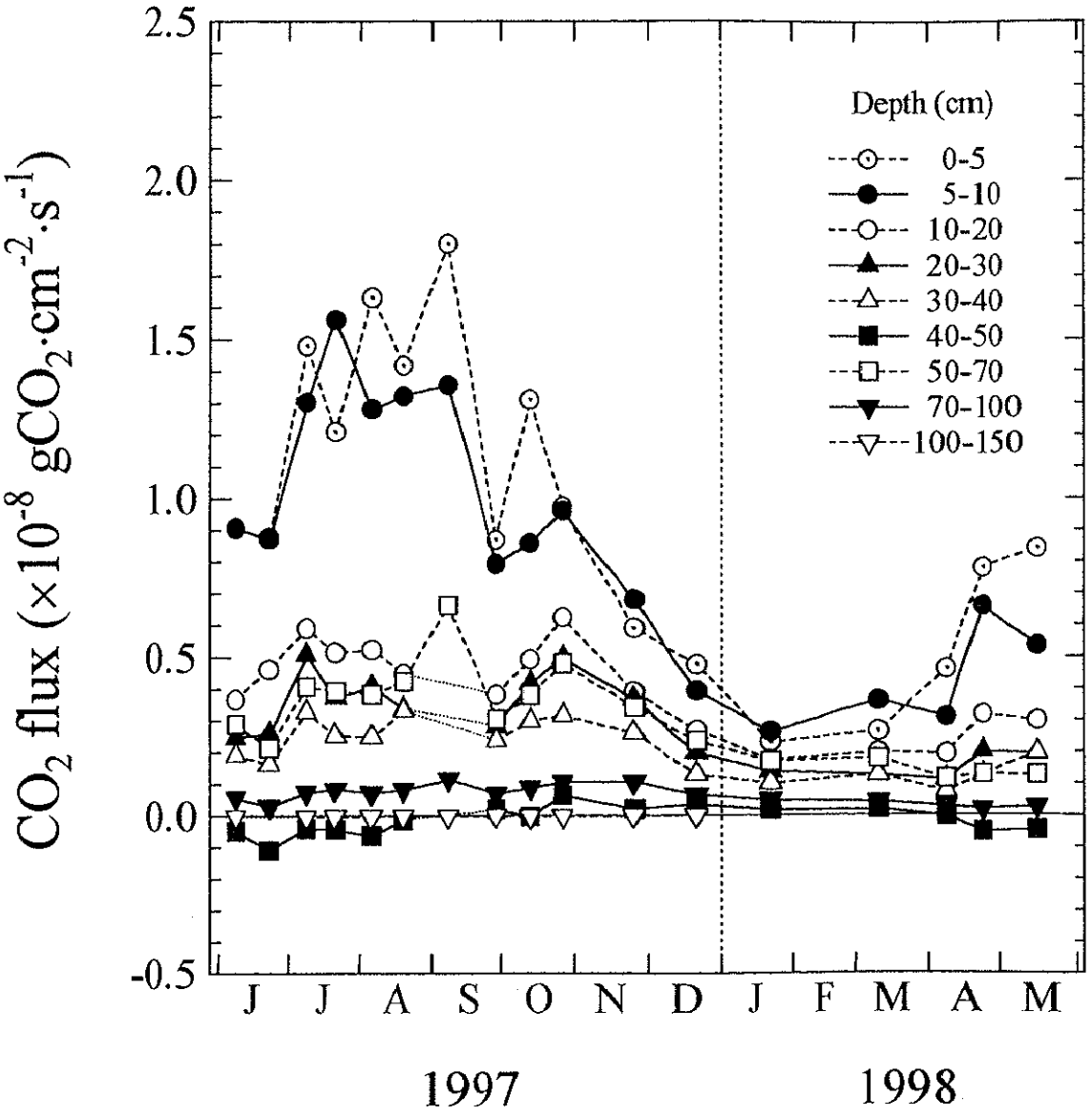

Figure 5.13. Seasonal variation of the diffusive flux of CO_2 in soil air at the forest site.

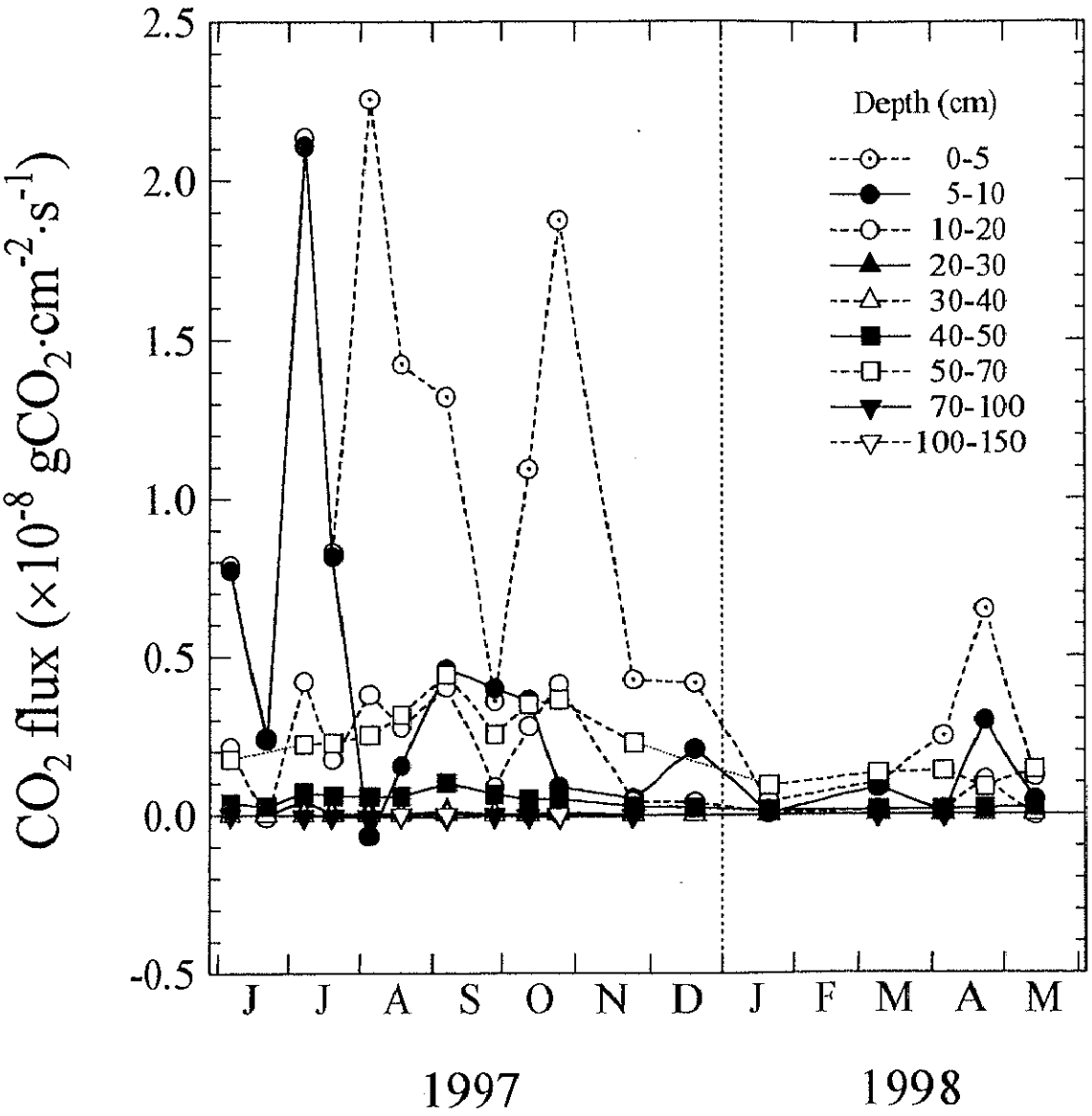

Figure 5.14. Seasonal variation of the diffusive flux of CO_2 in soil air at the grassland site.

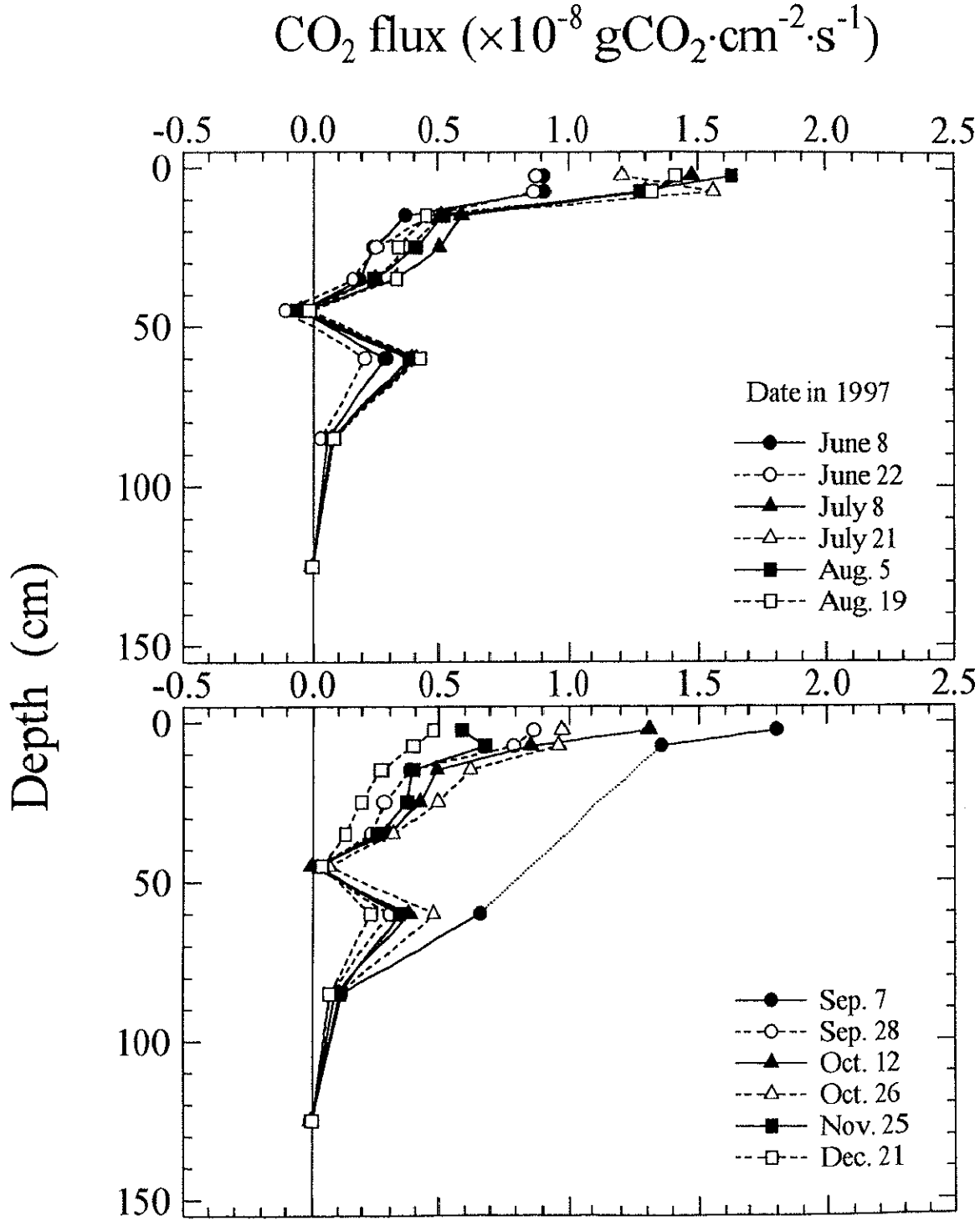

Figure 5.15a. Profiles of the diffusive flux of CO_2 in soil air at the forest site in 1997.

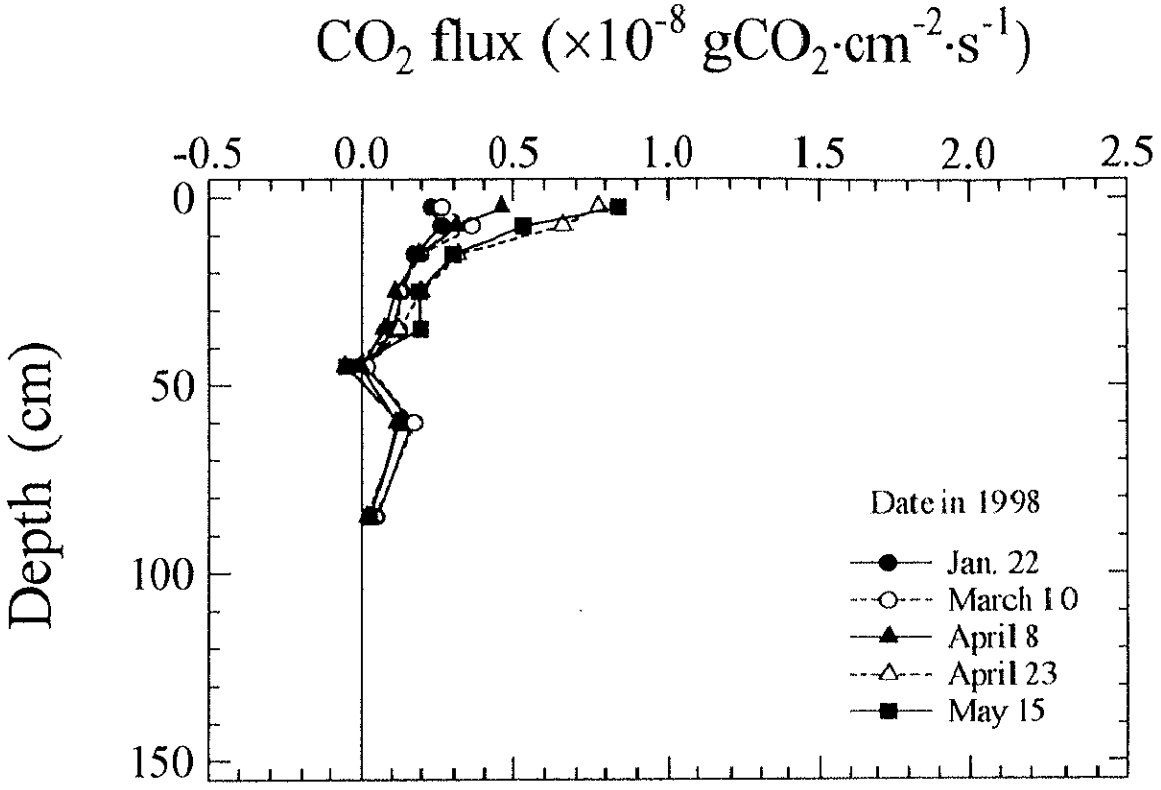

Figure 5.15b. Profiles of the diffusive flux of CO_2 in soil air at the forest site in 1998.

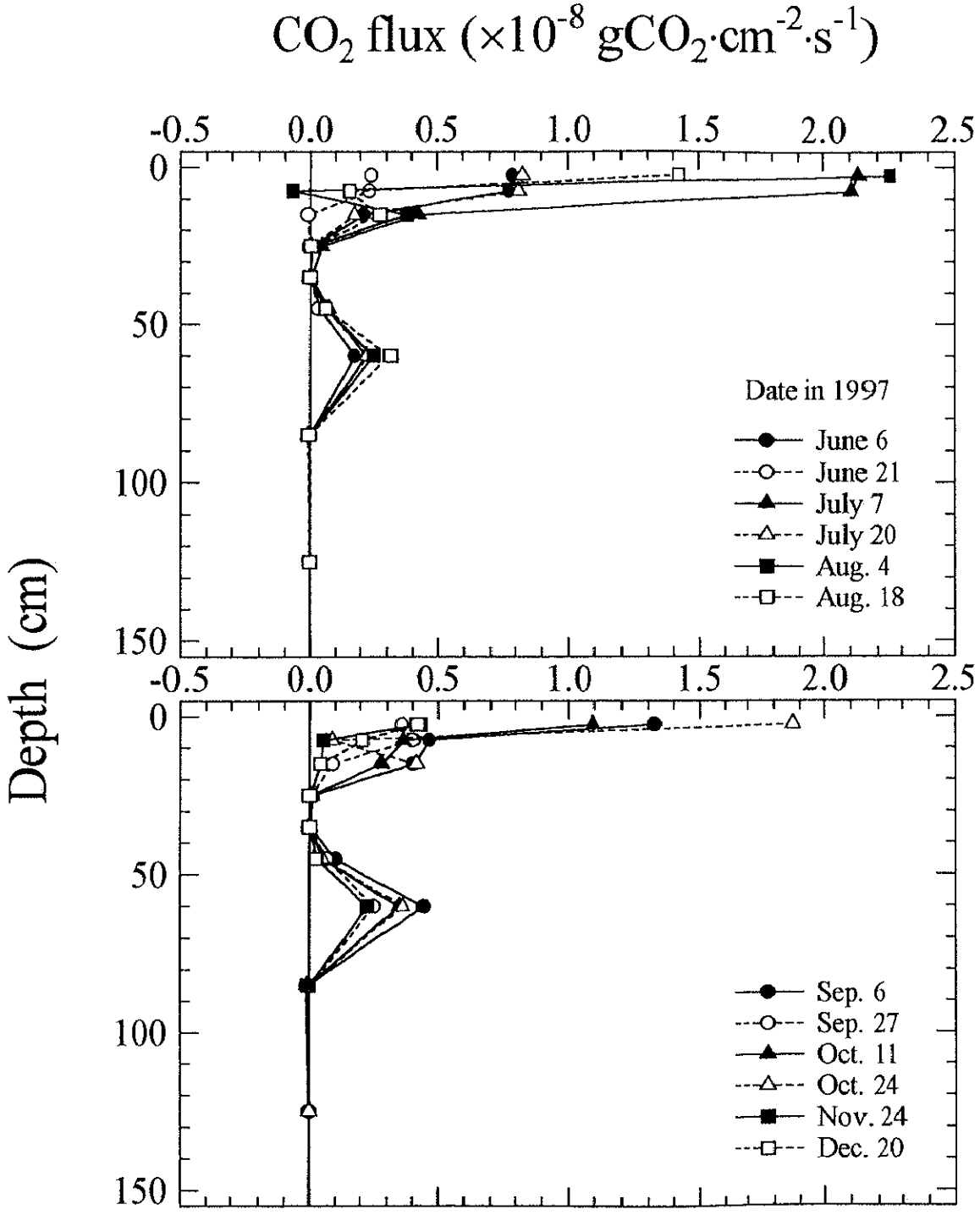

Figure 5.16a. Profiles of the diffusive flux of CO_2 in soil air at the grassland site in 1997.

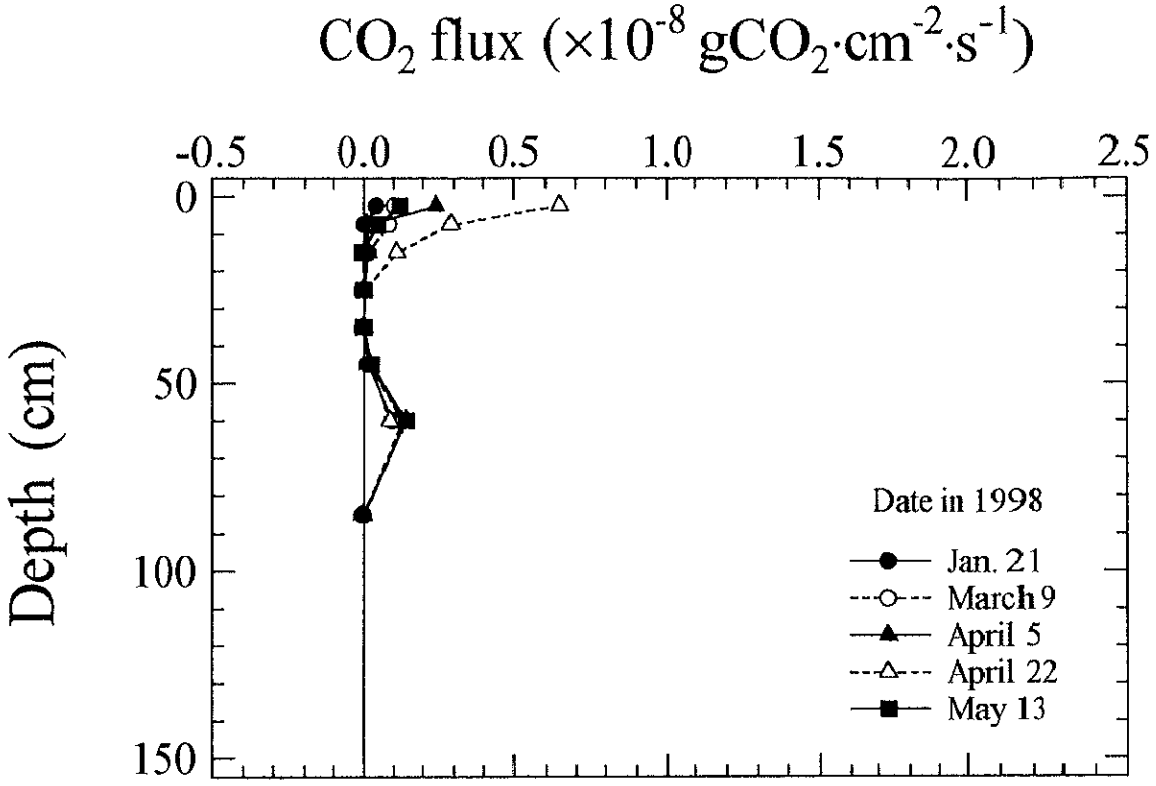

Figure 5.16b. Profiles of the diffusive flux of CO_2 in soil air at the grassland site in 1998.

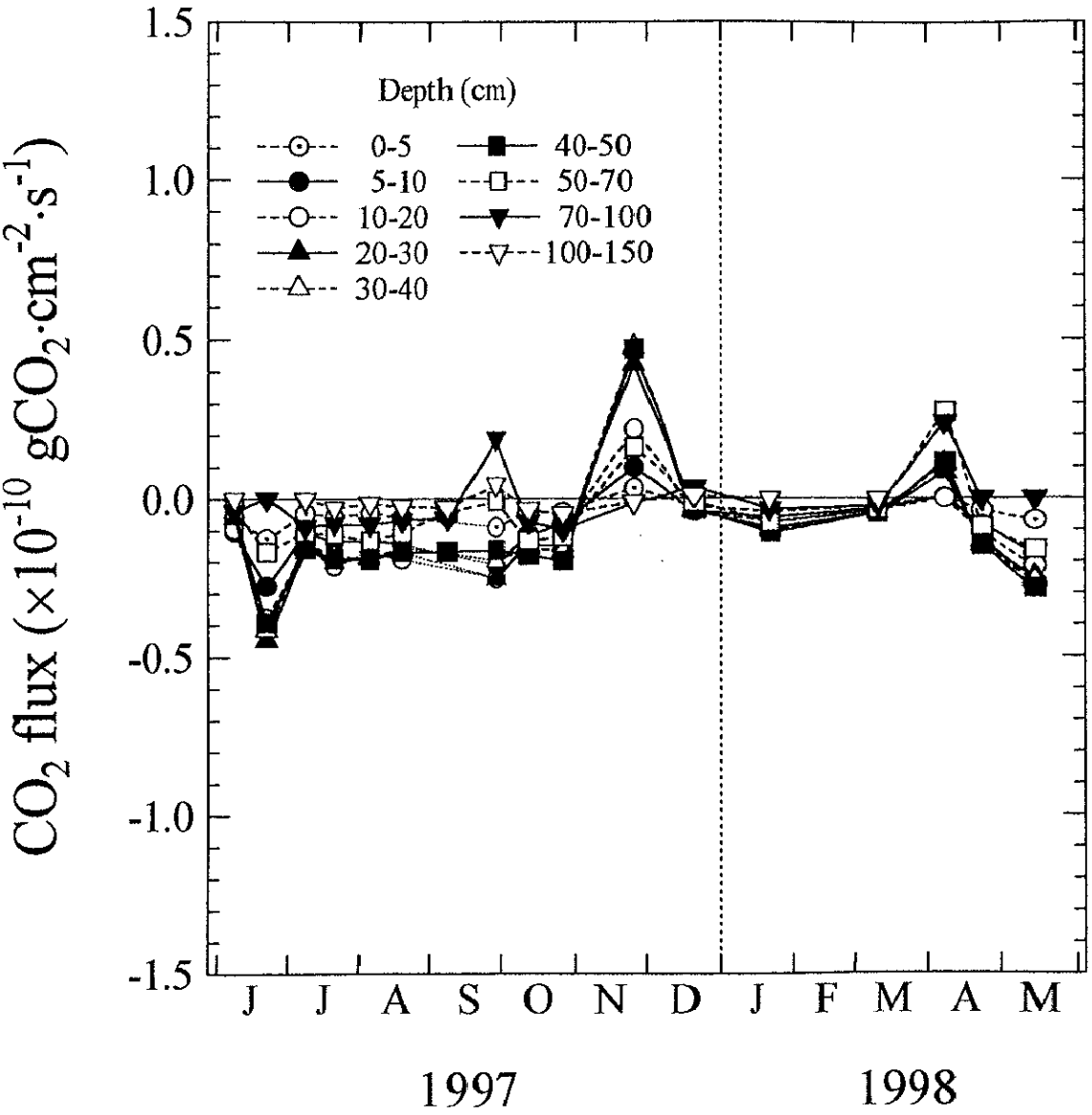

Figure 5.17. Seasonal variation of the advective flux of CO_2 accompanied by the mass flow of soil air at the forest site.

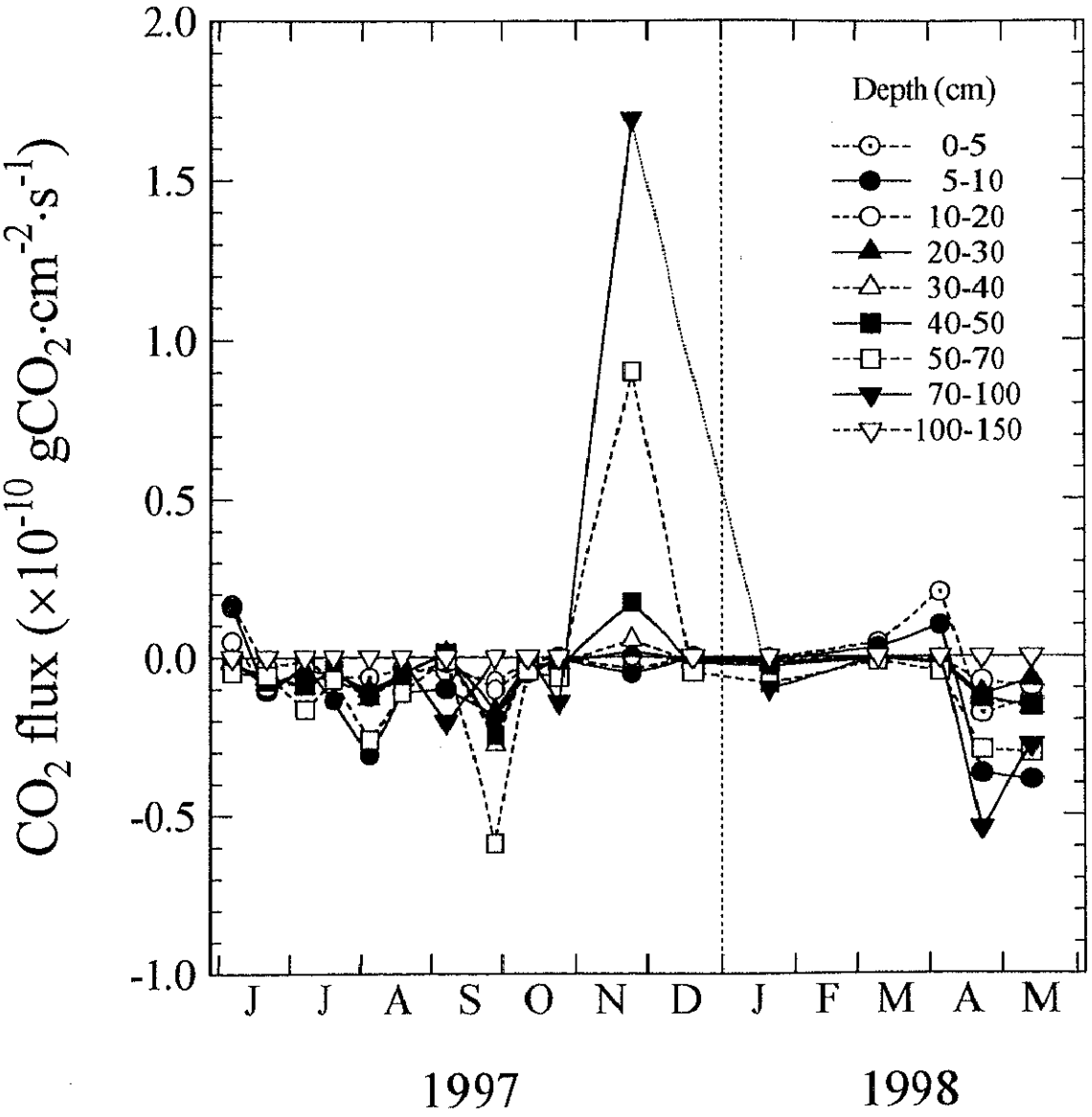

Figure 5.18. Seasonal variation of the advective flux of CO_2 accompanied by the mass flow of soil air at the grassland site.

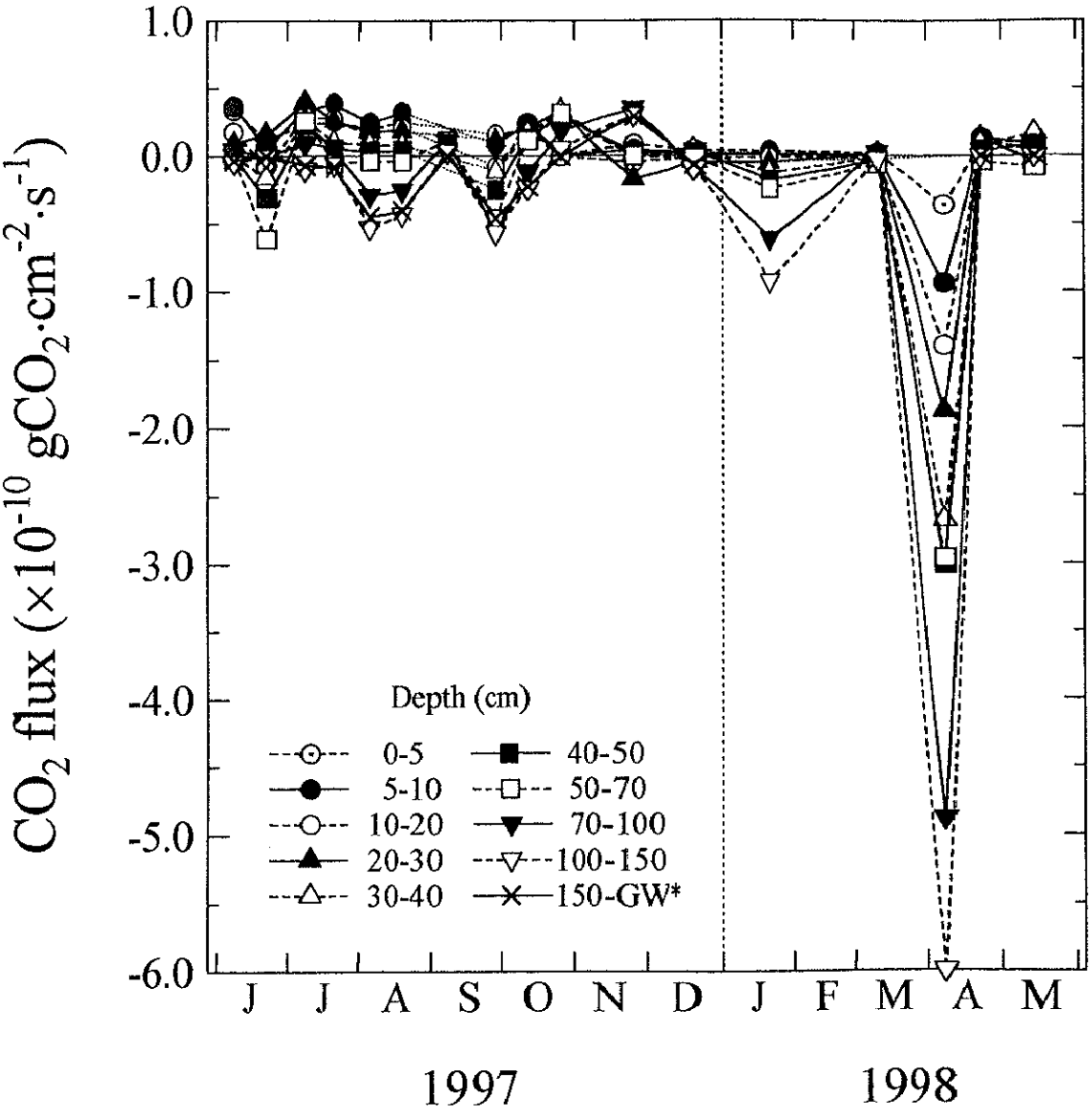

Figure 5.19. Seasonal variation of the advective flux of dissolved CO_2 accompanied by the movement of soil water at the forest site.

* Dissolved CO_2 flux across the lower boundary of the virtual soil column into or out of the groundwater.

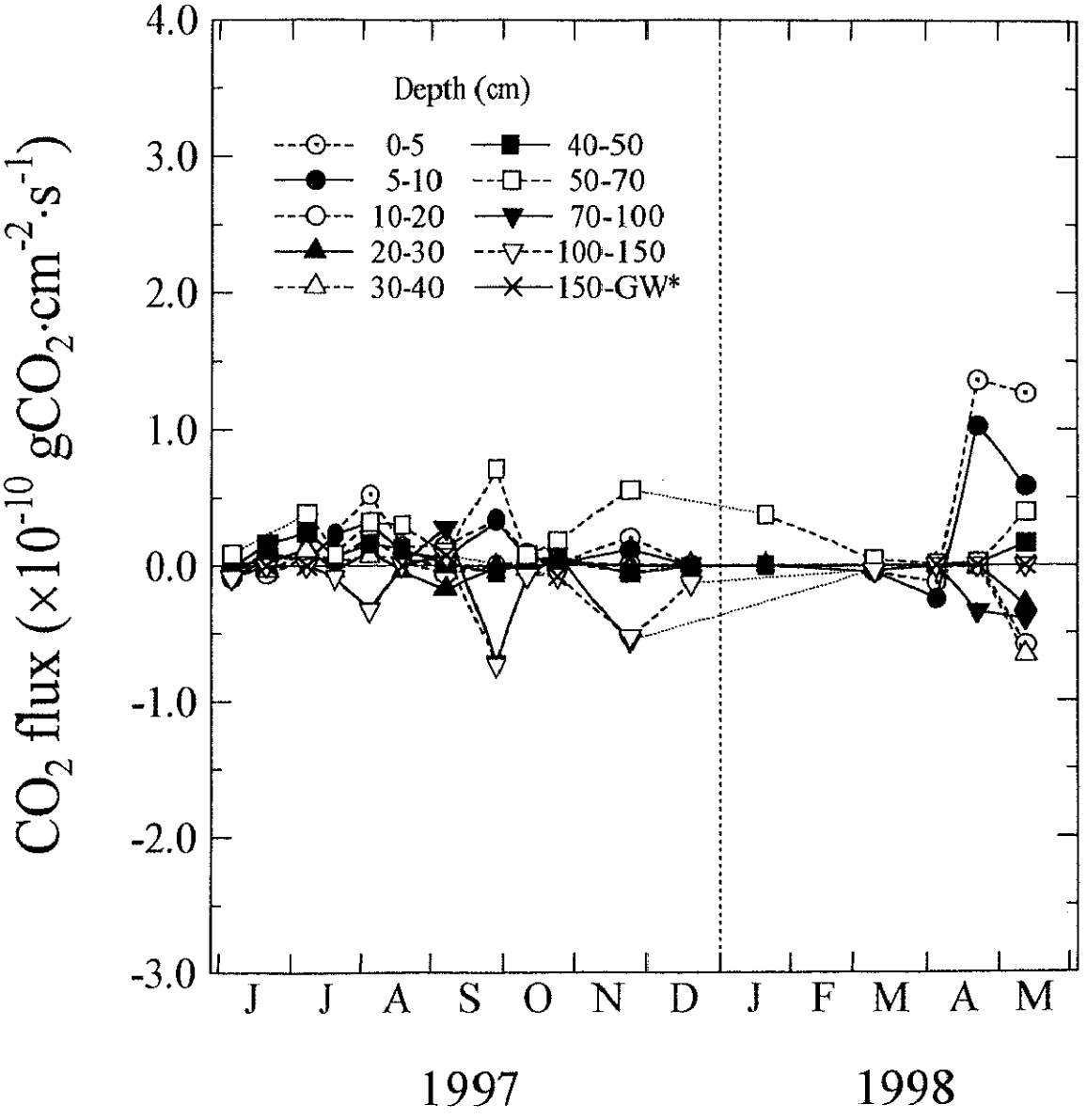

Figure 5.20. Seasonal variation of the advective flux of dissolved CO_2 accompanied by the movement of soil water at the grassland site.

* Dissolved CO_2 flux across the lower boundary of the virtual soil column into or out of the groundwater.

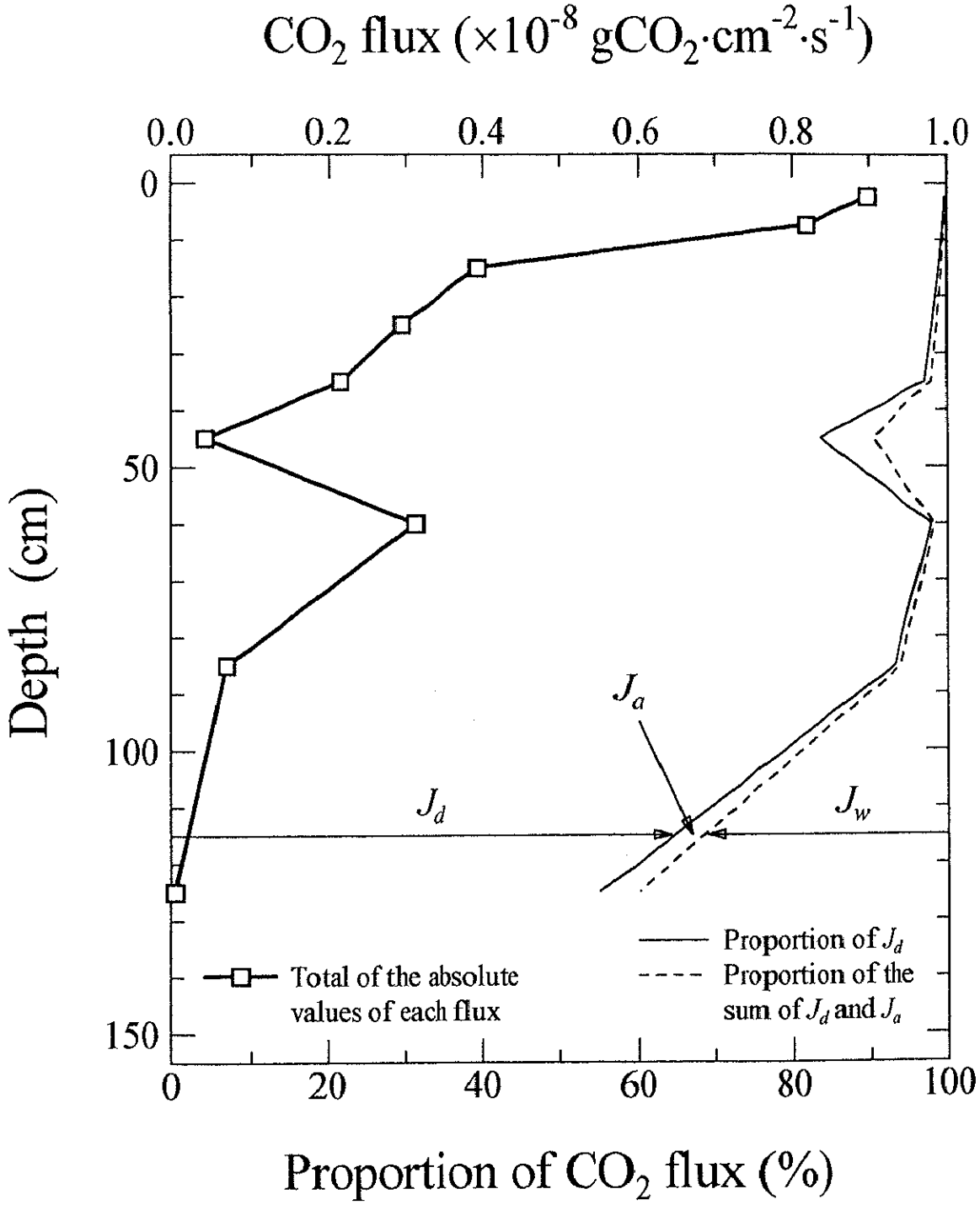

Figure 5.21. Profiles of the arithmetic mean of the total of absolute values of each CO_2 flux and the proportions of each flux — diffusive (J_d), advective (J_a) and dissolved (J_w) — to the total flux at the forest site.

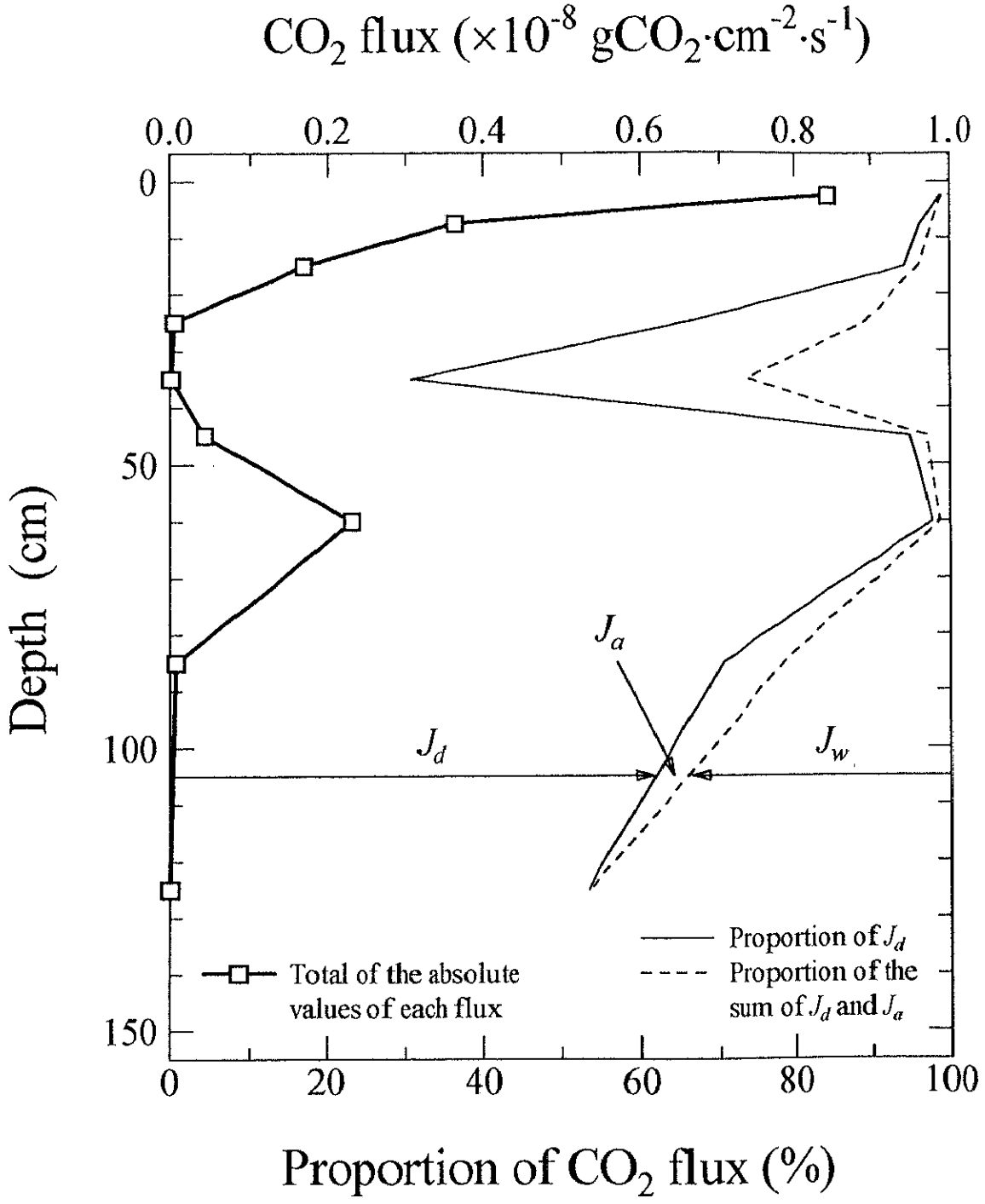

Figure 5.22. Profiles of the arithmetic mean of the total of absolute values of each CO_2 flux and the proportions of each flux — diffusive (J_d), advective (J_a) and dissolved (J_w) — to the total flux at the grassland site.

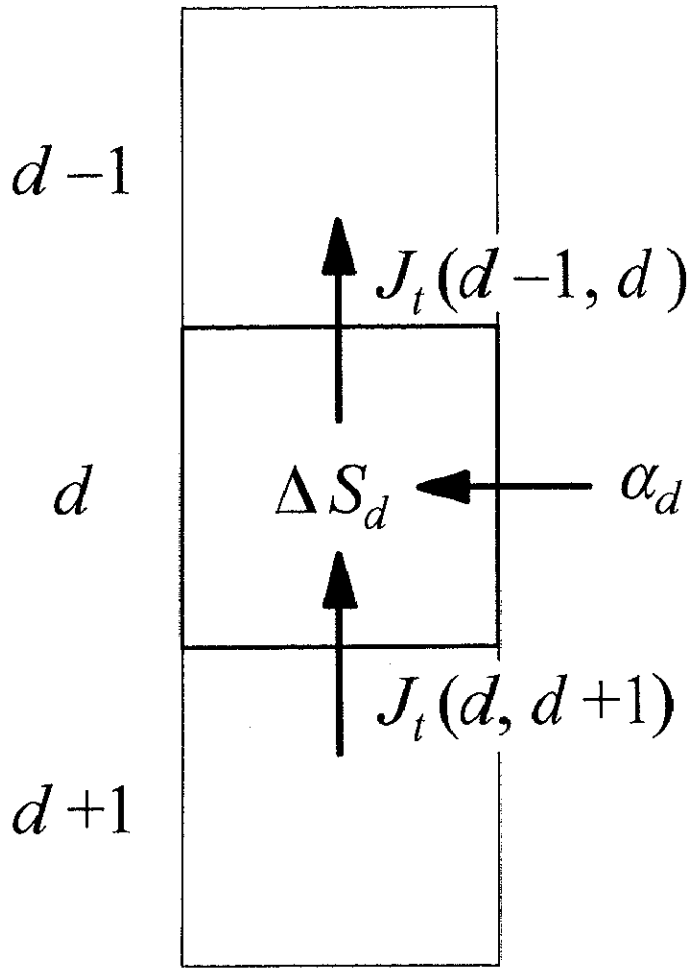

$$\alpha_d = J_t(d-1, d) - J_t(d, d+1) + \Delta S_d$$

Figure 5.23. Mass balance of CO_2 on the soil compartment d of the virtual soil column.

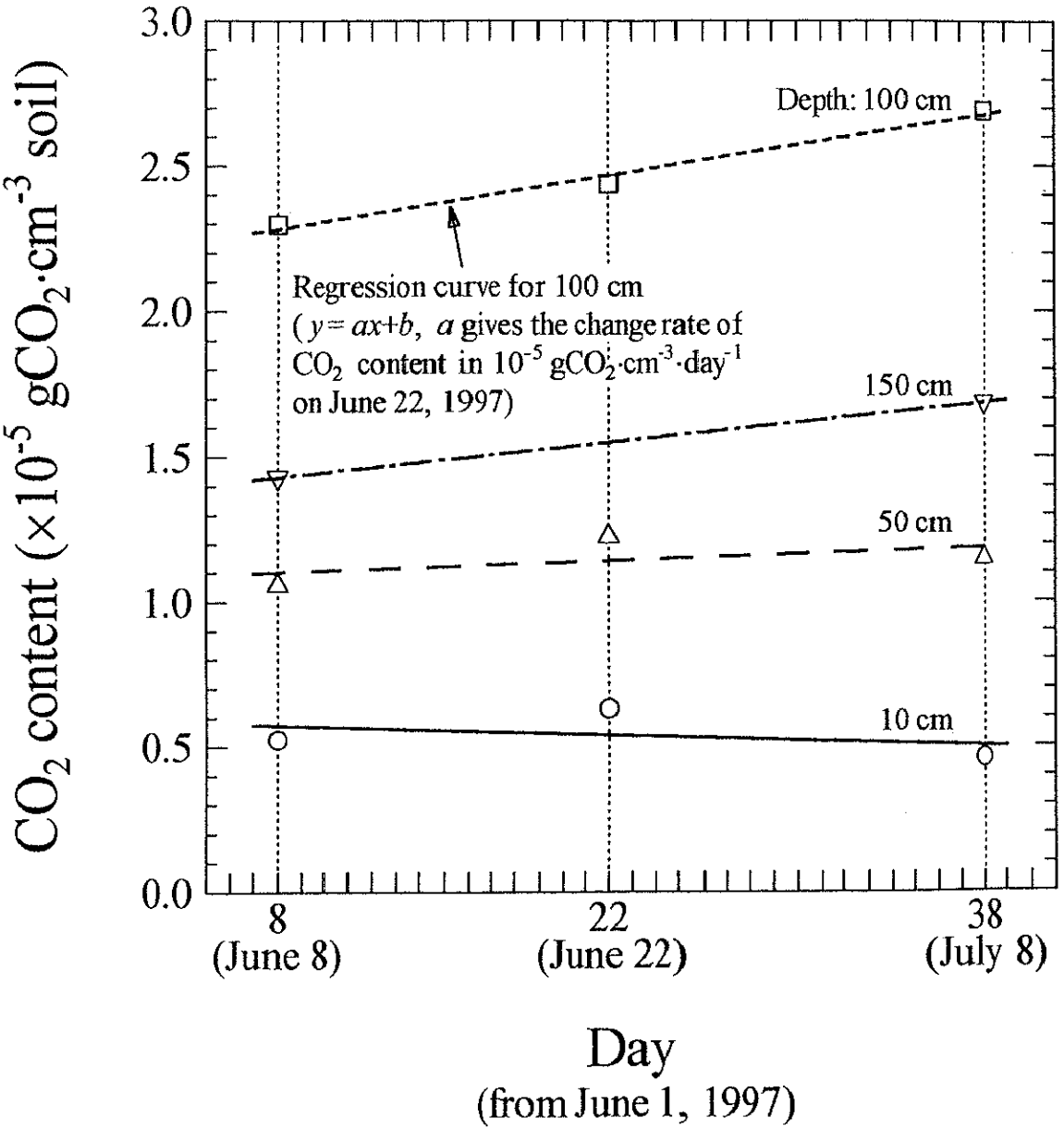

Figure 5.24. Method for determining the change rate of CO_2 content per unit volume of bulk soil at each depth.

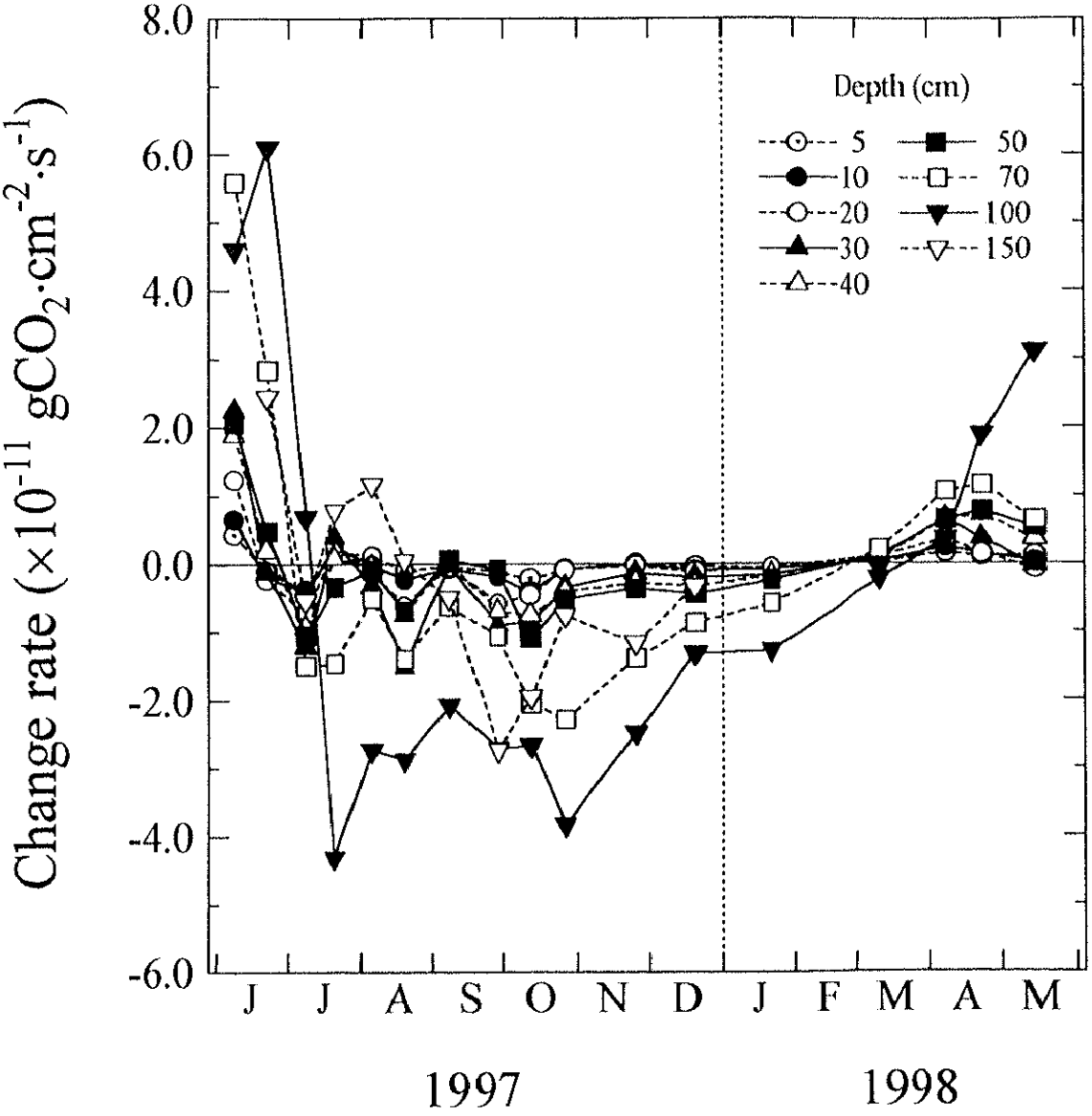

Figure 5.25. Seasonal variation of the change rate of CO_2 storage at the forest site.

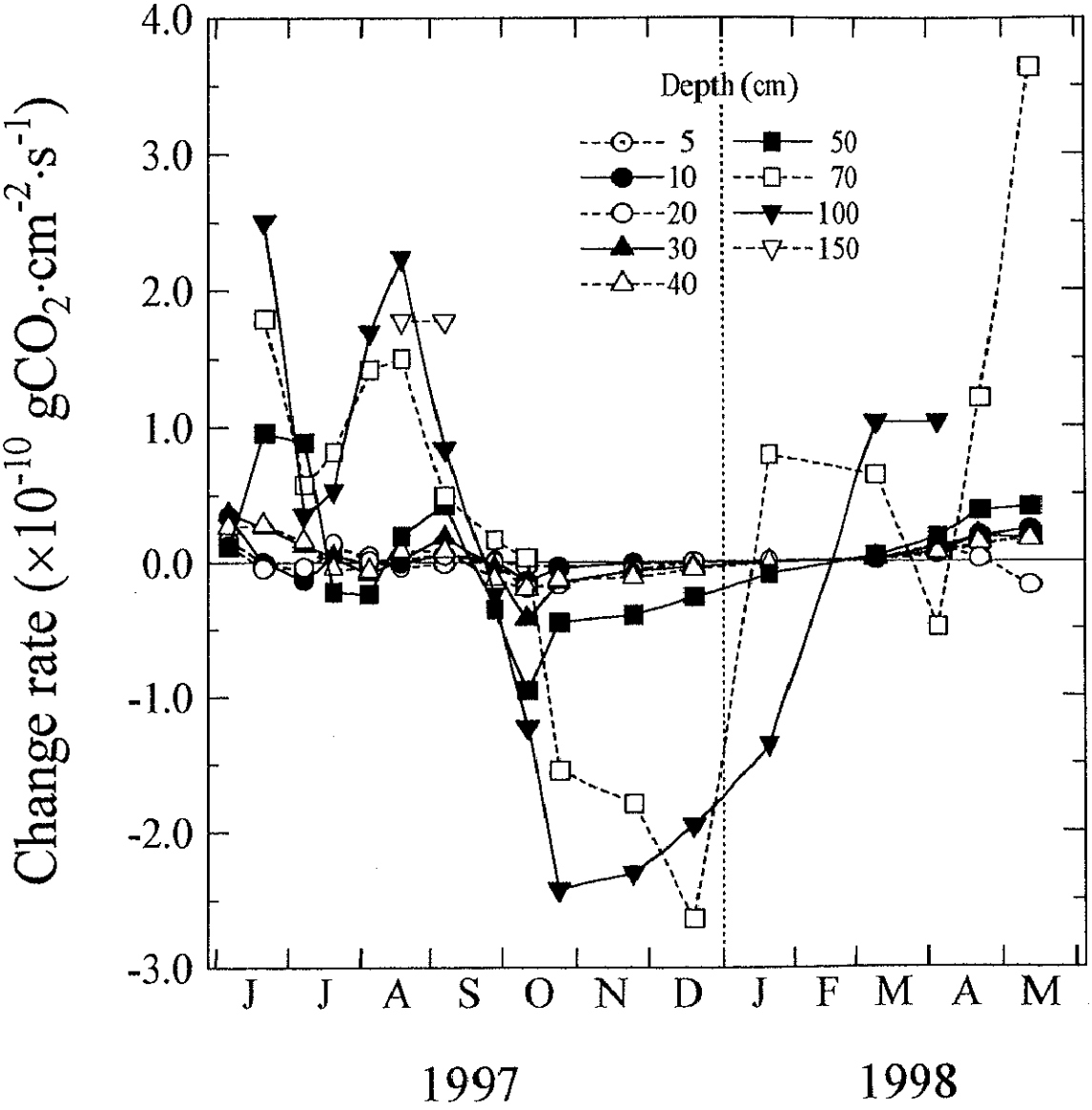

Figure 5.26. Seasonal variation of the change rate of CO_2 storage at the grassland site.

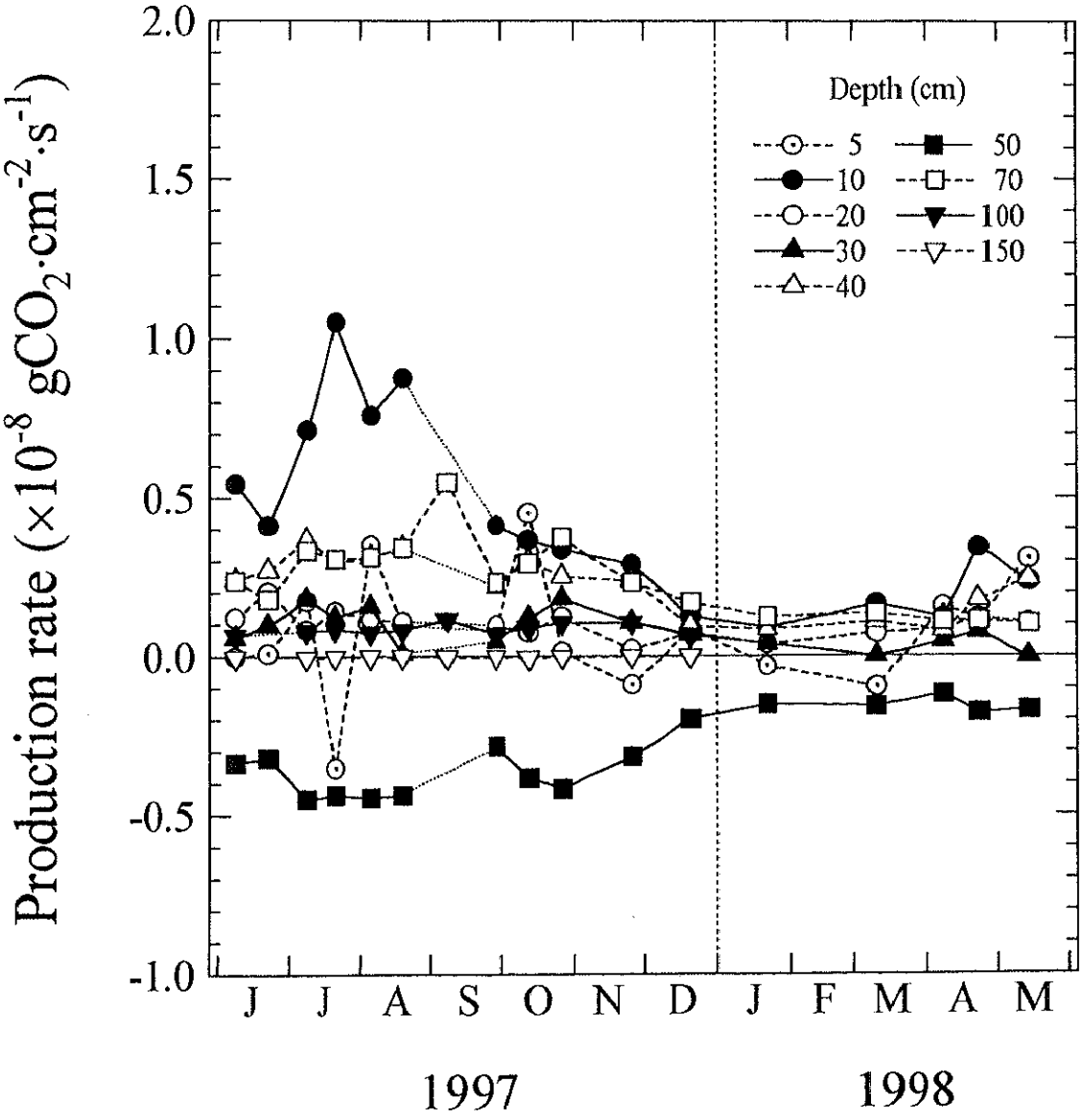

Figure 5.27. Seasonal variation of CO_2 production rate at the forest site.

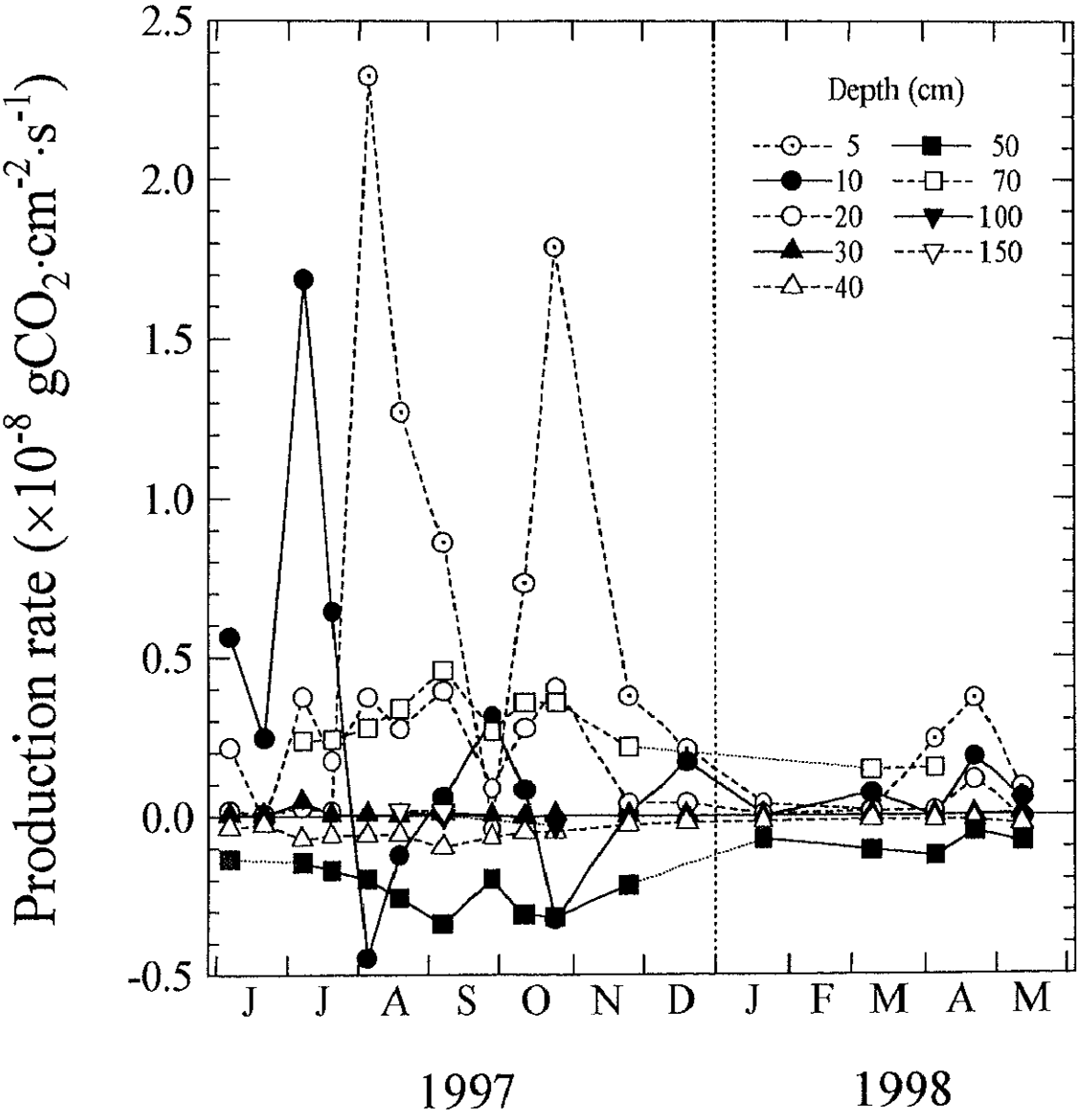

Figure 5.28. Seasonal variation of CO_2 production rate at the grassland site.

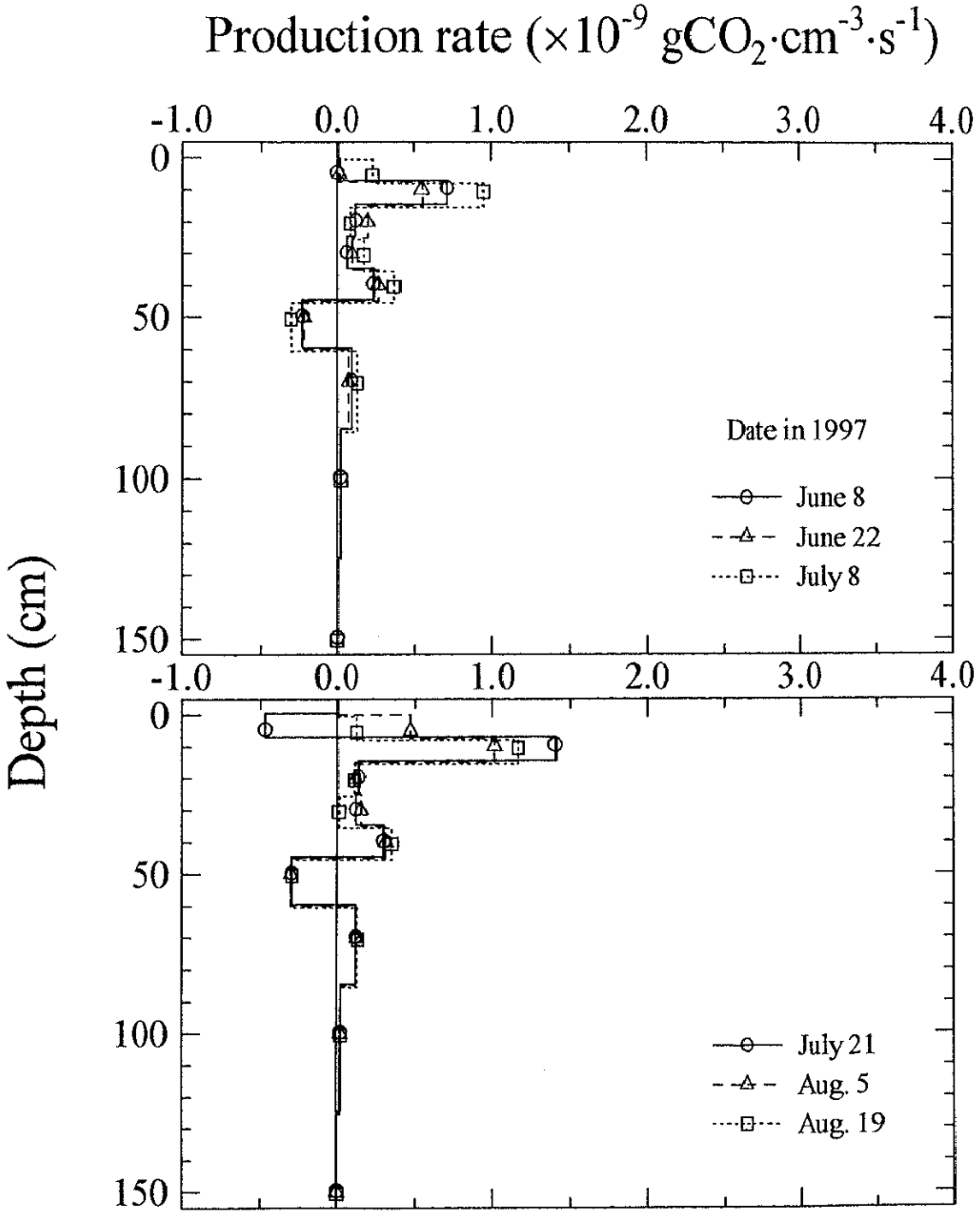

Figure 5.29a. Profiles of CO_2 production rate at the forest site from June to August, 1997.

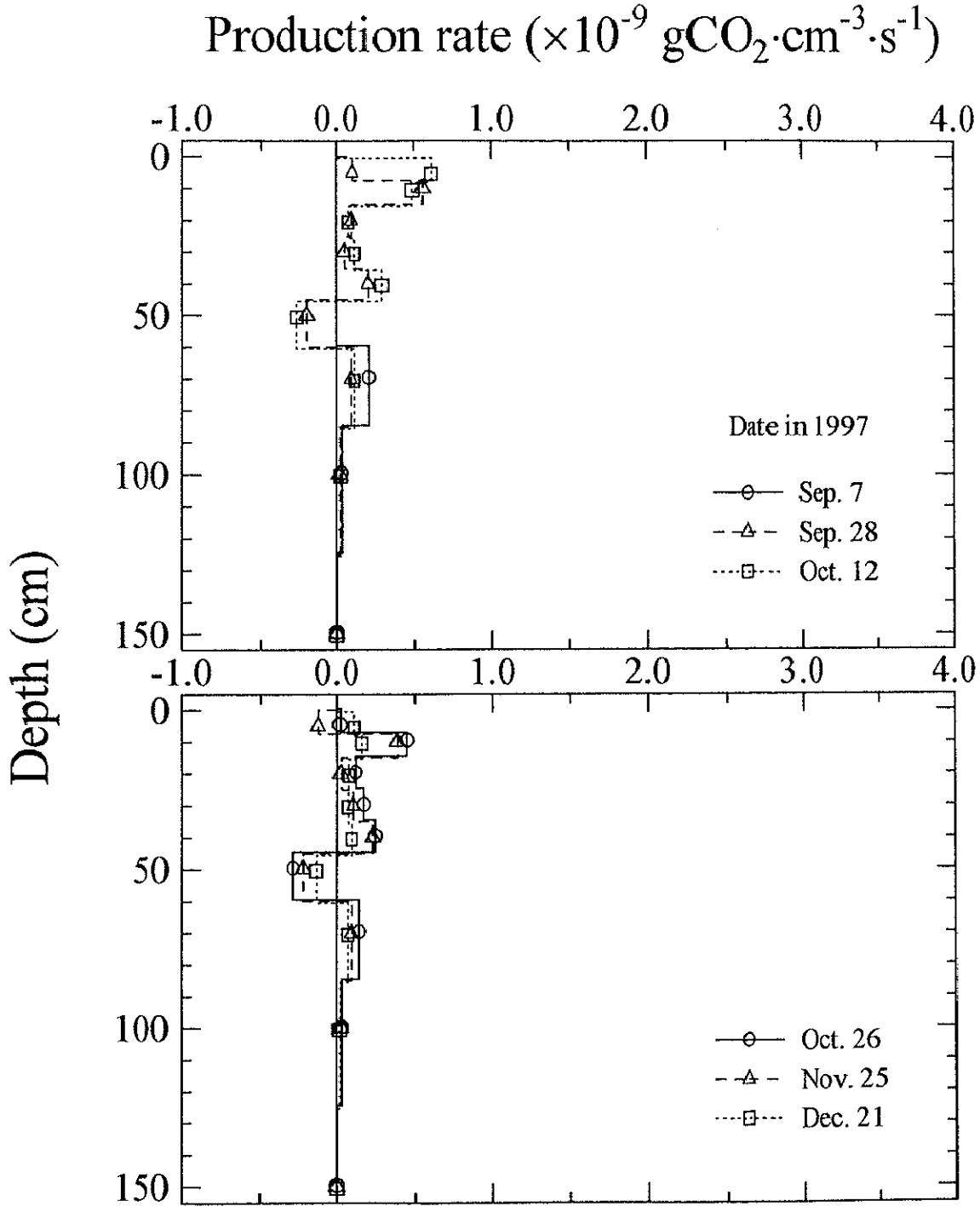

Figure 5.29b. Profiles of CO_2 production rate at the forest site from September to December, 1997.

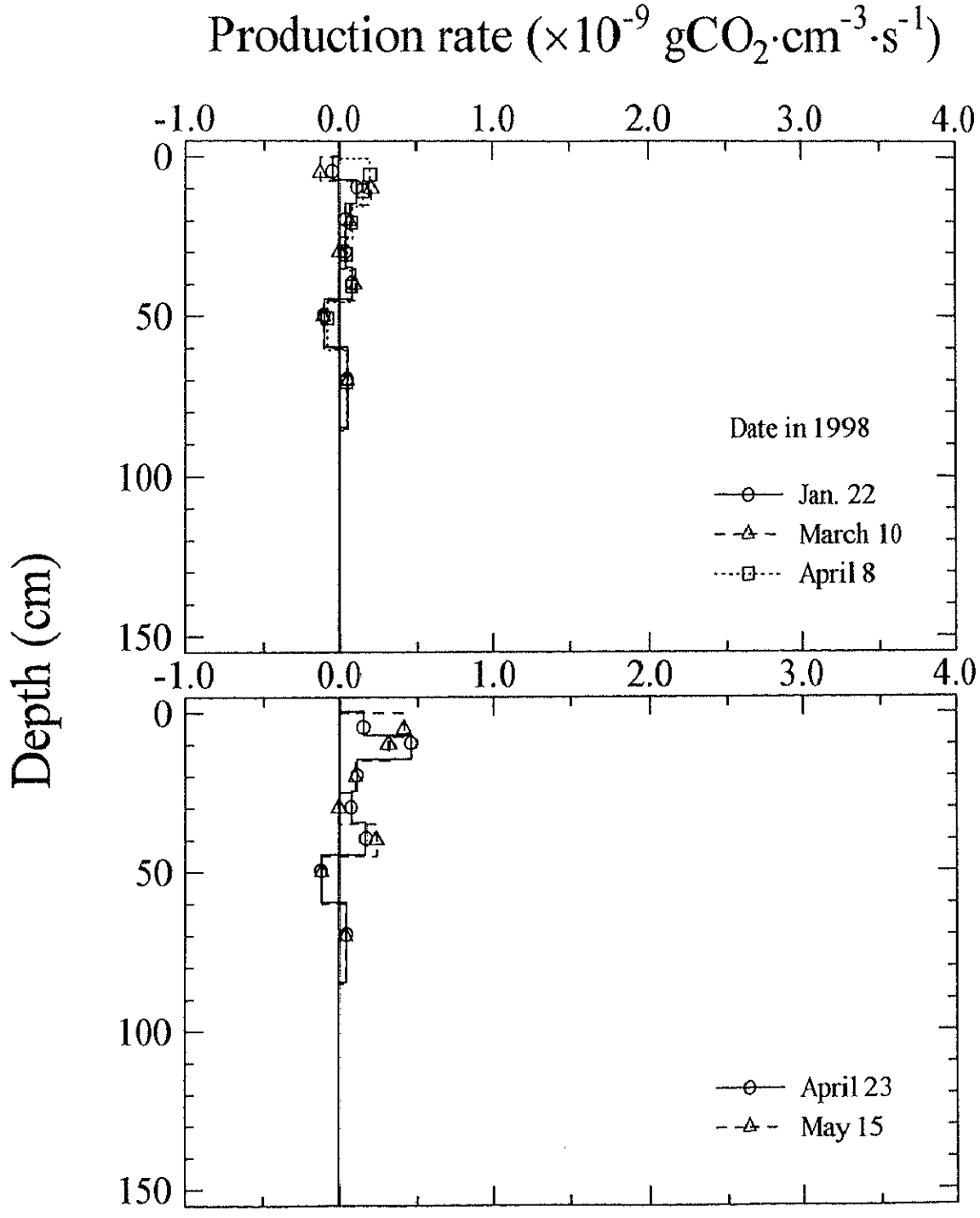

Figure 5.29c. Profiles of CO_2 production rate at the forest site from January to May, 1998.

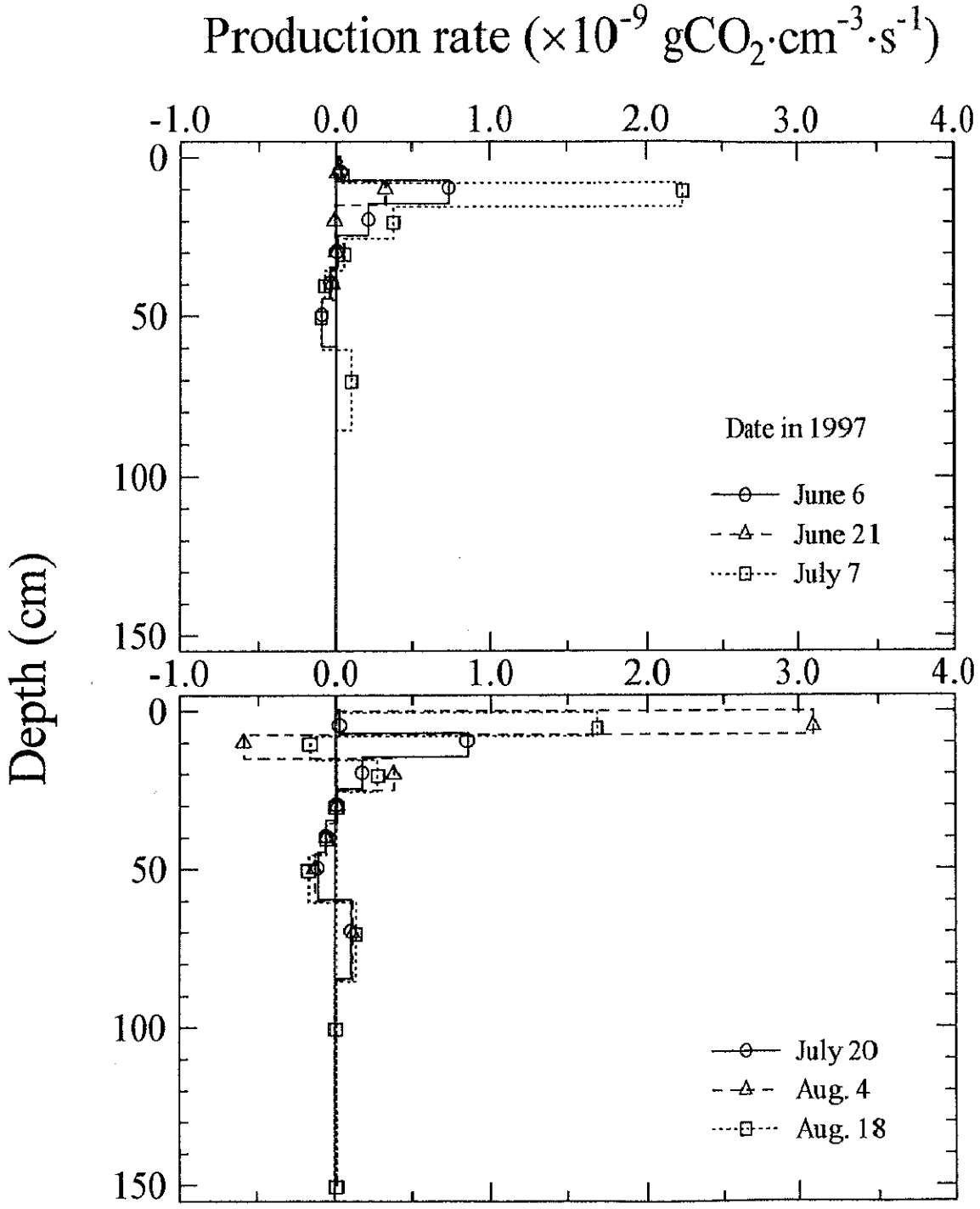

Figure 5.30a. Profiles of CO_2 production rate at the grassland site from June to August, 1997.

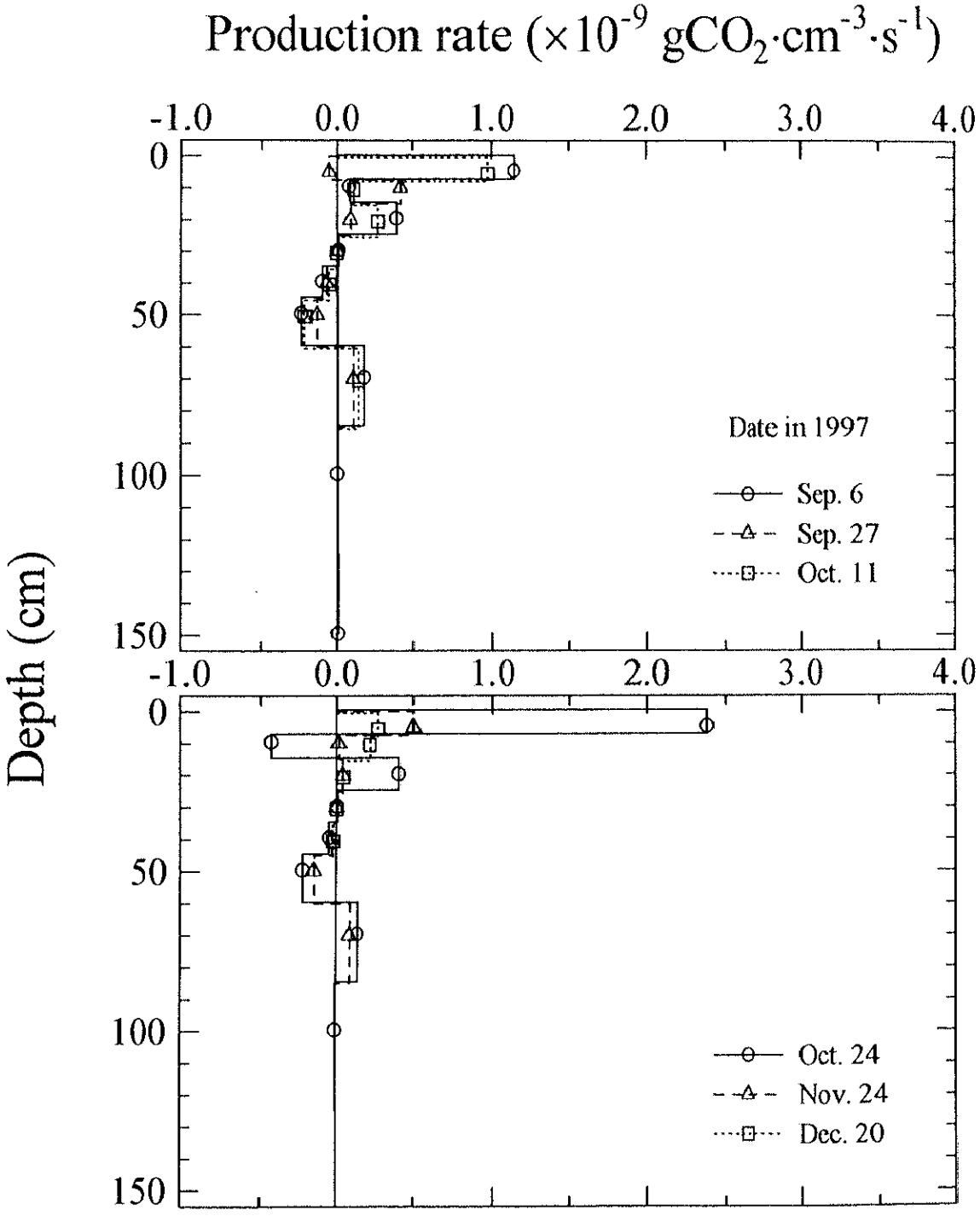

Figure 5.30b. Profiles of CO_2 production rate at the grassland site from September to December, 1997.

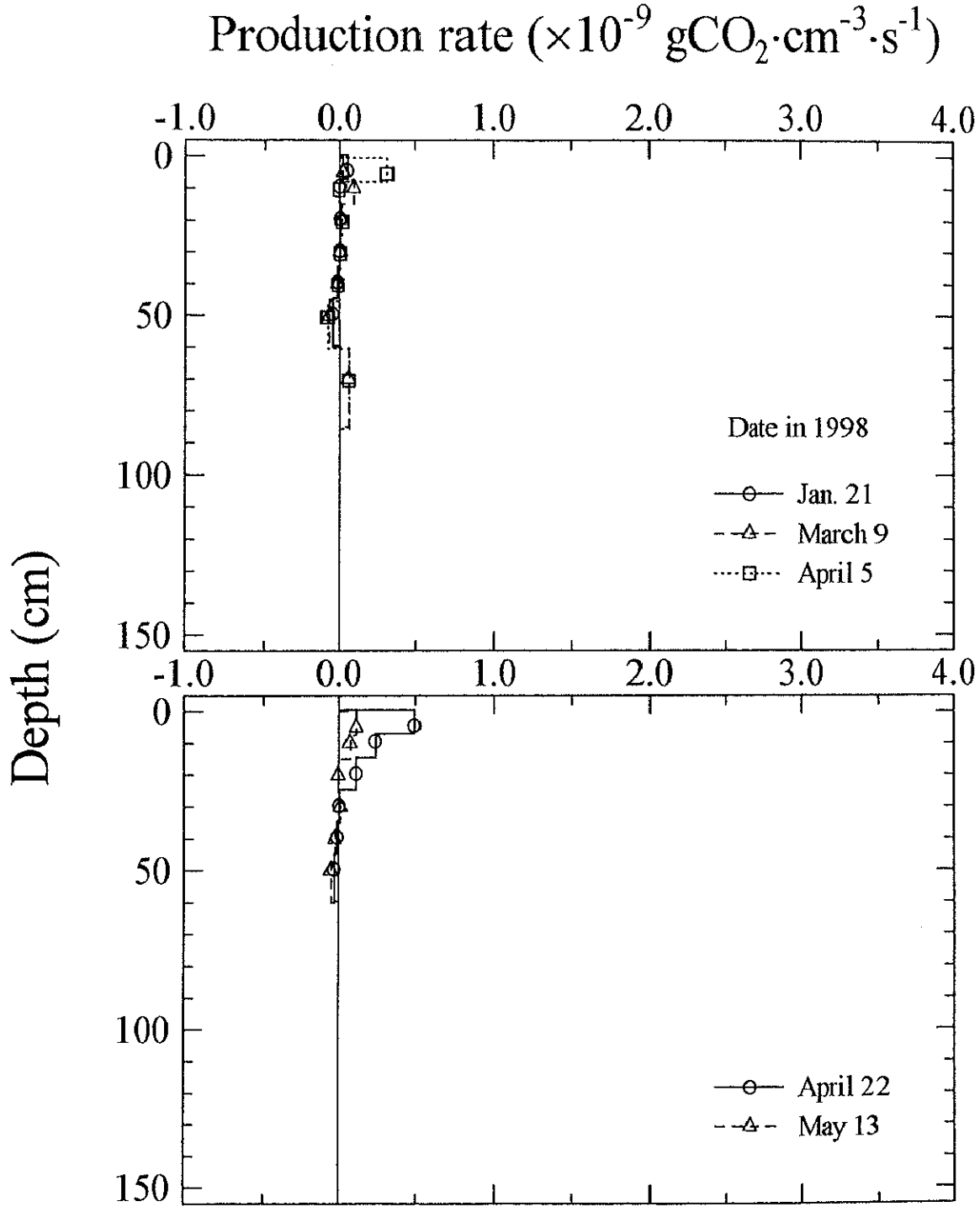

Figure 5.30c. Profiles of CO_2 production rate at the grassland site from January to May, 1998.

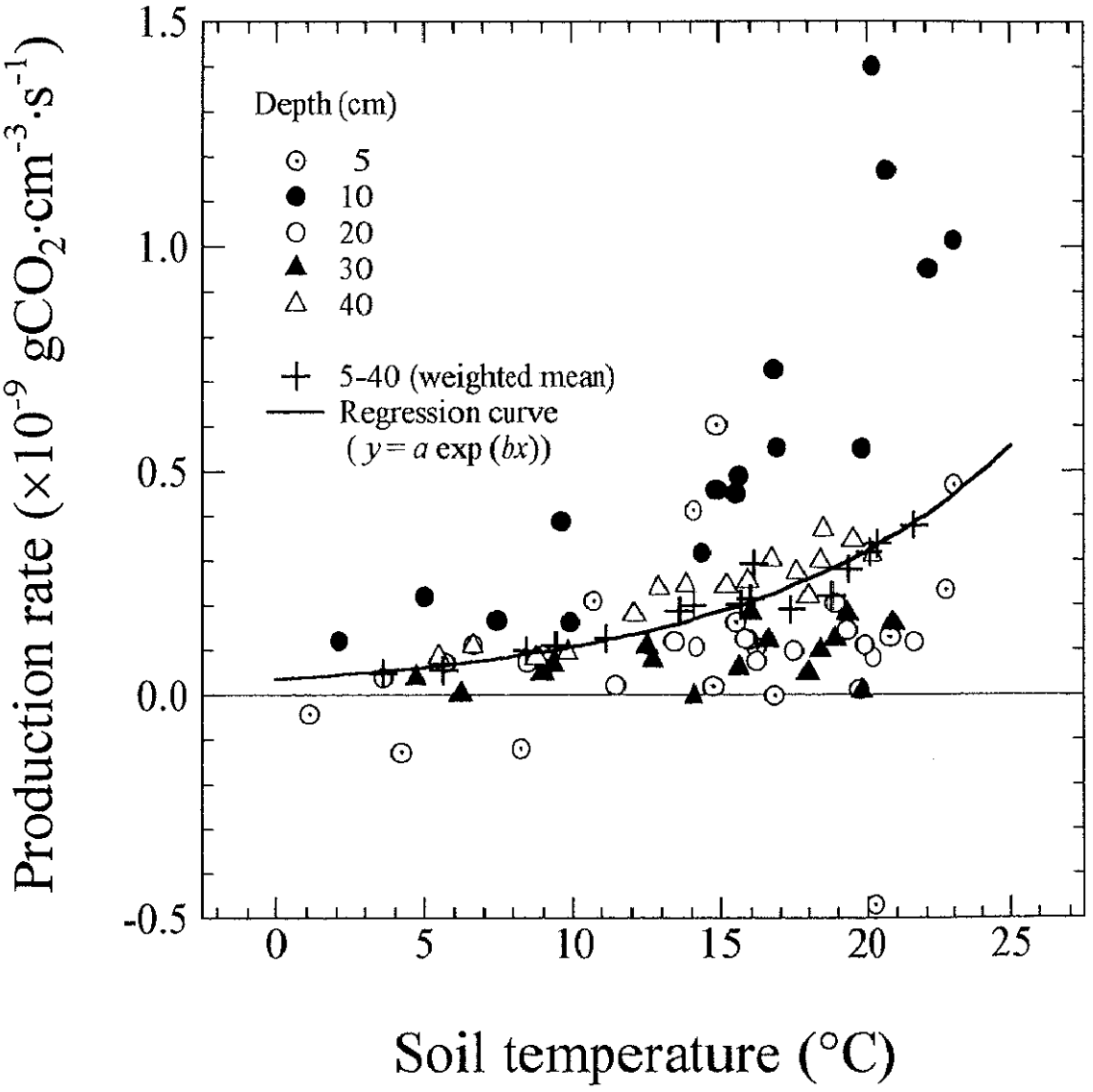

Figure 5.31. Relationship between CO_2 production rate and soil temperature at the forest site.

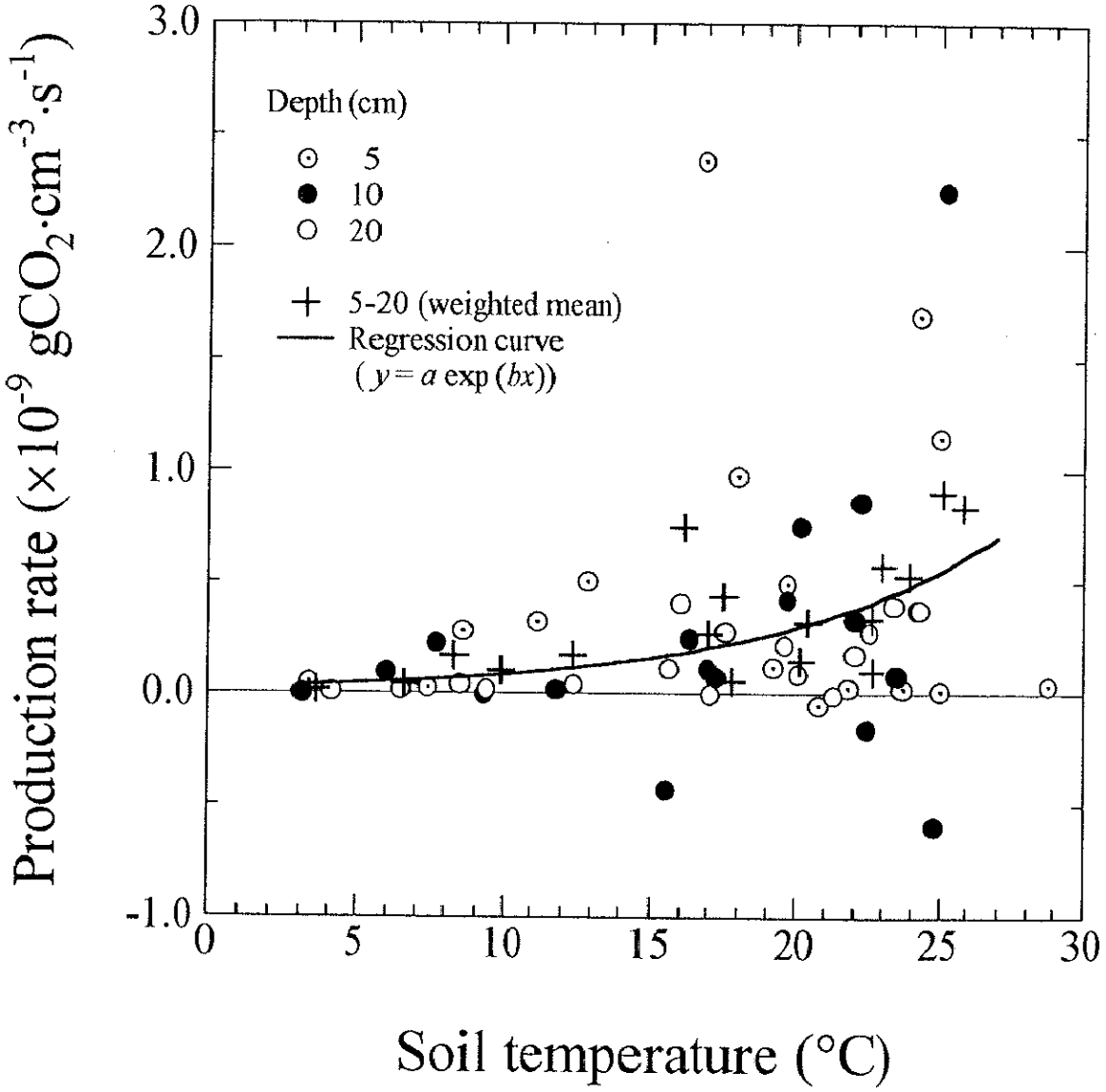

Figure 5.32. Relationship between CO_2 production rate and soil temperature at the grassland site.

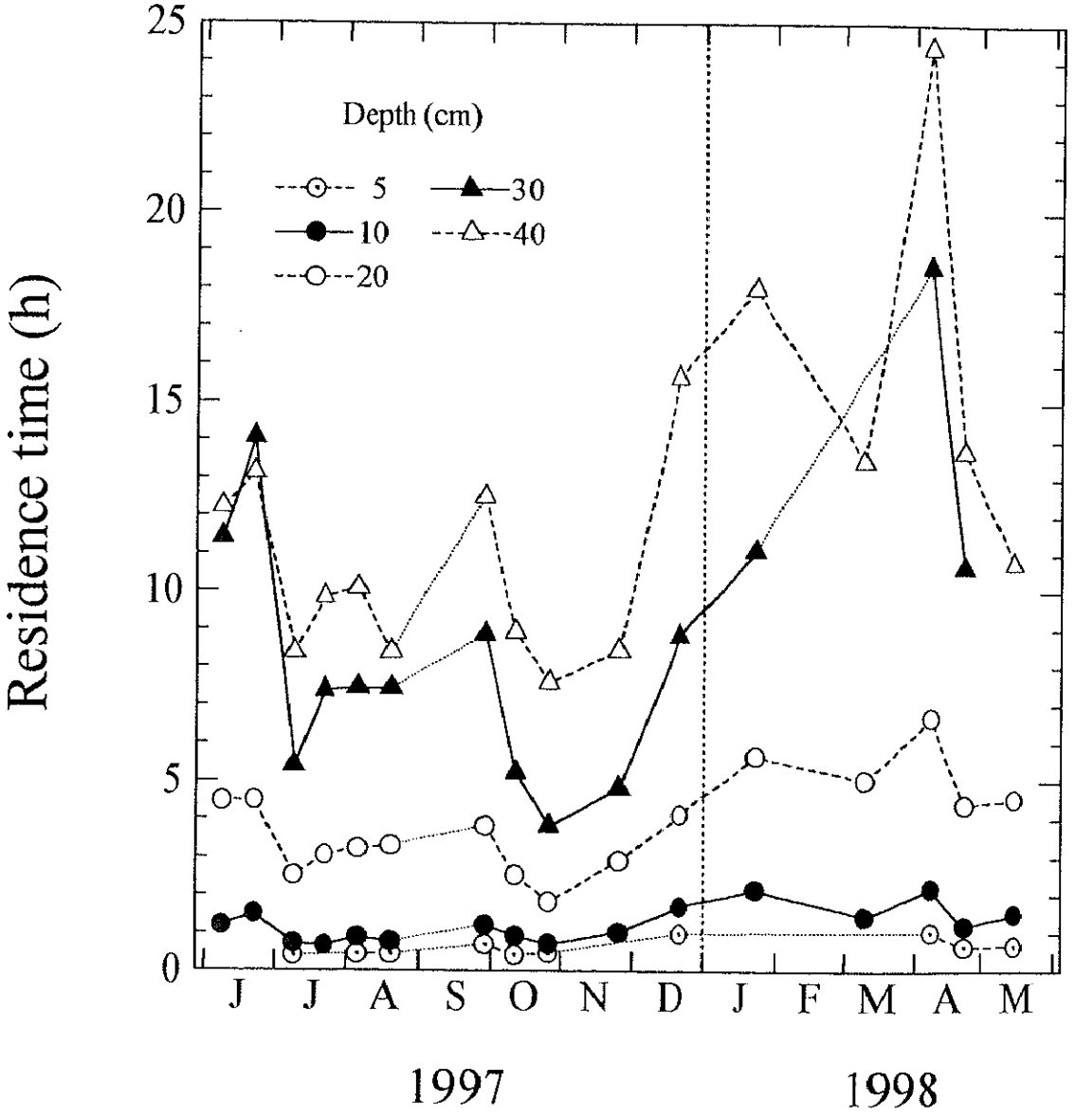

Figure 5.33. Seasonal variation of the mean residence time of CO_2 at the forest site.

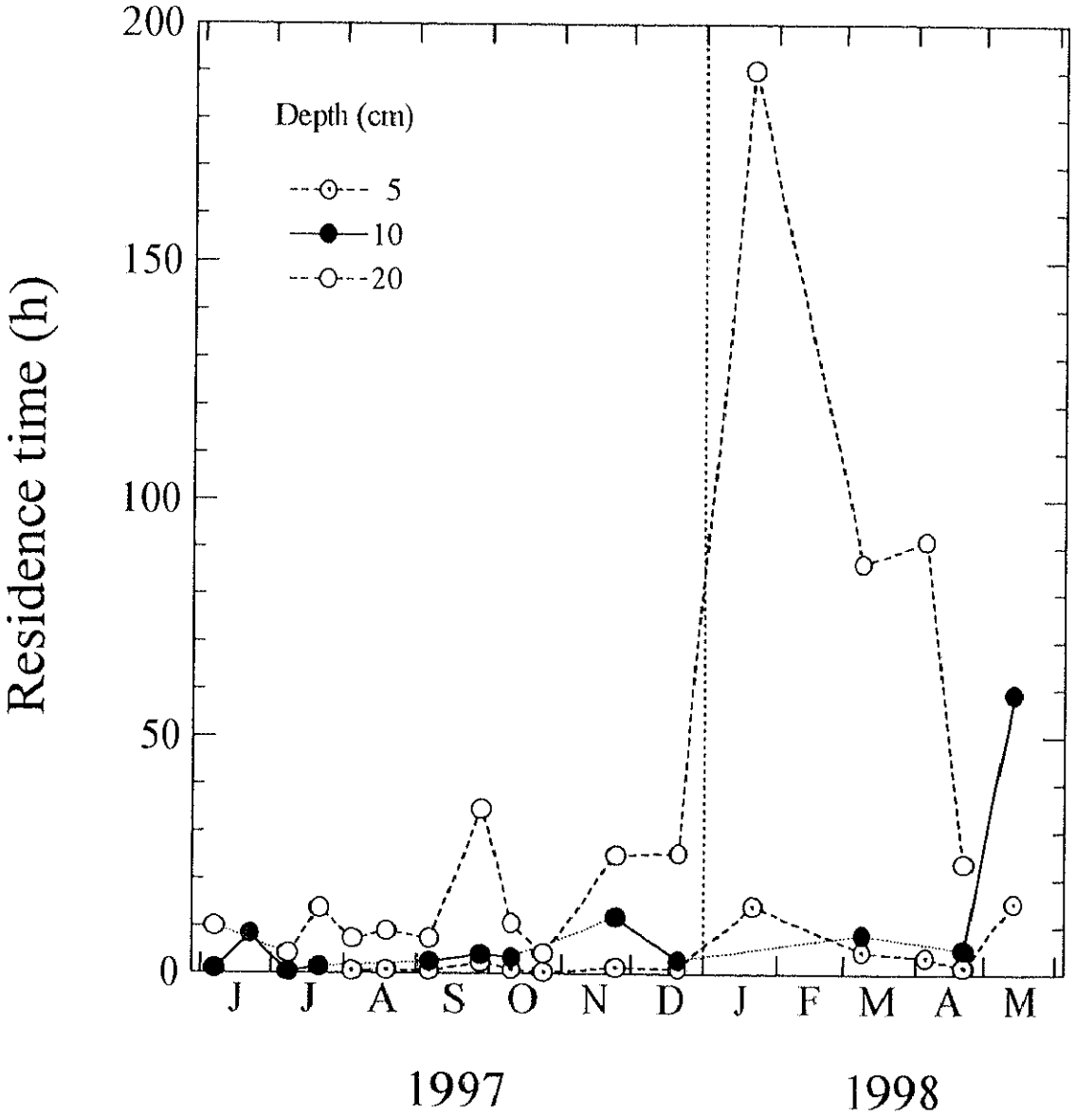

Figure 5.34. Seasonal variation of the mean residence time of CO_2 at the grassland site.

Chapter 6

General discussion

6.1 Processes of the formation of concentration profiles of carbon dioxide

From the deterministic approach used in this study, the processes of the production and transport of CO_2 were quantitatively assessed in the inverse order of the real processes. Here, the results obtained in Chapters 4 and 5 are generally reviewed, and the processes of CO_2 in soil profiles at the forest and the grassland site are presented in the same order of the actual processes; 1) production, 2) transport, and 3) formation of the concentration profiles.

At the forest site, significant CO_2 production was observed from the ground surface to a depth of 45 cm (Figure 5.29). Especially at the soil compartment of a depth of 10 cm, about a half of the total production of CO_2 in the soil was concentrated. This resulted from the relatively large amount of plant roots (Figure 3.7) and TOC (Figure 3.8) in shallow soils at the forest site. In addition, considerable upward fluxes of CO_2 were obtained at these depths (Figure 5.15). The total flux was dominated by the diffusive flux in soil air (Figure 5.21) due to the large air-filled porosity at these depths (Figure 3.1). Thus, in spite of the higher production rates of CO_2, the concentrations in soil air (Figure 4.13) and in soil water (Figure 4.24) and the total content in bulk soil (Figure 4.32) were kept lower than those in the deeper soils by the larger fluxes into the atmosphere. As a result, the mean residence time of CO_2 at these depths was relatively short, usually less than a day (Figure 5.33).

For the soil compartment at a depth of 50 cm, negative production rates were evaluated by the CO_2 mass balance (Figure 5.29). In practice, the net sink of CO_2 must be absent, but the real values of the production rates would be much smaller than those in the upper soils. Around the depth, some changes in the soil physical property were implied by the sudden decrease in saturated hydraulic conductivity (Figure 3.5), so that such physical properties might prevent the plant roots from penetrating into the depth. Probably because of the small production rate, the

inflow of CO_2 produced in the upper soils would occur in the summer, and therefore the downward gradient of CO_2 concentration (Figure 4.13) and the downward flux of diffusion (Figure 5.15) were found at the soil section of 40-50 cm in the summer, though the magnitude of the downward flux would be much smaller. In the winter, the inhibition of CO_2 production in shallow soils by the low temperatures would cause the evolution of CO_2 accumulated around a depth of 50 cm during the summer into the upper depths, and this might be the reason that the concentration gradient and the diffusive flux at 40-50 cm became upward in the winter. Consequently, CO_2 concentration at a depth of 50 cm was similar to that at 40 cm (Figure 4.11), and the mean residence time probably becomes much longer.

In contrast, for the soil compartments at depths of 70 and 100 cm, considerable production of CO_2 was estimated (Figure 5.29). The real values of production rate must be much lower because the evaluated production rates at these depths were almost offset by the negative production rates evaluated at 50 cm. The CO_2 produced at these depths were then probably accumulated within the depths due to the specific soil physical properties around a depth of 50 cm. As a result, large concentration gradients were formed at depth intervals between 50 and 100 cm (Figure 4.13). The relatively large diffusive fluxes evaluated from the concentration gradients (Figure 5.15), however, must be much smaller in reality. The accumulated CO_2 might be removed into the groundwater by the large advective flux of dissolved CO_2 during heavy rain (Figure 5.19). Consequently, the highest concentrations (Figures 4.9 and 4.24) and the largest total content (Figure 4.32) of CO_2 in the profiles was observed at a depth of 100 cm, probably due to the combination of the low production rate and the intensive inhibition of diffusion. Inevitably, the mean residence time at these depths would be extremely long.

Little CO_2 was produced at a depth of 150 cm, and much of the CO_2 around the depth would be brought from the upper soils, partly by the consistently downward flux of diffusion at the soil section of 100-150 cm (Figure 5.13). As the groundwater table approached, the proportion of the diffusive flux to the total flux became smaller whereas the proportion of the dissolved CO_2 flux became larger (Figure 5.21). The dissolved CO_2 flux is important as a source of carbonate species in groundwater, though its magnitude is much smaller than that of the diffusive flux into the atmosphere.

On the other hand, at the grassland site, the soil layer in which CO_2 was actively generated ranged from the ground surface to a depth of 25 cm (Figure 5.30), concentrated closer to the

surface than at the forest site. The four-fifth of the total CO_2 was produced in the soil compartments at depths of 5 and 10 cm. This profile of the production rate is in good agreement with the distribution of grass roots (Figure 3.8). Similar to the same depths of the forest, large upward fluxes of CO_2 were observed at these depths (Figure 5.16). Because of the higher production rates and the larger fluxes, consequently, the lower concentrations in soil air (Figure 4.12) and in soil water (Figure 4.25) and the smaller total content in bulk soil (Figure 4.33) were obtained in these depths than those found in the deeper soils. Due to the inhibition of the diffusive flux caused by the extremely low air-filled porosity (Figure 3.2), however, CO_2 concentration in soil air was higher than the concentration at the same depth of the forest. So that the mean residence time became much longer (cf Figures 5.33 and 5.34), nevertheless the production of CO_2 was concentrated closer to the ground surface and then the produced CO_2 could escape into the atmosphere more readily at the grassland.

The production rate of CO_2 in the soil compartment at a depth of 30 cm was extremely low (Figure 5.30). At the depth, the dressed clay layer was present (Table 2.1), which had little content of TOC (Figure 3.9) and probably prevented the grass roots from extending downward any further. Due to the clay layer, the total flux of CO_2 was also little (Figure 5.22), as a result CO_2 concentration at a depth of 30 cm was kept slightly higher than the concentration at 20 cm (Figure 4.12), but the mean residence time must be much longer.

For the soil compartments at depths of 40 and 50 cm, negative values were calculated as the production rate of CO_2, while relatively large production rates were obtained at 70 cm (Figure 5.30). As discussed previously, such production rates probably resulted from the overestimate of the diffusive fluxes at the soil sections among these depths (Figure 5.16), so that much less amount of CO_2 would be produced at these depths in fact. The old surface soils were deposited at these depths (Table 2.1); thus the old soil organic matter contained in the soils (Figure 3.9) might contribute to the CO_2 production. Moreover, slightly larger number of roots were observed at these depths (Figure 3.8), therefore the root respiration would also contribute to the production rate if the roots were the present vegetation's. Most of the produced CO_2 would be accumulated within the depths due to the clay layer that intensively prevented the CO_2 from diffusing into the upper soils. The large concentration gradients observed at the soil sections among these depths (Figure 4.14) were probably formed by this inhibition of diffusion. Due to the extremely low saturated hydraulic conductivity in the shallow soils (Figure 3.6), the removal of the accumulated

CO_2 into groundwater accompanied by large percolation during heavy rain could not be expected, but horizontally heterogeneous fluxes such as preferential flow of soil water might play important roles. Because of the relatively large amount of TOC and plant roots and the presence of the dressed clay layer, the concentrations (Figures 4.10 and 4.25) and the total content (Figure 4.33) of CO_2 became much higher than those at the same depths of the forest site. Also the mean residence time must be much longer.

The production rates of CO_2 were little below 100 cm (Figure 5.30). Usually downward concentration gradients were obtained at the soil sections between 70 and 150 cm (Figure 4.14) so that some of the CO_2 contained in these depths would have been carried from the upper soils by diffusion. Because of the closeness to the groundwater table, however, the proportion of the diffusive flux were low, while the proportion of the advective flux of dissolved CO_2 became high (Figure 5.22). The dissolved CO_2 flux must be important in the transport of CO_2 from the upper depths to these depths, and then into the groundwater.

Finally, the averaged profiles of the production rate, total flux and the proportions of each flux, concentration in soil air, and mean residence time of CO_2 in soils at the forest and the grassland site are summarized in Figure 6.1. Some data are arbitrarily corrected to agree with the above discussion, and plotted by dotted lines.

At both observation sites, the soil profiles are clearly classified into two layers by the processes of CO_2. In the shallow layer, in which CO_2 is actively produced, the flux of CO_2 is also large and mostly caused by diffusion in soil air; consequently, the concentration of CO_2 is kept small. Most of the CO_2 production in the soil are concentrated in the layer, and almost all the produced CO_2 are evolved as soil respiration, therefore the surface layer is important as a source of CO_2 in the atmosphere. On the other hand, in the deep layer, although the production rates are generally low, the diffusive fluxes are also small; consequently, relatively high concentrations are kept. The high concentrations of CO_2 in soil air will heighten the dissolved CO_2 concentration and then lower the pH in soil water, hence the deep layer plays an important role on the determination of groundwater chemistry.

6.2 Effects of vegetation and soil physical property on the production and transport of carbon dioxide

Plant roots, as well as soil organic matter, are the important source of CO_2 produced in a soil. Because of the adjacency of the forest and grassland sites, climate, geomorphology and underlying geology at both sites can be regarded as common. Thus, the effect of the difference in vegetation on CO_2 processes in the soil profiles could be examined by comparing the results obtained at both sites.

The soil layer in which significant production rate of CO_2 was observed ranged from the ground surface to a depth of 45 cm at the forest site (Figure 5.29). At the grassland, the active soil layer ranged from the surface to a depth of 25 cm (Figure 5.30), concentrated closer to the surface than at the forest. The ranges of distribution were in good agreement with the distribution of plant roots at both sites (Figures 3.7 and 3.8). In addition, soil respiration rate (Figures 5.3 and 5.4), the diffusive flux in soil air (Figures 5.13 and 5.14) and the production rate (Figures 5.28 and 5.29) near the ground surface varied more rapidly and more widely in response to the variation of micrometeorological conditions at the grassland than at the forest. This probably resulted from the high variability in the environmental conditions near the ground surface at the grassland, due to the lack of dense canopy. In addition, however, the response of the production rate to the change in environmental factors might be enhanced due to the high concentration of plant roots near the surface. Hence the temporal and spatial variations in CO_2 production can be explained generally by the difference in the distribution of plant roots, and therefore the difference in vegetation.

On the other hand, however, soil physical properties at both observation sites were largely different, too. At the grassland site, the soil had been strongly affected by artificial disturbance (Table 2.1). In the shallow soils, CO_2 concentrations in soil air were 1.4 to 1.9 times as high as those at the forest (cf Figures 4.9 and 4.10), nevertheless the CO_2 production was concentrated closer to the surface at the grassland and then it was expected that the produced CO_2 could be more easily evolved into the atmosphere. This would be caused by the inhibition of the diffusion of CO_2 due to the extremely low air-filled porosity (Figure 3.2). In the deep soils, CO_2 concentrations were 4.4 to 8.3 times as high as those at the forest. This was probably due to the strongly inhibited diffusive flux in soil air caused by the dressed clay layer (Table 2.1). Thus, the

differences in the flux and concentration of CO_2 between both sites were directly affected by the difference in soil physical properties rather than that in vegetation.

Actually, soil physical properties at the grassland site are highly affected by the artificial disturbance. In general, however, a grassland soil probably shows the physical properties more or less similar to the properties of the soil at the grassland site. Roots of trees are generally thicker than roots of grass and are likely to extend to deeper soils. In addition, trees are essentially perennial whereas many of grass species are annual. Consequently, the effect of tree roots on soil physical properties would be larger and more consistent than the effect of grass roots. Moreover, because of the lack of dense canopy, pore spaces in the surface soil of grassland can be easily packed or filled by the impact of raindrops. For these reasons, the possibility is suggested that even under natural conditions, grassland soils have more compact texture and lower permeability of substances than forest soils have.

For example, Hoover (1949) compared the hydrologic characteristics of soils between an old cotton field which had been abandoned 35 years before and a forest which had never been cultivated, in South Carolina, USA. The soils at the uncultivated forest showed their water retention properties similar to those at the forest site in this study. On the other hand, high water retention characteristics were shown by the old field soils except near the ground surface, as well as the soils at the grassland site. From the results, it is supposed that the soil physical properties at both observation sites in this study might be good examples of the properties at an undisturbed forest and a disturbed land that has been created by the deforestation of the forest.

As discussed above, soil physical properties are determined not only by parent material and by climatic condition, but also by vegetation as well as artificial disturbance. The grassland site has been highly influenced by anthropogenic effect. However, its soil physical properties might reflect the properties found in general grasslands except for the effects of the dressed clay layer that shows clearly different textures and the soil organic matter contained in the old surface soils.

Finally, the effect of vegetation on the processes of the production and transport of CO_2 in soil profiles is summarized as follows: The temporal and spatial distributions of CO_2 production generally correspond to the distribution of plant roots and the variation of the activity; the flux and concentration of CO_2 are directly affected by soil physical properties, but at the same time, it may be said that they are indirectly influenced by vegetation because of the considerable effect of the vegetation on the soil physical properties.

6.3 Contributions of soil air and soil water to the transport and storage of carbon dioxide

The two phases in which CO_2 in a soil can be stored, namely soil air and soil water, showed highly different contributions to the transport and storage of CO_2.

The transport of CO_2 in soil profiles mostly occurred as molecular diffusion in soil air (Figures 5.21 and 5.22). The proportion of the diffusive flux in soil air to the total flux was usually more than 99% at the soil sections between the ground surface to a depth of 40 cm at the forest, and between the surface to 20 cm at the grassland. The diffusive flux was also dominant at another depths in most cases. The low proportions of the diffusive flux always accompanied with the small total fluxes.

In contrast, the fluxes of CO_2 dissolved in soil water are generally small. The diffusion coefficient in water is about four orders of magnitude as low as that in air, so that the diffusive flux of CO_2 in soil water was not taken into consideration in this study. The advective flux of dissolved CO_2 accompanied by the movement of soil water is important as a source of carbonate species in groundwater, and actually the proportion of dissolved CO_2 flux to the total flux was relatively large in deep soils (Figures 5.21 and 5.22). However, the magnitude of the flux was much smaller than the magnitude of the diffusive flux evolved into the atmosphere. Except for the large proportions observed during heavy rain at the forest site (Figure 5.19), which might be important as a process removing the accumulated CO_2 in deep soils into groundwater, the proportion of dissolved CO_2 flux was relatively small in the whole profiles.

On the other hand, CO_2 concentration dissolved in soil water was generally higher than that in soil air (Figures 4.26 and 4.27). In most cases, the C_w/C_g ranged from 1.5 to 2.5 at the forest and from 1 to 2 at the grassland. In addition, volumetric water content generally exceeded air-filled porosity throughout the profiles (Figures 3.1 and 3.2). At the forest site, volumetric water content increased with depth; at the grassland site, air-filled porosity was extremely low except near the ground surface. As a result, the M_w/M_t at the forest increased with depth, 50 to 70% from depths of 5 to 20 cm, about 80% from 30 to 50 cm, and more than 90% from 70 to 150 cm; at the grassland, more than 95% except near the ground surface and the depths at which the old surface soils were lain (Figures 4.34 and 4.35). Thus, in quantitative aspect, soil water is much more important as a reservoir of CO_2 than soil air, due to the higher concentration of dissolved CO_2 and the volumetric water content larger than air-filled porosity.

Additionally, the temporal and spatial variations of dissolved CO_2 concentration was different from the variations of CO_2 concentration in soil air, due to the dependence of dissolved CO_2 on soil temperature and pH in soil water. In the summer, the concentrations of CO_2 became higher, while the C_w/C_g became lower in response to the low solubility of CO_2 caused by high temperature (Figures 4.26 and 4.27). In deep soils, the concentrations were also high, whereas the values of C_w/C_g were small due to the low pH values (Figures 4.20 and 4.21), caused by high CO_2 concentrations themselves in the deep soils. Because of the C_w/C_g that distributes inversely to the concentrations of CO_2, the variations of dissolved CO_2 concentration were moderated temporally and spatially compared to the concentration in soil air. At the forest site, the values of Max/Min of CO_2 concentration in soil air at each depth ranged from 1.9 to 4.3, while those of dissolved CO_2 concentration were from 1.8 to 2.8, less than the Max/Min of the concentration in soil air at all the depths. So that the Max/Min of the total content of CO_2 in bulk soil became 1.7 to 3.1. At the grassland site, the Max/Min of these variables were 3.3-8.6, 2.2-5.5 and 2.0-4.6, respectively, except for a depth of 150 cm where only a few measurements of CO_2 were carried out. Namely, the dissolution of CO_2 into soil water will decrease the range of the variation of CO_2 storage in bulk soil.

If the C_w/C_g never changed and were kept as a constant value of 1.0, the total content of CO_2 can be given by the product of CO_2 concentration in soil air and total porosity. In this case, at the forest site, the total content becomes 67.8 to 82.2% of the real values of the content averaged for each depth, and the Max/Min ranges from 1.9 to 4.0, larger than the true values of Max/Min. At the grassland site, the total content also shows small values, 71.3 to 90.8% of the real values and the Max/Min ranges from 2.8 to 6.3, also larger than its true values. In addition, the seasonal variation of the total content of CO_2 was also moderated by the change in the volume of liquid phase, which increased in the summer and decreased in the winter. Thus, the importance of soil water in the storage of CO_2 is not limited only in quantitative aspect, but also involves the moderation of the temporal and spatial variations of the storage.

Finally, the contributions of soil air and soil water to the transport and storage of CO_2 are summarized as follows: Soil air acts as the important media in which most of CO_2 is transported; soil water plays a role of the reservoir in which much of CO_2 is stored stably.

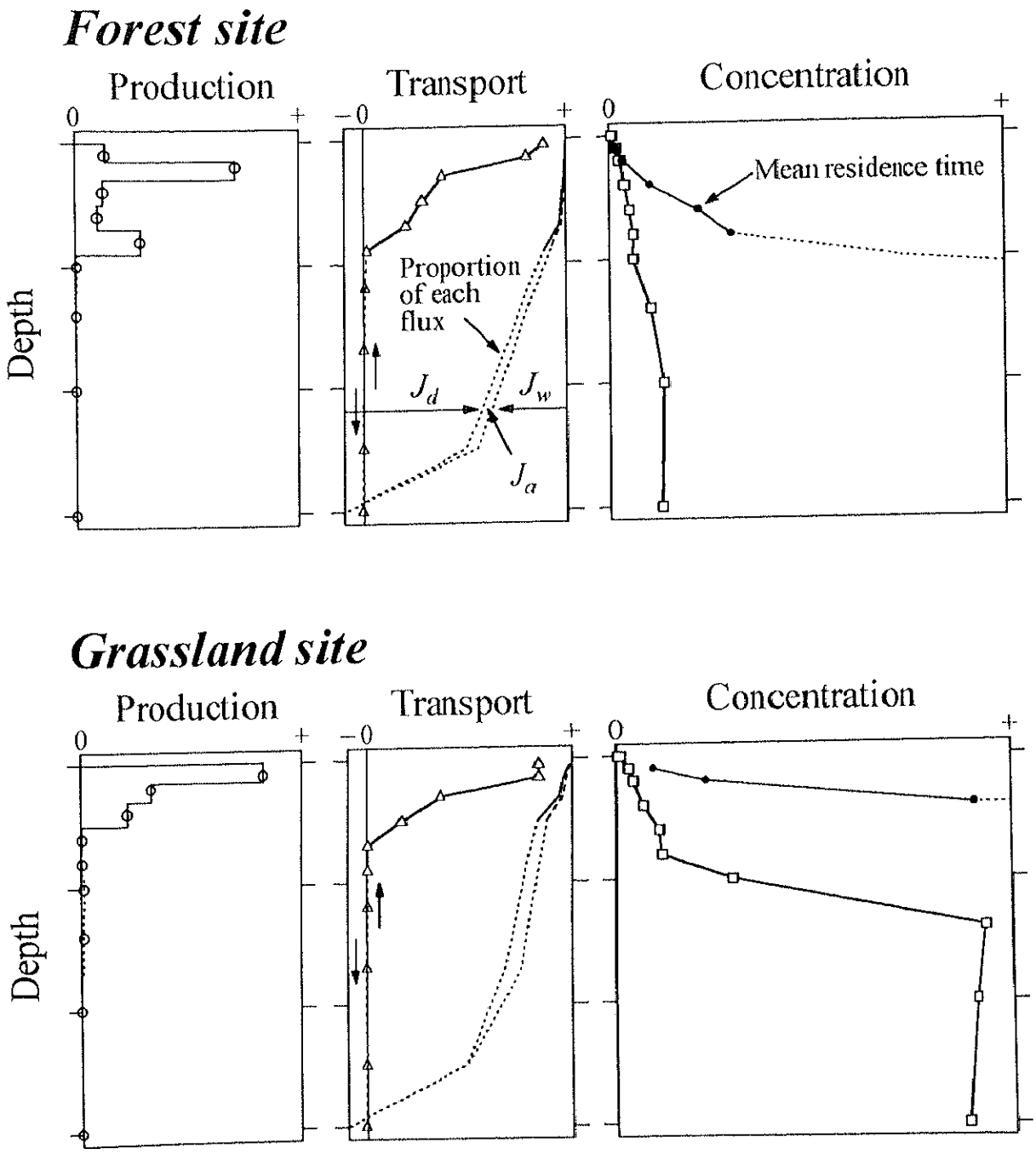

Figure 6.1. Averaged profiles of the processes of CO_2 in soils at the forest and the grassland site.

Arbitrarily corrected values are plotted by dotted lines.

Chapter 7

Conclusions

The conclusions obtained in this study are summarized as follows:

1) The concentration of CO_2 in soil air was always higher than that at the ground surface. The maximum values of the concentration were 1.26% at the forest site and 9.89% at the grassland site and the both were measured in the summer of 1997. The CO_2 concentration in soil air increased from spring to summer and decreased from autumn to winter, similar to the seasonal variation of soil temperature. The concentration of CO_2 in soil air was lowest near the ground surface and generally increased with depth. The maximum concentrations of CO_2 in the profile were observed at 100 cm in the forest, at 70 cm in the grassland.
2) The concentration of CO_2 dissolved in soil water varied seasonally and vertically corresponding to the variations of CO_2 concentration in soil air. The dissolved CO_2 concentrations were generally 1.5 to 2.5 times as high as the concentrations in soil air at the forest site, and were one- to twofold at the grassland site. The C_w/C_g was seasonally varied in an opposite way to soil temperature, mainly due to the CO_2 solubility into water which decreases with rising temperature. In addition, the C_w/C_g decreased with depth as well as the pH in soil water. As the result of such dependence of dissolved CO_2 concentration on soil temperature and pH, the ranges of the temporal and spatial variations of dissolved CO_2 concentration in soil water became smaller than the ranges of the variations in soil air.
3) The total CO_2 content per unit volume of bulk soil showed seasonal variations similar to those of CO_2 concentrations in soil air and soil water. At the forest site, the soil was classified into three layers by the magnitude of total CO_2 content; the total content of CO_2 increased with depth as well as the M_w/M_t, which was 50 to 70% at depths of 5 to 20 cm, about 80% at 30 to 50 cm, and more than 90% below 70 cm. At the grassland site, total CO_2 content was almost equal to the content in liquid phase, because of the extremely low air-filled porosity

throughout the profile except near the ground surface.

4) The soil respiration rates measured by closed chamber method were high in the summer and low in the winter. At the forest site, the rate ranged from 0.22-0.24 $gCO_2 \cdot m^{-2} \cdot day^{-1}$ in January 1998 to 17.3-18.1 $gCO_2 \cdot m^{-2} \cdot day^{-1}$ in late June and early July of 1997. At the grassland site, the difference in soil respiration rate between the measuring spots was large, and the rates ranged from 0.13 to 27.2 $gCO_2 \cdot m^{-2} \cdot day^{-1}$ at SR-G1 and nearly zero to 11.3 $gCO_2 \cdot m^{-2} \cdot day^{-1}$ at SR-G2. The soil respiration rates were exponentially increased with the soil temperature near the ground surface.

From the comparison of the measured soil respiration rate and the evaluated diffusive flux of CO_2 in soil air near the ground surface, the M-Q 2 equation was selected for estimating the relative diffusion coefficient.

5) The seasonal variation of the diffusive flux in soil air generally reflected the variation of the concentration gradient of CO_2 at the forest site. The diffusive flux decreased with depth mainly due to the decrease in the diffusion coefficient. The largest flux in the profile was always observed near the ground surface, and the maximum value of the flux was 1.80×10^{-8} $gCO_2 \cdot cm^{-2} \cdot s^{-1}$, observed in early September of 1997. The diffusive fluxes at the grassland were much lower than those at the forest due to the extremely low diffusion coefficients caused by the low air-filled porosity except near the ground surface. The diffusive flux at the soil section of 0-5 cm was much larger than any other depths and the maximum value of the flux was 2.26×10^{-8} $gCO_2 \cdot cm^{-2} \cdot s^{-1}$, observed in early August of 1997.

The advective flux of CO_2 accompanied by the mass flow of soil air was relatively high at the soil sections between 10 and 50 cm at the forest site, and the sections of 5-10 and 50-70 cm at the grassland site. The maximum downward flux of -0.45×10^{-10} $gCO_2 \cdot cm^{-2} \cdot s^{-1}$ was observed at 20-30 cm in late June of 1997 at the forest. At the grassland, the maximum values of the upward and downward fluxes reached 0.901 and -0.587×10^{-10} $gCO_2 \cdot cm^{-2} \cdot s^{-1}$. However, the advective fluxes at both sites were two orders of magnitude as small as the diffusive fluxes in soil air.

The advective flux of dissolved CO_2 accompanied by the movement of soil water reached about $\pm 0.5 \times 10^{-10} gCO_2 \cdot cm^{-2} \cdot s^{-1}$ at both sites, similar to the advective flux accompanied by the mass flow of soil air, and two orders of magnitude as small as the diffusive flux in soil air. In early April of 1998, however, exceptionally large downward fluxes were obtained throughout

the profile at the forest site because of the heavy rain and the corresponding specific calculation; the maximum downward flux of -5.99×10^{-10} $gCO_2 \cdot cm^{-2} \cdot s^{-1}$ was observed at the soil section of 100-150 cm.

Due to the extremely large values of the diffusive flux of CO_2 in soil air, the temporal and spatial distributions of total CO_2 flux were almost similar to the distributions of the diffusive flux. On the proportions of each flux of CO_2 to the total flux, the diffusive flux in soil air was dominant at most of the depths. The proportion of the diffusive flux was usually more than 99% of the total flux at the soil sections between the ground surface and a depth of 20 cm. The proportion of the advective flux was small throughout the profile. The proportion of dissolved CO_2 flux was also generally small, but increased with depth in deep soils.

6) The production rate of CO_2, which was evaluated as the remainder of CO_2 mass balance, was strongly affected by the seasonal and vertical distributions of the diffusive flux of CO_2 in soil air. The change rates of CO_2 storage were two or three orders of magnitude as small as the difference in the diffusive fluxes among the depths, so that the significance of the storage change in CO_2 mass balance was small.

The production rate of CO_2 was generally higher in the summer and lower in the winter. At the forest site, the largest production rate in the profile was observed at a depth of 10 cm and reached 1.40×10^{-9} $gCO_2 \cdot cm^{-3} \cdot s^{-1}$. About a half of the CO_2 production in the soil of the forest site concentrated around the depth. At the grassland site, the production rate at 5 cm reached 3.11×10^{-9} $gCO_2 \cdot cm^{-3} \cdot s^{-1}$. The four-fifths of the CO_2 generated in the soil of the grassland site concentrated between the ground surface and a depth of 15 cm. The active soil layer in which CO_2 was mainly produced ranged from the ground surface to a depth of 45 cm at the forest, and to 25 cm at the grassland. The profiles of the production rate reflected the distributions of plant roots at both sites. Due to the overestimate of the diffusive flux around a depth of 50 cm, the production rates below the depth could not evaluated correctly, but the CO_2 production in the deep soils would be much smaller than that in the shallow soils.

The production rate of CO_2 exponentially increased in response to the linearly rising soil temperature, indicating that the values of the evaluated production rate were reasonable. The production rates averaged for the active shallow soils were well expressed as exponential functions of the averaged soil temperatures at both sites. The coefficients of determination of the relationships were 0.939 at the forest site, and 0.551 at the grassland site.

The mean residence time of CO_2 was shortest near the ground surface and increased with depth. The mean residence time in the active shallow soils was within a day at the forest site, while the time reached nearly two hundred hours at the grassland site.

7) From the general discussion, the following suggestions were obtained: (1) The shallow soil layer is important for the place of CO_2 production, while the deep soil layer is important as the place keeping high CO_2 concentrations and then determining the rate of the supply of carbonate species into groundwater. (2) The difference in vegetation directly affects the production rate of CO_2 by the difference in the distribution of plant roots, and indirectly influences the transport processes of CO_2, and then its concentration, by affecting the soil physical properties. (3) Soil air is the important media in which much of the CO_2 is transported whereas soil water is important as the reservoir in which CO_2 is stored.

Acknowledgements

The author wishes to express his gratitude to his adviser, Professor Norio Tase, Institute of Geoscience, University of Tsukuba, and his former adviser, Professor Kazuo Kotoda, Toyo University, for their guidance and suggestions during his graduate work. Special thanks are extended to Dr. Tadashi Tanaka, Institute of Geoscience, University of Tsukuba, for drawing the author's attention to this problem and for his continuing guidance and encouragement. The author is also grateful to Dr. Jun Shimada and Dr. Michiaki Sugita, Institute of Geoscience, University of Tsukuba, for their helpful suggestions.

The author would like to thank Professor Takehisa Oikawa, Institute of Biological Science, University of Tsukuba, for his suggestive comments from a biological viewpoint. The author also wishes to thank Professor Franz-Dieter Miotke, Geographical Institute, University of Hannover, for his technical advice on the gas detection tubes and for providing his book free. The author is indebted to Dr. Shin'ichi Onodera, Department of Natural Environmental Sciences, Faculty of Integrated Arts and Sciences, Hiroshima University, and Dr. Maki Tsujimura, Department of Environmental Earth Sciences, Aichi University of Education, for their assistance and advice especially on the field observation.

The author is grateful to Mr. Yoshikazu Kobayashi, Miss Aneeta Rosari Indra Fernando and Mr. Sin'ichi Iida, Doctoral Program in Geoscience, University of Tsukuba, for their cooperative fieldwork and discussions. Special thanks are extended to Mr. Seiichiro Ioka, Doctoral program in Geoscience, University of Tsukuba, and Mr. Takaya Ono, Master's Program in Environmental Science, University of Tsukuba, for their assistance on the survey of soil horizon at the grassland site. The author would like to appreciate Dr. Noriko Niimura and the staff members of Environmental Research Center, University of Tsukuba, for their support on the field observation at the forest and the grassland site. Thanks are also extended to the staff members of Institute of Geoscience, University of Tsukuba, and the author's colleagues, for their supports and discussions.

The soil physical properties at the observation sites were determined in the Laboratory Works

on Hydrology, First Cluster of Collages, University of Tsukuba. The quantitative analysis of soil organic carbon was entrusted to Geo-Science Laboratory Co. Ltd. This study was supported financially in part by the Research Fellowships of the Japan Society for the Promotion of Science for Young Scientists.

Finally, the author would like to express his acknowledgement to his parents for their continuing financial support and encouragement.

References

Allison, G. B., Colin-Kaczara, C., Filly, A. and Fontes, J. Ch. (1987): Measurement of isotopic equilibrium between water, water vapour and soil CO_2 in arid zone soils. *J. Hydrol.*, **95**, 131-141.

Betsumiya, Y. (1992): A study on soil respiration and carbon balance in a field ecosystem. Master of Environ. Sci. thesis, Univ. of Tsukuba, 86 p (in Japanese).

Blake, G. R. and Page, J. B. (1948): Direct measurement of gaseous diffusion in soils. *Soil Sci. Soc. Am. Proc.*, **13**, 37-41.

Bolt, G. H. and Bruggenwert, M. G. M. eds. (1978): *Soil Chemistry, A. Basic Elements.* Elsevier, 281 p.

Bouten, W., de Vré, F. M., Verstraten, J. M. and Duysings, J. J. H. M. (1984): Carbon dioxide in the soil atmosphere: Simulation model parameter estimation from field measurements. *IAHS Publ.*, No. 150, 23-30.

Breymeyer, A. I., Hall, D. O., Melillo, J. M. and Ågren, G. I. eds. (1996): *Global Change: Effects on Coniferous Forests and Grasslands.* Wiley, 459 p.

Brook, G. A., Folkoff, M. E. and Box, E. O. (1983): A world model of soil carbon dioxide. *Earth Surf. Processes Landf.*, **8**, 79-88.

Buyanovsky, G. A. and Wagner, G. H. (1983): Annual cycles of carbon dioxide level in soil air. *Soil Sci. Soc. Am. J.*, **47**, 1139-1145.

Castelle, A. J. and Galloway, J. N. (1990): Carbon dioxide dynamics in acid forest soils in Shenandoah National Park, Virginia. *Soil Sci. Soc. Am. J.*, **54**, 252-257.

Currie, J. A. (1960): Gaseous diffusion in porous media. 2. Dry granular materials. *Br. J. Appl. Phys.*, **11**, 318-324.

Currie, J. A. (1961): Gaseous diffusion in porous media. 3. Wet granular materials. *Br. J. Appl. Phys.*, **12**, 275-281.

Davidson, E. A. and Trumbore, S. E. (1995): Gas diffusivity and production of CO_2 in deep soils of the eastern Amazon. *Tellus*, **47B**, 550-565.

De Jong, E. and Schappert, H. J. V. (1972): Calculation of soil respiration and activity from CO_2 profiles in the soil. *Soil Sci.*, **113**, 328-333.

Fernandez, I. J. and Kosian, P. A. (1987): Soil air carbon dioxide concentrations in a New England spruce-fir forest. *Soil Sci. Soc. Am. J.*, **51**, 261-263.

Fernandez, I. J., Son, Y., Kraske, C. R., Rustad, L. E. and David, M. B. (1993): Soil carbon dioxide characteristics under different forest types and after harvest. *Soil Sci. Soc. Am. J.*, **57**, 1115-1121.

Gash, J. H. C., Nobre, C. A., Roberts, J. M. and Victoria, R. L. eds. (1996): *Amazonian Deforestation and Climate.* Wiley, 611 p.

Grossmann, J. and Udluft, P. (1991): The extraction of soil water by the suction-cup method: a review. *J. Soil Sci.*, **42**, 83-93.

Gunn, J. and Trudgill, S. T. (1982): Carbon dioxide production and concentrations in the soil atmosphere: A case study from New Zealand volcanic ash soils. *Catena*, **9**, 81-94.

Haibara, K., Shimada, H., Toda, H. and Koike, T. (1997): Concentrations of gaseous CO_2 in a forest soil and the dependence of CO_2 flux on the temperature. In: *Report of a Grant-in-Aid for International Joint Research, Ministry of Education, Science and Culture, Japan, IGBP-MESC H8-3*, 243-265 (in Japanese).

Hamada, M., Ohte, N. and Kobashi, S. (1996): A measurement of soil CO_2 profile in a forest watershed. *J. Jpn. For. Soc.*, **78**, 376-383 (in Japanese with English abstract).

Hamada, Y., Indra, A. R. F. and Tanaka, T. (1998): Physical properties of soils of Red Pine forest and heat balance and water balance experimental field in Environmental Research Center, University of Tsukuba. *Bull. Environ. Res. Center*, No. 23, 1-10 (in Japanese).

Hamada, Y., Kobayashi, Y. and Tanaka, T. (1997): Distribution of root system in the soil of a Japanese larch and an Oak Forest. *Bull. Tsukuba Univ. Forests*, No. 13, 103-118 (in Japanese with English abstract).

Hamada, Y. and Tanaka, T. (1995): A simple method for measuring CO_2 concentration in soil air using gas detection device. *J. Jpn. Assoc. Hydrol. Sci.*, **25**, 123-130 (in Japanese with English abstract).

Hamada, Y. and Tanaka, T. (1997): Temporal and spatial distribution of carbon dioxide concentration in forest soil air. *J. Jpn. Assoc. Hydrol. Sci.*, **27**, 3-16 (in Japanese with English abstract).

Hendry, M. J., Lawrence, J. R., Zanyk, B. N. and Kirkland, R. (1993): Microbial production of CO_2 in unsaturated geologic media in a mesoscale model. *Water Resour. Res.*, **29**, 973-984.

Hoover, M. D. (1949): Hydrologic characteristics of South Carolina Piedmont forest soils. *Soil Sci. Soc. Am. Proc.*, **13**, 353-358.

Howard, D. M. and Howard, P. J. A. (1993): Relationships between CO_2 evolution, moisture content and temperature for a range of soil types. *Soil Biol. Biochem.*, **25**, 1537-1546.

Indra, A. R. F. (1997): Soil water dynamics in natural pine forest and disturbed grassland. M. S. thesis, Univ. of Tsukuba, 62 p.

Inokuchi, M., Ikeda, H., Hayashi, Y. and Sakura, Y. (1977): Outline of the Environmental Research Center. *Bull. Environ. Res. Center*, No. 1, 77-91 (in Japanese).

Ishii, T., Kazahaya, K., Yasuhara, M., Marui, A. and Sato, T. (1996): High-temperature anomaly of groundwater and stable carbon isotope ratio of total carbonic acid in and around Kobe City. *Geographic Review of Japan*, **69A**, 493-503 (in Japanese with English abstract).

Jin, Y. and Jury, W. A. (1996): Characterizing the dependence of gas diffusion coefficient on soil properties. *Soil Sci. Soc. Am. J.*, **60**, 66-71.

Kiefer, R. H. (1990): Soil carbon dioxide concentrations and climate in a humid subtropical environment. *Professional Geographer*, **42**, 182-194.

Kirita, H. (1971): Studies of soil respiration in warm-temperate evergreen broadleaf forests of Southwestern Japan. *Jpn. J. Ecol.*, **21**, 230-244 (in Japanese with English abstract).

Kumagai, T. (1998): Process of formation of CO_2 gas environment in forest soil—Examination using numerical model—. *J. Jpn. For. Soc.*, **80**, 214-222 (in Japanese with English abstract).

Liu, S. and Oikawa, T. (1993): Seasonal changes of the biomass in grassland and the environmental conditions at ERC, University of Tsukuba. *Bull. Environ. Res. Center*, No. 18, 69-75 (in Japanese).

Marshall, T. J. (1959): The diffusion of gases through porous media. *J. Soil Sci.*, **10**, 79-82.

Millington, R. J. (1959): Gas diffusion in porous media. *Science*, **130**, 100-102.

Millington, R. J. and Quirk, J. P. (1961): Permeability of porous solids. *Trans. Faraday Soc.*, **57**, 1200-1207.

Miotke, F. D. (1974): Carbon dioxide and the soil atmosphere. Abh. Karst-u Höhlenkunde Ser. A, 9, 1-49.

Mizutani, Y. and Yamamoto, K. (1993): Sources of dissolved carbonates in the shallow groundwater of the Tonami plain, Toyama. *J. Groundwater Hydrol.*, **35**, 77-86 (in Japanese with English abstract).

Nakano, M. (1991): *Movement of substances in the soil.* Tokyo Univ. Press, 189 p (in Japanese).

Ohte, N., Tokuchi, N. and Suzuki, M. (1995): Biogeochemical influences on the determination of water chemistry in a temperature forest basin: Factors determining the *p*H value. *Water Resour. Res.*, **31**, 2823-2834.

Penman, H. L. (1940): Gas and vapor movements in the soil. I. The diffusion of vapors through porous solids. *J. Agric. Sci.*, **30**, 437-462.

Romell, L.G. (1922): Luftväxlingen i marken som ekologisk faktor. Medd. *Statens Skogs-farsöks-anstalt*, **19**.

Seto, M., Matsumae, K. and Tazaki, T. (1978): Seasonal changes of evolution rate of carbon dioxide from forest floor and some considerations on soil organisms and environmental factors. *Environ. Control Biol.*, **16**, 103-108 (in Japanese with English abstract).

Solomon, D. K. and Cerling, T. E. (1987): The annual carbon dioxide cycle in a montane soil: Observation, modeling, and implications for weathering. *Water Resour. Res.*, **23**, 2257-2265.

Stumm, W. and Morgan, J. J. (1981): *Aquatic Chemistry, An Introduction Emphasizing Chemical Equilibria in Natural Waters, 2nd ed.* Wiley, 780 p.

Suarez, D. L. (1986): A soil water extractor that minimizes CO_2 degassing and pH errors. *Water Resour. Res.*, **22**, 876-880.

Suarez, D. L. (1987): Prediction of pH errors in soil water extractors due to degassing. *Soil Sci. Soc. Am. J.*, **51**, 64-67.

Suchomel, K. H., Kreamer, D. K. and Long, A. (1990): production and transport of carbon dioxide in a contaminated vadose zone: A stable and radioactive carbon isotope study. *Environ. Sci. Technol.*, **24**, 1824-1831.

Sugita, M., Yamashita, K. and Kotoda, K. (1986): Geometric structure of a Red Pine tree. *Bull. Environ. Res. Center*, No. 10, 47-52 (in Japanese).

Uchida, M. (1995): Determination of CO_2 flux from forest soil using ^{222}Rn and diffusion process of soil CO_2 to the atmosphere. Master of Environ. Sci. thesis, Univ. of Tsukuba, 67 p.

Usami, T. and Oikawa, T. (1993): Growth of *Quercus myrsinaefolia* seedlings as influenced by microsite light availability in a Red Pine forest. *Bull. Environ. Res. Center*, No. 17, 79-89 (in Japanese).

Van Bavel, C. H. M. (1952): Gaseous diffusion and porosity in porous media. *Soil Sci.*, **73**, 91-104.

Wood, B. D., Keller, C. K. and Johnstone, D. L. (1993): In situ measurement of microbial activity and controls on microbial CO_2 production in the unsaturated zone. *Water Resour. Res.*, **29**, 647-659.

Wood, W. W. and Petraitis, M. J. (1984): Origin and distribution of carbon dioxide in the unsaturated zone of the Southern High Plains of Texas. *Water Resour. Res.*, **20**, 1193-1208.

Yamamoto, S ed. (1986): *Terminology in Groundwater Hydrology.* Kokon-Shoin, 141 p (in Japanese).

Yasui, Y. and Oikawa, T. (1993): Daily and seasonal changes of soil respiration rates and micrometeorological conditions of a Red Pine forest floor in University of Tsukuba. *Bull. Environ. Res. Center*, No. 18, 77-91 (in Japanese).

Zabowski, D. and Sletten, R. S. (1991): Carbon dioxide degassing effects on the pH of spodosol soil solutions. *Soil Sci. Soc. Am. J.*, **55**, 1456-1461.